Calix[n]tetrahydrofuran[4-n]pyrrolidines: Optimized synthesis *via* hydrogenation of calix[n]furan[4-n]pyrroles, conformational study and preliminary work on their transition metal complexes

Thèse soutenue le 23 septembre 2016 à l'Université de Neuchâtel pour l'obtention du titre de Docteur ès Sciences par

William Maupillier

Ingénieur Chimiste diplômé de l'École Nationale Supérieur de Caen (ENSICAEN)

Membres du jury :

Prof. Reinhard Neier	(Directeur de thèse)
Prof. ass. Bruno Therrien	(Rapporteur interne)
Prof. Helen Stoeckli-Evans	(Rapporteur interne)
Prof. Christophe Thomas	(Rapporteur externe)

FNSNF
FONDS NATIONAL SUISSE
DE LA RECHERCHE SCIENTIFIQUE

unine
UNIVERSITÉ DE
NEUCHÂTEL

UNIVERSITÉ DE NEUCHÂTEL

Faculté des sciences
Secrétariat-décanat de Faculté
Rue Emile-Argand 11
2000 Neuchâtel - Suisse
Tél: + 41 (0)32 718 2100
E-mail: secretariat.sciences@unine.ch

IMPRIMATUR POUR THESE DE DOCTORAT

La Faculté des sciences de l'Université de Neuchâtel autorise l'impression de la présente thèse soutenue par

Monsieur William Maupillier

Titre:

"Calix[n]tetrahydrofuran[4-n]pyrrolidines: optimized synthesis *via* hydrogenation of calix[n]furane[4-n]pyrroles, conformational study and preliminary work on their transition metal complexes"

sur le rapport des membres du jury composé comme suit:

- Prof. hon. Reinhard Neier, directeur de thèse, Université de Neuchâtel, Suisse
- Prof. ass., Bruno Therrien, Université de Neuchâtel, Suisse
- Prof. Emerit Helen Stoeckli-Evans, Université de Neuchâtel, Suisse
- Prof. Christophe Thomas, Paris Tech, France

Neuchâtel, le 10 octobre 2016 Le Doyen, Prof. R. Bshary

Remerciements

Ce travail a été effectué d'octobre 2012 à septembre 2016 à l'institut de Chimie de l'université de Neuchâtel sous la direction du Prof. Reinhard Neier. Je tiens tout particulièrement à le remercier pour m'avoir donné l'opportunité de travailler au sein de son groupe de recherche et la confiance qu'il m'a apportée avec l'objectif de conclure un sujet qui lui tient à cœur : le sujet « calix ». Je voudrais le remercier pour la liberté de travail qu'il m'a offerte et son enthousiasme pour la recherche.

J'adresse mes sincères remerciements aux Prof. Helen Stoeckli-Evans, Prof. Bruno Therrien et Prof. Christophe Thomas qui ont pris part à mon jury de thèse, pris le temps de lire et corriger le manuscrit ainsi qu'apporter de précieux conseils concernant mon manuscrit lors de la présentation privée de thèse. Je remercie tout particulièrement le Prof. Helen Stoeckli-Evans pour l'élucidation de nouvelles structures rayon X, sa disponibilité, sa gentillesse ainsi que sa patience pour l'analyse répétitive d'une même structure lors de la recherche de polymorphe.

Je tiens à remercier chaleureusement le Dr. Aurora Cruz-Cabeza pour avoir réalisé les calculs d'énergies de mes composés ce qui a donné une nouvelle dimension au projet grâce à cette étude conformationelle.

Je tiens à remercier tous les apprentis que j'ai encadrés lors de ces quatre années pour leur implication et leur sérieux dans leur travail ainsi que leur bonne humeur : Csilla Horvath (nos incompréhensions linguistiques ont provoqué de nombreux fous rires entre nous), Line Wehren, Loic Da Costa, ~~Sébastien~~ Capelli, Tracy Rosselet et Edy Flückiger.

J'adresse mes remerciements aux membres du service analytique de Neuchâtel (NPAC) : Dr. Armelle Vallat, Dr. Gaétan Glauser et Laurence Lachat (spectrométrie de masse) ainsi que Dr. Claudio Dalvit et Dr. Diego Carnevale (spectroscopie RMN). Merci pour leur travail de caractérisation analytique indispensable à la synthèse organique.

Je tiens à adresser un énorme merci à tous les membres de notre groupe pour les moments passés ensembles à l'institut ou en dehors autour d'une bonne bière : Dr. Damien Thevenet, Dr. Christian Invernizzi, Dr. Sara Santi, Ewa Banach, Dr. Christelle Schenk ainsi que les anciens que j'ai pu croiser lors de plusieurs événements comme Dr. Guillaume Journot, Dr. Christophe Letondor, Dr. Inga Zaitseva et Dr. Anca Pordea.

Je remercie tout particulièrement toutes les personnes que j'ai rencontrées à Neuchâtel et qui ont égayés ma vie ici: mes colocataires Thomas et Mendes pour toutes les soirées passées dans le salon, sur la console ou les sorties en ville, Damien avec qui j'ai partagé mon labo et de nombreuses fondues chinoises, mes italiens préférés Christian, Sara et Matteo, Julien (a.k.a bûcheron) pour m'avoir motivé au fitness, Minghui et la nouvelle génération Marie, Fan, Cristina, Giau et Yassine.

Mes pensées vont également à tous les autres étudiants doctorants et post-doctorants de l'université de Neuchâtel.

Je voudrais aussi remercier tous mes amis de France. Les moments partagés ensembles ces dernières années ont été limités mais essentiels lors de mes retours. Un merci particulier pour Iano, Paulo, Ben & Jess, Flow, Stéphanie, Jérémy, Baptiste ainsi qu'à ma team de l'ENSICAEN avec Marine, Élodie, Christelle, Adèle, Sandra, Simon, Din, Tony et Ben.

Je tiens à remercier chaleureusement Zsofia Tatar qui partage ma vie pour m'avoir supporté et épaulé durant toutes ces années. De nouvelles perspectives s'offrent à nous maintenant et je sais que tu te réjouis de me retrouver les weekends.

Enfin, ces remerciements se concluent par un énorme merci à toute ma famille, particulièrement à mes parents Christine et Marc ainsi qu'à mon frère Thomas pour leur soutien tout au long de ces années et leur précieuses visites à Neuchâtel.

“Every chemical substance, whether natural or artificial, falls into one of two major categories, according to the spatial characteristic of its form. The distinction is between those substances that have a plane of symmetry and those that do not. The former belong to the mineral, the latter to the living world.”

(Louis Pasteur)

Kewords

Calix[n]furan[4-n]pyrrole, calix[n]tetrahydrofuran[4-n]pyrrolidine, macrocycle, optimized synthesis, hydrogenation, plate and bowl conformations, transition metal complexes, ligand

Abbreviations

AcOH: Acetic acid

$AcONH_4$: Ammonium acetate

$CHCl_3$: Chloroform

CH_2Cl_2: Dichloromethane

CH_3CN: acetonitrile

DFT: Density Functional theory

DNA: Deoxyribonucleic acid

Equiv.: Equivalent

EtOAc: Ethyl acetate

GC: Gas Chromatography

HCl: Hydrochloric acid

HIV: Human Immunodeficiency virus

UPLC: Ultra Performance Liquid Chromatography

IR: Infrared

IUPAC: International Union of Pure and Applied Chemistry

MS: Mass Spectroscopy

NMR: Nuclear Magnetic Resonance spectroscopy

r.t.: Room temperature

SCE: Saturated calomel electrode

TFA: Trifluoroacetic acid

THF: Tetrahydrofuran

TLC: Thin-layer chromatography

Summary

An hydrogenation method for the reduction of the easy accessible *meso*-octaalkylporphirinogen (calix[4]pyrrole) has previously been reported in our group. This "*standard method*" leads to an unsatisfactory conversion to the saturated analogue, calix[4]pyrrolidine (18% yield determined by GC). However using large excess of the catalyst leads to total conversion. In order to study the sequence of the reduction reaction, the replacement of one or several pyrrole ring(s) by furan ring(s) in the macrocycle was proposed and studied. For this study an access to the mixed calix[n]furan[4-n]pyrrole analogues had to be developed. Some of these macrocycles mixing furan and pyrrole rings have been reported in the literature by French almost 60 years ago: the yields reported were extremely low. No other method leading to the four isomers was described in the literature and only six studies were reported on these products. The previously developed procedure was fully optimized giving access to the four isomers by a selective ring-opening of calix[4]furan followed by a ring-closing reaction to form the pyrrole rings. This optimized procedure led to sufficient amounts of the four isomers to study their hydrogenation under our previously developed "*standard conditions*". Hydrogenation of these isomers gave good to excellent yields compared to the hydrogenation of calix[4]pyrrole with an impressively high diastereoselectivity. Computational and NMR in solution conformational studies were carried out to characterize the conformational equilibria of these fully saturated calix[n]tetrahydrofuran[4-n]pyrrolidines as observed in solution and in the solid state. In a preliminary study the synthesis of a series of transition metal complexes using these macrocycles was undertaken.

Table of Contents

Chapter 1. Introduction

1. Macrocycles present in Nature

Nature, during its evolution over billions of years, has created an incredible and seemingly unending variety of different molecular structures. Chemists have since the very beginning of their science been interested in understanding and explaining the biological phenomena that surrounds us based on a molecular description. In order to have a chance to understand what nature has to offer, organic chemists developed a variety of tools for the isolation, detection and structure characterization of important natural products involved in biological processes. As extraction of molecules directly from nature usually starts from complex mixtures, the development of chromatographic techniques such as HPLC and GC allowed more rapid isolation of pure compounds starting from natural sources. In parallel the development of efficient techniques such as NMR and mass spectroscopy allowed the identification and characterization of complex unknown molecules with a high degree of certainty.

Nature generates with ease both small active molecules, e.g. alkaloids, as large and much more complex structures, e.g. DNA or large proteins, thanks to programmed biological synthesis. One of the surprising features analyzing highly active natural compounds and pharmaceutical products is the presence of a macrocyclic unit in a large proportion of these functionally important structures. Molecules are usually classified as macrocycles when their central core contains a cyclic framework of twelve or more atoms. The classification is based on the ease or reversely the difficulty of access encountered by the synthetic chemist during the first part of the 20th century. Chemists classified cyclic structures as small rings, three and four membered rings, normal rings, five and six membered rings, medium sized rings, ring sizes between seven and eleven and macrocycles equal or bigger then twelve membered rings. For a long time, macrocycles were extremely challenging to synthetize in laboratory. An additional obstacle to the synthesis of the natural macrocycles was the number of stereocenters contained in this class of compounds. Chemists had to develop powerful methods to make these macrocyclic molecules synthetically accessible. To our knowledge the first examples of natural products with macrocyclic structures are muscone with one stereocenter and civetone with a (*Z*)-double bond (Figure 1). Both compounds revealed to be difficult to synthesize. Muscone and civetone are two compounds with strong odor used in perfumery coming from glandular secretion of animals, the musk deer and the civet respectively. Until the late 19th century, natural musk was extensively used until economic and ethical motives led to the adoption of synthetic musk. Although muscone was known for a long time, only its first synthesis described by Leopold Ruzicka in 1926[1-2] elucidated and secured the constitution. Nowadays, synthetic racemic mixture is on the market and chemists work on efficient and scalable synthesis of the enantiopure form.[3]

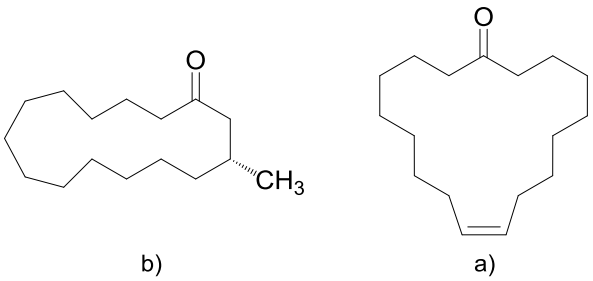

Figure 1. Structure of two macrocyclic musks. a) Muscone; b) Civetone

Macrocycles have been intensively explored by many synthetic groups as challenging goals for total synthesis[4-12] and in medicine in modern drug discovery.[13-16] One of the largest classes of macrocycles found in Nature are the macrolides. These molecules are used in medicine as natural products or chemically modified derivatives of the natural products are sold as drugs. They typically contain a large macrocyclic lactone ring to which one or more deoxy sugars may be attached. Usually, the lactone ring is composed of a 14-, 15-, or 16-membered ring. One of the high points for the use of this type of molecules came with the discovery of erythromycin (Figure 2) in the early 1950s, isolated from the bacteria *Saccharopolyspora erythraea*. This macrocycle became the first macrolide antibiotic applied for the treatment of a number of bacterial infections, including upper and lower respiratory tract infections, soft tissue infections and syphilis (especially for penicillin-allergic individuals). Due to frequent side effects such as abdominal cramps and gastrointestinal intolerance, chemists developed advanced macrolide antimicrobials by altering the basic structure of erythromycin resulting in compounds with extended spectrum of activity and tolerability. For example, beginning of the 1990s, the US Food and Drug Administration (FDA) approved the use of clarithromycin (the 6-O-methylerythromycin analogue) and azithromycin, for clinical use as second generation of macrolides.[17] The increased acid stability of clarithromycin reduced gastrointestinal intolerance.[18]

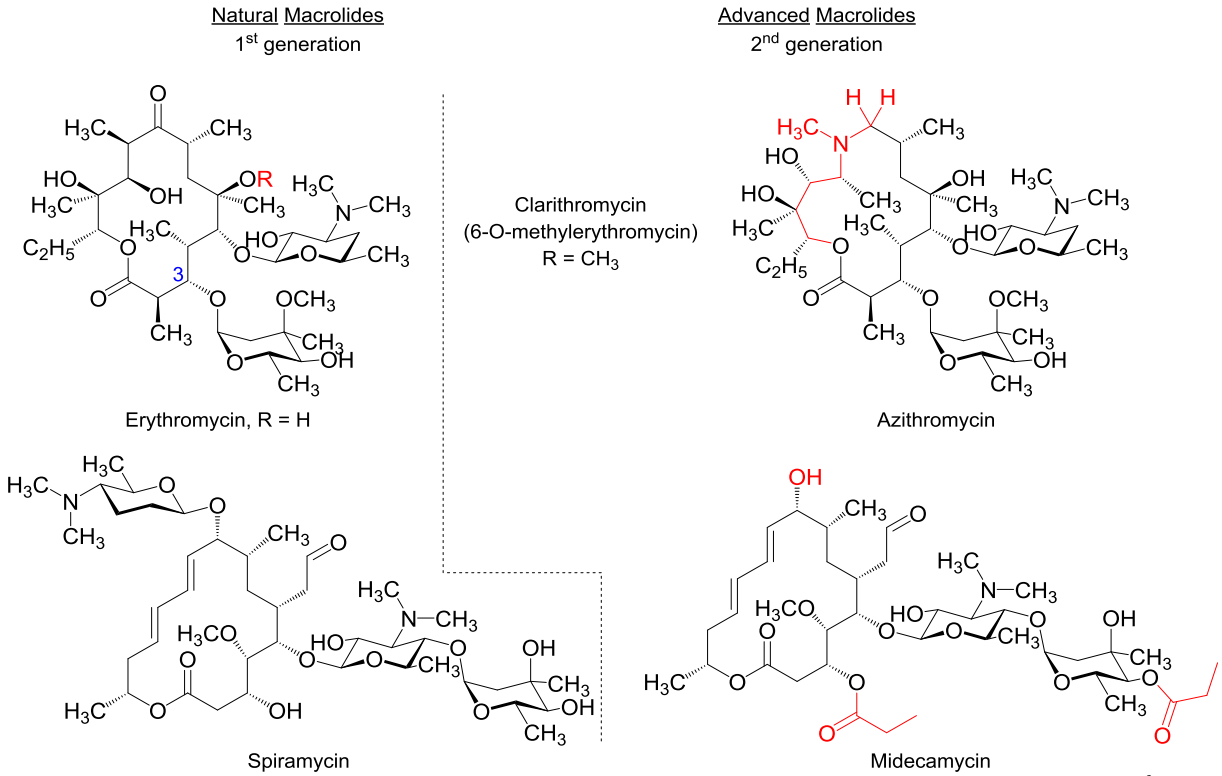

Figure 2. Natural and advanced macrolides used as antibiotic. Modified section in the 2nd generation compared to their predecessors are shown in red

Ketolides, structurally related to the 14-membered macrolides, characterized by a keto group at the C-3 position (position shown in blue on erythromycin, Figure 2), were developed to include good antibacterial activity against Gram-positive organisms which are resistant to classical macrolides.

Several other macrocycles isolated from natural sources such as plants, fungi, and mainly from bacterial sources present drug-like physicochemical and pharmacokinetic properties and offer popular targets for developing novel therapeutic derivatives, most notably as anti-tumor and antibiotics derivatives (Figure 3).[15, 19]

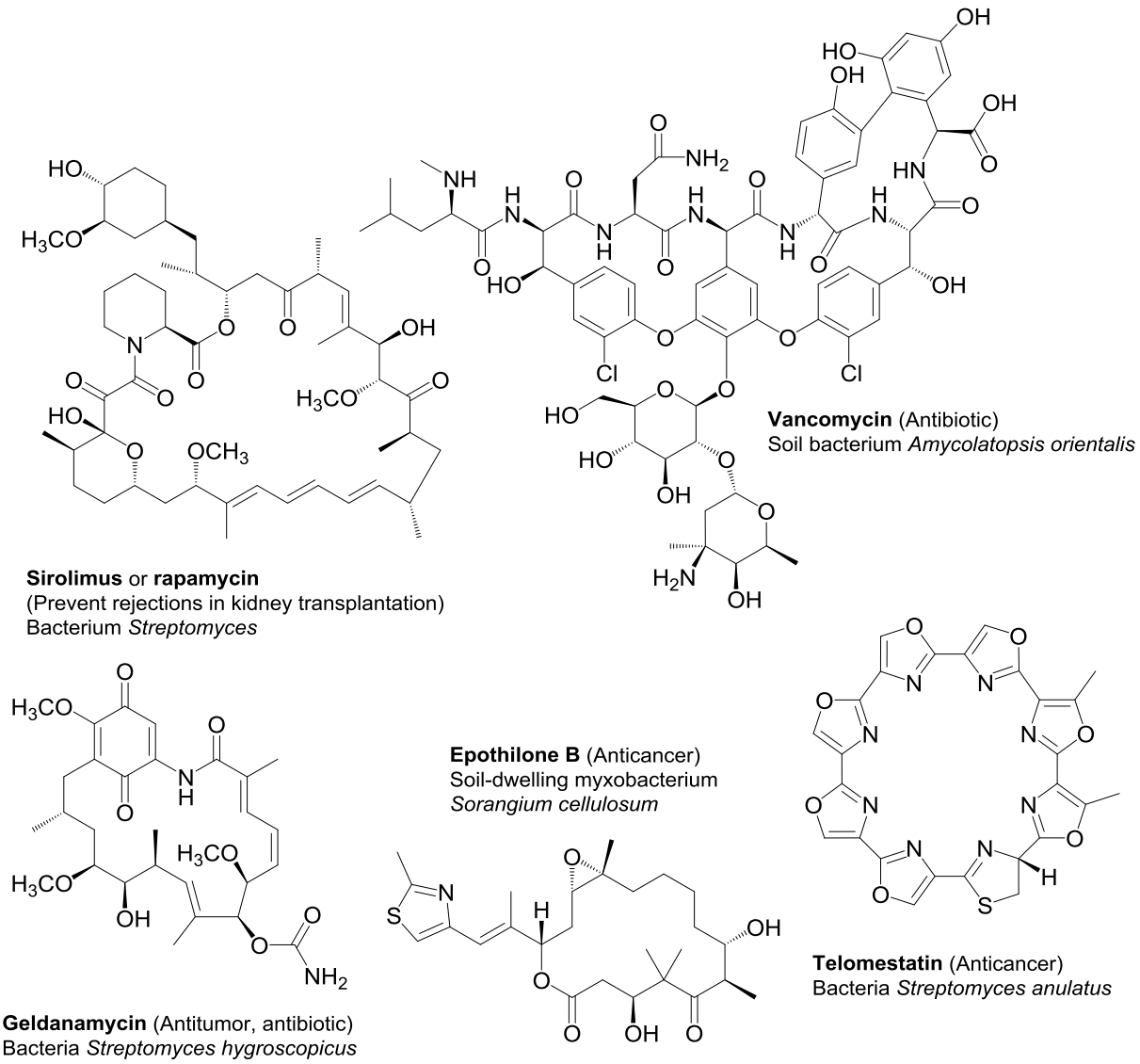

Figure 3. Selected natural macrocycles employed as therapeutic agents (Vancomycin is the antibiotic of last resort in the case of resistant strains)

Macrocycles are not limited in their use as drugs. Indeed, some macrocyclic structures show notable abilities to ion-binding. These macrocycles play the role of ionophores by reversibly binding cations, thereby facilitating the transport of these cations through membranes. Two well-known macrocyclic ionophores found in nature are nonactin[20], a representative of the macrotetrolide family, and valinomycin[21], a dodecadepsipeptide (Figure 4).

While both of them exhibit high cation selectivity for potassium ion over sodium or rubidium ions, nonactin also possesses the highest selectivity for ammonium ions, which gave it the nickname of "ammonium ionophore". Taking nonactin as example, the eight oxygen atoms coming from the tetrahydrofuran rings and the four carbonyl groups bind the potassium ion in the center of a structure which resembles a "tennis ball". All the non-polar methyl groups and the methylene groups from the tetrahydrofuran rings point outside, building a hydrophobic surface making the complex soluble in lipidic membranes.[20]

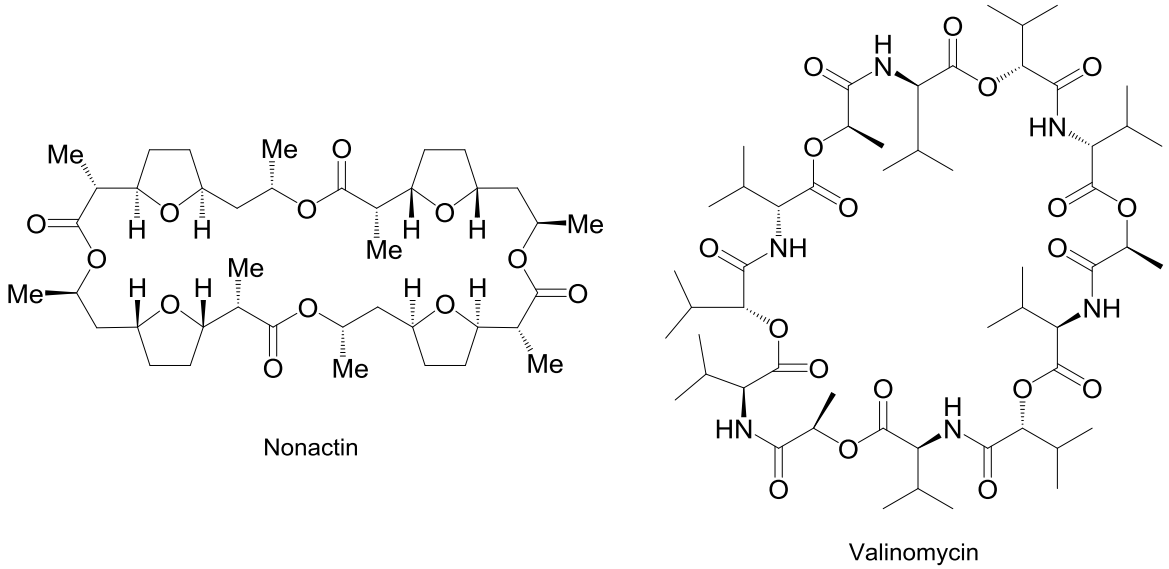

Figure 4. Natural potassium selective ionophoric macrocycles, technically used in ion selective electrodes

2. "Pigments of life"

Nature has achieved the stable binding of cations, mainly transition metals using another family of macrocyclic ligand. Many important processes of life like the transport of electrons, oxygen and photosynthesis depend on the presence of these metal complexes with tetrapyrrolic macrocycles.[22-26] These metal complexes have been called "pigments of life" thereby indicating the fundamental roles played by these metal complexes (Figure 5).[27-29] The structural parent of the tetrapyrrolic natural product family is the porphin. Porphin is not present in nature but several substituted porphins, called porphyrins, are natural products. Porphyrins are fully conjugated 16-membered macrocycles containing four modified pyrrole subunits connected to each other at the α–positions by four methine bridges (one-carbon bridges formed by a C-H unit). Several related heterocycles are well-known members of this family: the reduction of one double bond leads to chlorins (represented by chlorophyll), of two double bonds leads to bacteriochlorophylls while if one of the bridging carbons is missing, creating a direct link between rings A and D to the skeleton, the corrin system is obtained. The corrin chromophore, a highly reduced version of this basic structure, is present in vitamin B_{12}. Another highly reduced tetrapyrrolic product sharing the core of porphyrins with a 16-membered structure is Factor F430, a co-enzyme which catalyzes one step in the conversion of carbon dioxide to methane in methanogenic Archaea.

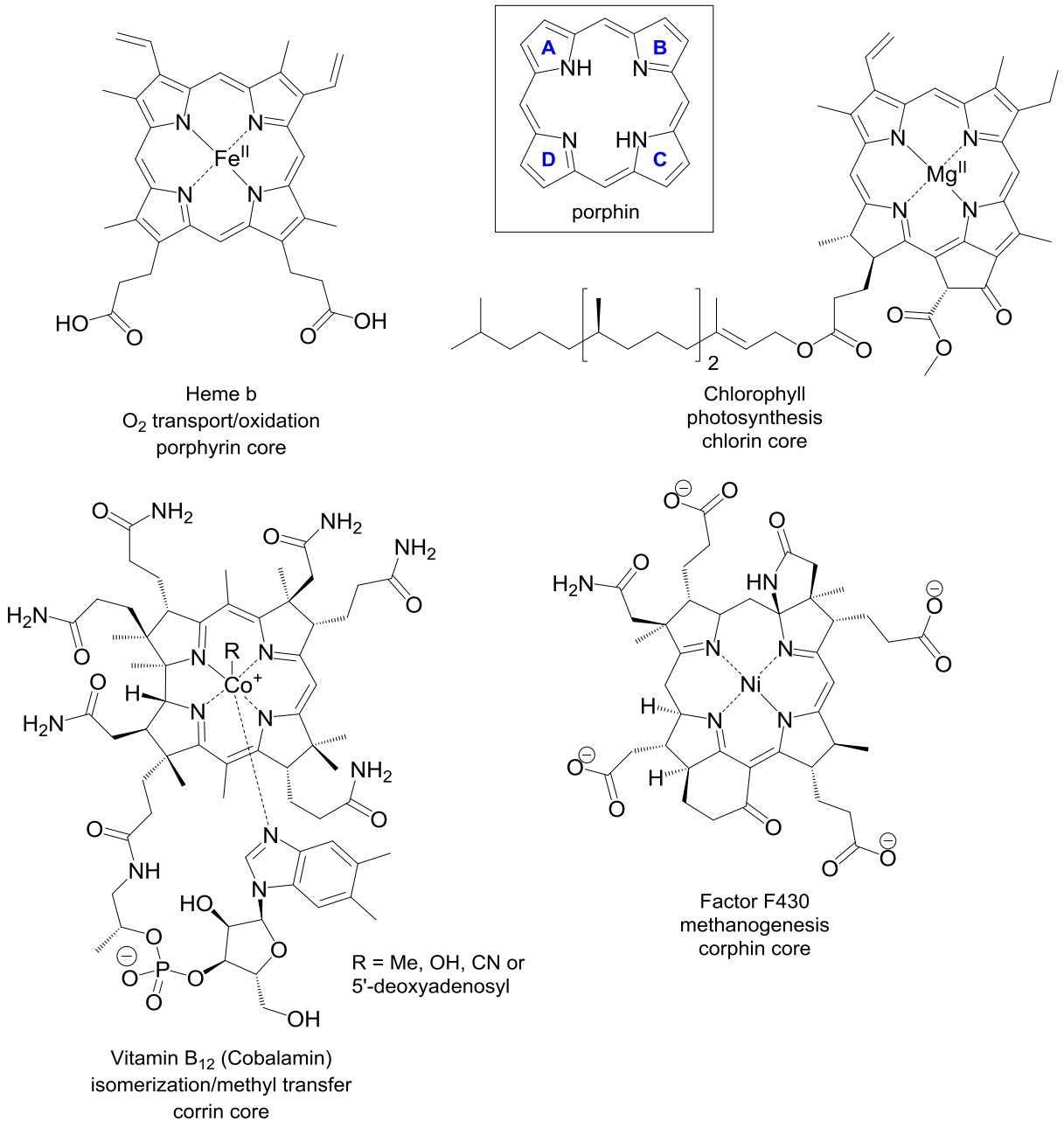

Figure 5. The structures of four "pigments of life", the processes they perform and the trivial name given to their heterocyclic basic system

Due to their particular electronic structure (relatively long extended or even cyclic π-systems) all of these compounds strongly absorb visual light. For the natural products derived from chlorins and bacteriochlorophylls the capacity to absorb visual light is a compulsory precondition to function as chromophores in photosynthesis. The scientific community broadly explored the utility of these structures as photosensitizers in photodynamic detection (PDD) and photodynamic therapy (PDT). In photodynamic therapy a photosensitizer is used to elicit cancer cell death, when excited by light energy in presence of oxygen. The first photosensitizer to gain regulatory approval for clinical PDT was Photofrin, a porphyrin macrocycle (Figure 6). A second and a third generation of photosensitizers has been

developed to overcome the disadvantages of skin sensitivity and weak absorption of light of the first generation.

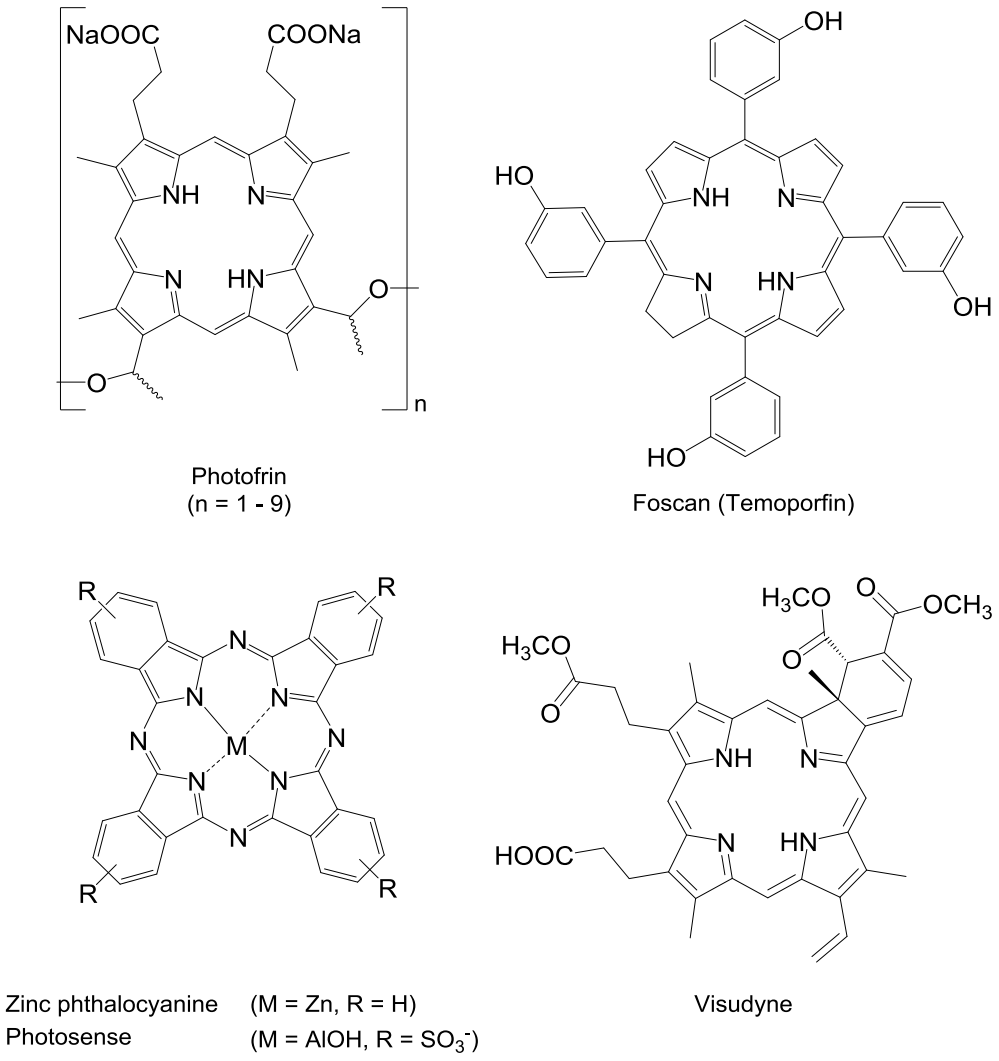

Figure 6. Selection of well-studied photosensitizers

To quote just a few, Foscan, based on chlorin core (Figure 6), is approximately 100 times more photoactive than photofrin but it is not selective enough against cancer cells. Zinc phthalocyanine CGP55847 and photosense, phthalocyanines derivatives, also entered clinical trials against squamous cell carcinomas of the upper aerodigestive tract and malignancies, respectively. With the ageing of populations, some diseases are becoming more prevalent such as age-related macular degeneration (ARMD), a disease of the retina causing significant weakening of the visual capacities. Visudyne is a treatment in PDT to treat blood vessels disorders in the eyes and other ocular diseases. Several porphyrins, chlorins and phthalocyanines derivatives are nowadays in different phases of clinical trials.[30-33]

3. Calix[4]arenes and heterocyclic calix[4]arenes macrocycles

In order to mimic the active site of enzymes, chemists intensively studied synthetic macrocycles, capable to form Werner complexes and later host-guest complexes using artificially created cavities. The discovery and the studies of the calixarenes and then heterocalixarenes represent pioneering work in the area of creating artificial biomimetic enzymes.

Calix[4]arenes

In 1872, Adolf von Baeyer mixed phenols with formaldehyde in strong acidic solution resulting in the formation of a resinous product, suggesting a polymerization process.[34-35] Beginning of the 1900s, Baekeland exploited this process and manufactured a hard moldable early plastic under the name of Bakelite.[36-37] In the 1940s, Zinke and Ziegler first described the formation of a cyclic tetramer using *p-tert*-butylphenol and formaldehyde (Figure 7).[38-40] Gutsche developed a procedure allowing large scale synthesis of these types of molecules.[41] He recognized the calix shape of the cyclic tetramer and introduced the name of calix[n]arene: "calix" from the Greek name of a chalice, "arene" for the presence of aromatic rings and [n] inserted between the two components to specify the number of aromatic rings incorporated into the macrocycle.[41] The presence of a bulky alkyl group in the *para*-position of the phenol in conjunction with the presence of the phenolic H-bonding groups on the opposite site blocked the conformation of the macrocycles into a cone-like arrangement (see Chapter 4 for the different conformations of calix[4]arenes and heterocyclic calix[4]arenes).

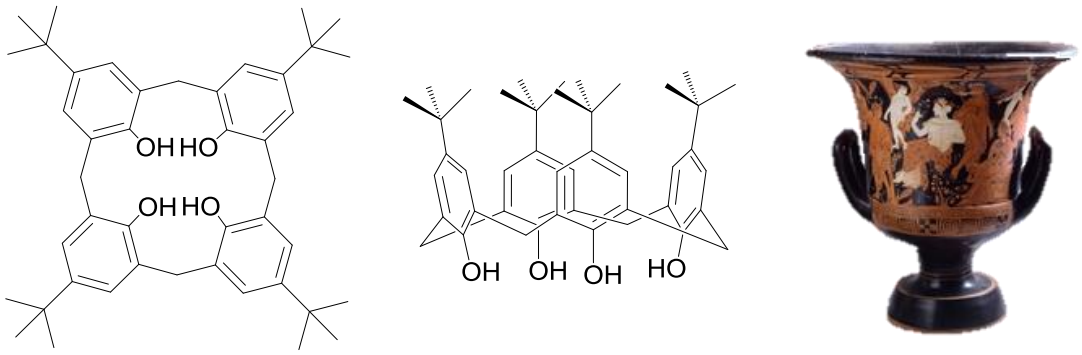

Figure 7. Structure of *p-tert*-butylcalix[4]arene and a Greek chalice

Certain derivatives were synthetized from differently *p*-substituted phenolic precursors or by stepwise syntheses allowing forming non symmetrical calixarenes. However, *p*-tert-butylphenol remains the best reactant. Larger calix[n]arenes were reported in the literature (n = 5 – 20). These compounds could be classified depending on the ease of closing the macrocycle. Calix[n]arenes (n = 4, 6 and 8) are called "major calixarenes" and are the most represented in literature. The cyclic pentamer and heptamer are obtained with lower yields and are named "minor calixarenes" and finally the others (n > 9) are called "large calixarenes".[42] The capacities of calixarenes to form non covalent, apolar host guest

interactions has been used applying adequate derivatives as ionophores, sensors, ion selective electrodes, enzyme mimetics and in catalysis.

Calix[4]pyrroles

In 1886, von Baeyer and his group extended their systematic studies on condensation reactions by mixing pyrrole and acetone in the presence of HCl. Von Baeyer called this product "acetonepyrrole". The product precipitates out of the solution in pure, crystalline form. The ease of the reaction and of the isolation are remarkable but the structure characterization proofed to be tedious. Indeed, it took more than 40 years until Chelintlev *et al*. first proposed the correct structure in 1916 (Figure 8a).[43] Hans Fischer had given the name α, β, γ, δ-octamethylporphyrinogen suggesting the close structural similarity of compound **1** to the porphyrins, more especially to the uroporphyrinogen III (Figure 8b), the first macrocyclic intermediate in the biosynthetic pathway to heme and as known today to all other natural tetrapyrrolic macrocycles.

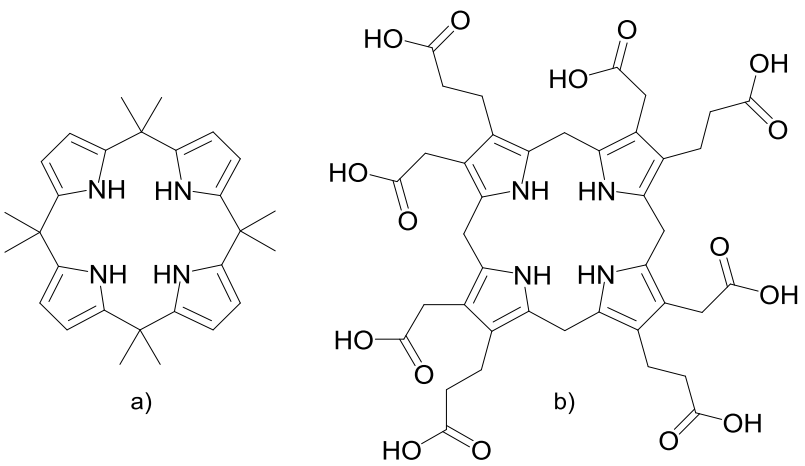

Figure 8. a) *meso*-octamethylporphyrinogen **1** (calix[4]pyrrole); b) uroporphyrinogen III

In 1955, Rothemund finally proved the α, α'-linkage between the pyrrole rings.[44] It was not until 1996 that the X-ray structure determination was presented by Sessler revealing the alternating conformation of adjacent pyrroles in the solid state.[45] In this 1,3-alternating conformation the pyrrole rings opposite to each other were nearly parallel forming a cavity (Figure 9). In the same paper, the X-ray structures of these macrocycles binding anions like fluoride and chloride disclosed a significant change of conformation. In the complexes, all the –NH were pointing towards the anion and the anion is taking up a position between the pyrrole rings. The conformation adopted by these complexes is the cone-like conformation previously observed for calixarenes (Figure 9 and see Chapter 4).

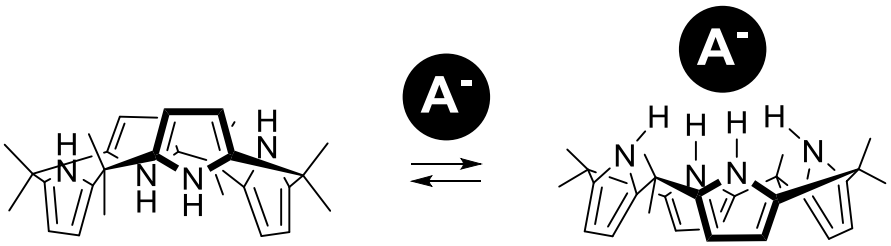

Figure 9. Calix[4]pyrrole **1**: Conformation of the free ligand and influence of an anion

Based on this observed conformation induced by anion binding and the fact that *meso*-octamethylporphyrinogen were not *bona fide* precursors of porphyrins, Sessler proposed to change the name of macrocycle **1** to calix[4]pyrrole or *meso*-octamethylcalix[4]pyrrole. Although the term *meso*-octaalkylporphyrinogen remains commonly used in the literature. "Calix[4]pyrroles" in the plural form includes all the macrocycles with four pyrrole rings independent of the type of the alkyl chains present in the *meso* position.

The pioneering work published by Sessler in 1996[45-47] on the anion binding properties of calix[4]pyrroles stimulated an intense activity on the use of this macrocycle as anion transporters. In the same period, the use of calix[4]pyrroles as macrocyclic ligands was also explored by Floriani but the synthesis of metal complexes appeared to be difficult.[48-51] While porphyrins and porphyrins derivatives form Werner complexes (transition metal complexes) with great ease, the lone pairs of the four pyrrole rings of calix[4]pyrroles are not available for coordination as they are involved in the aromaticity of the heteroaromatic ring. The tetraanion intermediate needs to be prepared using four equivalents of *n*-butyllithium before adding the metal source in order to introduce the metal cation into the macrocycle. This was in line with observations made with uroporphyrinogen III which does not form metal complexes at this stage in the biosynthesis of heme. In contrast to porphyrin and their derivatives who are widely used as catalysts for various reactions, calix[4]pyrroles have mainly (almost exclusively) found applications as anion receptors.

Calix[4]furans

The oxygen version calix[4]furan **2** also interested chemists. Its first synthesis was described by Ackman *et al* in 1955.[52] The reaction conditions are similar to the conditions used for the synthesis of calix[4]pyrrole **1**. However the yields are generally lower. This can be attributed to the increased solubility of the macrocycle, which leaves greater quantities of linear condensation products in the solution. The best conditions were reported by Chastrette using a large excess of $LiClO_4$ to enhance the reaction and reach a 25% yield *via* a template effect (Scheme 1).[53-54]

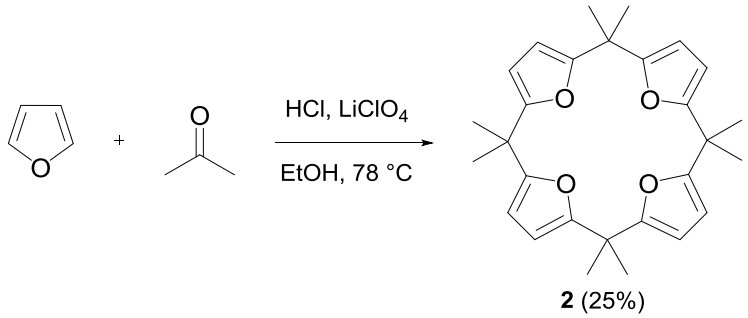

Scheme 1. Synthesis of calix[4]furan **2** by Chastrette

In 1985 de Sousa Healy and Rest reported a study of the role of metal salts in the synthesis of furan-ketone condensation claiming that the template effect is not the major effect influencing the formation of the tetramer.[55] They support their assumption of an acidity effect on the condensation as a direct consequence of the presence of the different metal salts. They performed the reaction in the absence of salts by varying the amount of hydrochloric acid added and managed to have 30% yield of product of condensation. In the presence of transition metal and alkaline-earth metal salts, good yields situated between 12 and 33% of the macrocycle **2** were obtained. In all cases, best yields were obtained using perchlorate as the anion. Condensation of furan with other ketones to vary the alkyl chain in the *meso*-position was also reported but leads to lower yields. Recently, new procedures were described for the synthesis of sterically demanding calix[4]furans. Lee *et al.*[56] reported the cyclization of arylalkenes to calix[4]furans with the aid of iodonium ion coming from *N*-iodosuccinimide (NIS) (Scheme 2a) and Banerji *et al*.[57] used stannic chloride as Lewis acid (Scheme 2b).

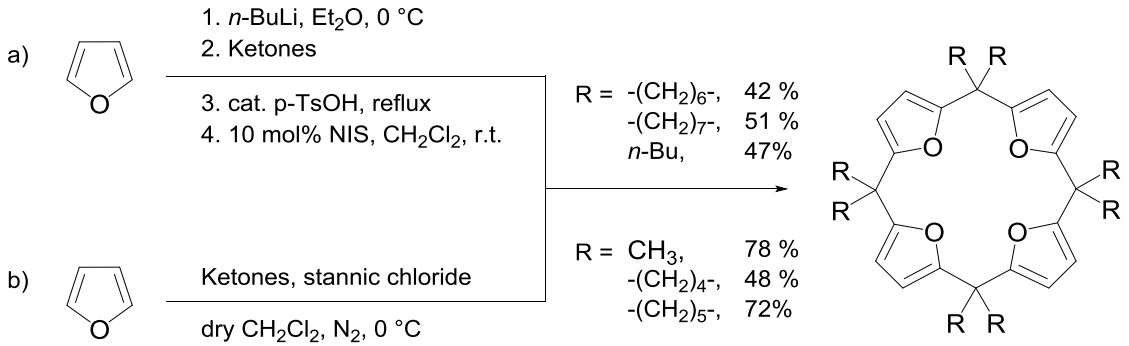

Scheme 2. Recent synthesis of calix[4]furans. a) Lee *et al*.; b) Banerji *et al*.

Calix[4]arenes and heterocyclic calix[4]arenes **1** and **2** are easy to make but the synthesis of larger macrocycles and the variability of the alkyl groups on the *meso*-position has stayed limited. Other synthetic macrocyclic structures emerged as "competitors" allowing to remove these limitations.

4. Simple synthetic nitrogen- and oxygen-containing macrocycles

Synthetic macrocyclic chemistry has expanded phenomenally since the 1960s making a broad catalogue of structures available. The goal of chemists in this field was to synthesize novel and much simpler purely synthetic macrocycles varying systematically the compounds and thereby adapting the structure to specific applications. The goal to develop these ligands was to find a cheap route to synthesize in a modular way macrocyclic ligands which allows to reach the following goals: 1) Vary the size of the central "hole" in order to optimally adapt the ligand to the metal which has to be incorporated. 2) Vary and mix the donor atoms in the macrocycle in order to extend the structural "alphabet" explored by Nature by introducing in the same macrocycle both nitrogen and oxygen atoms. The known natural products contain either only nitrogen or oxygen atoms but they are not mixing the donor atoms. 3) Vary systematically the flexibility of the structures exploring the influence of substituents or types of connectivity between the donor atoms on the stability and properties of the complexes.

In the synthesis of aza- and oxa-macrocycles metal ion template effects are often used to facilitate their synthesis. The number of studies of these macrocycles has grown constantly in literature, especially since the Nobel-prize winning discovery of crowns ethers (see page 16 Chapter 1). The thia- and phospha-macrocycles have been less studied in literature probably due to difficulties in the synthetic procedure.[58] With the presence of four (or more) donor sites located in a macrocyclic structure, these ligands present high affinity for many metal ions. Applications to such metal complexes range from catalysis to medicine.[58] The coordination chemistry of such macrocyclic ligands has been widely reported in literature. Several reviews described hundreds of different structures, ranging from the simplest, bare macrocycle to more elaborated compounds.[58-62] As it is impossible to summarize all the field the discussion here will exclusively focus on the literature of aza and oxa-macrocycles containing typically four heteroatoms. These structures are directly related to our project.

4.1. Synthetic polyazamacrocycles

In the 1930s, J. van Alphen worked on the synthesis of aliphatic polyamines and first described the synthesis of 1,4,8,11-tetraazacyclotetradecane (IUPAC name), known as cyclam (Figure 12a).[63-64] The appeal of these nitrogen-containing ligands will only be revealed in the 1960s with the introduction of the "Curtis macrocycles": nickel(II) Schiff bases efficiently synthesized by the mediated condensation of $[Ni(en)_3]^{2+}$ with acetone (Figure 10b). [65]

In 1960, Curtis knew that no primary amine remained in the compound. He isolated the metal complex and suggested the formation of four isopropyl imino functions (Figure 10c). The reaction was quickly extended to other amines, carbonyls, copper(II) and the correct structures where the acetone residues link the amine groups to form amine-imine chelate rings was elucidated.[66-70]

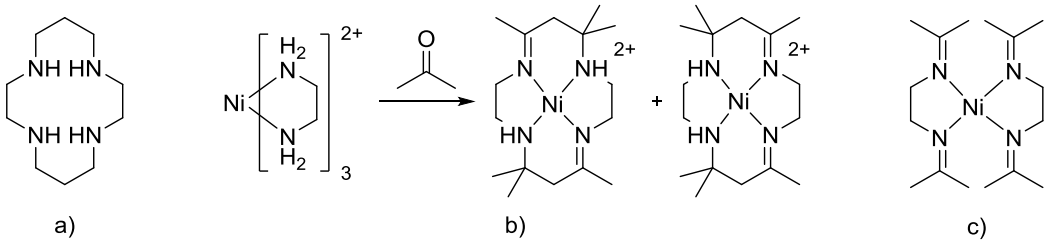

Figure 10. First synthetic azamacrocycle. a) Cyclam; b) Synthesis of the first Curtis ligand; c) initially proposed structure.

Since then, a large member of other synthetic polyazamacrocycles like cyclens[1], [16]aneN$_4$[2] and then bigger polyazamacrocycles have been reported (Figure 11).[61-62] These structures are the most studied and widely used. Their resemblance of the connectivity between the nitrogen donor atoms to the natural tetraazamacrocycles, the porphyrins and the corrins, was certainly critical for the increased interest in these classes of compounds. These nitrogen donor macrocycles appear to complex well with transition metals and form more stable complexes than the open-chain polyamines containing the same number of amino groups. The increase of the stability has been called macrocyclic effect.[71] The topological similarity of cyclam and [16]aneN$_4$ to the inner rim of the porphinoid ligand system inspired chemist to study metal complexes of these polyazamacrocycles and their small derivatives in various applications as example as contrast agents and as oxidation and bleaching catalysts, to cite just a few.[72-75]

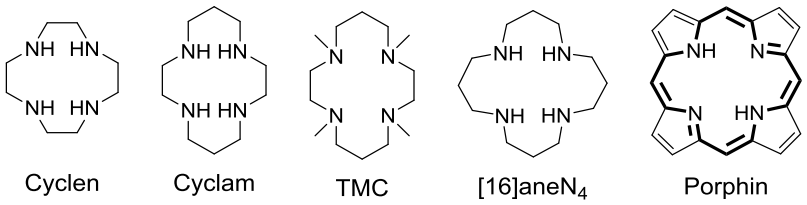

Figure 11. Classes of synthetically studied azamacrocycles close to porphin

To avoid the oxidative degradation of cyclam metal complexes by deprotonation of the amine, azamacrocycles often contain tertiary amines. The *N*-tetramethylcyclam (or TMC, Figure 11), readily synthesized by methylation of cyclam using formaldehyde and formic acid, has been widely studied.[76]

Further generations of synthetic macrocycles containing nitrogen or both nitrogen and oxygen atoms have typically used tertiary amines as donor ligand in order to avoid the stability problem mentioned above.

[1] IUPAC name: 1,4,7,10-tetraazacyclododecane
[2] IUPAC name: 1,5,9,13-Tetraazacyclohexadecane

4.2. Crown ethers and azacrown ethers

Crown ethers

In 1967, Pedersen published an investigation describing the synthesis of thirty three cyclic polyethers of varying sizes from nine to sixty atoms including three to twenty oxygen atoms in the ring (Figure 12).[77] The use of the IUPAC nomenclature revealed to be difficult for these cyclic structures. For convenience, Pedersen gave a name to this class of molecules, "crown" compounds, and established a systematic rule to name the different analogues.[3] The main types of crown ethers are represented in Figure 12. The most common crown ethers are cyclic oligomers of ethylene oxide with repeating $–CH_2CH_2O–$ units.

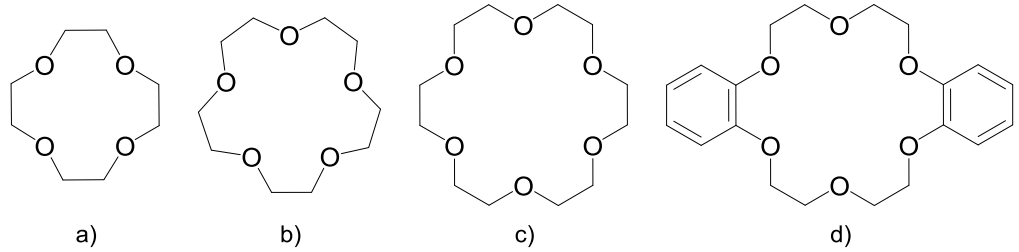

Figure 12. Common crown ethers and the cation for which they have affinity. a)12-crown-4; b) 15-crown-5; c) 18-crown-6; d) dibenzo-18-crown-6

The term "crown" was coined to express the resemblance of the macrocycle complexed to a cation with a crown sitting on a person's head. Pedersen not only reported the synthesis of these compounds he also described the capacity of most crown ethers to form stable complexes with different metal cations. It is for this property that this class of compounds was studied and used as ionophores and as phase-transfer agents.

A phase-transfer agent, or phase-transfer catalyst, is according to IUPAC an agent allowing the phenomenon of rate enhancement of a reaction between chemical species located in different phases (immiscible liquids or solid and liquid) by extraction of one of the reactants across the interface into the other phase so that reaction can proceed.[78] Cations are highly soluble in polar solvents like water and methanol. When the cation is forming a complex with the crown ether through the oxygen atoms, only the hydrophobic outside of the ring is exposed and thereby migration through organic phases becomes possible.

In term of metal coordination, oxygen donor containing macrocycles like crown ethers strongly bind alkali and alkaline earth metal ions whereas nitrogen containing macrocycles preferentially complex transition metals. A few metal ions such as Pb^{2+} and Hg^{2+} bind to both oxygen and nitrogen containing macrocycles. The investigation of macrocycles containing both oxygen and nitrogen atoms was the logical next step in coordination chemistry.[79]

[3] Nomenclature for crown ethers proposed by Pedersen: 1) the name of the external substituent (in case there is a substituent); 2) the total number of atoms in the polyether ring; 3) the term "crown" for this class of compound; 4) the number of oxygen atoms in the macrocycle.

Azacrown ethers

In the simplified nomenclature used by the community, azacrown ethers, or azacrown macrocycles, are macrocycles containing both oxygen and nitrogen donor atoms. Two nomenclatures can be used for these structures. The first is the crown ether nomenclature proposed by Pedersen in 1967,[77] where the position of the nitrogen atom replacing the oxygen atom is indicated. As an example of using this nomenclature, the 18-membered macrocycle (Figure 13a) is named 1,10-diaza-18-crown-6. The second nomenclature was proposed by Busch[4].[80] The position of the nitrogen atoms is not stated so three isomers could be drawn for this molecule, named [18]N_2O_4 with this method.

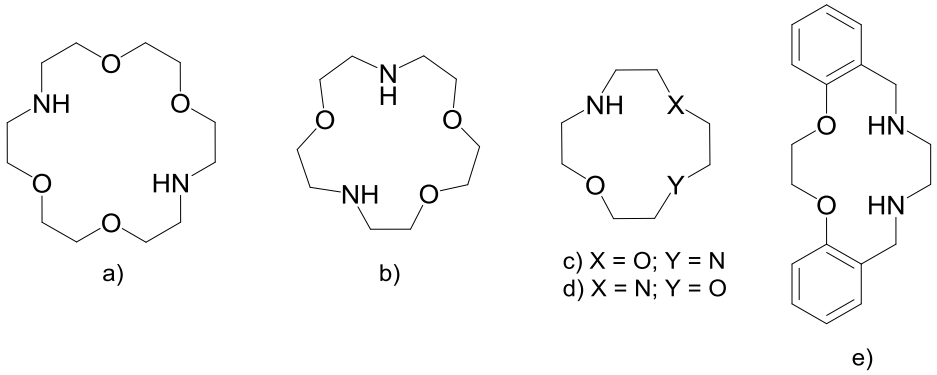

Figure 13. Selection of some small azacrown macrocycles. a) 1,10-diaza-18-crown-6; b) 1,7-diaza-15-crown-5; c) 1,7-diaza-12-crown-4; d) 1,4-diaza-12-crown-4; e) 3,4:9,10-Dibenzo-1,12-diaza-5,8-dioxacyclotetradecane

The azacrown ethers have also been studied extensively and several structures have been synthesized (Figure 13).[60] As for the synthesis of the crown ethers, the influence of the template effect was also studied for their synthesis. In the case of azacrown ethers the template effect revealed to be less pronounced because the nitrogen donor atoms formed weaker complexes with alkali metal cations. Azacrown macrocycles revealed to possess proprieties and thereby found applications related to their analogues containing either exclusively oxygen on nitrogen donor atoms.[81]

In order to increase the thermodynamic strength of the complexation constants of some crown ethers a subclass of these molecules was developed by Gokel: the lariat ethers (Figure 14a).[82-83] These molecules are crown ethers with flexible sidearms which could create an additional interaction with the metal cations. For synthetic reasons, the sidearm for lariat ethers coming from azacrown ethers is often connected to the nitrogen atoms (Figure 14b and 14c). Compound 1,10-diaza-18-crown-6 (Figure 13a) was an important starting material for the synthesis of these lariat ethers.

[4] Nomenclature for crown ethers proposed by Busch: the size of the macrocycle is given in a bracket followed by the number and types of heteroatoms.

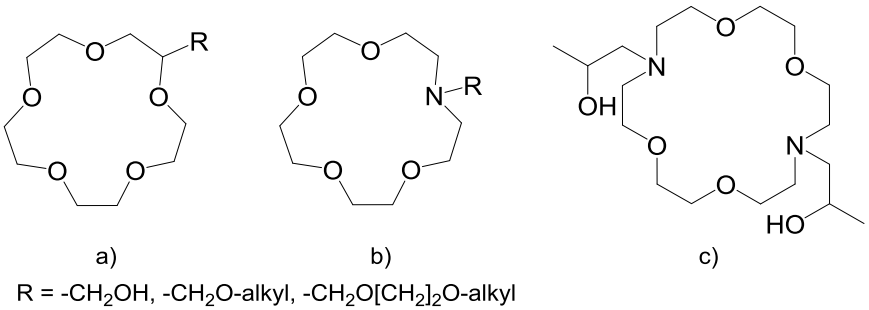

Figure 14. Examples of lariat ethers

4.3. Bridged azamacrocycles and cryptands

In order to induce topological constraints and enhance the complex stability, additional bridges were added to form polycyclic multidentate structures to encapsulate metal ions in a cage-like structure. This concept was designed by Jean-Marie Lehn in 1969 with the synthesis of cryptands (or cryptates), the three dimensional analogues of crown ethers.[84] The name came from the latin *crypta* meaning "cavity, cave". The main protagonist of this family is the 1,10-diaza-4,7,13,16,21,24-hexaoxabicyclo[8.8.8]hexacosane (also called [2.2.2]cryptand[5]) [85] presented below (Figure 15a). A huge effort has been dedicated to the synthesis of bridged or strapped tetraazamacrocycles and the study of their metal complexes (Figure 15c).[86-87]

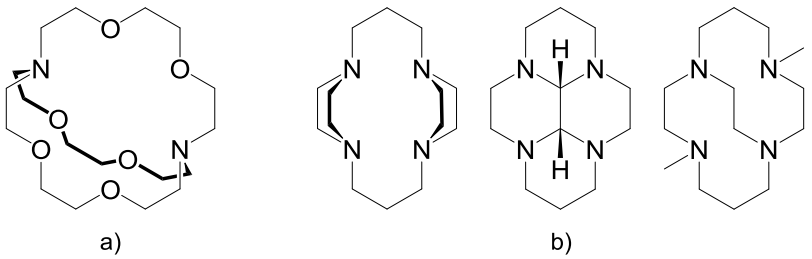

Figure 15. Bridged or strapped macrocycles reported and studied. a) Lehn's cryptand; b) Examples of strapped tetraazamacrocyles

The synthetic strategies limited and directed the design of the structures synthesized. Better complexations were observed using bridged macrocycles compared to their non-linked analogues but their synthesis was often difficult, thereby limiting the availability of these interesting structures. The most famous compound of this class of molecules remains the [2.2.2]cyptand.

The 1987 Nobel Prize in Chemistry awarded Pederson, Lehn and Cram "*for their development and the use of molecules with structure-specific interactions of high selectivity*".[88] Their work led to dramatic advancement in coordination chemistry followed by broader applications of the metal complexes formed from these macrocyclic structures.

[5] Nomenclature for cryptands: cryptands are assumed to be macro-bicyclic compounds and nitrogen is assumed to be the bridgehead. The number of heteroatoms in each ethylenoxy chain is assigned in bracket.

Nowadays several crown ethers, azacrown ethers and [2.2.2]cryptand are common reagents commercially available from various suppliers.

5. Known hydrogenations of heterocyclic calix[4]arenes

The two heterocyclic calix[4]arenes calix[4]pyrrole **1** and calix[4]furan **2** are easy to synthesize in one step *via* the procedure pioneered by von Baeyer. For this reason, the two macrocycles were well studied contrary to the analogue calix[4]tiophenes containing four sulfur atoms which is more difficult to obtain.[89]

Although tetrapyrrole macrocycle **1** is easy to synthesize its applications were limited. The synthetically easiest way to reduced macrocycles breaking the aromaticity is the exhaustive hydrogenation of the corresponding heterocyclic calix[4]arenes. Only the transformation of the calix[4]furan **2** to the calix[4]tetrahydrofuran **4** has been reported in the literature before our studies on the hydrogenation of calix[4]pyrrole to the calix[4]pyrrolidine **3** in 2009 (Figure 16).[90]

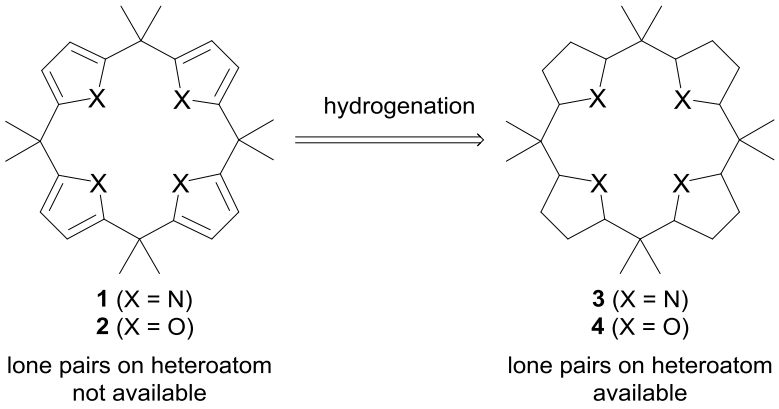

Figure 16. Synthesis of reduced heterocyclic calix[4]arenes by hydrogenation

5.1. Hydrogenation of calix[4]furan 2

The catalytic hydrogenation of the calix[4]furan **2** was mentioned by Chastrette in 1973 using Raney nickel but no experimental data were given.[53] The hydrogenation was first fully described by Kobuke *et al*. in 1976 using ruthenium on carbon as catalyst.[91] High H_2-pressure and temperature (respectively 120 atm of H_2 and 190 °C for 6 h) were needed to obtain the totally reduced macrocycle **4** in 73% yield. Other groups were interested in this transformation and procedures using Pd/C were reported by Chastrette[54] and by Wiegers and Smith.[92] The pressure reported for the reduction varied from 110 to 170 atm of hydrogen at 105 °C for yields of **4** between 57 and 72%. Using these conditions, de Sousa Healy and Rest[55] were not able to carry out the reduction in ethanol. They only recovered starting materials. Changing to THF as solvent and Raney Ni as catalyst while maintaining similar conditions of temperature and H_2-pressure they isolated and separated a mixture consisting of

38% of the fully reduced macrocycle **4** and 18% of the half reduced intermediate **5** by successive recrystallization (Scheme 3).

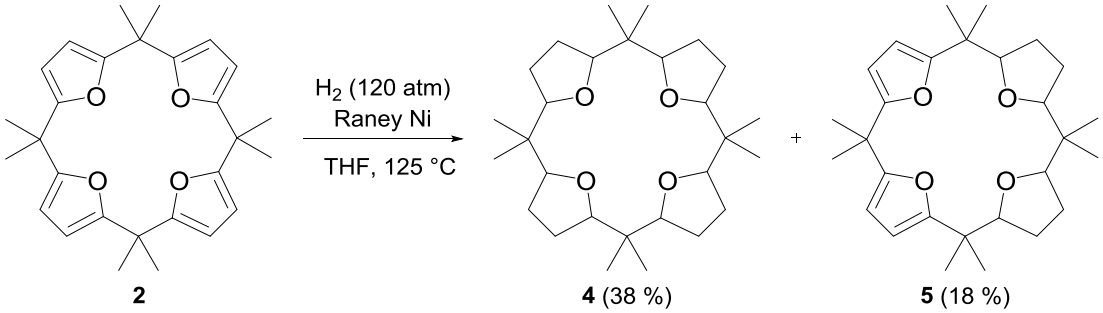

Scheme 3. Catalytic hydrogenation of calix[4]furan **2** according to Sousa Healy and Rest

These different conditions led to uncharacterized isomeric mixtures of calix[4]tetrahydrofuran **4** until van Beylen *et al*. reported the isolation and separation of two isomers **4a** and **4b** (Scheme 4).[93] The authors also reported the reaction under significantly milder conditions for the hydrogenation (Pd/C, 1 atm of H_2, r.t., 48 h) leading to the two isomers **4a** and **4b** in a 70/20 ratio. The remaining 10% corresponded to a mixture containing other isomers and partially reduced products. After the isolation of **4a** and **4b** in 49% and 14% respectively they secured the stereostructure of the two isomers by obtaining crystals suitable for an X-ray structure determination for both compounds. These two diastereoisomers are reminiscent of simplified version of the natural product nonactin presented in Figure 4 (with four tetrahydrofuran rings) and crown ethers.

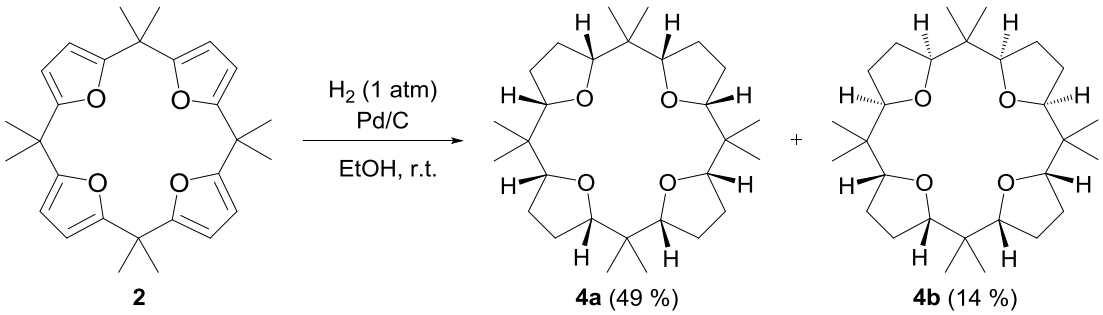

Scheme 4. Catalytic hydrogenation of calix[4]furan **2** and separation of the two diastereoisomers **4a** and **4b** according to van Beylen

5.2. Hydrogenation of calix[4]pyrrole 1

To the best our knowledge only one report on the hydrogenation of calix[4]pyrrole **1** has been published in 1955 by Rothemund and Gage[44] before our work on this transformation. At this time, the authors wanted to confirm the structure of calix[4]pyrrole **1** called "acetonepyrrole" by von Bayer. Using harsh conditions, the goal was to degrade the starting material and analyze the resulting fragments to justify the position of the linkage connecting the neighboring pyrrole rings in the macrocycle. They proofed the position of the links in the 2 and 5 positions of the pyrrole rings since the fragments were exclusively substituted in these

two positions (Scheme 5). In an investigation of heterocyclic calix[4]arenes as ligands, Corsini mentioned the hydrogenation test of calix[4]pyrrole **1** (177 atm of H_2, 160 °C, 12 h, Raney Ni). He only commented that the reaction had failed.[94]

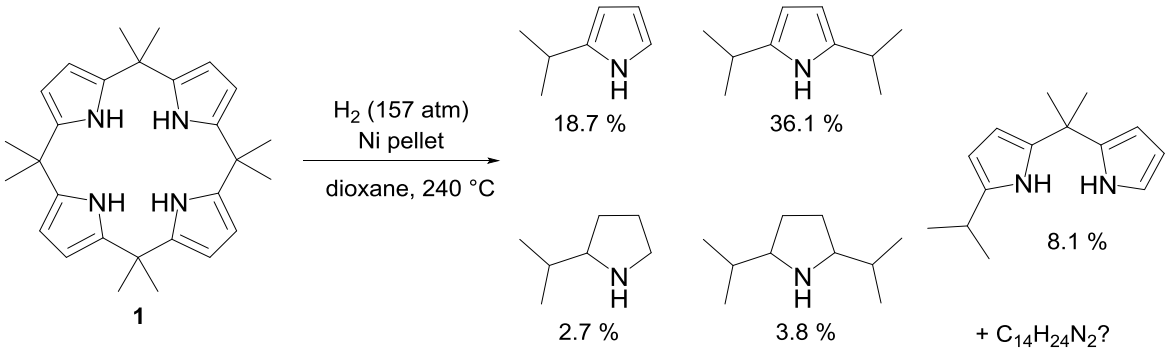

Scheme 5. Degradation of calix[4]pyrrole **1** under heterogeneous catalytic hydrogenation reported by Rothemund and Gage

Since we were interested in the synthesis of the fully saturated calix[4]pyrrolidine **3**, we started to screen reduction conditions with the hope of finding an experimental procedure which would allow the reduction of calix[4]pyrroles. After a considerable screening effort (catalysts, hydrogen pressure, temperature, solvent) we could report the first successful hydrogenation of calix[4]pyrrole **1** to a small but reproducible amount of the totally reduced macrocycle **3** (Scheme 6).[90, 95]

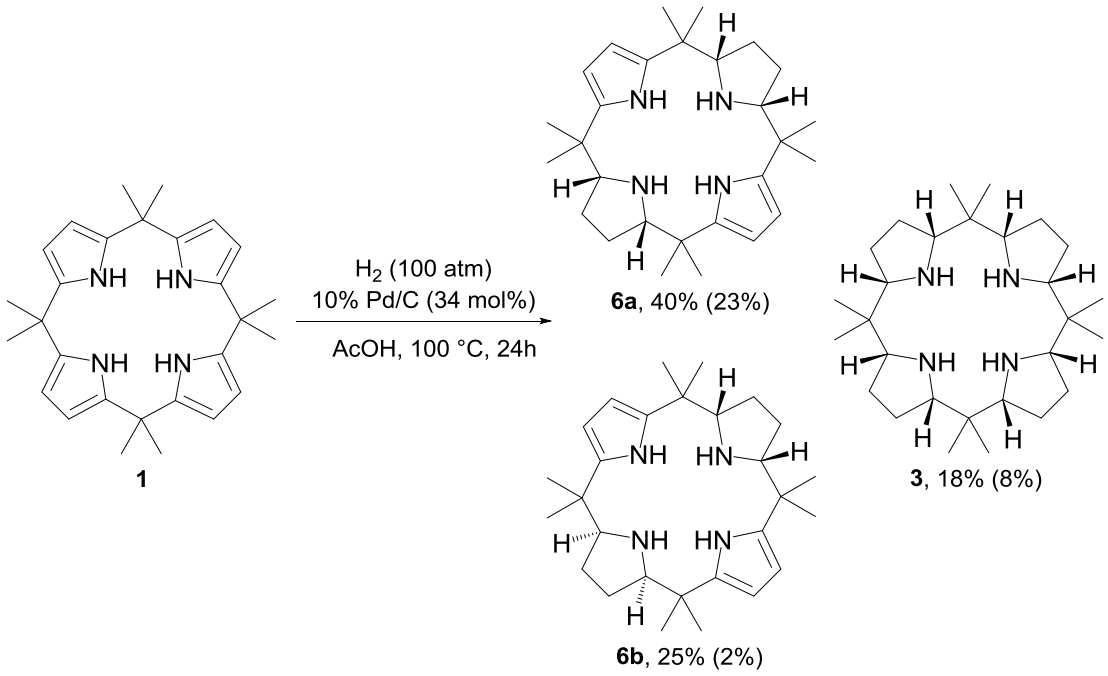

Scheme 6. Optimized catalytic hydrogenation of calix[4]pyrrole **1** giving the macrocycles **6a** – **6b** and **3**.[95] GC yields are given; yields of isolated products are shown in parentheses

To achieve the reduction of the four pyrrole rings of the calix[4]pyrrole **1**, harsh conditions were needed. Our optimized "best" conditions are the following: 10% Pd/C (34 mol% of Pd compared to the substrate) as catalyst, 100 atm of H_2, AcOH, 100 °C, 24 h. A GC method using *n*-eicosane as internal standard was developed to analyze the complex mixtures obtained and calculate the GC yields of the different products of the transformation. The totally reduced calix[4]pyrrolidine **3** was the minor product of the transformation (18% GC yield) accompanied with the two half-reduced isomers **6a** and **6b** as major compounds (40% and 25%, respectively) where the two pyrrole rings located opposite to each other were reduced while the two others did not react. Higher hydrogen pressure or longer reaction time did not lead to a better formation of macrocycle **3**.

As expected, our novel tetraazamacrocycle **3** proved to be a good ligand allowing the smooth, high-yielding synthesis of several transition metal complexes such as Cu^{II}, Ni^{II}, Pd^{II} and Mn^{II} (see Chapter 5).[90] In order to test potential applications of this type of complexes, the catalytic epoxidation of alkenes was studied using the Mn^{II} complex as catalyst with reasonable to good yields.[96]

6. Goals

The hydrogenation of calix[4]pyrrole **1** was only a half success considering the low yield of isolated totally reduced calix[4]pyrrolidine **3**. Hydrogenations of pyrroles into heterocyclic calix[4]arene structures seem to require more stringent conditions than the hydrogenations of corresponding furan derivatives.

We decided to study the hydrogenations of the series of mixed calix[n]furan[4-n]pyrrole **7** – **10** (Figure 17). The following two reasons motivated our studies: 1) Since furan rings revealed to be hydrogenated more easily than the pyrrole rings, the hydrogenation of the mixed macrocycles should allow a better conversion to the fully reduced analogues **11** – **14**. 2) The products of the hydrogenation **11** – **14** are in themselves attractive ligands for studying the capacities to complex metals and finally to study their potential catalytic activity. Keeping the connectivity and the constitution of the heterocyclic calix[4]arenes, but removing the π-system creates structural analogues, which will allow studying the interplay of the geometrical, stereoelectronic and electronic factors. The "exocyclic" addition of four five membered rings introduces conformational restrictions, keeping a degree of rotational freedom not available to the aromatic porphyrins. These target compounds will allow the experimentally based comparison between the influences exercised by the topology and by the π-system on the physical chemical properties of the compounds, on the complexation behavior and on the catalytic activity of the macrocyclic metal complexes.

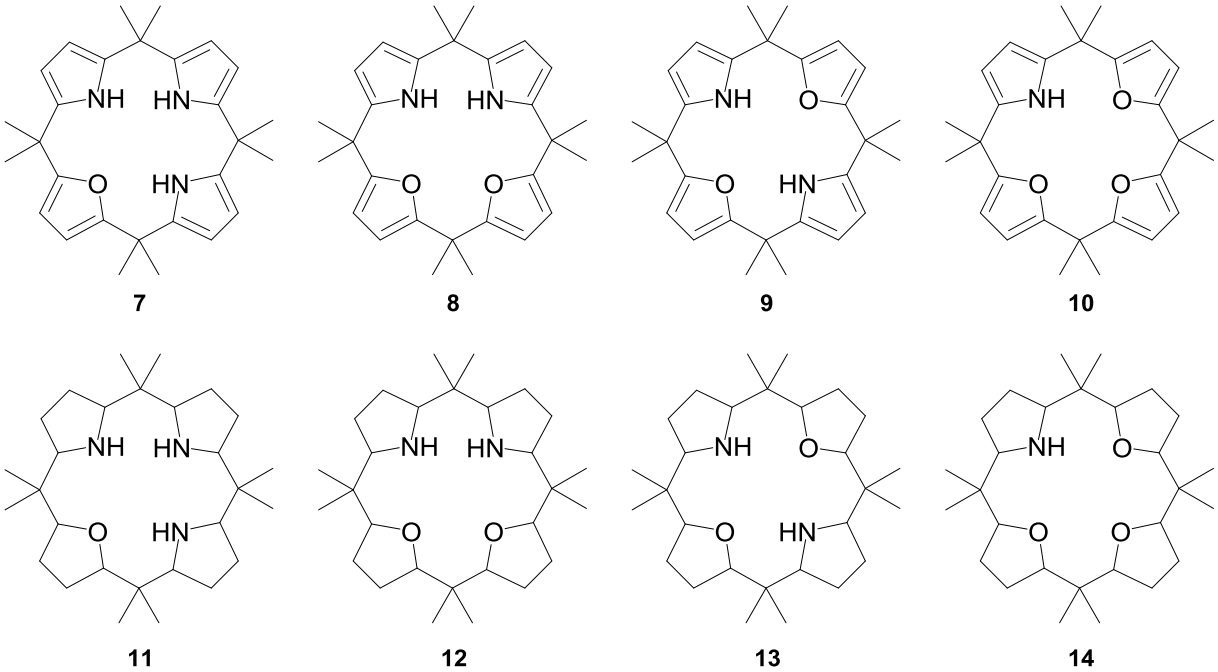

Figure 17. Targeted calix[n]tetrahydrofuran[4-n]pyrrolidines **11** – **14** by catalytic hydrogenation from their aromatic calix[4]furan[4-n]pyrrole analogues **7** – **10**

Chapter 2. Synthesis of calix[n]furan[4-n]pyrroles

1. Introduction

To be able to study the hydrogenation reaction leading to the calix[n]tetrahydrofuran[4-n]pyrrolidines **11** – **14** we had to have an efficient synthetic access to the calix[n]furan[4-n]pyrroles **7** – **10**. Only few publications were reported in the literature on the synthesis of one or several macrocycles of the type described by structures **7** – **10**. Three different approaches for the synthesis of calix[n]furan[4-n]pyrroles have been described in the literature.[97-100] Among these procedures, one provided macrocycles **8** – **10** while the two others afforded exclusively calix[2]furan[2]pyrrole **9**. To the best of our knowledge, calix[1]furan[3]pyrrole **7** was not reported in the literature so far. The difficulty of the access to the different macrocycles may explain the lack of studies on their anion and cation binding compared to the simple calix[4]pyrrole **1** and calix[4]furan **2**. Besides publications on the synthesis, only six studies have been reported so far including the anion-[101] and cation-[94] binding abilities, the synthesis of a cobalt-complex with molecule **9** as ligand,[98] the use of these macrocycles as ionophores in silver ion-selective electrodes[102-103] and recently a DFT study on macrocycle **9** to form host-guest type complexes with alkali and alkaline-earth metal ions.[104]

French *et al*. reported in 1958 the first syntheses of caliy[n]furan[4-n]pyrrole **8** – **10**.[97] They proceeded by stepwise condensation of a substituted furylcarbinol at the α–position of furan or pyrrole ring (Scheme 7a). The overall yields observed for these transformations are extremely low (1 – 4% for four steps depending on the final macrocycle). The authors specified that they did not succeed to obtain compound **7** with their method. More than forty years later Lee *et al*. described the synthesis of calix[n]furan[n]pyrroles and calix[n]thiophene[n]pyrroles (n = 2, 3, 4) using a similar synthetic strategy based on the "3 + 1" condensation between furyl- or thiophenylcarbinol and oxa- or thiatripyrromethane (Scheme 7b).[99-100] Compound **9** was reported in a considerably improved 30% overall yield. Their method required a cumbersome separation and purification procedure to isolate the desired macrocycle **9** from the other larger macrocycles. Moreover this method gave access to only one member of the calix[n]furan[4-n]pyrrole family. The third procedure was reported by Floriani *et al*. again with the synthesis of only macrocycle **9**.[98] It was based on the substitution of furan by pyrrole rings in the calix[4]furan **2**. The method consisted first in the selective ring-opening of calix[4]furan **2** to a tetraketone with the *trans*/*trans*-configuration of the two double bonds positioned one opposite to the other followed by the reduction of these unsaturations described by LeGoff *et al*. (Scheme 7c).[105] A Paal-Knorr ring closing reaction afforded the macrocycle **9** in around 60% overall yield.

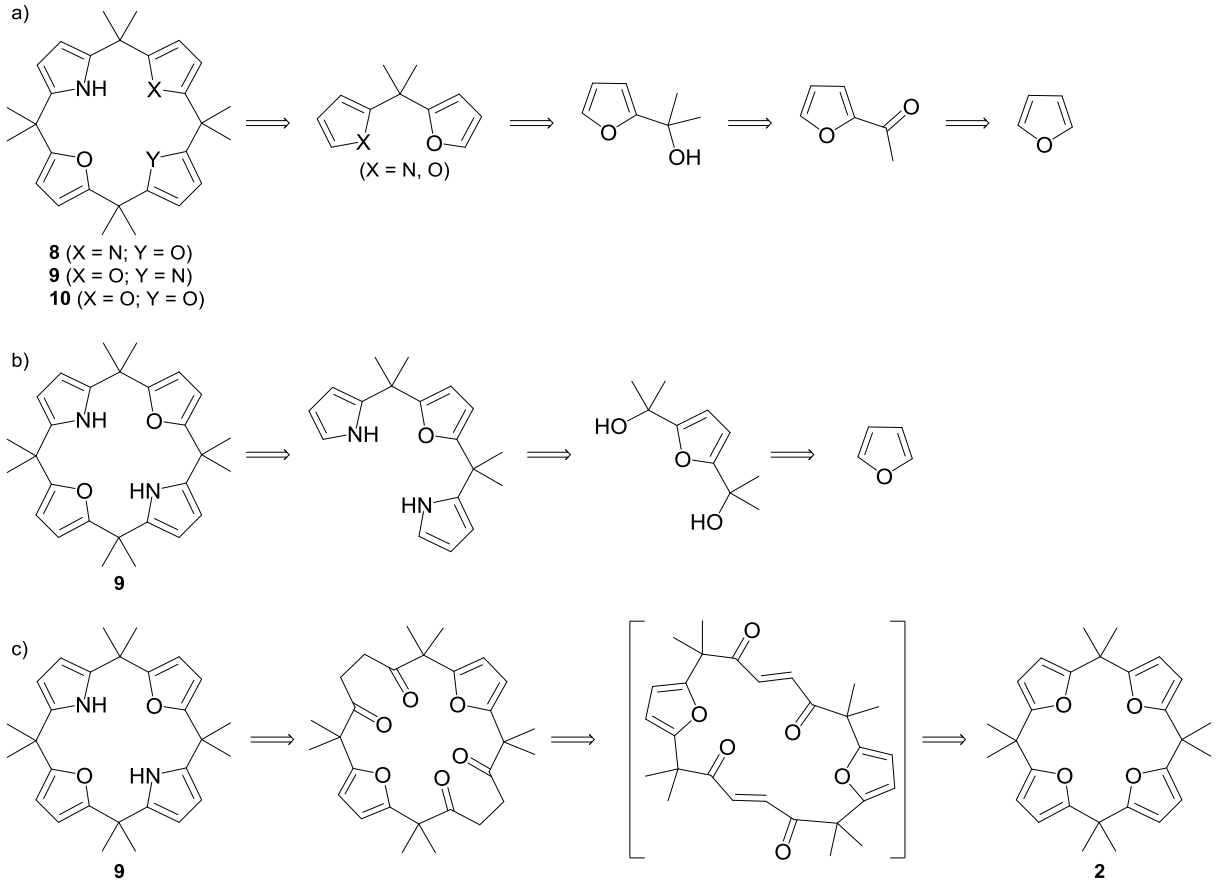

Scheme 7. Synthesis of calix[n]furan[4-n]pyrroles reported in the literature. a) First stepwise synthesis of **8** – **10** by French using a "2 + 2" macrocyclization; b) The synthesis of **9** using a "3 + 1" macrocyclization reported by Lee. c) The synthesis of **9** using the LeGoff's ring-opening procedure as applied by Floriani

The synthetic route described by French *et al*. is the only one affording the synthesis of three of the four possible calix[4]furan[4-n]pyrroles but the very poor yields observed in the condensation reactions could not provide appropriate quantities for our studies. Although macrocycle **9** aroused interest and could be selectively synthesized, no improved experimental procedures were reported in the literature for the synthesis of the other three calix[n]furan[4-n]pyrroles **7**, **8** and **10**.

2. Our synthetic approach

An approach allowing the preparation of all four possible calix[n]furan[4-n]pyrrole regioisomers **7** – **10** was developed inspired by the work of LeGoff *et al*.[105] and Kohnke *et al*.[106-107] using a sequence of transformations starting from the all-furan macrocyclic structure **2** (Scheme 8). Our approach is based on a mono, bis or tris oxidative furan ring-opening reaction of calix[4]furan **2** allowing to obtain sufficient quantities of the selectively opened macrocycles, followed by a reduction of the C–C double bond to form the

corresponding 1,4-dicarbonyl compounds reported by LeGoff in his work on the oxidative ring-opening of calix[4]furan and calix[6]furan.

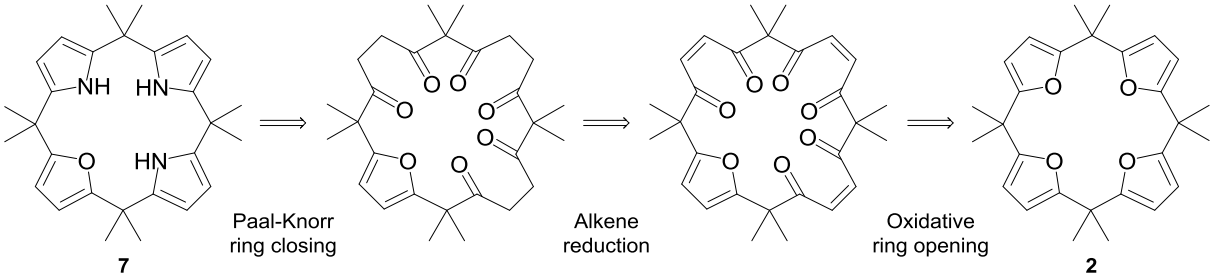

Scheme 8. The retrosynthetic sequences for the synthesis of calix[4]furan[4-n]pyrroles taking macrocycle **7** as example

The controlled oxidation of calix[4]furan **2** using adequately chosen amounts of *meta*-chloroperbenzoic acid (*m*-CPBA) has been reported to form di- and tri-ring-opened macrocycles with *cis*-configurated double bonds (Scheme 8). Alternatively, if bromine was used as oxidative agent, the selective ring-opening of two opposite furan rings of calix[4]furan **2** leading to a compound with the *trans*/*trans*-configuration of the two double bonds has also been reported by LeGoff and applied in the synthesis of macrocycle **9** by Floriani (Scheme 7c). The pyrrole ring(s) was (were) then formed using the Paal–Knorr condensation reaction after the reduction of the double bonds. This sequence has been successfully applied for the synthesis of calix[n]furan[6-n]pyrroles (17 – 41% yield)[106] and calix[5]pyrrole (1% yield).[107]

Using this strategy, the starting material for all the mixed calix[n]furan[4-n]pyrroles **7** – **10** was the calix[4]furan **2**. This approach should for the first time allow the synthesis of calix[1]furan[3]pyrrole **7** (Scheme 9). The efficient alternative oxidation method using bromine as oxidative agent was chosen for an easy and selective access to calix[2]furan[2]pyrrole **9** once the reaction conditions had been optimized. The *m*-CPBA based oxidative ring-opening was chosen for the synthesis of the three other macrocycles **7**, **8** and **10**. In contrast to the reaction with bromine, which yielded exclusively the bis-ring opened product, the oxidation with *m*-CPBA did not show any appreciable selectivity. The oxidation of the furan rings was "quasi" independent of the number of furan rings, which had already been ring opened. Using *m*-CPBA, we could therefore not avoid the formation of side products due to over-oxidation or to incomplete oxidation. As we were forced to separate these side products by chromatography we recovered them and they could be used in parallel syntheses of the corresponding alternative calix[n]furan[4-n]pyrrole analogues.

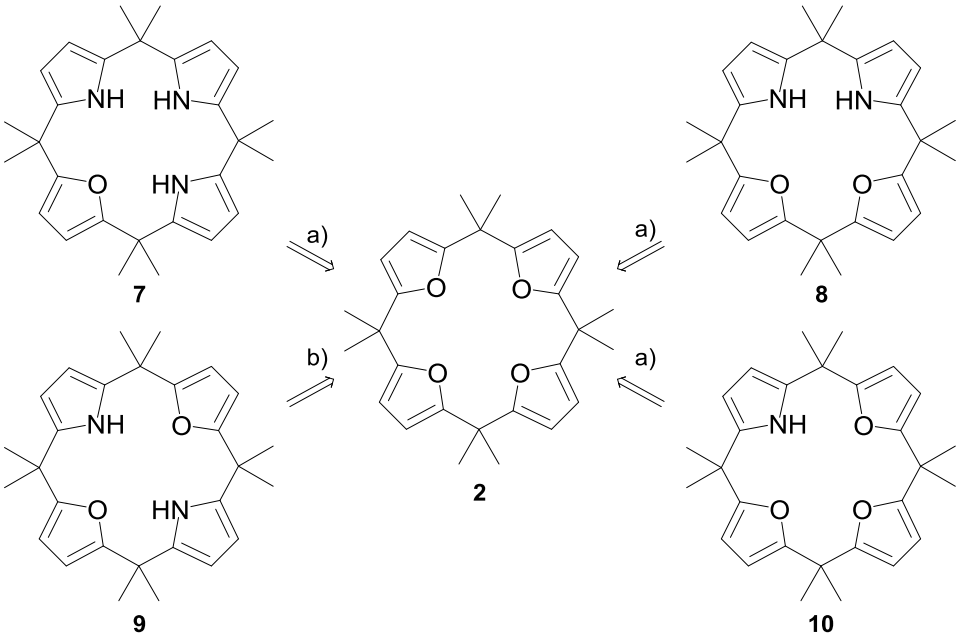

Scheme 9. The four calix[n]furan[4-n]pyrroles **7** – **10** coming from calix[4]furan **2** and the oxidation process involved. a) use of *m*-CPBA as oxidative agent; b) selective oxidation *via* the bromine procedure

The work of LeGoff and Kohnke has been already cited by Jae Sang Kim as procedure for the synthesis of macrocycles **8** – **10** for their study as ionophores in silver ion-selective electrodes but no experimental data could be found.[102] Surprisingly, macrocycle **7** was not synthesized whereas the ring-transforming method should allow its synthesis. The full optimization on the synthesis of the four calix[n]furan[4-n]pyrroles will be reported.

3. First results (Thesis of Guillaume Journot)[108]

3.1. Synthesis of calix[2]furan[2]pyrroles 8 and 9

In our first studies Guillaume Journot concentrated on a proof-of-principle approach, which allowed us to prove the feasibility of the whole sequence and give access to the aromatic calix[n]furan[4-n]pyrroles for the further investigation on their ability to be hydrogenated.

The synthesis of calix[4]furan, our starting material for all the four isomers, was investigated with the goal to obtain the product in large scale. An experimental procedure described by Jurczak *et al.*[109] in 2000 reported to afford calix[4]furan with 70% yield was used. The authors reported the influence of the concentration of sulfuric acid on the yields of calix[4]furan. The condensation between furan and acetone in dioxane using a 90.5% solution of sulfuric acid afforded calix[4]furan in 35% yield in our case, after recrystallization of the crude material. Despite a low yield the reaction is cheap, easy to manage in large scale and sufficient amount of starting material could be quickly and efficiently obtained.

The oxidative ring-opening of **2** was carried out with 2.2 equivalents of *m*-CPBA in cold $CHCl_3$. This reaction provided three different products: two di-ring-opened tetraketones **15a** and **16** and one tri-ring-opened unsaturated hexaketone **17** (Scheme 10). Compounds **15a** and **16** were obtained as a mixture, after column chromatography in 45/55 ratio respectively and 60% combined yield. Compound **17** has been isolated after column chromatography with 28% yield. In their experimental part, French *et al*. succeeded in isolating each product by column chromatography. In his hands Guillaume Journot was not able to separate compound **15a** and **16** following their conditions. Nevertheless, he continued with the mixture in the aim to separate the two regioisomers in a later step. The mixture of **15a** and **16** was submitted to the reduction of the α,β-unsaturated ketones using zinc dust and glacial acetic acid at 100 °C to provide the mixture of compounds **18** and **19** in 92% yield after chromatography. Unfortunately the separation by column chromatography of the regioisomers was still impossible. When trying to perform the next step from the mixture of regioisomers, he realized that only one of the two compounds, compound **19,** was soluble in ethanol, the solvent used for the reaction, even at 80 °C.

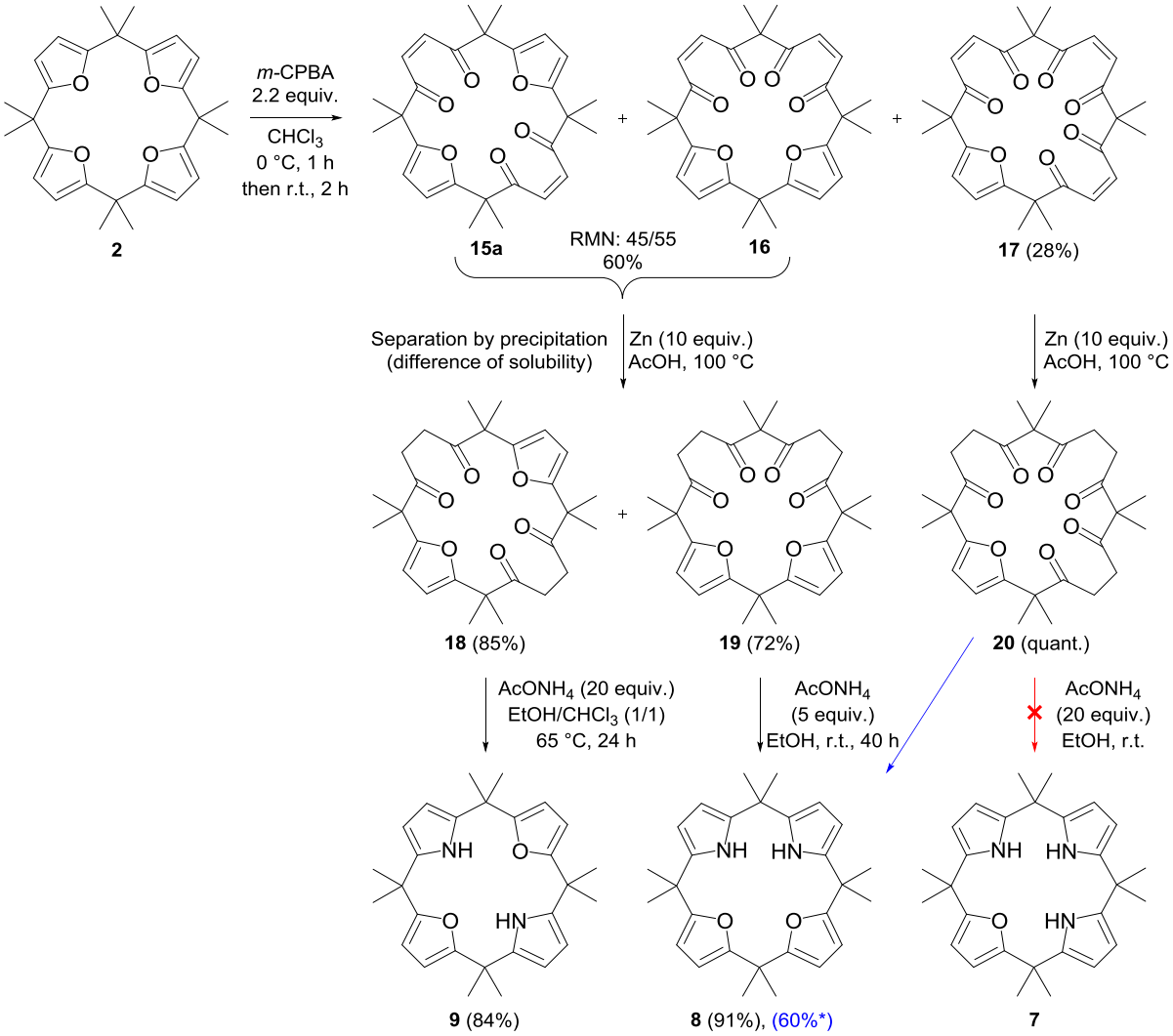

Scheme 10. Summary of the synthesis of macrocycles **7** – **9** coming from the same oxidation reaction using 2.2 equiv. of *m*-CPBA. *: Yield of **8** obtained starting from hexaketone **20**

Thanks to this difference of solubility, the separation of the regioisomers was achieved by successive washing with 80 °C ethanol. Using this procedure he successfully separated the reduced tetraketones **18** and **19** from each other, isolating the two isomers with respectively 85 and 72% yield. The next step is the formation of pyrroles by Paal-Knorr reaction. A special effort optimizing the reaction conditions had to be done, especially for the reaction using **18** as starting material. The synthesis of calix[2]furan[2]pyrrole **8** was carried out using 5 equiv. of ammonium acetate ($AcONH_4$) as source of ammoniac in a mixture of EtOH/$CHCl_3$ (1/1) at 65 °C overnight. After reducing the solvent volume in the rotavap, compound **9** was filtered off in 84% yield (>99%, GC). The reduced tetraketone **19** smoothly reacts with ammonium acetate, in ethanol at room temperature, to afford after filtration the calix[2]furan[2]pyrrole **8** with 91% yield.

The reduction of the three double bonds of the macrocycle **17** by adding zinc dust in a warm solution of **17** in glacial acetic acid provides the hexaketone **20** in quantitative yield without purification. In his thesis, the Paal-Knorr reaction on compound **20** provides, surprisingly, only the unsaturated macrocycle **8** in 60% yield. No traces of compound **7** have been detected in this reaction.

3.2. Synthesis of calix[3]furan[1]pyrrole 10

This reaction has been done using 1.2 equiv. of *m*-CPBA in chloroform at 0 °C. This reaction unfortunately affords also a non-negligible amount of side products from the multiple opening. The reduction of the double bond was performed directly after a simple workup of the reaction mixture, without separating the desired product from the side products. The two consecutive steps afforded the macrocycle **21** in 28% overall yield after chromatography (Scheme 11). The ring closing reaction to pyrrole was carried out very smoothly at room temperature giving calix[3]furan[1]pyrrole **10** in 90% after a simple filtration, in a high purity.

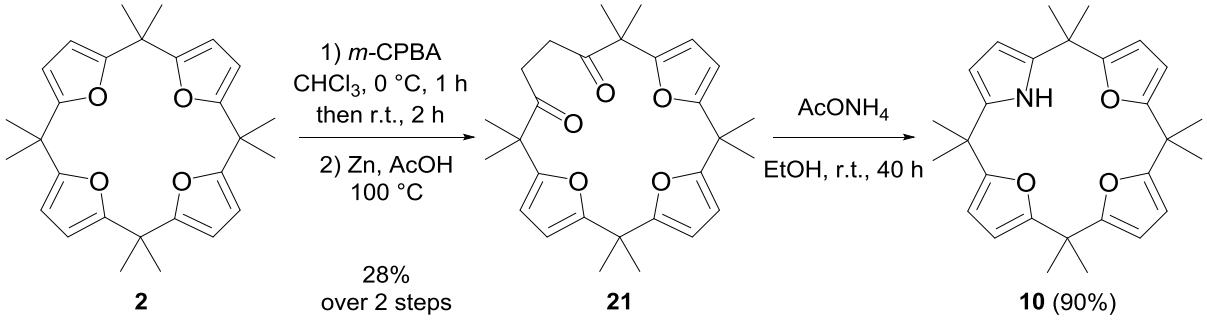

Scheme 11. Synthesis of macrocycle **10**

4. What had to be improved

Once it was clear that the proposed retrosynthesis could be successfully carried out efforts had to be focused on making the individual steps efficient and scalable. Indeed, in order to claim

that our compounds could potentially become novel ligands or compounds of interest we must propose an efficient, reproducible and scalable procedure with as high selectivity as possible.

The treatment of calix[4]furan (700 mg scale) with 2.2 equiv. of *m*-CPBA afforded the three intermediates **15a**, **16** and **17** leading to the synthesis of **9**, **8** and **7** respectively (Scheme 10). This protocol was a good starting point but the reaction is complicated to implement on a larger scale since we have to separate by chromatography three compounds with similar structures. The quantity of *m*-CPBA used should be related to number of rings opened. The synthesis of calix[1]furan[3]pyrrole **7** should therefore start with the oxidation of calix[4]furan with around three equivalents of the peracid. To achieve our goal we need to obtain the formation of this calix[1]furan[3]pyrrole **7** never observed so far. In case of failure we should be able to explain the reasons why this compound could not be obtained with this method. Since the addition of bromine could selectively open two furan rings located in front of each other in the macrocycle, this method was obviously selected for the synthesis of calix[2]furan[2]pyrrole **9**.

Obtaining the tetraketone **16** without the presence of its regioisomer **15a** seemed from the outset of our studies to be difficult. Even if the amount of *m*-CPBA is carefully adapted to the required bis-ring opening, it seemed to be difficult to avoid the concomitant formation of a significant quantity of hexaketone **17**. An important goal of our studies was to improve the purification of the mixture with the prime objective to isolate compound **16**, the most difficult to selectively synthesize. The formation of the diketone **21** with 28% yield over two steps on 500 mg scale without intermediate purification is as well not optimal. These two steps should also be improved.

5. Optimization of the synthesis of calix[n]furan[4-n]pyrroles 7 – 10

Our observations on the first two steps (ring-opening of calix[4]furan **2** and reduction of the unsaturated 1,4-diketone function) were similar to the results described by LeGoff.[105] Our work further includes procedures on larger scales compared to the previously reported experimental procedures of LeGoff, the synthesis of the mono ring-opened diketone **22a** (Scheme 12c) and modifications in the purification step of the treatment of calix[4]furan **2** with 2.2 equivalents of *m*-CPBA leading to the di-ring-opened compounds **15a** and **16**.

5.1. Oxidation of calix[4]furan using *m*-CPBA

To optimize the reaction conditions, the crude materials obtained from the reaction without purification were analyzed by GC to determine the optimal amount of *m*-CPBA to be added. The attribution of the GC peaks to the structures of the intermediates is based on GC-MS and ^{1}H NMR data. The analysis of the crude materials of different reaction conditions are compiled at the end of this chapter (Table 1). The remaining percent were attributed to uncharacterized products.

The opening of three rings was best achieved adding at once a small excess of 3.1 equiv. of *m*-CPBA to a solution of the starting material **2** in chloroform at r.t. leading after 4.5 h of stirring to the hexaketone **17** in satisfactory 60 – 63% yields after chromatography (Scheme 12a). The GC analysis of the crude material showed a mixture containing compound **17** as major product (70%) with small amounts of **21** (3%) and **15a** (13%) (Table 1, Entry 7). Since still a residual amount of tetraketone **15a** was present, the use of 3.30 equiv. of oxidative agent was tried and led to a small diminution of **17** (64%) in the crude material (Table 1, Entry 8).

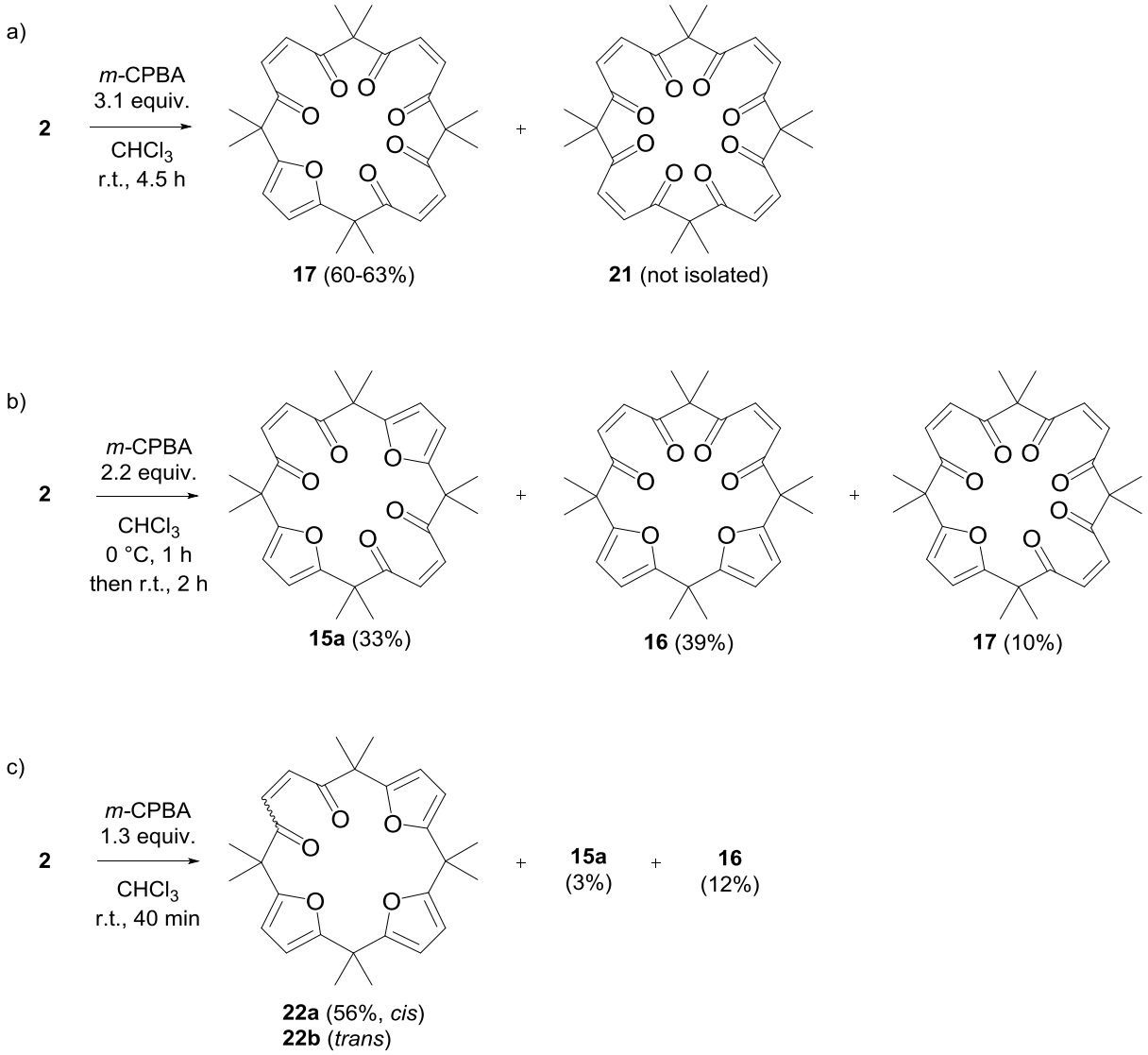

Scheme 12. Oxidative rings-opening reactions of calix[4]furan **2** using varying amounts of *m*-CPBA. a) Process optimized for obtaining product **17** by opening of three rings. b**)** Process optimized for the synthesis of the two bis-opened products **15a** and **16**. c) Using 1.1 equiv. of *m*-CPBA the mono-opened product **22a** was obtained as major product

Obtaining selectively the tetraketone **16** proofed to be challenging. The best proportion of compound **16** was obtained when calix[4]furan **2** was treated with 2.2 equiv. of *m*-CPBA in cold chloroform for 1 h followed by stirring at r.t. for additional 2 h with the presence of 43%

of intermediate **16** (Table 1, Entry 6). The use of 2.0 equivalents slightly decreased the amount of **16** formed (40% compared to 43%) and in the same time more of the mono-opened compound **22a** remained in the crude material (18% compared to 4%). At the same time, a decreased of the more oxidized compounds **15a** and **17** was detected in the mixture (Table 1, Entry 5).

The reaction conditions were not changed from our previous tests but the purification was optimized to isolate essentially compound **16**. The mobile phase reported by LeGoff for the chromatography was $CHCl_3$/EtOAc (9/1). The TLC using this mobile phase is shown above (Figure 18a). These conditions did not allow us to separate the two regioisomers **15a** and **16**. We have not been able to find a unique mobile phase allowing the separation of the three components of the mixture. When chloroform or dichloromethane was the major component of the mixture, the two tetraketones **15a** and **16** migrated with the same retention factor (Figure 18a and 18c) while when cyclohexane is the major solvent these two compounds showed different retention values (Figure 18b, cyclohexane/EtOAc (8/2)). In this condition, intermediate **16** showed a higher R_f value than the two others and can be isolated. The chromatography was successfully applied on a scale up reaction (based on the transformation of 3.0 g of calix[4]furan) to isolate first compound **16** with a cyclohexane/EtOAc (9/1) mixture. Once the tetraketone was isolated, the mobile phase was changed to CH_2Cl_2/EtOAc (97/3) to successively isolate compounds **15a** and **17**.

This purification by flash chromatography on SiO_2 afforded the tetraketones **15a**, **16** and the hexaketone **17** in respectively 33%, 39% and 10% yields (Scheme 12b). Around 1.2 grams of macrocycle **16** were isolated (reaction and purification were repeated three times).

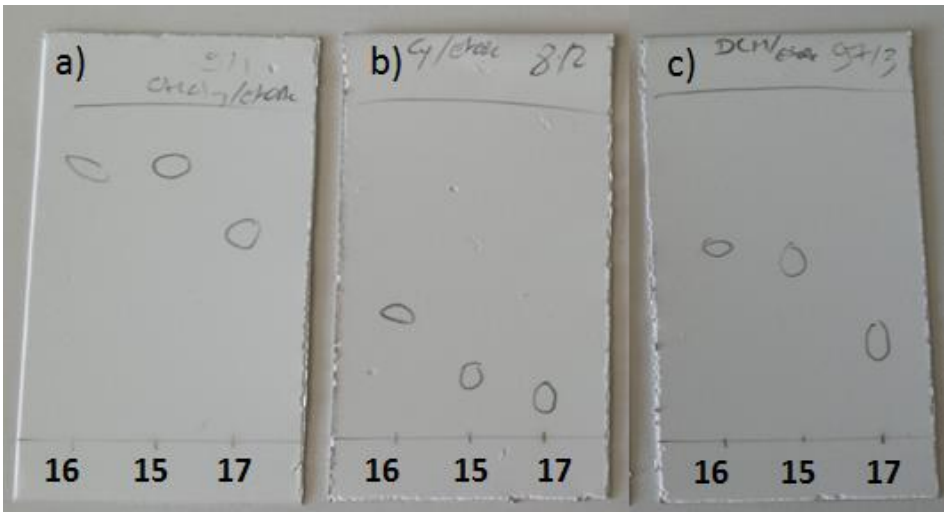

Figure 18. TLC of compounds **15**, **16** and **17** with different mobile phase. a) $CHCl_3$/EtOAc (9/1); b) Cyclohexane/EtOAc (8/2); c) CH_2Cl_2/EtOAc (97/3)

The other delicate transformation was the selective synthesis of the diketones **22a** (Scheme 12c). In order to avoid over-oxidation we started with the use of 1.1 equivalents of *m*-CPBA in chloroform at r.t. No further transformation was observed after 20 min with a proportion of 69% and 2% for **22a** and **22b**, respectively. A significant amount of starting material **2** remained in the mixture (18%) as well as product of over-oxidation **16** and **15a** in respectively 7% and 2% (Table 1, Entry 1). Using 1.3 equivalents of *m*-CPBA, the reaction was finished after around 40 minutes. The GC of the crude showed a mixture of unreacted starting material **2** (4%), diketone **22a** (73%), tetraketone **16** (15%) and traces of tetraketone **15** (6%) (Table 1, Entry 2). After chromatography, 56% yield of pure **22a** was obtained. In large scale experiments (10 grams of calix[4]furan **2**) we obtained more than 5.70 grams of compound **22a** and we recovered significant amounts of starting material **2** (880 mg) and tetraketones **16** and **15a** (respectively 1.32 g and 321 mg). Since the synthesis of tetraketone **16** was not sufficiently selective, its isolation as side product in this reaction was an added bonus.

In an effort to avoid over-oxidation, we tried to slowly add a solution of *m*-CPBA in chloroform instead of adding the entire reagent at once. A solution of 1.1 (or 1.25) equivalents were added over 1 h at r.t. then the solution was stirred for 15 min before quenching the reaction with an aqueous saturated solution of sodium bicarbonate. The composition of the crude of these experiments did not change compared to the addition of solid *m*-CPBA in one go (Table 1, Entries 3 and 4, respectively).

During chromatographic purification, a spot close to our mono-opened compound **22a** appeared as function of the time needed for the purification. This compound was obtained as a mixture with **22a** but it was never isolated pure. After analysis, it revealed to be the result of the isomerization of the unsaturated 1,4-diketone function from the *cis*-isomer **22a** to the *trans*-isomer **22b** (Figure 19). The two isomers were easy to differentiate using our GC method (1 min difference in the retention time between the two isomers) and a distinctly different ^{1}H NMR, especially for the proton of the double bond with a chemical shift of 5.88 compared to 6.79 for **22a** and **22b**, respectively (Figure 19).

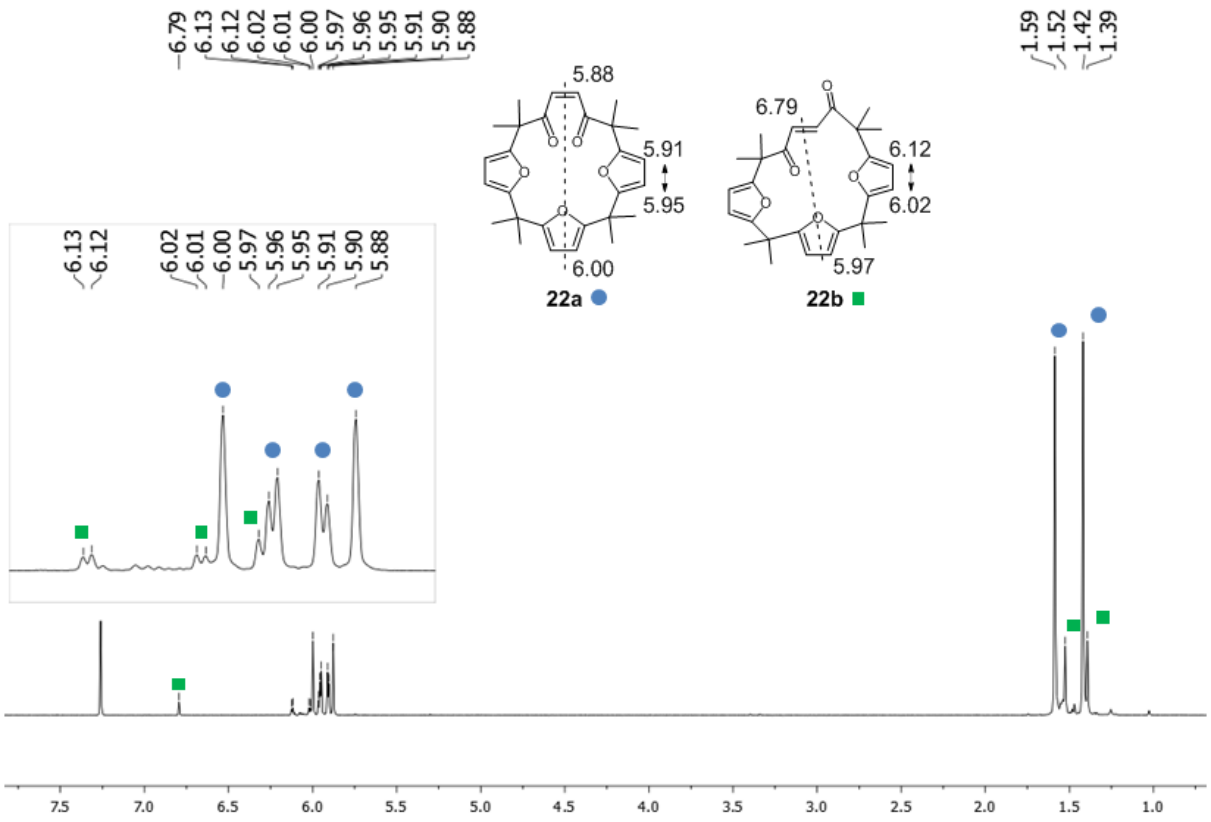

Figure 19. 400-MHz ^{1}H NMR spectra of a mixture of isomers **22a** and **22b**

The chromatographic separation has to be performed quickly in order to avoid this isomerization catalyzed by the silica gel. The use of a large column (diameter: 8 cm) allowed an efficient and quick purification with the recovery of the products directly in Erlenmeyer flasks. The identification of the product was facilitated due to the yellow color of the ring-opened products. Synthetically, the contamination of **22a** with its isomer **22b** was not a problem, because the double bond will be reduced in the next step (Scheme 16c). Performing the chromatography quickly we isolated compound **22a** before a significant isomerization had occurred and usually we obtained a 98/2 mixture in favor of the *cis*-isomer **22a**.

Starting from the *cis*-isomer **22a**, some short tests were tried to fully isomerize the double bond to the *trans*-isomer **22b**. A solution of **22a** in $CHCl_3$ was stirred with silica or with a catalytic amount of hydrochloric acid but each time a mixture of the two isomers was obtained. As compound **22b** did not have real interest for us we did not go any further.

Entry	Equiv. of *m*-CPBA	**2**	**22a**, **22b**	**16**	**15a**	**17**	**21**
1[a]	1.10	18%	**22a** 69%, **22b** 2%	7%	2%	-	-
2[a]	1.30	4%	**22a** 73%, **22b** 2%	15%	6%	-	-
3[b]	1.10	13%	**22a** 71%, **22b** 1%	11%	4%	-	-
4[b]	1.25	5%	**22a** 73%, **22b** 1%	13%	6%	-	-
5	2.00	1%	**22a** 18%	40%	23%	8%	-
6	2.20	-	**22a** 4%	43%	33%	16%	-
7	3.10	-	-	1%	13%	70%	3%
8	3.30	-	-	1%	13%	64%	6%

Table 1. GC analysis of crude materials of the ring-opening reaction using varying equiv. of *m*-CPBA.[a] One pot addition of *m*-CPBA (1 h at 0 °C then 2 h at r.t.); [b] Dropwise addition of a solution of *m*-CPBA in $CHCl_3$ (1 h addition + 15 min stirring, r.t.)

5.2. Synthesis of 15b via the bromine oxidation

For the synthesis of the tetraketone **15b** a transformation avoiding chromatography could be developed following the procedure reported in the literature.[105] Slowly adding a bromine solution in glacial acetic acid over a 3 h period to a suspension of calix[4]furan **2** in a glacial acetic acid/water solution gave selectively tetraketone **15b** (Scheme 13). Since **15b** was not soluble in the reaction mixture at r.t., filtration of the solid and washing the crude material with methanol allowed the isolation of **15b** in 65 – 70% yield as a yellow powder. It was mentioned by LeGoff that acetic acid was trapped in crystals of **15b**. A recrystallization in cold $CHCl_3$ allowed the elimination of the small amount of solvent present. As acetic acid was the solvent for the next transformation no further purification of the crude product was necessary.

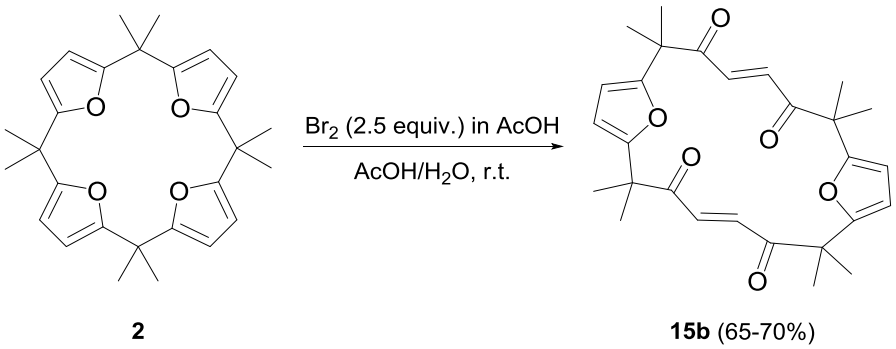

Scheme 13. Selective synthesis of **15b** with the bromine oxidation

A faster addition in less than 3 h or an increase of the amount of bromine diminished the yield of **15b** by forming side product **23** (Scheme 14) by the addition of bromine to one of the double bonds of **15b**. Indeed both starting material **2** and tetraketone **15b** are very slightly soluble in the solvent mixture of the reaction. A slow addition was absolutely necessary to favor the precipitation of compound **15b** before an over-addition of bromine on the product could occur.

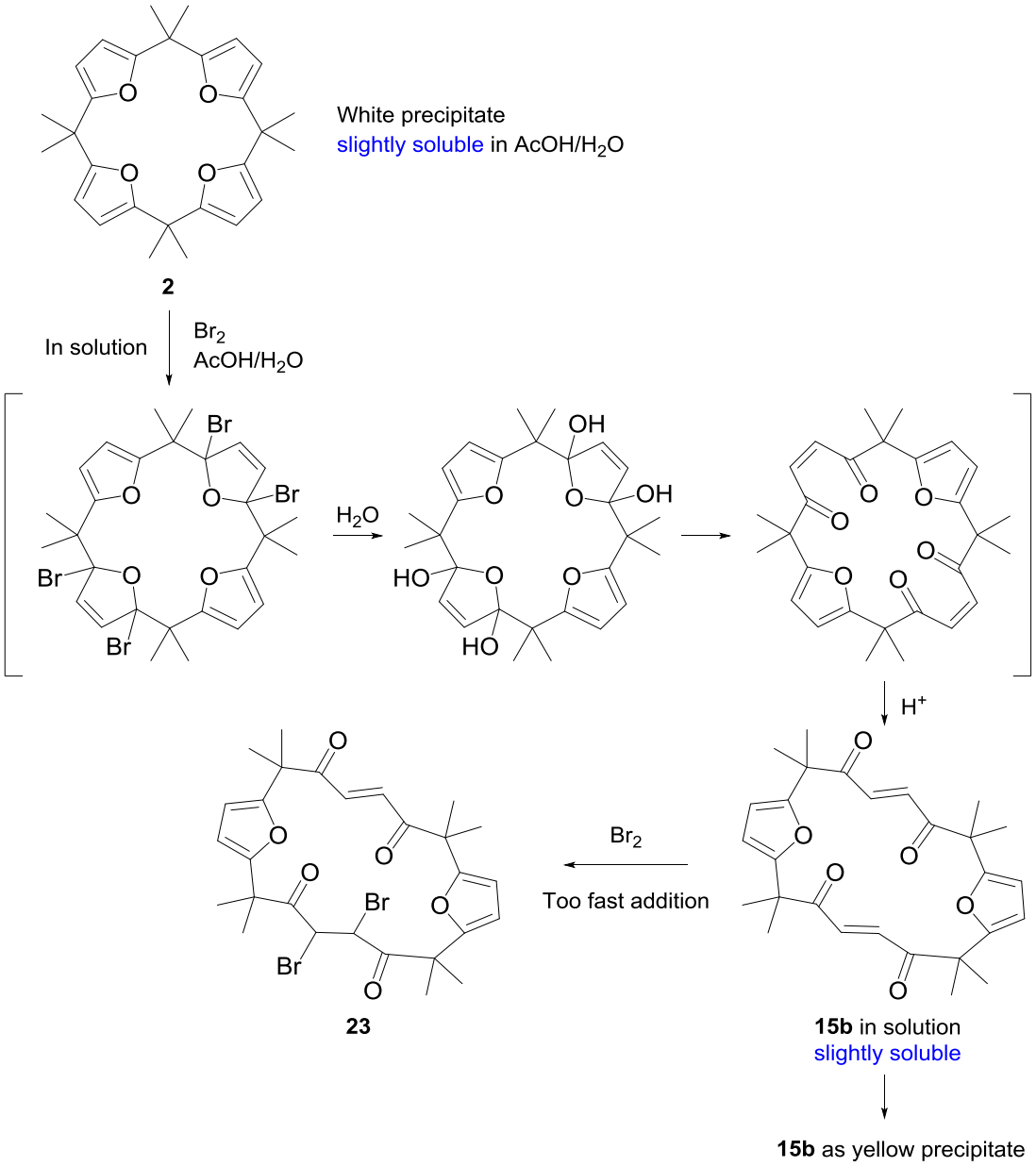

Scheme 14. Process to the formation of compounds **15b** and **23**

5.3. Reduction of the unsaturated 1,4-diketone

For the reduction of the two *trans*-double bonds of **15b** a hot glacial acetic acid solution containing the tetraketone **15b** was treated with excess of zinc dust (Scheme 15). The yellow solution became colorless in few seconds after the addition of the zinc dust. After treatment and evaporation of the organic phase, and in accordance with the high solubility of **18** in ethanol we had previously observed, the crude material was washed with ethanol to obtain reduced compound **18** in 95% yields. Starting from calix[4]furan **2**, the reduction product **18** was obtained in 62 – 67% yields in two steps without chromatographic purification. Synthesizing **18** in one step starting form calix[4]furan **2** by heating the reaction mixture

without workup after the bromine addition gave in our hands slightly lower overall yields (50% yield on two steps) although Floriani reported 65% with this process.[98]

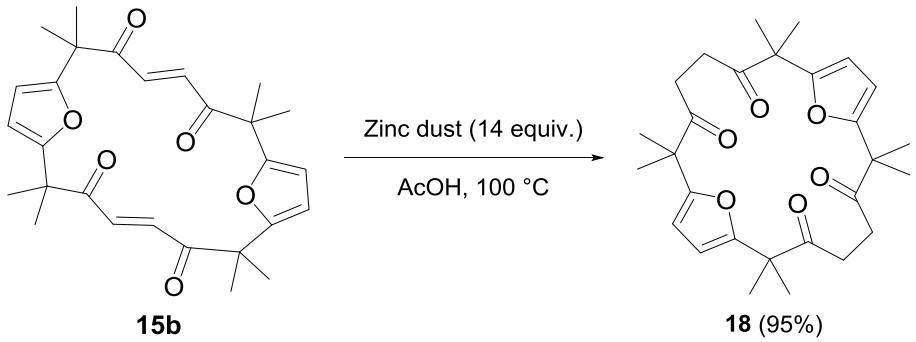

Scheme 15. Reduction of **15b** with the zinc/AcOH method

Tetraketone **18** could also be obtained by reduction of the previously synthesized *cis*-configurated compound **15a** using the same method (zinc dust, hot AcOH) with similar results (95% yield).

The reduction of the double bonds of the macrocycles **16**, **17** and **22a** in grams scale using zinc in hot acetic acid led only to incomplete transformations and difficult purifications. So we moved towards protocols reported by LeGoff using hydrogenation for the reduction of these intermediates. Catalytic hydrogenation of compounds **16** and **17** in a Parr apparatus under 4.5 bars of H_2 using Pd/C as catalyst in EtOAc as solvent at r.t. led to full conversion. After recrystallization in EtOH, **20** and **19** were obtained in 70% and 78% yield, respectively (Scheme 16a and 16b). Hydrogenation of **22a** under the same conditions led to a more complicated mixture of products for reasons, which were not explored. The major product of this transformation was present in 60% by GC analysis. Pleasingly using the Lindlar catalyst instead afforded the formation of **21** as unique product, which was identical with the major compound obtained with the reduction using Pd/C. The crude solid was washed with EtOH to obtain **21** in 95% yield with 99% purity (Scheme 16c). This quantitative reduction was efficiently realized on a 4.5 g scale.

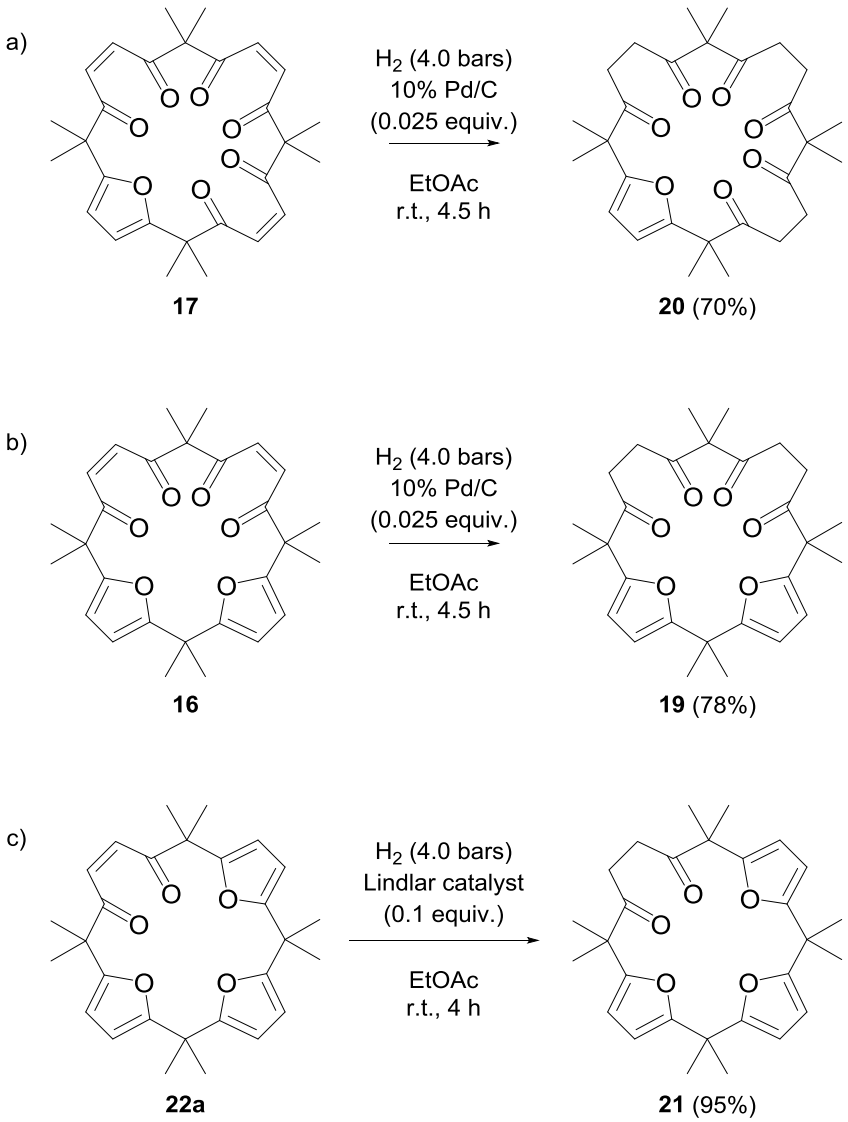

Scheme 16. Synthesis of **19** – **21** by heterogeneous catalytic hydrogenation

The success of the hydrogenation reactions could be easily observed once the catalyst is removed. Indeed the discoloration of the solution is a reliable indicator for the success of the hydrogenation process. This simple color change was reliable for the reduction of **15b** to **18**. The same color change could be used for the transformation of the starting materials **16**, **17** and **22a**, which are yellow and which are after hydrogenation transformed to colorless macrocycles **19** – **21**.

5.4. Synthesis of calix[n]furan[4-n]pyrroles 7 – 10

The last step for the synthesis of calix[n]furan[4-n]pyrroles **7** – **10** is the Paal-Knorr reaction starting with the corresponding ketones **18** – **21**. We based our work on Kohnke's conditions ($AcONH_4$, 1.5 equiv. per 1,4-diketone units in the macrocycle, EtOH, reflux, 30 h).[106] Purity of the final compounds **7** – **10** were determined by GC and NMR analysis.

5.4.1. Synthesis of calix[2]furan[2]pyrrole 9

As compound **18** was poorly soluble in ethanol, the reaction had therefore to be carried out in a 1/1-mixture of EtOH/$CHCl_3$. A large excess of $AcONH_4$ acetate was reported in our preliminary tests on this synthesis of compound **9** (20 equiv.) in contrast to the reaction carried out at room temperature using its regioisomer compound **8** (Scheme 10). Ammonium acetate was used as reactant to liberate *in situ* ammoniac (NH_3) which reacts with the saturated 1,4-diketone function to form the pyrrole rings. As ammoniac is a gas and the reaction was performed at reflux, it is likely we lost the reactant during the reaction despite the presence of a condenser. Reaction carried on Schlenk tubes, a closed system, helped to greatly reduce the amounts of $AcONH_4$ used. Kinetic studies of the reaction showed that using a slight excess of $AcONH_4$ (4.5 equiv., Table 2, Entries 2 and 4) allowed a faster reaction compared to the standard conditions (3 equiv., Table 2, Entries 1 and 3). In this way the reaction stopped after 24 h with a satisfying 95% conversion (Table 2, Entry 4) while a lower 79% conversion was observed using only three equivalents of $AcONH_4$ (Table 2, Entry 3).

Entry	Equivalent	Reaction time (h)	Crude material analysis (GC)
1	3	17	**9** (71%), **int.**[6] (29%)
2	4.5	17	**9** (89%), **int.** (11%)
3	3	24	**9** (79%), **int.** (21%)
4	4.5	24	**9** (95%), **int.** (5%)

Table 2. Kinetic study of the synthesis of **9**

Removing the solvent in the rotavap the calix[2]furan[2]pyrrole **9** started to precipitate (Scheme 17). After removing around 80% of the solvent the crude reaction mixture was obtained as a slurry. Filtration and washing of the solid with EtOH gave **9** in 96 – 98% purity. A quick filtration/purification on SiO_2 gave pure **9** in 84% yield. Calix[2]furan[2]pyrrole **9** could be selectively and efficiently synthesized (2 grams) in three steps in 54% overall yield in only 2 – 3 days starting from calix[4]furan **2**.

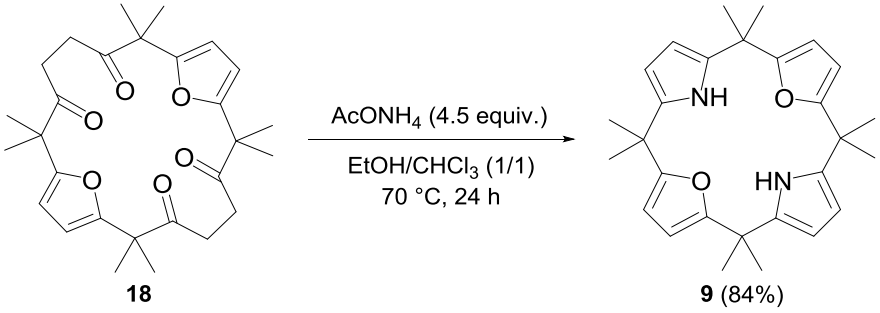

18 **9** (84%)

Scheme 17. Synthesis of calix[2]furan[2]pyrrole **9**

[6] Reaction intermediate

5.4.2. Synthesis of calix[n]furan[4-n]pyrroles 7, 8 and 10

The triple Paal-Knorr reaction on compound **20** leading to the formation of calix[1]furan[3]pyrrole **7** occurred smoothly at room temperature with the use of 6 equiv. of $AcONH_4$. Macrocycle **7** precipitated in EtOH during the reaction. After a 40 h reaction, filtration and washing of the white solid with EtOH, calix[1]furan[3]pyrrole **7** was obtained in 51% yield, 98% purity. The reaction was also carried out at 85°C in a Schlenk tube. After a reaction time of 40 h, the crude mixture was concentrated under vacuum leading to the precipitation of **7**. Before removing all the solvent, the white solid was filtered and the crude product was obtained in 93% purity. Recrystallization in EtOH yielded 60% of **7** in excellent purity (Scheme 18a). Longer reaction time than 40 h afforded the same 60% yield. Following the same process but by stopping the reaction after 24 h at 85 °C afforded macrocycle **7** in 50% yield.

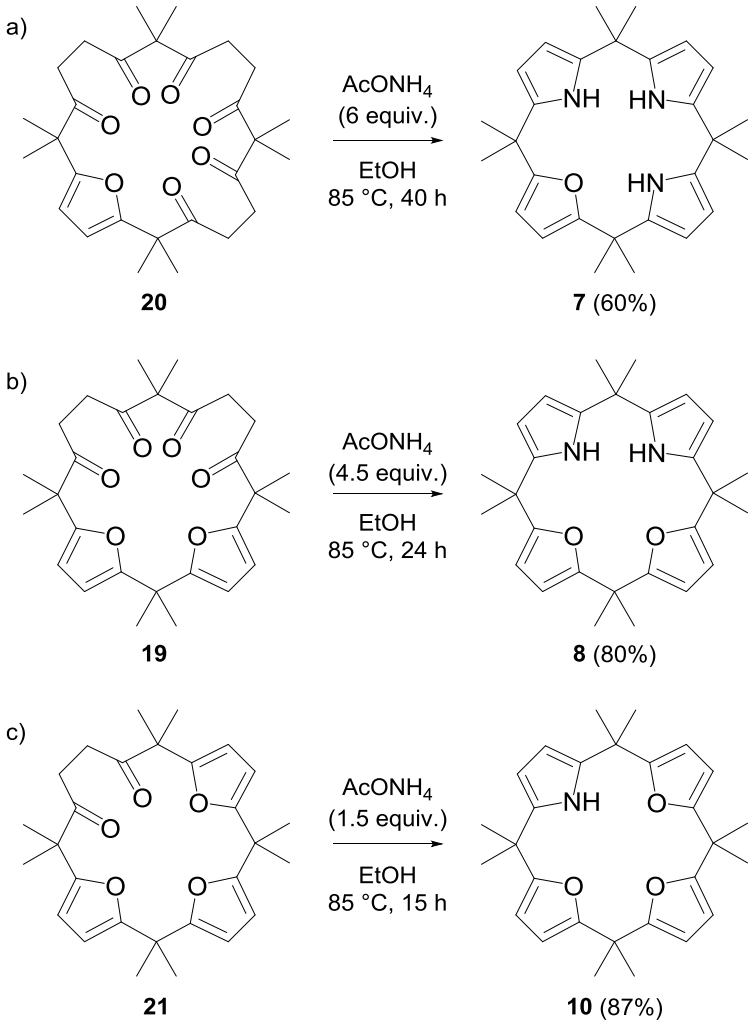

Scheme 18. Synthesis of calix[n]furan[4-n]pyrroles **7**, **8** and **10**

Treating of the tetraketone **19** as described for **20** at r.t. using 4.5 equiv. of $AcONH_4$ induced the precipitation of the calix[2]furan[2]pyrrole **8** in good yield (80%) and excellent purity directly from the reaction mixture after a 40 h reaction time. The yield observed was slightly different with the results obtained by Guillaume (80% yield compared to 91% previously

described). No further purification was needed to obtain calix[2]furan[2]pyrrole **8** in pure form. The reaction was carried out at 85 °C in a Schlenk tube. In these conditions, the same maximum yield (80%) was obtained after 24 h of reaction. Pure **8** was obtained after filtration and washing of the white solid with EtOH (Scheme 18b).

The same procedure in a Schlenk tube could be applied for the saturated diketone **21**. The calix[3]furan[1]pyrrole **10** precipitated in excellent yield and in good purity also directly from the reaction mixture. After 15 h reaction at 85 °C, the reaction mixture was concentrated in the rotavap, the precipitate was filtered and washed with EtOH. The crude calix[3]furan[1]pyrrole **10** was obtained in better than 99% purity. Recrystallization of the crude white powder in dioxane gave big crystals of **10** ($P4_1$ space group) in 87% yield (Scheme 18c). The efficient synthesis of macrocycle **10** allowed having more than two grams of final product within three days of work. The overall yields of compounds **7** – **10** starting from calix[4]furan **2** were summarized in Figure 20.

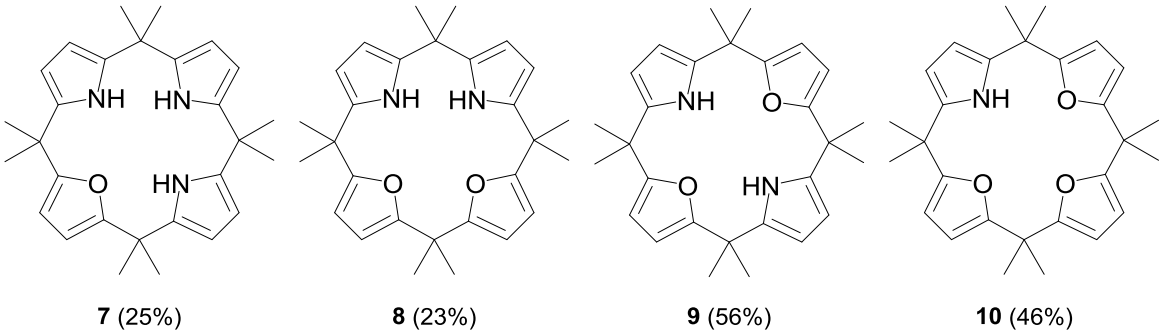

7 (25%) **8** (23%) **9** (56%) **10** (46%)

Figure 20. Overall yields for the synthesis of calix[n]furan[4-n]pyrroles **7** – **10** starting from calix[4]furan **2**

6. Electrochemical properties

The characteristic and unique features of tetrapyrrolic macrocycles is their π-system, which confers to them special physicochemical properties. Studying their photophysics, photochemistry and often in parallel their electrochemistry has become a hallmark and at the same time a routine procedure for the characterization of novel macrocyclic tetrapyrrolic complexes,[110-112] and more recently for the free tetrapyrrolic macrocycles.[113-116] Our optimized process afforded sufficient quantities of the four calix[n]furan[4-n]pyrroles **7** – **10** to explore the characteristic physicochemical properties of this family of compounds.

We recently started a collaboration with the group of Professor Karl Kadish to systematically investigate the electrochemical behavior of the calix[n]furan[4-n]pyrroles family. The study includes the parent compounds n = 0 (calix[4]pyrrole **1**) and n = 4 (calix[4]furan **2**) together with the mixed nitrogen and oxygen containing calix[n]furan[4-n]pyrroles **7** – **10**. At this point in time only preliminary results are available but future, more extensive studies are planned. Cyclic voltammetry (CV) is widely used to determine the redox potentials of electroactive compounds and it allows to characterize the (electro-)chemical reactions of the

oxidized or the reduced species.[117] In CV the voltage is swept between two set values. The CV set-up is a one compartment experiment where a working electrode and a reference electrode are immersed into a solution containing the compound to be analyzed.

The reported results have been collected by Xiangyi (Florence) Ke, PhD student in the group of Professor Kadish. We are obliged to Mrs. Ke and Professor Kadish for the collaboration and for their careful experimental work and for sharing their results with us.

In order to successfully measure CV of organic compounds a solvent must be chosen, which allows dissolving the studied compound in sufficient quantities and at the same time dissolving the needed electrolyte. For organic compounds acetonitrile is therefore often the preferred solvent, using TBAP (tetrabutyl ammonium perchlorate) as electrolyte. In a first approach the Houston group studied the oxidation of the six compounds **1**, **4** and **7** to **10** by cyclic voltammetry using acetonitrile (CH_3CN), benzonitrile (C_6H_5CN) and CH_2Cl_2 as solvents (Figure 21). The oxidation potentials of the six calix macrocycles as determined from the cyclic voltammetry experiments are summarized in Table 3.

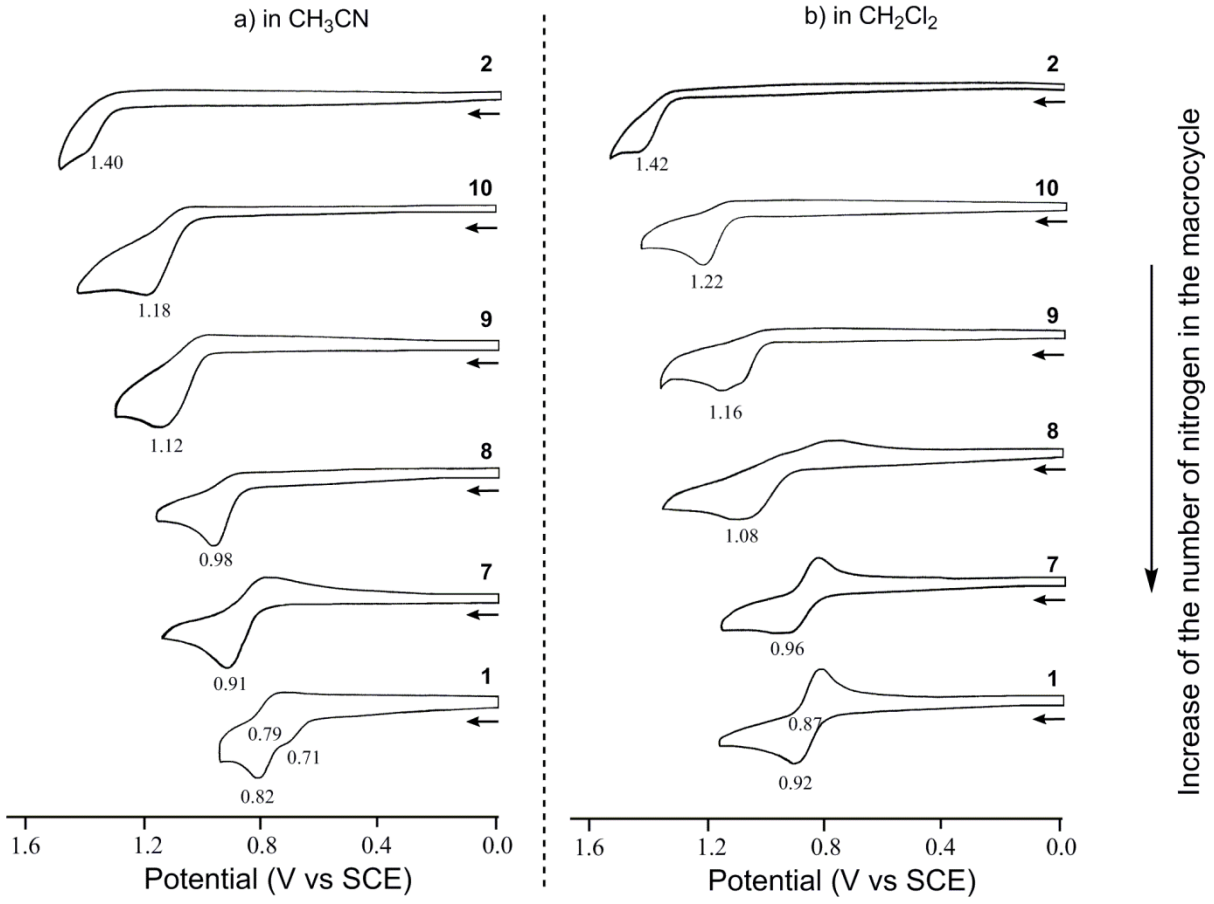

Figure 21. Cyclic voltammetry of investigated compound **1**, **2** and **7** – **10** in CH_3CN (left) and in CH_2Cl_2 (right), 0.1M TBAP. [7] Scan rate = 0.1 V/s

[7] SCE: Saturated calomel electrode (reference electrode)

Description and preliminary discussion on the results

As seen in Figure 21, both CH_3CN and CH_2Cl_2 solvents showed oxidation at the anode for all the tested compounds. Calix[4]pyrrole **1** and calix[1]furan[3]pyrrole **7** are characterized by a reversible 1st oxidation in CH_2Cl_2 at a half-wave potential ($E_{1/2}$) of respectively 0.87 and 0.88 V (Figure 21 and Table 3, Entries 5 and 6). Working in CH_3CN, a similar reversible 1st oxidation was observed for compound **7** ($E_{1/2}$ = 0.86 V, Table 3 Entry 11) whereas the cyclic voltammogram of compound **1** showed two successive irreversible oxidations at anodic peak potential E_{pa} = 0.71 and 0.82 V (Figure 21 and Table 3 Entry 12). The other compounds **8** – **10** and **2** showed, in both solvents, irreversible 1st oxidation at anodic peak potential (E_{pa}) from respectively 1.08 to 1.42 V in CH_2Cl_2 (Figure 21 and Table 3, Entries 1 to 4). In CH_2Cl_2, compound **9** showed two successive irreversible oxidations at anodic peak potential E_{pa} = 1.09 and 1.16 V (Figure 21 and Table 3 Entry 3).

Entry	Solvent	Compound	E_{pa} (Ox_1)	$E_{1/2}$ (Ox_1)	E_{pa} (Ox_2)	$E_{1/2}$ (Ox_2)	E_{pa} (Ox_3)	$E_{1/2}$ (Ox_3)
1	CH_2Cl_2	**2** – OOOO	1.42		1.72*			
2		**10** – NOOO	1.22		1.66*			
3		**9** – NONO	1.09		1.16		1.42*	1.39*
4		**8** – NNOO	1.08		1.72*			
5		**7** – NNNO	0.96	0.88	1.44	1.41		
6		**1** – NNNN	0.92	0.87	1.30	1.25		
7	CH_3CN	**2** – OOOO	1.40		1.66*			
8		**10** – NOOO	1.18		1.82*			
9		**9** – NONO	1.12		1.36*	1.33*		
10		**8** – NNOO	0.98		1.62*		1.82*	
11		**7** – NNNO	0.91	0.86	1.40*	1.37*		
12		**1** – NNNN	0.71		0.82	0.79	1.14*	1.11*

Table 3. Redox potential (V vs SCE) of investigated calix compounds in CH_2Cl_2 and CH_3CN containing 0.1 M TBAP. Scan rate = 0.1V/s. *Values sent by Xiangyi Ke for which we do not have voltammograms in our possession

Cyclic voltammograms of the two parents calix[4]pyrrole **1** and calix[4]furan **2** in CH_2Cl_2 showed distinct differences: compound **1** with the four pyrrole rings shows a fully reversible CV wave for the 1st oxidation ($E_{1/2}$ = 0.87 V) whereas the wave of calix[4]furan **2** clearly indicates an irreversible oxidation at anodic peak potential E_{pa} = 1.42 V. The behavior of the mixed compounds can be empirically classified as being a function of the relative number of furan rings present. The calix[1]furan[3]pyrrole **7** incorporating only one furan ring in the macrocycle still showed a reversible cyclic voltammogram (Figure 21b). Once two or more furan rings are present in the macrocycle, irreversible electron transfer processes were observed. The electron transfer reaction seems to become increasingly irreversible as the number of oxygen atoms in the macrocycle increased.

The reversibility observed in the cyclic voltammogram of calix[4]pyrrole **1** suggested the formation of a relatively stable radical cation after the 1st oxidation (Figure 22a). the electrochemically formation of a relatively stable radical cation from pyrrole is in accordance

with the proposed mechanisms reported for the synthesis of polypyrrole by electropolymerization of pyrrole.[118] Due to the irreversible oxidation of calix[4]furan **2**, the radical cation formed may undergo a nucleophilic addition e.g. with traces of water present in the solvent (Figure 22b). The product formed is more easily oxidizable than the starting furan ring. The oxidation of calix[4]furan **2** in AcOH/H_2O medium with bromine, peroxides or peracids as oxidative agent proceeds *via* a similar sequence of steps (see page 35 Chapter 2).

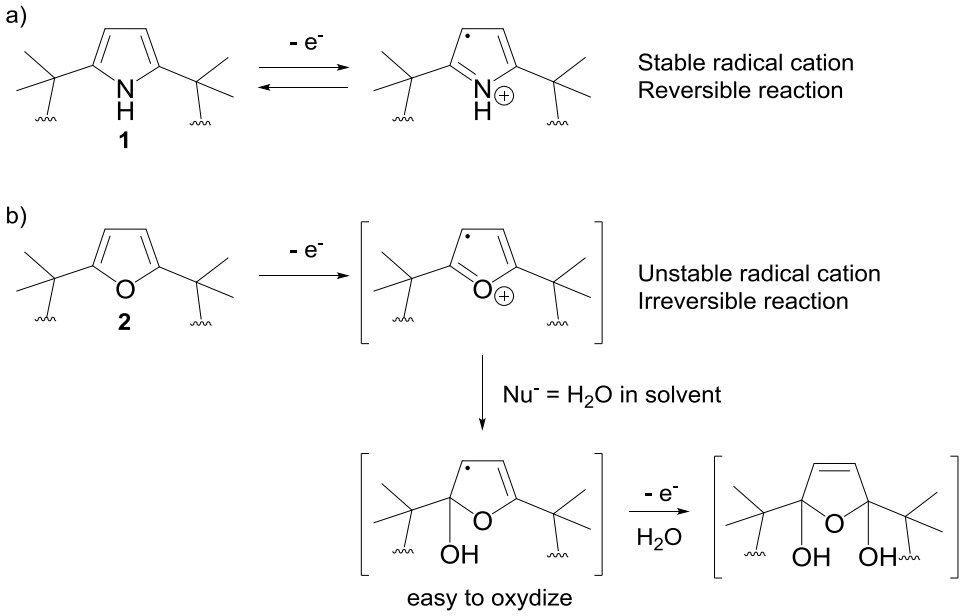

Figure 22. Schematic scheme for the proposed mechanism of the 1st oxidation as observed in the cyclic voltammetry experiments. In this simplified scheme one of the four heterocycles in the calix[4]heterocyclic macrocycles and its reaction during the oxidation process are highlighted a) Oxidation of one pyrrole ring representative for the calix[4]pyrrole **1**; b) Oxidation of one furan ring representative for the calix[4]furan **2**

To quantify the number of electrons used in the oxidation process the cyclic voltammograms were also measured in the presence of 1.0 equiv. of ferrocene. This experiment with calix[4]pyrrole **1** is reproduced in Figure 23 showing unequivocally that the 1st oxidation is a reversible one electron oxidation.

The cyclic voltammetry analysis was performed until 1.6 V revealing the 2nd oxidation ($E_{1/2}$ = 1.25 V, Figure 23 and Table 3, Entry 6). Cyclic voltammograms of the other compounds in the presence of ferrocene are shown in the annex (page 161).

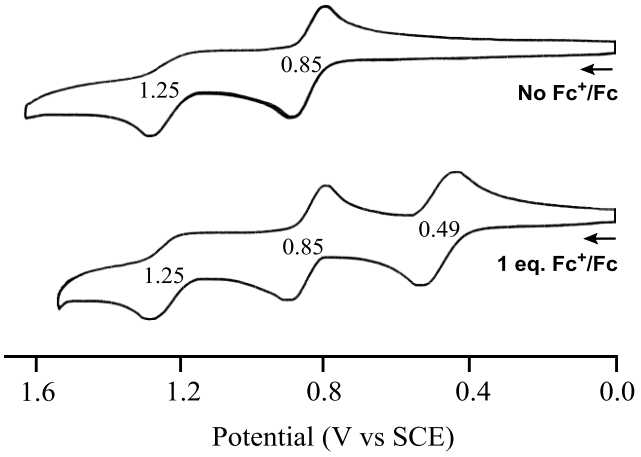

Figure 23. Cyclic voltammetry of **1** in CH_2Cl_2, with and without Fc^+/Fc, 0.1M TBAP. Scan rate = 0.1V/s

The potential observed for the 1st oxidation peak in CH_2Cl_2 was plotted as a function of the number of oxygen atoms present (= number of furan rings) in the macrocycle (Figure 24). As the two compounds **8** and **9** both have two furan rings in the macrocycle and showed slightly different peak potential at the anode (respectively E_{pa} = 1.08 and 1.09 V), two different points are plotted for the value of two furan rings. An empirical linear correlation could be established between the number of furan rings contained in the calix-macrocycle and the 1st oxidation with a correlation efficient of 0.945. Considering compounds **7** – **10** without the two parents **1** and **2**, the points are almost perfectly aligned and the correlation coefficient increases to 0.998.

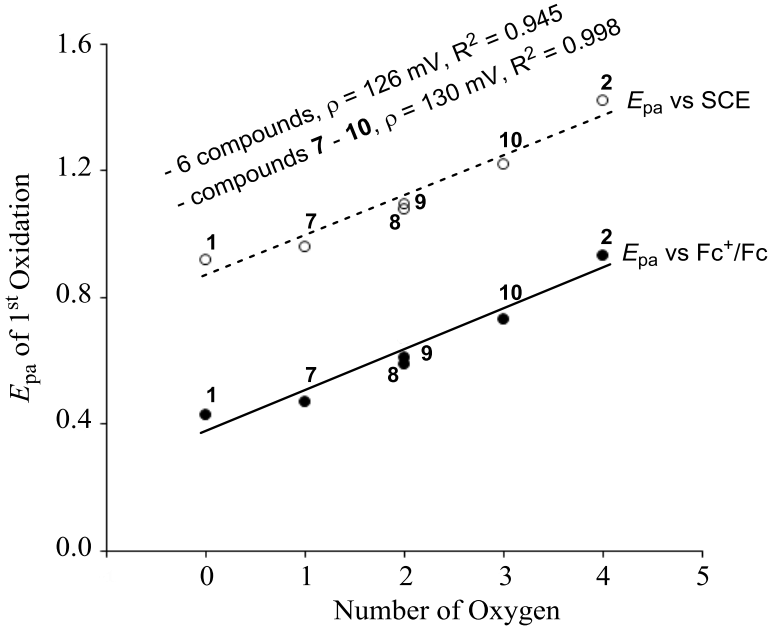

Figure 24. Plots of 1st oxidation peak potential vs the number of oxygen atoms contained in each calix compound in CH_2Cl_2, 0.1M TBAP. Scan rate = 0.1V/s.

Further experiments are in progress to fully explore the properties of this type of compound into electrochemical processes.

7. Conclusion

The analytical data of the macrocycles **8** – **10** reported in the literature were not complete. French[97] reported in 1958 the melting points, the mass analysis and the percent N (partial combustion analysis) contained in compounds **8** and **10**. The melting point, the mass analysis and the complete CHN combustion analysis was reported for compound **9**. Floriani[98] reported the ^{1}H NMR and the IR spectrum of compound **9**. Guillaume Journot successfully characterized the three unsaturated macrocycles **8** – **10** fully by ^{1}H and ^{13}C NMR, IR and HRMS spectroscopy as well as determining their melting points. He successfully grew single mono-crystals of macrocycles **8** and **9**, structures already reported in literature.

Thanks to an optimization work on this project, the synthesis of calix[1]furan[3]pyrrole **7** had been achieved for the first time. The procedure was successfully optimized with a modest 25% overall yield over three steps starting from calix[4]furan **2**. A single crystal of macrocycle **7** was successfully grown, as well as a crystal for compound **10** already listed in literature. The X-ray diffraction analyses of these heterocyclic calix[4]arenes **7** – **10** will be presented and discussed in the corresponding chapter (page 63, Chapter 4).

Our optimized procedures allowed synthesizing sufficient quantities (from 600 mg to 2.2 g per batch depending of the macrocycle) of the mixed compound **7** to **10**. With these quantities in hand we could explore the hydrogenation. As starting point of our studies reported in the next chapter (Chapter 3) we used the methods successfully applied for the synthesis of calix[4]pyrrolidine **3**.

Chapter 3. Synthesis of calix[n]tetrahydrofuran[4-n]pyrrolidines

1. Introduction

Before the studies published by our group only the hydrogenation of calix[4]furan **2** had been reported in the 1970s (see Chapter 1). First uncharacterized mixtures were reported until van Beylen *et al.*[93] described in 1985 the isolation and characterization of the two calix[4]tetrahydrofuran diastereoisomers **4a** and **4b** (Figure 25). Hydrogenation of calix[4]furan **2** under milder conditions (Pd/C, 1 bar of H_2, EtOH, r.t., 48 h) described by van Beylan yielded the two calix[4]tetrahydrofuran **4a** and **4b** (Scheme 4) in a combined 70% (in a 70/20 ratio, respectively). Our group reported in 2009[90] and 2010[95] the hydrogenation of calix[4]pyrrole **1** leading to two half-reduced diastereoisomers **6a** and **6b** in 23% respectively 2% isolated yields. The totally reduced calix[4]pyrrolidine **3** was isolated as one single diastereoisomer in an unsatisfactory yield of 8% (Scheme 6).[90, 95]

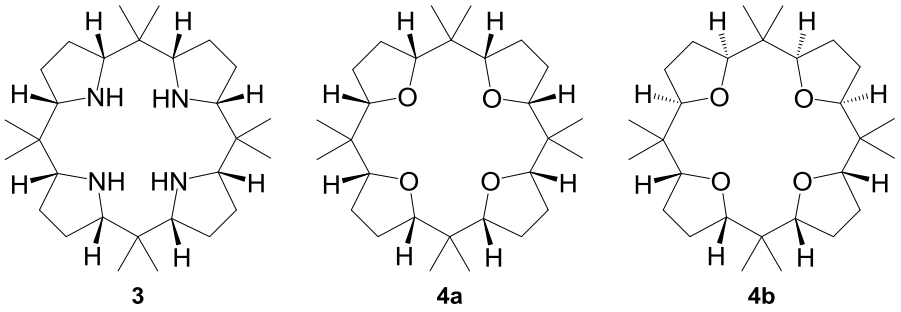

Figure 25. Reported isomers of totally reduced heterocyclic calix[4]arenes before our work on calix[n]tetrahydrofuran[4-n]pyrrolidines

While mild conditions could be applied to hydrogenate calix[4]furan **2**, the hydrogenation of calix[4]pyrrole **1** giving the calix[4]pyrrolidine **3** had been more recalcitrant. The method successfully applied to the hydrogenation of **1** employs 10% Pd/C as catalyst, high hydrogen pressure (100 bars of H_2), high temperatures (100 °C) using acetic acid as reaction medium. These conditions have led to the success of the hydrogenation but only 18% GC yields (8% isolated yield) of product **3** were obtained.

These two macrocycles, calix[4]pyrrole **1** and calix[4]furan **2** respectively, showed dramatic differences in their ease respectively their resistance towards hydrogenation: calix[4]furan **2** can easily be hydrogenated using a variety of different methods, whereas calix[4]pyrrole **1** is "resisting" against most hydrogenation methods and only very specific conditions successful hydrogenation has been reported so far. However the hydrogenation reaction of both compounds was highly diastereoselective. Indeed, the fully reduced macrocycles **3** and **4** possess eight stereogenic centers, all at the α-position of the heteroatoms. The maximum theoretical number of possible stereoisomers is therefore 256 but symmetry within the

macrocycle considerably reduces the number of stereoisomers to "only" 45 isomers. This symmetry was first mentioned by van Beylen for the calix[4]tetrahydrofuran **4**.[93] Only one diastereoisomer of the fully saturated macrocycle for the hydrogenation of calix[4]pyrrole **1** and two diastereoisomers for the hydrogenation of calix[4]furan **2** were observed, isolated and characterized.

2. Hydrogenation using our standard conditions (with Guillaume Journot)

Having developed an access to three isomers of the calix[n]furan[4-n]pyrroles, Guillaume Journot tested the hydrogenation of macrocycles **8** – **10** (Figure 20) under his previously developed conditions with the best amount of palladium catalyst (standard conditions: 100 bars of H_2, 0.3 equiv. of Pd/C, AcOH, 100 °C, 24 h). The three macrocycles were completely soluble at 90 °C in acetic acid. This first investigation led to the synthesis, isolation and full characterization of the corresponding calix[n]tetrahydrofuran[4-n]pyrrolidines **12** – **14** in small quantities per batch of reaction (Figure 26). Single crystals of the three macrocycles were grown for X-ray analysis and will be presented later (page 79, Chapter 4).

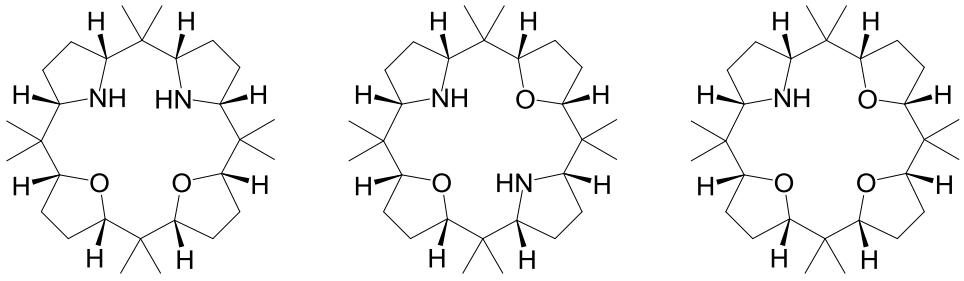

Figure 26. Calix[n]tetrahydrofuran[4-n]pyrrolidines **12** – **14** and their quantities reported by Guillaume Journot

With the development of a scalable access to the four different isomeric calix[n]furan[4-n]pyrroles **7** – **10** the investigation on their hydrogenation was continued on larger scales. The GC yields obtained in the hydrogenation reaction were collected in Table 4 in the next subchapter "screening of the hydrogenation reaction". If this is not specified, the remaining percent were attributed to uncharacterized products. The reductions of calix[4]pyrrole **1** and calix[4]furan **2** (Table 4, Entries 1 and 12) served as reference points. Indeed, in a parallel project, the hydrogenation of the calix[4]furan **2** carried out by Guillaume Journot and Dr. Damien Thevenet under our forcing conditions led without surprise to a complete transformation yielding **4a** and **4b** in an excellent 96% GC yield with an almost 49/45 proportion between the two diastereoisomers (Table 4, Entry 12).

Hydrogenation of **7**, the macrocycle containing three adjacent pyrrole rings, led to **11** as the major compound in 69% GC yield (Table 4, Entry 2) accompanied with four minor compounds in 6:5:4:4 distribution (GC yields in %). No more starting material **7** was detected

in the GC analysis. Two recrystallizations (one crystallization of the crude material followed by a second recrystallization of the resulting filtrate after its evaporation, products was left crystallized in the fridge) of calix[1]tetrahydrofuran[3]pyrrolidine **11** in EtOAc gave the product in disappointing 35% yield due to losses, >99% pure, as very thin colorless needles (Scheme 19). The replacement of only one pyrrole ring with a furan ring compared to calix[4]pyrrole **1** completely changed the outcome of the hydrogenation reaction and permitted a high conversion from compound **7** to **11** when conversion from calix[4]pyrrole **1** to calix[4]pyrrolidine **3** stopped to 18% (Table 4, Entry 1). We were pleased to observe that the reaction did not stop at intermediates and continue towards the formation of the wanted product **11**. The hydrogenation reaction was carried out with a maximum of 450 mg scale of starting material **7** affording 164 mg (35%) of calix[1]tetrahydrofuran[3]pyrrolidine **11**. A single crystal of compound **11** was grown and its X-ray structure in the solid was determined.

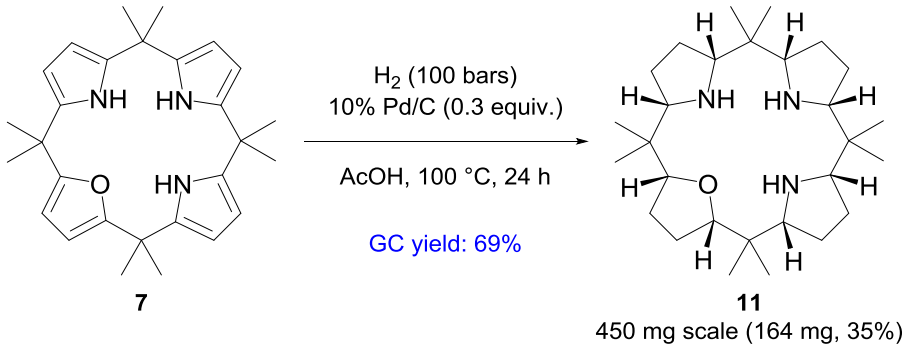

Scheme 19. Catalytic hydrogenation of calix[1]furan[3]pyrroles **7**

The C_{2v} symmetric calix[2]furan[2]pyrrole **8** containing two contiguous pyrrole rings showed a distinctively different behavior. As firstly observed by Guillaume, the catalytic hydrogenation of **8** under the conditions, which had been successful for **7** with three pyrrole rings in the macrocycle, surprisingly afforded a multitude of products. Five major products were detected by GC analysis (with a 30:12:20:4:9 distribution, GC yield in %) accompanied with several other minor peaks (around 2% each). The absence of the starting material **8** was also observed. The crude analysis of the reaction is presented in Figure 27 compared to the crude analysis of the hydrogenation of its isomer **9**. The wanted C_{2v} symmetric macrocycle **12** revealed to be the major product in up to 30% (Table 4, Entry 4). Recrystallization in EtOAc and a silica gel chromatography afforded in Guillaume's hands calix[2]tetrahydrofuran[2]pyrrolidine **12** in 15% yield, 80% pure (Scheme 20). Our attempts to have compound **12** in better purity with additional crystallization or chromatography have all failed. With the low isolated yield and unsatisfied purity of macrocycle **12**, no further hydrogenations were carried out in these reaction conditions (100 bars of H_2).

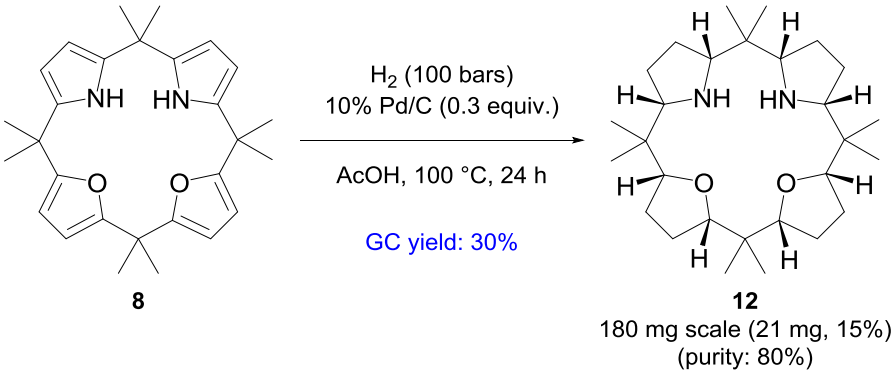

8 **12**
180 mg scale (21 mg, 15%)
(purity: 80%)

Scheme 20. Catalytic hydrogenation of calix[2]furan[2]pyrroles **8**

Hydrogenation of the D_{2h} symmetric calix[2]furan[2]pyrrole **9** by Guillaume gave excellent results with the formation of only one major product according to the GC analysis, in 83% GC yield with no more starting material **9** (Table 4, Entry 5). Recrystallization in EtOAc gave in his hand the fully saturated calix[2]tetrahydrofuran[2]pyrrolidine **13** in 70% yield, 95% pure (Scheme 21). The reaction was scaled up to 1.0 g of starting material without any loss of reactivity and yield (GC yield unchanged). A small decrease of the isolated amount of macrocycle **13** was obtained in this condition after two recrystallizations (same procedure as compound **11**). With the 1.0 g scale experiment, 668 mg (64%) of compound **13** were isolated from the 1.0 g crude material in 98 – 99% purity as big needles. The GC analysis of the mother liquor (100 mg) showed after these two crystallizations a mixture still containing 33% of product **13** but nothing precipitated with an additional crystallization. A chromatography should bring the remaining amount of **13**.

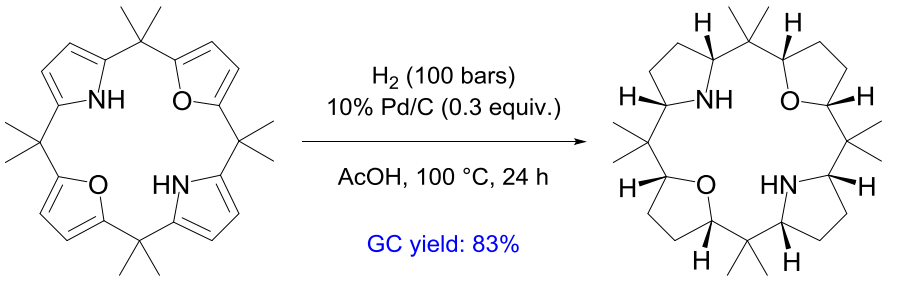

9 **13**
200 mg scale (142 mg, 70%)
1.0 g scale (668 mg, 64%)
(Purity: 98%)

Scheme 21. Catalytic hydrogenation of calix[2]furan[2]pyrrole **9**

Although macrocycles **8** and **9** are two isomers containing both two pyrrole and two furan rings, their hydrogenation with our conditions led to diametrically different results (GC analysis of the crude materials, Figure 27). The hydrogenation of compound **8** with two adjacent pyrrole rings in the macrocycles resulted in a low yield of the desired totally saturated macrocycle **12** (30%) accompanied with several other products while compound **9** with alternated pyrrole and furan rings could be fully reduced efficiently with the formation of **13** in 83% and with excellent diastereoselectivity.

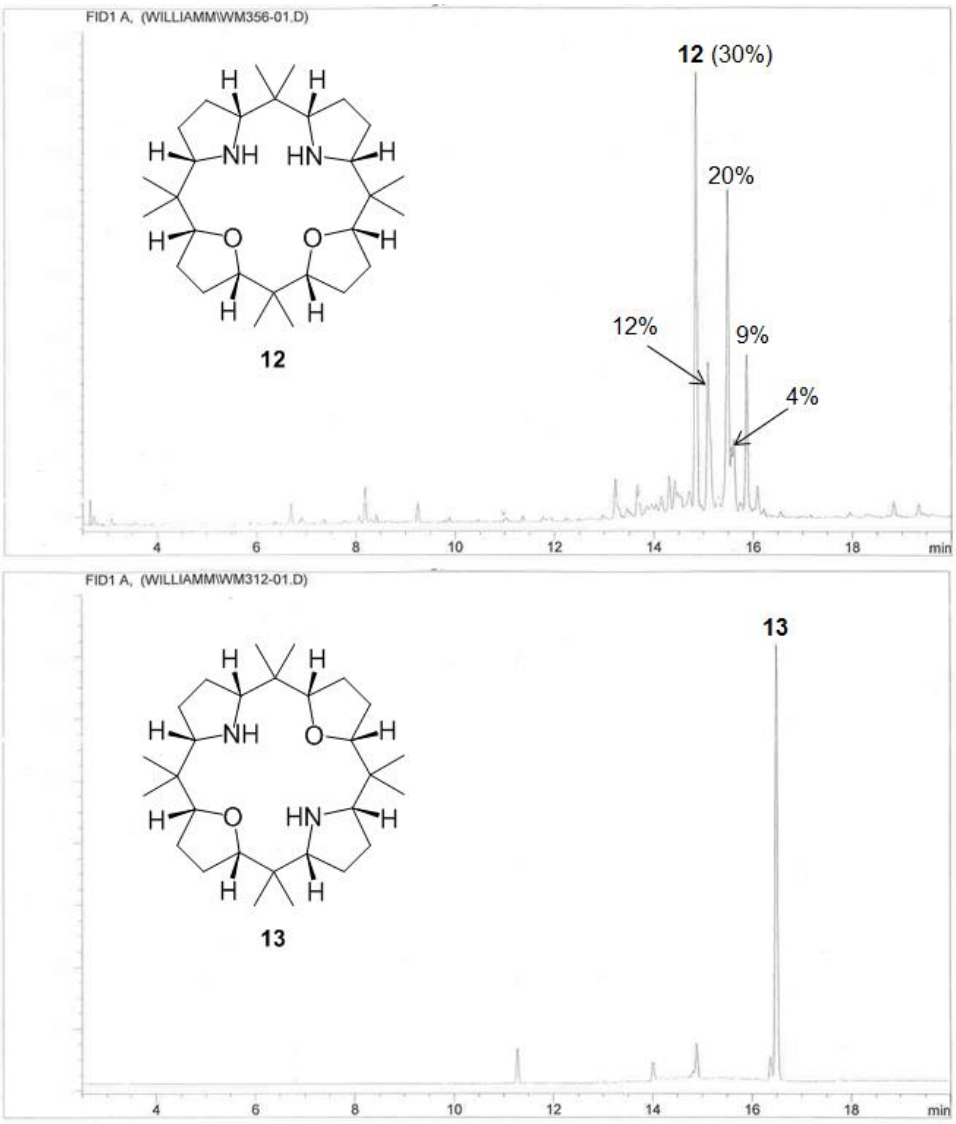

Figure 27. GC analysis of the crude materials obtained after hydrogenation of the two calix[2]furan[2]pyrroles **8** and **9**. Hydrogenation of **8** (above); hydrogenation of **9** (below)

The calix[3]furan[1]pyrrole **10** was reduced smoothly to give compound **14**. The GC analysis of the crude reaction mixture indicated the formation of only one major product in 87% GC yield with no more starting material **10** (Table 4, Entry 8). After recrystallizations in EtOAc, 62 mg of compound **14** were isolated by Guillaume in a 78% yield with a purity >99% (Scheme 22). Since compound **10** could be efficiently obtained in good quantities, its hydrogenation was carried out in up to 1.0 g scale experiments. On the large scale experiment (1.0 g of starting material **10**), the same GC yield were observed (87%) with around 1.0 g of crude material. After two recrystallizations (same procedure as compound **11**), a small decrease was observed in the isolated yield (71%) and the oily resulting filtrate did not crystallize.

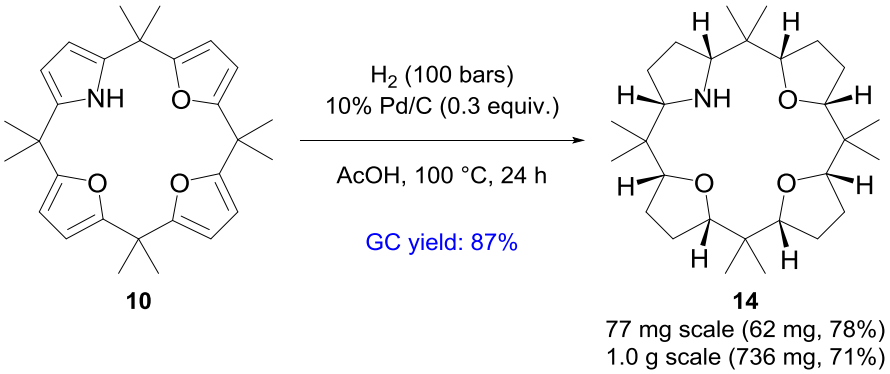

Scheme 22. Catalytic hydrogenation of calix[3]furan[1]pyrrole **10**

To summarize the hydrogenation of calix[n]furan[4-n]pyrroles **7** – **10** using our method with a pressure of 100 bars of hydrogen, three compounds of the four isomers could be smoothly reduced to their fully saturated analogues with good to excellent GC yields. In all reactions, the consumption of the starting materials **7** – **10** was always complete under these conditions and no intermediates were observed as major product. We can affirm that the replacement of at least one pyrrole ring in the macrocycle with its oxygen counterpart, a furan ring, considerably changed the reactivity and allowed the reduction of the macrocycle to proceed.

3. Screening of the hydrogenation conditions

Using the harsh conditions developed for the hydrogenation of calix[4]pyrrole **1** all the macrocycles **7** – **10** could be successfully fully hydrogenated. The hydrogenation of the C_{2v} symmetric ligand **8** was the least satisfactory as the diastereoselectivity of the process was disappointingly low and thereby the isolated yield was comparatively low. To test if the hydrogenation of our products required the application of these harsh conditions, we varied the H_2 pressure. Arbitrarily we tested the hydrogenation using to two considerably reduced H_2 pressures (50 bars and 15 bars) and analyzed the outcome using our GC-based analytics.

Reducing the pressure to 50 bars for the hydrogenation of **7** dramatically decreased the amount of **11** detected to 3% GC yield (Table 4, Entry 3) and mostly led to the accumulation of seven other products. Only 12 mg of crude material were recovered on the 20 mg submitted to the hydrogenation. The major product was detected in 39% (23% GC yield) and the others were between 6% and 12% (respectively 3% to 7% GC yield) in the crude with the absence of starting material. In view of this result we renounced to test this transformation at lower pressures. The hydrogenation behavior of compound **7** (three pyrrole rings compared to four pyrrole rings) shows a close similarity with calix[4]pyrrole **1**. High hydrogen pressures (100 bars) are also required to reduce the three pyrrole rings of macrocycle **7** in order to form the wanted product **11**.

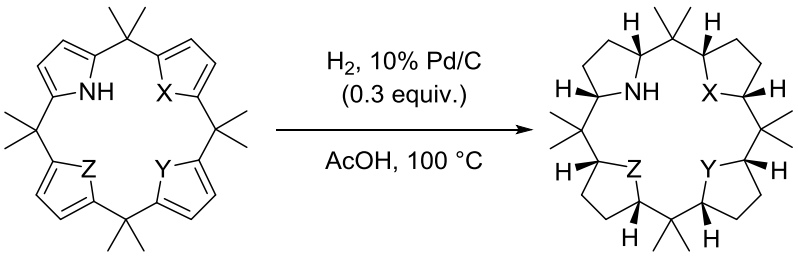

7 - 10
7 (X = Y = N; Z = O)
8 (X = N; Y = Z = O)
9 (Y = N; X = Z = O)
10 (X = Y = Z = O)

11 - 14

Entry	Macrocycle[a]	P. (bars)	Reaction time (h)	Yields (GC) [b] [c]
1	**1**[d]	100	24	**3** (18%)
2	**7**[e]	100	24	**11** (69%)
3	**7**	50	24	**11** (3%)
4	**8**	15 – 100	15 – 24	**12** (30%)
5	**9**[f]	100	24	**13** (83%)
6	**9**	50	15	**13** (75%)
7	**9**	15	15	**13** (65%)
8	**10**[f]	100	24	**14** (87%)
9	**10**	50	2	**14** (94%)
10	**10**	15	2	**14** (89%)
11	**10**	15	1	**14** (69%)
12	**2**[d]	100	24	**4a** (49%), **4b** (45%)

Table 4. Catalytic hydrogenations of calix[n]furan[4-n]pyrroles **7** – **10** compared to calix[4]furan **2** and calix[4]pyrrole **1**. [a] The reactions were performed in an autoclave in acetic acid at 100 °C under variable H_2 pressure using 30 mol% loading of 10% Pd/C. Without any indications the reaction was performed on a 0.046 mmol scale; [b] Yields calculated by GC analysis and mass of the crude material; [c] No more starting material was detected in these experiments; Scale of the reactions: [d] 0.47 mmol scale[95]; [e] 1.05 mmol scale; [f] 2.23 mmol scale

To test the hydrogenation of the D_{2h} symmetric macrocycle **9** we lowered the H_2 pressure to 50 respectively 15 bars leading to full conversion of the starting material. Significantly the product distribution changed: reduced amounts of the macrocycle **13** were observed (at 100 bars: 83%; at 50 bars: 75% and at 15 bars: 65%; see Table 4, Entries 5 to 7). The presence of intermediates or side products renders the purification process more difficult and we did not find conditions were the hydrogenation formed an intermediate as major product. Using 100 bars of H_2 pressure was kept as our preferred conditions for the reduction of the macrocycle **9**. However the reaction could be stopped after 15 h giving the same results as the 24 h reaction. For the complete reduction of compound **9** to obtain compound **13** the pressure could be drastically reduced to 15 bars of hydrogen with only a negligible reduction in the yield of the totally reduced macrocycle. The hydrogenation of **9** shows a different behavior compared to the hydrogenation of the all nitrogen containing calix[4]pyrrole **1**.

Testing the milder hydrogenation conditions using **10** at lower pressure also led to full conversion after only 2 h of reaction. Even under these much milder conditions (50 and 15 bars) the GC yield of **14** were excellent and the values of conversions were essentially the same independently of the H_2 pressure (respectively 94% and 89%) (Table 4, Entry 9 and 10). Reducing the reaction time to 1 h at 15 bars an uncomplete transformation was observed with a reduced GC yield of 69% (Table 4, Entry 11). On larger scale experiment (500 mg of **10**, 20 mg/ml compared to 4 mg/ml for the screening experiments), the hydrogenation occurred more slowly and an unsatisfactory 18% GC yield was obtained after 2 h at 15 bars. Increasing the pressure to 50 bars allowed retrieving an excellent 93% GC yield (70% isolated yield) after only 2 h with the same scale of 500 mg and a 20 mg/ml concentration.

Hydrogenation of **8** carried out at 50 and 15 bars realized by Guillaume gave similar results than the experiment performed at 100 bars with a formation of compound **14** in around 30% (Table 4, Entry 4). These results were reproducible in my hands. In order to have a clue on the structures of the other products formed in this reaction a GC/MS was performed on the crude material of a hydrogenation of calix[2]furan[2]pyrrole **8** after 2 h at 50 bars (Figure 28). Besides the presence of starting material **8** in these conditions, the profile of the GC spectra was similar to the one obtained with our GC method: macrocycle **12** (17.098 min) was obtained as major product with several other compounds. This indicates that the formation of the wanted compound **12** occurred quickly.

GC/MS analysis of the crude material revealed that most of the other products could be reactional intermediates, where part of the eight double bonds has been reduced: 15.58 min (three reduced double bonds), 16.18 min, 17.60 min, 17.68 min and 18.46 min (six reduced double bonds) and 15.85 min (seven reduced double bonds). The analysis also revealed the possible presence of another diastereoisomer of the fully reduced compound **12** at 16.58 min. No assumption was attributed to the second major product of the reaction with a mass of 433.4 at 17.84 min. None of these compounds were isolated.

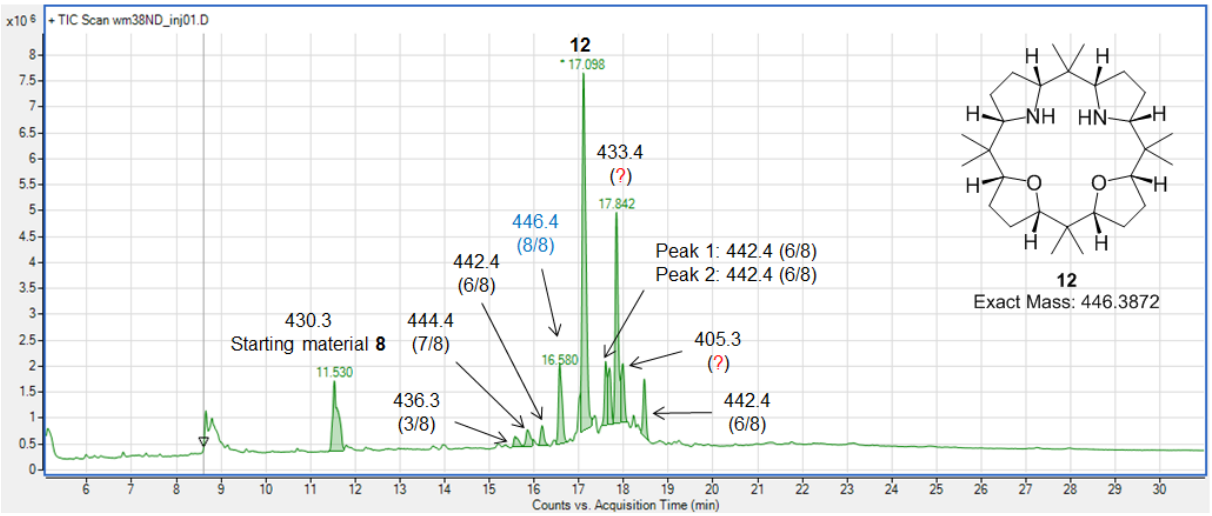

Figure 28. GC/MS analysis of the crude materials obtained after a 2 h hydrogenation of compound **8** at 50 bars. The exact mass of the peaks were presented as well as the hypothetical number of reduced double bonds on the eight double bonds is showed in parentheses.

These results meant the hydrogenation of macrocycle **8** was easily accomplished at low H_2 pressure (15 bars) but an insufficient diastereoselectivity to the formation of the fully saturated macrocycle **14** was observed.

4. Hydrogenation of models 24 and 25

To understand the observed reactivity sequence for the hydrogenation of pyrrole rings depending on the type of neighboring heterocycle, namely either pyrrole or furan, we intended to study the hydrogenation of the small models **24** and **25** (Figure 29).

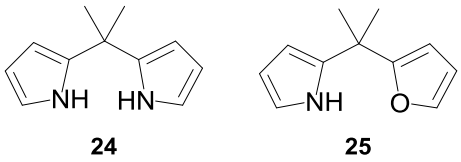

24 **25**

Figure 29. Half macrocycle models **24** and **25**

The synthesis of compound **24** and its hydrogenation into **26** were already described by Guillaume Journot and Anca Pordea in our group. Dipyrromethane **24** was synthetized according to the reported procedure (Scheme 23).[108, 119-120] Condensation of pyrrole in the presence of TFA yielded dipyrromethane **24** in one step. The purification was carried out using a Kugelrohr instead of the purification by column chromatography. The isolated yield and the purity of the product were not diminished by this change in the purification procedure. Compound **24** was submitted to the reported hydrogenation under 65 bars of hydrogen in a MeOH/AcOH (4/1) solvent mixture at r.t. The reaction stopped after the reduction of only one pyrrole ring with forming compound **26** in an excellent 81% isolated yield. Standard

conditions led to the reduction of the two pyrrole rings of **24** with the presence of two diastereoisomers in a 50/50 ratio (GC/MS). The presence of a Brønsted acid was required for the reduction of pyrrole ring(s) of compound **24**. While acetic acid needed to be the solvent of the reaction for the hydrogenation of macrocycles **7** – **10**, the use of acetic acid as additive with methanol as solvent, applying a H_2-pressure of 65 bars and performing the reaction at r.t. was sufficient for the successful transformation to the half-reduced compound **26** in 81% yield.

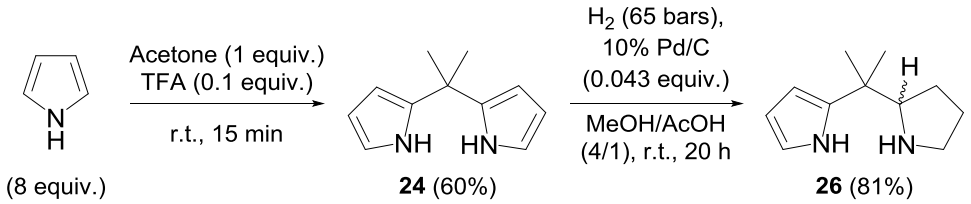

Scheme 23. Synthesis of **24** and its hydrogenation to **26**

We hypothesized that the difficult reduction of calix[4]pyrrole **1** came from the presence of adjacent pyrrole rings in the macrocycle. To explain our results observed in the hydrogenation of the calix[n]furan[4-n]pyrroles **7** – **10**, we were interested to compare these results with the hydrogenation of the model compound **25** containing both pyrrole and furan rings (Figure **29**). We suggested that the presence of only one pyrrole ring should led to the full reduction of compound **25** under the following conditions: 65 bars of H_2, MeOH/AcOH (4/1) at r.t.

Compound **25** was synthesized in two steps starting from furan. We did not optimize the synthesis as we just needed the compound **25** as starting material in order to test its hydrogenation with the previously reported conditions for the hydrogenation of dipyrromethane **24**.

The *ortho*-lithiation of furan by slow addition of *n*-BuLi to a solution of furan in anhydrous THF at -78 °C followed by the addition of anhydrous acetone afforded the dimethylfurylcarbinol **27** in 46% yield (Scheme 24). The condensation of intermediate **27** with pyrrole was proceed following the procedure described by Brown and French.[97] Pyrrole and hydrochloric acid were cold at 0 °C in ethanol and then dimethylfurylcarbinol **27** was added dropwise. After stirring 2 h at r.t., treatment of the reaction and purification by silica gel chromatography compound **25** was isolated in 16% yield as colorless fluorescent oil. This colorless oil slowly turned dark orange after few days in the fridge although it was kept under argon. Nevertheless, the ^{1}H NMR and the GC analysis didn't change. The low 16% yield observed in the condensation reaction is similar to the result of Brown and French (20%) and confirm the drawback of this method for the synthesis of calix[n]furan[4-n]pyrroles.

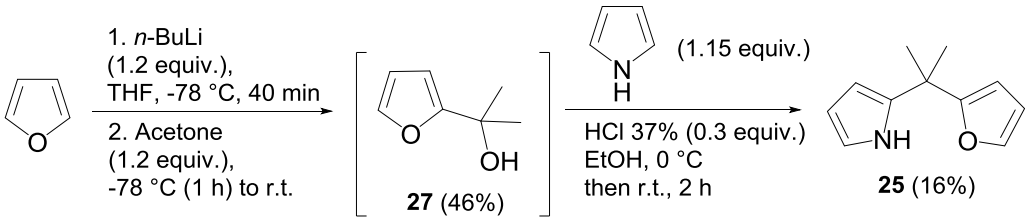

Scheme 24. Synthesis of compound **25**

With compound **25** in hand we could proceed to its hydrogenation. According to our successful hydrogenation of calix[2]furan[2]pyrrole **9** with alternating pyrrole and furan rings in the macrocycle we attended to go to the complete reduction of both heterocycles of compound **25**.

Model compound **25** was hydrogenated using similar conditions used for dipyrromethane **24** (Scheme 25). GC analysis of the crude material showed the presence of a major product in 90% accompanied with two minor products (4% each). GC-MS analysis revealed that the major compound is the wanted product resulting of the full hydrogenation of **25**. Purification on neutral alumina afforded compound **28** in a low 28% yield. Purification on neutral alumina revealed to be unsatisfying to isolate compound **28**.

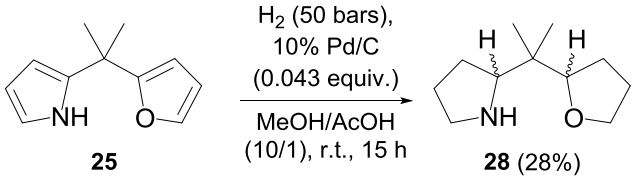

Scheme 25. Catalytic hydrogenation of **25**

The saturated product **28** possesses two stereocenters therefore four isomers could be drawn (Figure 30).

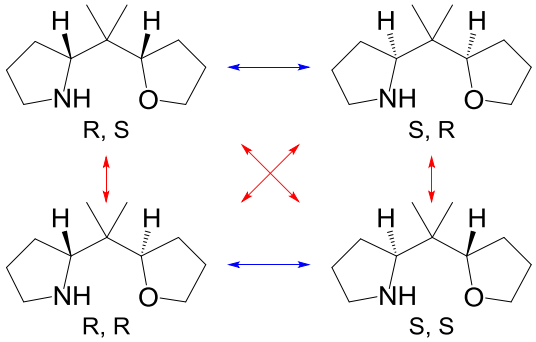

Figure 30. Possible isomers of **28**. Blue arrows: enantiomers; red arrows: diastereoisomers

NMR analyses revealed the presence of two isomers in the isolated fraction in a ratio 70/30. This observation could be easily affirmed with the methyl signals on the ^{1}H NMR (Figure 31, above) and more easily with the ^{13}C NMR where all the signals are doubled (Figure 31, below). Compound **28** is therefore present as a mixture of diastereoisomeric pairs of enantiomers (a total of 4 stereoisomers).

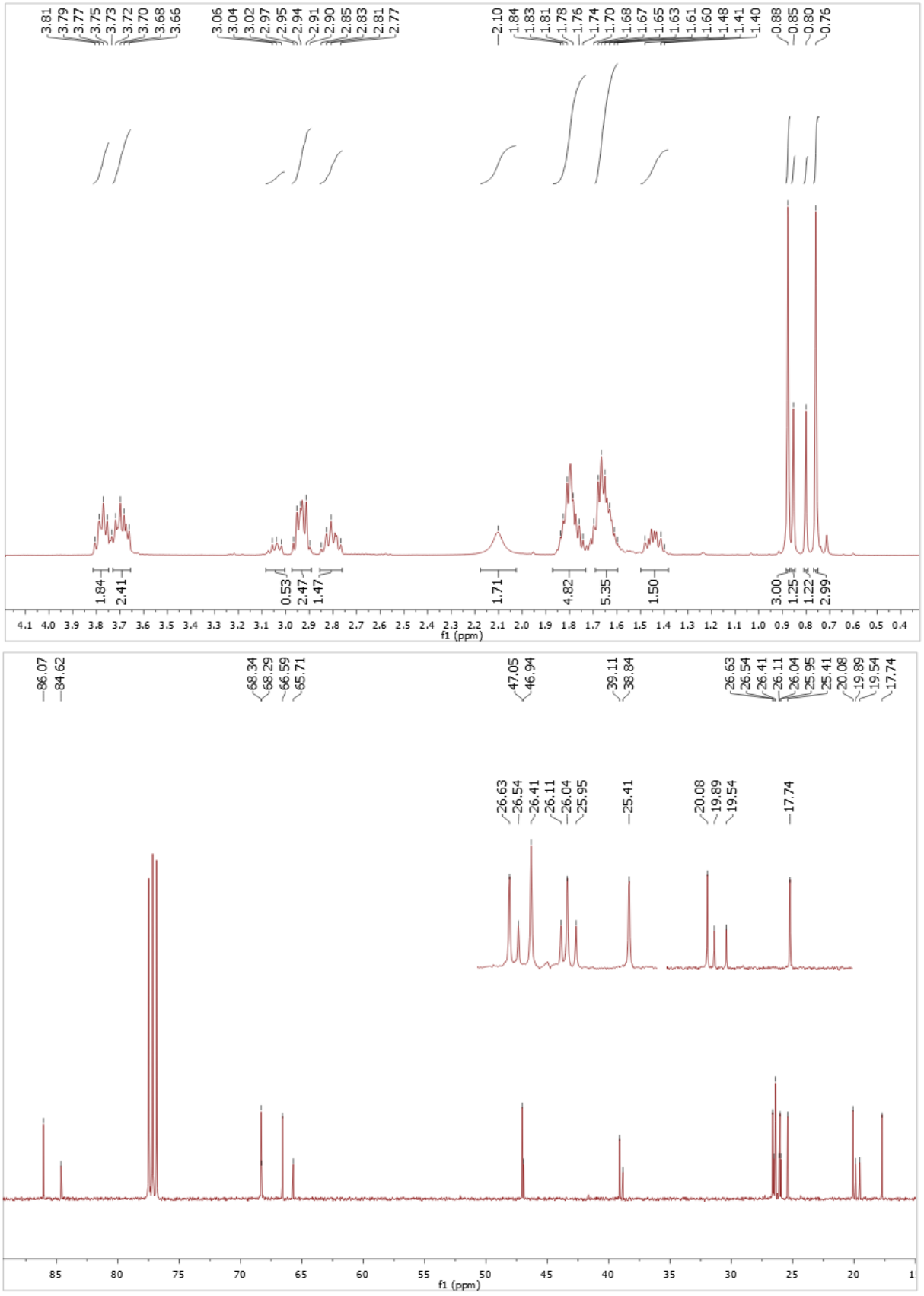

Figure 31. ^{1}H and ^{13}C NMR of isolated compound **28**

The hydrogenation of the model compound **25** containing one pyrrole and one furan ring led to the totally reduced compound **28** whereas the reduction of its analogue **24** with two pyrrole rings stopped to the reduction of only one pyrrole ring.

Our model studies allow us to formulate empirical rules classifying the ease or inversely the difficults to the hydrogenation of the mixed calix[4]furanopyrroles. The empirical rule states, that neighboring pyrrole rings lead to a situation which makes the hydrogenation to the totally reduced macrocycle difficult. This rule is compatible with the difficulties observed to reduce calix[4]pyrrole **1** and calix[2]furan[2]pyrrole **8**. It could also explain the efficient reduction of calix[2]furan[2]pyrrole **9** and calix[3]furan[1]pyrrole **10** (Figure 32). The only one compound which did not follow the predictions using these models is calix[1]furan[3]pyrrole **7**. Although macrocycle **7** possesses three contiguous pyrrole rings this product was efficiently reduced to calix[1]tetrahydrofuran[3]pyrrolidine **11** with a satisfying 69% GC yield.

These models could afford hints on the hydrogenation of macrocycles **7** – **10** but other parameters we did not identify should occur in the reaction allowing either an excellent diastereoselectivity as observed with a unique diastereoisomer for the hydrogenation of **7**, **9** and **10** or low diastereoselectivity to the full saturated compound observed in the reduction of **8**.

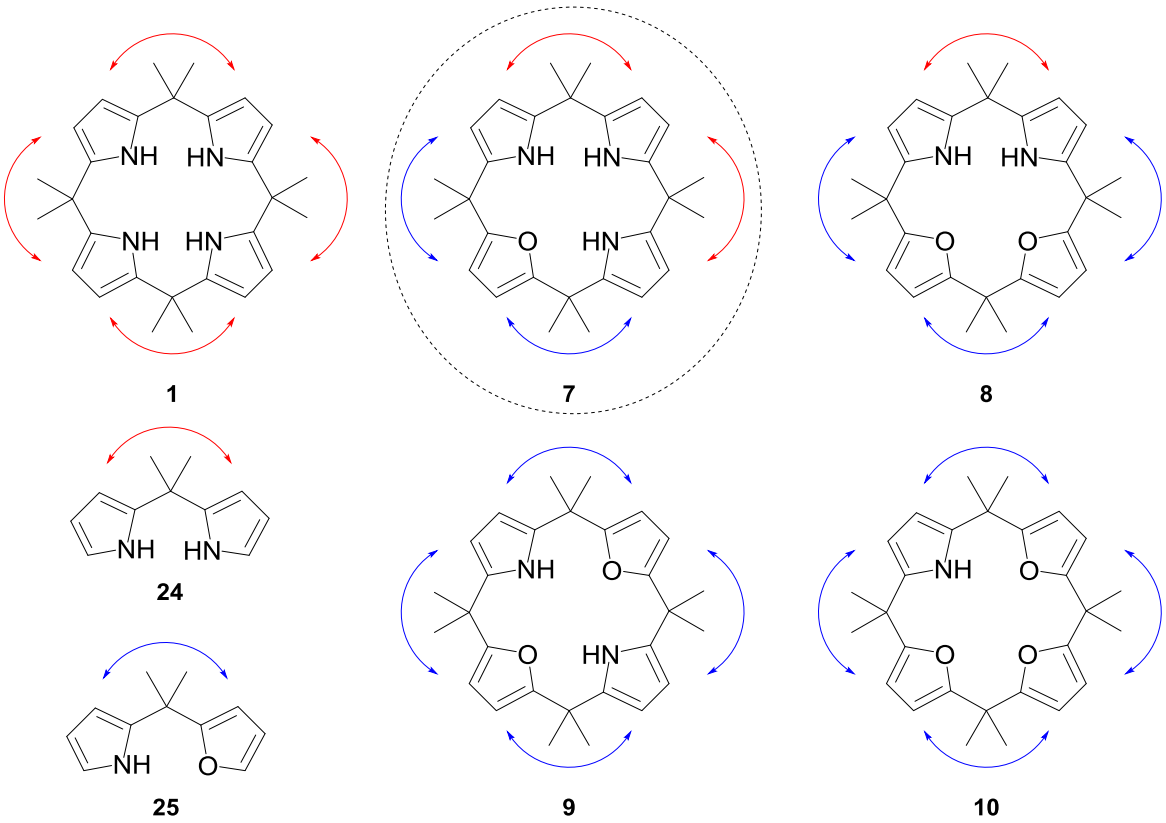

Figure 32. Predicted hydrogenation of pyrrole rings based on our models. Red arrows: difficult reduction; blue arrows: easy reduction

5. Conclusion

The hydrogenations of three of the four macrocycles **7**, **9** and even of **10** proceeded smoothly to give the totally reduced ligands **11**, **13** and **14** respectively with good to excellent yield and in an impressive diastereoselectivity. Although macrocycles **8** and **9** contain both two furan rings and two pyrrole rings, the different positioning of the heterocycles, C_{2v} respectively D_{2h} symmetric, induced significant difference for their reactivity. Isomer **9** with alternating pyrrole and furan rings underwent the hydrogenation smoothly and with good diastereoselectivity, whereas isomer **8** with adjacent pyrrole respectively furan rings showed facilities to be reduced regardless the pressure of hydrogen submitted but a low diastereoselectivity (30% yield) was obtained. The low diastereoselectivity observed in this transformation is so far not explained.

Hydrogenation of models **24** and **25** showed that the reduction of two neighboring pyrrole rings was more complicated compared to the reduction of a pyrrole-furan analogue. Indeed, hydrogenation of model **24** with two pyrrole rings under 65 bars of H_2 stopped to compound **26** with the reduction of one of the two pyrroles in 81% yield. Hydrogenation of model **25** with both furan and pyrrole rings lead to the full saturated compound **28** in a 70/30 mixture of two isomers under 50 bars of H_2). Hydrogenation of calix[1]furan[3]pyrrole **7** went in the same direction with the need of our standard conditions (100 bars of H_2) to be reduced to compound **11**. Reduction of **7** carried out at 50 bars of H_2 dramatically decreased the GC yield to 3%.

Two different conformations in the solid state were obtained among the four calix[n]tetrahydrofuran[4-n]pyrrolidines **11** – **14**. In order to understand and find the reason of these two conformations related to the N/O ratio and position in the macrocycle, a conformational study was realized.

Chapter 4. Conformational study of the calix[n]tetrahydrofuran[4-n]pyrrolidines 11 – 14

1. Conformations of calix[4]arenes and heterocalix[4]arenes

1.1. Conformations of calix[4]arenes

The archetypical calix[4]arenes are composed of four phenols or phenol derivatives linked together in the two *ortho*-*ortho'*-positions by methylene groups (Chapter 1). These four methylene groups are approximately located in a plane according to the data from the crystal structure determination by X-ray diffraction. It is generally believed that the X-ray data are representative for the average conformation of these compounds in solution. The presence of methylene groups allows a relatively free rotation of the aromatic groups. Four possible conformers can be formed, as has been recognized first by Cornforth.[121] These four conformers were named "cone", "partial cone", "1,3-alternate" and "1,2-alternate" by Gutsche depending on the position of the four phenol groups respectively the position of the alkyl substituents in the *para*-position of the –OH (Figure 33a).[122]

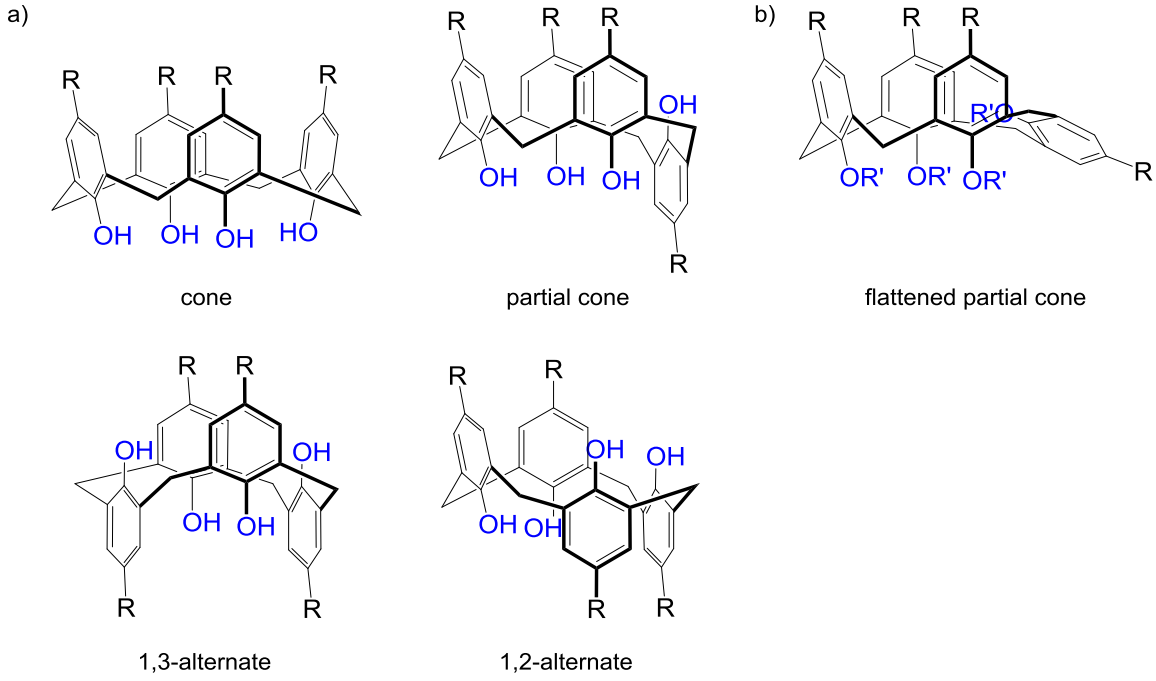

Figure 33. Conformation of calix[4]arenes. a) the four conformational isomers of calix[4]arenes; b) flattened partial conformation of tetra-*O*-substituted calix[4]arenes

For the calix[4]arenes composed of phenol rings, the cone conformation revealed to be the most stable. The consensus rationale for the preponderance of this conformer is to invoke the hydrogen bonding between the four –OH groups. The other forms are however also present in solution but in lower concentrations. Bulky alkyl substituents in the *para*-position of the phenol groups blocked the rotation and locked the conformation in the cone conformer in the

solid state. The *p-tert*-butylcalix[4]arene (Figure 7), the most studied calix[4]arenes with four bulky *tert*-butyl groups, was the first compound to show this cone conformation in the solid state as reported in 1979.[123] The name "calix" of this family of compound is directly linked to this observation. A slightly change in the conformation is observed when some are all of the oxygen atoms of calix[4]arenes are substituted. This is mainly observed with tetra-*O*-substituted compounds which crystallized in the partial cone conformation. These structures are often referred as "flattened partial cone" due to a distortion in the crystal structure (Figure 33b).[42, 124]

1.2. Conformation of heterocalix[4]arenes

1.2.1. Aromatic heterocalix[4]arenes

Like calix[4]arenes, their heterocyclic analogues calix[4]pyrroles and calix[4]furans are flexible molecules with the same conformational properties. They can adopt the same four conformations as the calix[4]arenes (Figure 34). While the cone conformation usually is the most stable conformation for calix[4]arenes, it was shown by Sessler *et al.* by calculation and in the solid state that the 1,3-alternate conformation is preferred for calix[4]pyrroles.[125-127] This 1,3-alternate structure is also the conformation reported in literature in the solid state for calix[4]furans with methyl or cyclohexyl group at the *meso*-position.[128-129] In the presence of anions, the neutral macrocyclic calix[4]pyrroles undergo a change of conformation: due to hydrogen binding of its four –NH protons with the anion the macrocycles adopt a cone conformation (Figure 34).[125, 130-131]

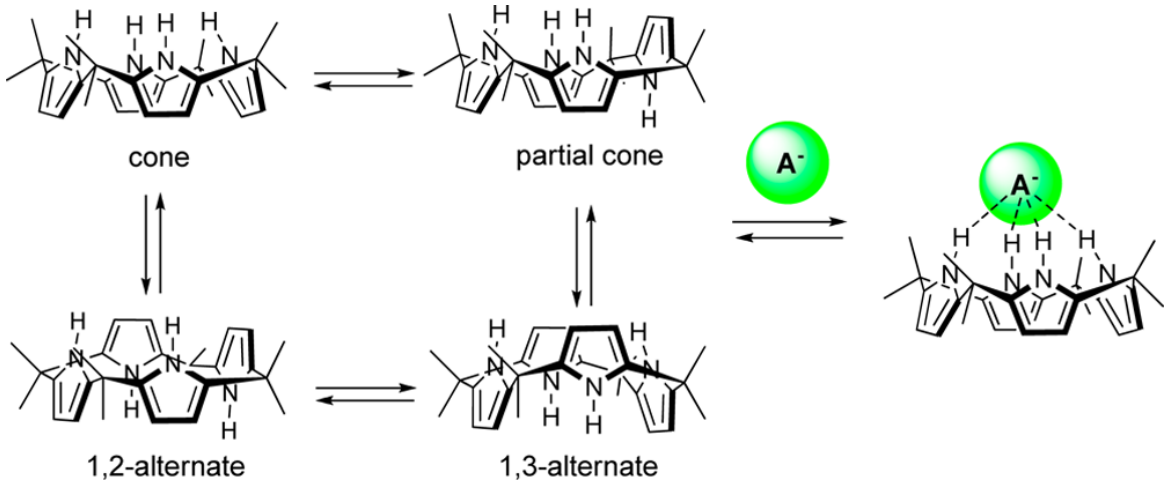

Figure 34. Scheme of the four conformational isomers of calix[4]pyrrole **1** and the change of conformation in presence of anion sources as described by Sessler.[131] Figure taken from the publication

We report in this thesis the optimized synthesis of calix[n]furan[4-n]pyrroles **7** – **10**. Suitable crystals of these four compounds were grown for X-ray analysis (Figure 35). The four structures crystallized in the same tetragonal $P4_1$ or $P4_3$ space groups in the solid state with the 1,3-alternate conformation as the all nitrogen- or all oxygen-containing analogues **1** and **2**.

We are the first to report crystal structures of macrocycles **7** and **8**. The structures obtained by our group and the previously reported structures in the literature are compiled in Table 5.

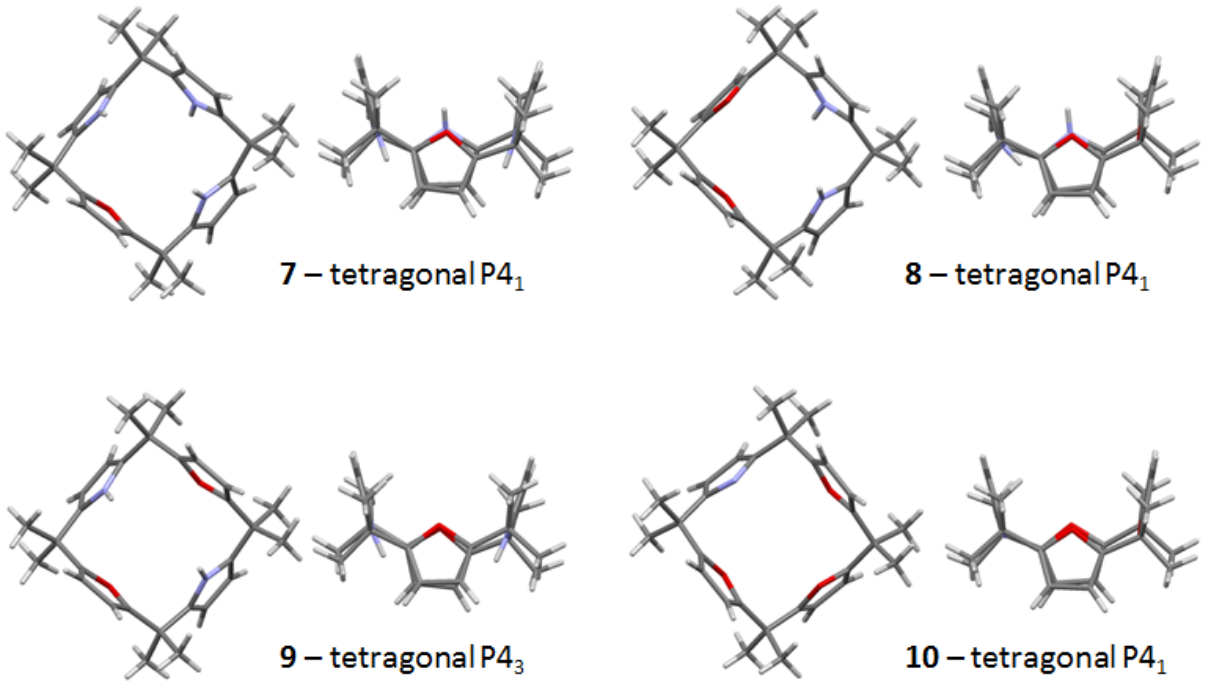

Figure 35. Molecular structures and space groups of calix[n]furan[4-n]pyrroles **7** – **10** obtained in our study. Top views (left); side views (right)

Macrocycles	CSD Refcodes	Space groups
1 – NNNN	VUSFIY[132]	P-1
	VUSFIY01[45]	P4$_1$
	VUSFIY02[133]	P4$_1$
7 – NNNO	Us	P4$_1$
8 – NNOO	Us	P4$_1$
9 – NONO	DUDHEP[99]	P4$_1$
	Us	P4$_3$
10 – NOOO	MOWKEO[102]	P4$_3$
	Us	P4$_1$
2 – OOOO	KADPOU[128]	P4$_1$
	KADPOU01[134]	P-1
	KADPOU02[57]	P-1

Table 5. Space groups of calix[n]furan[4-n]pyrroles. Blue: structures obtained in our group

The calix[4]pyrrole **1** and calix[4]furan **2** both crystallized in two different space groups: the triclinic P-1 and in the tetragonal P4$_1$ space groups. The reported X-ray structures specified that compounds **9** and **10** had crystallized in the tetragonal P4$_1$ and P4$_3$ space group, respectively. The space groups of the two new crystal structures obtained for macrocycles **7**

and **8** both belong to the $P4_1$ group. Compounds **9** and **10** crystallized in our hands in the enantiomeric space group of the one reported in the literature. Macrocycle **9** reported to crystallize in the $P4_1$ space group[99] was crystallized in the $P4_3$ space group in our hand. Similarly the macrocycle **10**, whose crystals were reported belong to the $P4_3$ space group,[102] crystallized in the $P4_1$ space group (Table 5).

1.2.2. Saturated heterocalix[4]arenes

The two fully saturated heterocalix[4]arenes known in the literature are calix[4]pyrrolidine **3** and calix[4]tetrahydrofuran **4a** and **4b** obtained by the hydrogenation of calix[4]pyrrole **1** and calix[4]furan **2**, respectively (Figure 36).

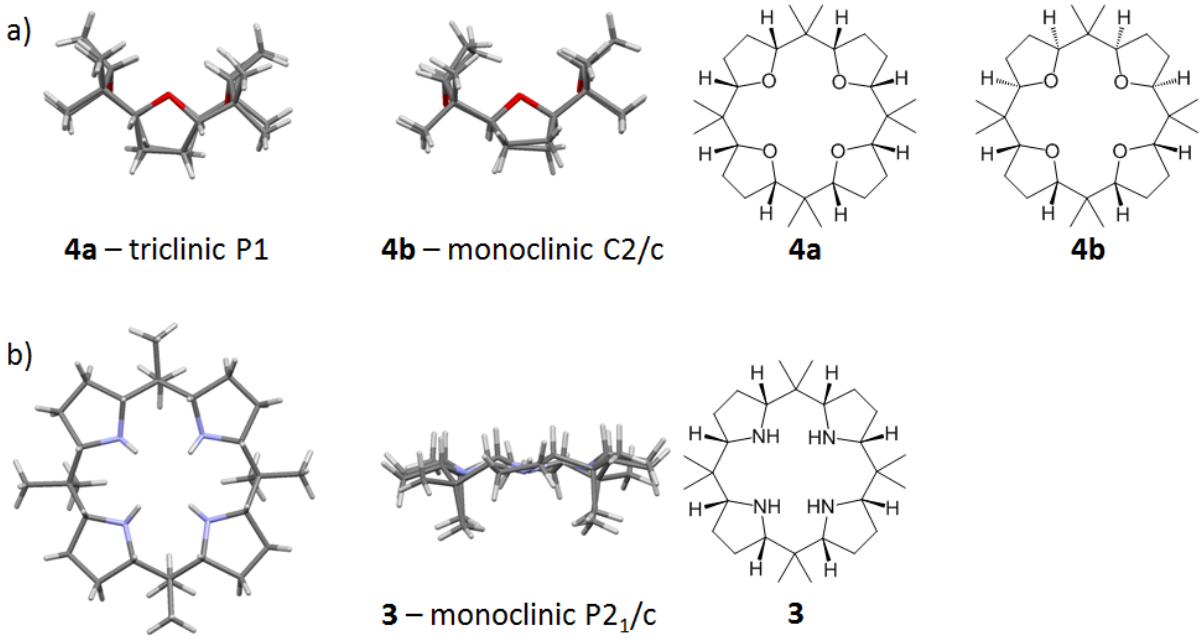

Figure 36. Structural formula and molecular structures determined by X-ray diffraction of: a) Isomers **4a** and **4b** of calix[4]tetrahydrofuran; b) calix[4]pyrrolidine **3**

Isomers **4a** and **4b** of calix[4]tetrahydrofuran were the first representative of this class of compounds reported by van Beylen to adopt the usual 1,3-alternate conformation crystallizing in the triclinic P-1 space group.[93] In our group, these two compounds were synthesized by Guillaume Journot and diastereoisomer **4b** crystallized in his hand in the monoclinic C2/c space group. This new crystal still adopt the 1,3-alternate conformation (Figure 36a).

Calix[4]pyrrolidine **3** reported by our group was the first heterocalix[4]arene which did not crystallize in one of the four conformations of the calix[4]arenes family.[95] Compound **3** crystallized in the monoclinic $P2_1/c$ space group and adopted a unique plate-like conformation (Figure 36b).

2. Introduction to conformational study and polymorphism

X-ray diffraction together with NMR are the two most important techniques for the determination of the structure of organic compounds. Molecular connectivity information together with conformational data in solution can be derived from NMR experiments. NMR data, however, are harder to interpret than X-ray data and they are often strongly temperature and concentration dependent.

With X-ray diffraction, one can determine with high certainty the structure of organic compounds and even their chirality. Beyond molecular structure, X-ray crystal structures also provide a wealth of information on molecular conformations as well as intermolecular interactions involving neighboring molecules in crystals. In solution, molecules are free to vibrate, translate, rotate and even change conformations. In the solid state, however, (and in perfectly ordered crystals in particular), molecules can only vibrate. This restriction in entropy is compensated by the favorable interactions that molecules have in crystals (enthalpy).

Polymorphism is the ability of certain compounds to crystallize in more than one crystal structure.[135] This phenomenon is of particular interest to the pharmaceutical industry because most drugs are delivered as crystalline solid forms.[136] The challenges with polymorphism are that 1) the phenomenon remains unpredictable and 2) that changes in polymorphic form may have important effects on the properties of a material. For example, a change in polymorphic form may impact materials properties such as stability, hygroscopicity, color, mechanical properties, solubility or dissolution rate, some of which are keys to bioavailability.[137]

Polymorphs can be very similar but they can also differ significantly in structural aspects such as crystal symmetry, number of symmetrically independent molecules in the unit cell, the type of interactions present in crystals and even their conformations. Polymorphs displaying significant changes in their conformations may be referred to as *Conformational Polymorphs*.[138-139] Conformational polymorphs are of particular interest to the scientific community because they differ in properties more significantly than polymorphs and they may also be much harder to realize experimentally (compared to packing polymorphism when the difference is a result of a crystal packing). This is the case, for example, of compounds that need to access high-energy conformers in solution in order to crystallize in their most stable polymorphic form.[140]

There is a lack of understanding of how solution chemistry may affect conformational preferences in solution and therefore alter the outcome of crystallizations. In this regard, we present here a combination of computer simulations, crystallization experiments, X-ray diffraction analysis together with solution NMR in order to: 1) determine conformational preferences in the calix[n]tetrahydrofuran[4-n]pyrrolidines **11** – **14** synthesized in this thesis, 2) understand the ability of these compounds to crystallize in several polymorphic forms with various conformations and 3) understand the relationships between solution conformational preferences with the crystallization outcomes.

3. Methods

3.1. Shorthand nomenclature of the studied compounds

The saturated macrocycles **11** – **14** synthesized in this thesis consist of calix[4]arene derivatives containing all possible combinations of four saturated five-member-rings containing either pyrrolidines or tetrahydrofurans. For clarity and to avoid representing each time the structures of compounds **11** – **14**, we will use in this chapter the abbreviation "calix" to refer to these compounds followed by four letters corresponding to the nature of the heteroatoms in the rings in consecutive order. For example, calix-OOOO **4a** corresponds to the all oxygen containing derivative, the calix-NNNN **3** corresponds to the all nitrogen containing derivative and calix-NONO **13** corresponds to the compounds with 50:50 pyrrolidine:tetrahydrofuran alternated (Figure 37). The molar fraction of oxygen (X_O) or nitrogen (X_N) is defined as the amount of oxygen/nitrogen atoms of the total of the four heteroatoms present in the calix compound.

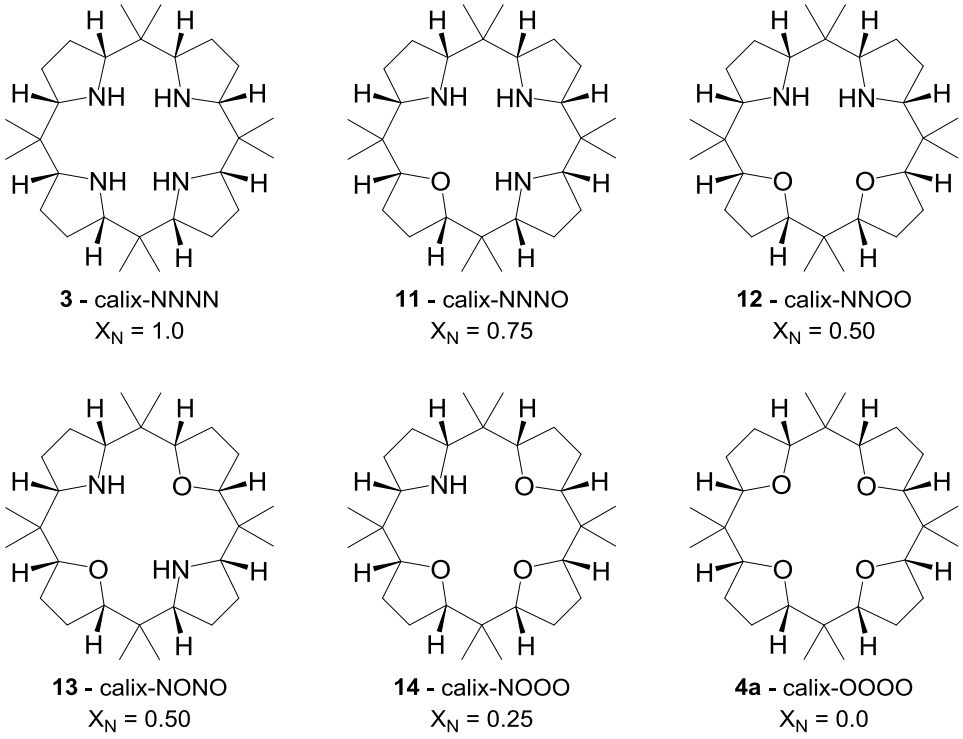

Figure 37. Nomenclature of the calix[n]tetrahydrofuran[4-n]pyrrolidines used in this chapter

3.2. Computational methods (calculations done by Prof. Aurora Cruz-Cabeza)

CSD searches. A search of the Cambridge Structural Database (CSD)[141-142] for crystal structures of calix-compounds returned two entries with CSD refcodes DIVVOT and MUYWOT.

Stability of the various conformations in the gas-phase. Analysis of the conformations found in the structures of DIVVOT and MUYWOT confirmed that the calix-compounds may

display two main conformers (Figure 38): 1) a bowl-like conformer and 2) a plate-like conformer (see below for more information). Based on these, structures of bowls as well as plates were generated with aid of the open-software *Avogadro*[143] for all the calix-compounds synthesized in this thesis.

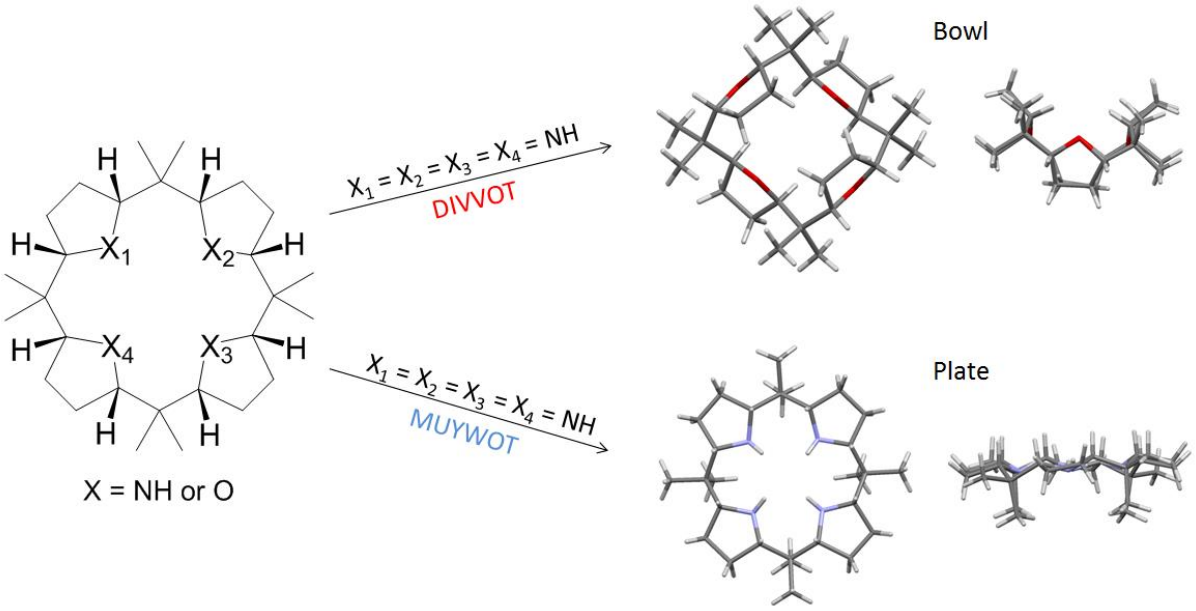

Figure 38. Bowl-like (above) and plate-like (below) conformations found in the calix-OOOO **4a** and calix-NNNN **3**

We note that in the bowl geometry, rings 1 and 3 (containing atoms X_1 and X_3) are equivalent and rings 2 and 4 (containing atoms X_2 and X_4) are also equivalent. As we can see in Figure 38, rings 1 and 3 have the CH_2-CH_2 atoms pointing inside the bowl. By contrast, rings 2 and 4 have the CH_2-CH_2 atoms pointing away from the center of the bowl. If we were to introduce a nitrogen ring, then, it could be sitting in a ring pointing inwards or pointing outwards the bowl center. We will refer to these configurations as N_ring-IN and N_ring-OUT (Figure 39). These two configurations can be easily interconverted by rotations of the all rings simultaneously and they have different energies.

We also note that the position of the proton on the nitrogen atoms is not resolved with X-ray diffraction and so several sub-conformations of the bowls and the plates need to be considered. Nitrogen atoms display pyramidalisation and so the proton can be located in two configurations. We will refer to these configurations as NH-IN, when the proton points towards the center of the bowl/plate, and NH-OUT, when the proton points away from the center of the bowl/plate (Figure 39). These two configurations (NH-IN and NH-OUT) can have significantly different energies and need to be computed separately. We note that these configurations might interconvert via pyramidalisation of the nitrogen. As the nitrogen content increases, so does the number of configurations that need to be considered for simulations.

Molecular geometries for all bowl/plate conformations were generated with the considerations of the configurations above. This resulted in a total of 57 different molecular geometries.

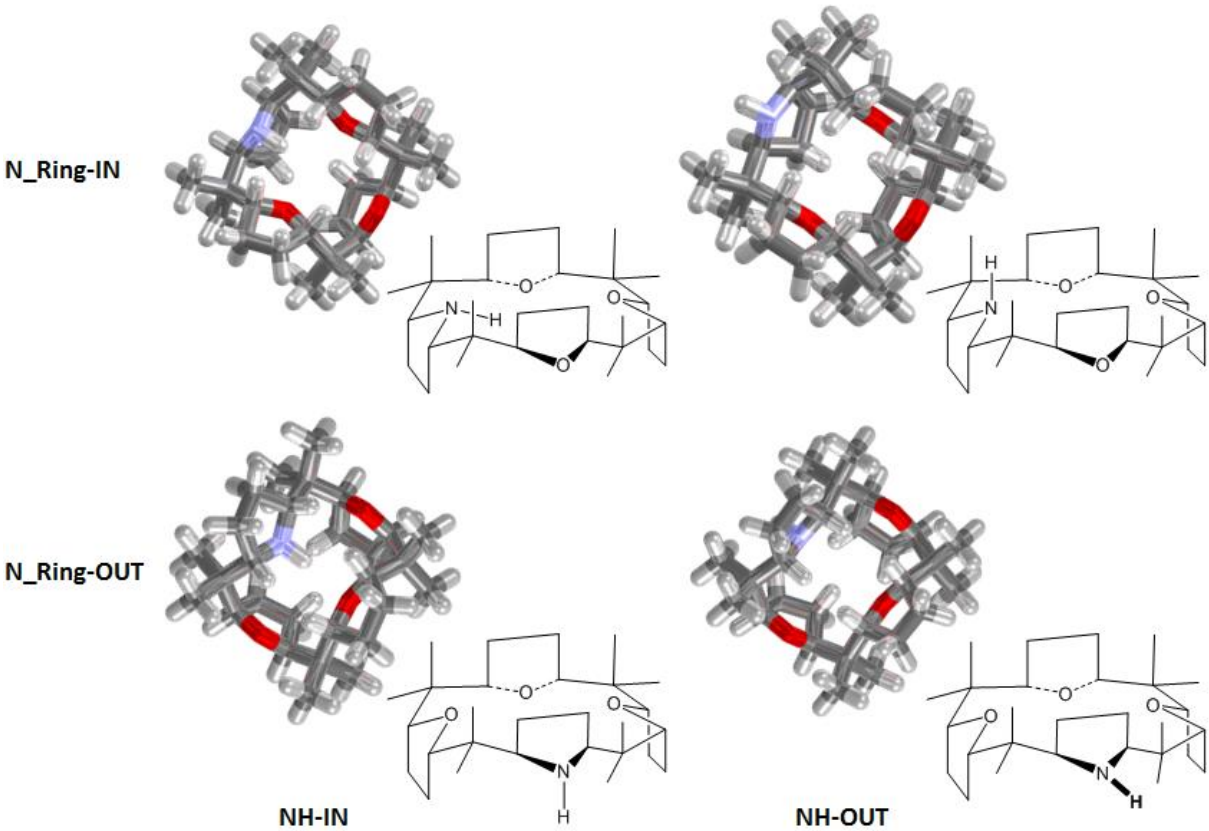

Figure 39. Configurations N_Ring (IN and OUT) and NH (IN and OUT) considered for the bowl conformation of calix-NOOO **14**

The molecular geometries were then geometry optimized in the gas-phase using density functional methods with van der Waals corrections with the software GAUSSIAN09.[144] For this, the B97-d functional[145] was used together with the 6-31+G(d,p) basis set. Geometries were fully relaxed in the gas-phase and molecular frequencies were calculated. Free energies at 298 K were then computed from the vibrational analysis. Energies and free energies were given as the difference between the conformer under study and the most stable conformer for each family of compounds.

^{1}H NMR analysis. Temperature dependent ^{1}H NMR analysis were recorded using a Bruker Avance 400 spectrometer operating at 400.13 MHz (^{1}H) and 100.63 MHz (^{13}C). ^{1}H NMR spectroscopy chemical shifts are quoted in ppm relative to $CDCl_3$ (δ = 7.26 ppm).

PIXEL calculations. PIXEL calculations were used to evaluate the energetics between individual pyrrolidine and tetrahydrofuran rings at different distances. This was done in order to understand the relative changes in stabilities between plates and bowls. The PIXEL method allows the evaluation of intermolecular interactions at a good accuracy and with a relatively low computational cost. The method treats molecules as a grid of approximately 10^6 points (pixels) grouped in super pixels where the electron density is derived from the wave function of a QM calculation.

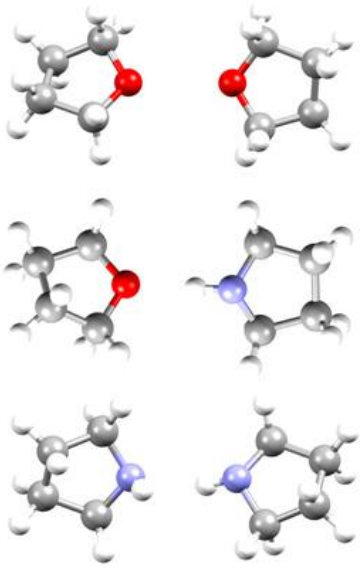

Figure 40. Dimers of THF and pyrrolidine placed at 2.84 Å

Geometry optimisations of tetrahydrofuran as well as pyrrolidine were performed at the B3LYP/6-31G(d,p) level of theory in the gas-phase and using GAUSSIAN09. Electron densities were then derived from those geometries at the MP2/6-31G(d,p) level of theory and were used to derive the PIXEL grids. Rings were then oriented pointing the heteroatoms at each other and the shortest distances found in the bowl conformations, which was 2.84 Å (Figure 40). The intermolecular interactions were then evaluated as the sum of pixel–pixel interactions in the system with the program OPIX. The total PIXEL energy is given the sum of the independent contributions to the intermolecular energy: coulombic, static polarisation, dispersion and repulsion.

Crystal Structure Optimisations and Energies. Density Functional Theory with van der Waals corrections (DFT-d) was used for crystal geometry relaxations of the crystal structures presented in this chapter. Structural relaxations were performed allowing all possible structural parameters to relax (unit cell parameters as well as atomic positions). The PBE functional[146] was used with PAW pseudopotentials[147-148] and the Grimme's van der Waals corrections (d2)[149] as implemented in the VASP 5.3.3 code.[150-153] The Brillouin zone was sampled using the Monkhorst-Pack approximation[154] and a variety of k-point grids. Structural relaxations were halted when the calculated force on every atom was less than 0.003 eV/Å. VASP energies are given per unit cell and so they were divided by the number of molecules in the unit cell for normalization. Energies presented in the text are always given relative to the most stable crystal structure.

3.3. Experimental methods

Microscopy. Images of the calix-crystals were captured on a Zeiss Axioplan 2 polarising microscope with aid of the Linksy software for image editing.

Melting point measurements. Melting points of the calix-crystals were measured with two methods: 1) visually using a hot-stage plate linked to the Zeiss Axioplan 2 microscope and 2) using a Buchi 510 melting instrument. For this, compounds were heated up to 200 °C very fast (10 °C/per minute) and then the heating rate was reduced to 2 °C/per minute until melting was observed. On cooling to room temperature (via fast cooling), recrystallization temperatures were noted.

Differential Scanning Calorimetry (DSC). DSC experiments were performed using a Mettler Toledo DSC 30 instrument controlled by Mettler TC15. A start temperature of 30 °C and a heating rate of 5 °C/min were used up to a final heating temperature of 280 °C. Between 2 and 4 mg of the solid sample was used for the DSC experiments.

4. Conformal aspects of the calix[n]tetrahydrofuran[4-n]pyrrolidines 11 – 14

4.1. Stabilities of bowls and plates

The energies calculations of both bowl and plate conformations for each calix-compound in their different possible geometries were compiled in Table 6. Blue values represent the most stable conformation of each macrocycle considering both bowl and plate models. Red values are the lowest energy geometries calculated for the alternative less stable conformation (very often one or several structures with the same conformation have lower calculated energies than the lowest energy structure with the alternative conformation). We notice that the most stable conformer for all compounds is always a bowl-like conformer except for the calix-NNNN **3**. As the content of nitrogen increases, the plate conformations become more stable relative to the bowl ones.

The 57 geometries were drawn and classified according to their growing calculated energy (Figure 41). We can notice that in several cases the rings-OUT prefer to have their –NH pointing in the macrocycle. This could be observe for calix-NNOO **12** (bowl-1), calix-NONO **13** (bowl-1 and bowl-3), calix-NNNO **11** (bowl-1 and bowl-4) and calix-NNNN **3** (bowl-1 and bowl-2). This could be explain by the fact of the charge of the –NH tried to point toward another oxygen or nitrogen atom. The long distance did not allow a hydrogen bonding but it certainly promoted this type of geometries. Considering calix-NOOO **14**, the –NH of the rings-OUT prefers to point outside the macrocycle (bowl-2 compared to bowl-4).

Compound (X_N)	Bowl-Models*		RE	RE+ZPE	RFE	Plate-Models		RE	RE+ZPE	RFE
OOOO	Bowl-1	----	0.0	0.0	**0.0**	Plate-1	----	70.6	68.1	**64.2**
NOOO (0.25)	Bowl-1	i---	0.0	0.0	**0.0**	Plate-1	i---	42.0	38.1	**32.5**
	Bowl-2	-o--	8.2	4.4	1.7	Plate-2	o---	58.9	54.4	53.8
	Bowl-3	o---	11.1	8.7	6.1					
	Bowl-4	-i--	18.8	17.3	13.2					
NNOO (0.50)	Bowl-1	o--i	0.0	0.0	**0.0**	Plate-1	ii--	26.3	24.7	**23.9**
	Bowl-2	o--o	10.8	9.5	10.5	Plate-2	io--	31.0	31.4	31.1
	Bowl-3	i--i	11.3	13.1	13.9	Plate-3[§]	oo--	-	-	-
	Bowl-4	i--o	19.4	20.6	19.2					
NONO (0.50)	Bowl-1	-o-i	0.0	0.0	**0.0**	Plate-1	i-i-	22.0	17.0	**7.4**
	Bowl-2	o-o-	6.5	1.4	1.6	Plate-2	i-o-	28.2	25.0	21.1
	Bowl-3	-i-i	9.8	7.0	5.6	Plate-3	o-o-	42.8	39.9	38.6
	Bowl-4	o-i-	13.3	11.0	8.9					
	Bowl-5	-o-o	14.3	11.9	5.6					
	Bowl-6	i-i-	19.4	20.4	18.1					
NNNO (0.75)	Bowl-1	o-oi	0.0	0.0	**0.0**	Plate-1	ioi-	5.7	7.7	**6.1**
	Bowl-2	-ioo	0.6	3.4	4.5	Plate-2	oii-	19.6	20.2	21.5
	Bowl-3	o-oo	8.2	7.0	7.1	Plate-3	iii-	19.8	20.6	18.9
	Bowl-4	-ioi	5.1	8.2	10.4	Plate-4	ioo-	18.9	21.5	22.8
	Bowl-5	-ooo	12.2	12.1	13.1	Plate-5	oio-	21.9	24.1	22.8
	Bowl-6	o-ii	9.9	13.7	17.0	Plate-6	ooo-	39.4	40.1	40.7
	Bowl-7	-oii	10.3	15.5	16.8					
	Bowl-8	i-oo	15.9	19.1	17.8					
	Bowl-9	-iii	18.2	20.9	22.0					
	Bowl-10	i-ii	17.6	23.4	25.6					
	Bowl-11	i-io	19.6	25.1	23.3					
	Bowl-12	-oio	23.0	26.8	26.7					
NNNN (1.0)	Bowl-1	oioi	7.8	6.1	**5.4**	Plate-1	oioi	0.1	1.5	**0.0**
	Bowl-2	oioo	8.5	9.2	12.5	Plate-2	oiii	0.0	0.0	0.5
	Bowl-3	oooo	17.3	13.4	15.1	Plate-3	ooii	27.8	25.8	20.4
	Bowl-4	iioo	16.5	18.0	19.5	Plate-4	iiii	33.0	27.2	26.6
	Bowl-5	iioi	19.0	20.0	21.1	Plate-5[§]	oooi	-	-	-
	Bowl-6	ioii	21.6	25.7	28.1	Plate-6[§]	oooo	-	-	-
	Bowl-7	ooio	26.9	28.6	30.6					
	Bowl-8	ioio	24.2	29.7	31.2					
	Bowl-9	iiii	33.3	35.3	38.5					

Table 6. Relative energies (RE), relative energies plus zero point energies (RE+ZPE) and relative free energies (RFE, 298 K) for the models considered. The energies are always given relative to the most stable model for each compound, usually the most stable bowl. Values are given in kJ/mol.*Ring order: Ring-IN (1), Ring-OUT (2), Ring-IN (3), Ring-OUT (4); i = NH-IN, o = NH-OUT; [§]There geometries converged to a different one via amine inversion

Calculations of the plate forms of calix-NNOO **12** afforded the same energies for plate-2 (one –NH-IN and one –NH-OUT) and plate-3 (two –NH-OUT) (Table 6 and Figure 41). Geometry plate-3 with the two –NH-OUT revealed to be unstable and automatically converged in the plate-2 configuration by migration of a –NH in the macrocycle. This inversion of geometry was also observed with calix-NNNN **3** for which plate-5 (three –NH-OUT) and plate-6 (four –NH-OUT) underwent the same inversion of geometry (Table 6 and Figure 41). Interestingly, plate-6 of calix-NNNO **11** with three –NH-OUT did not converge to another configuration but a significant difference of energy was observed compared to the other plate geometries (> 17 kJ/mol, Table 6).

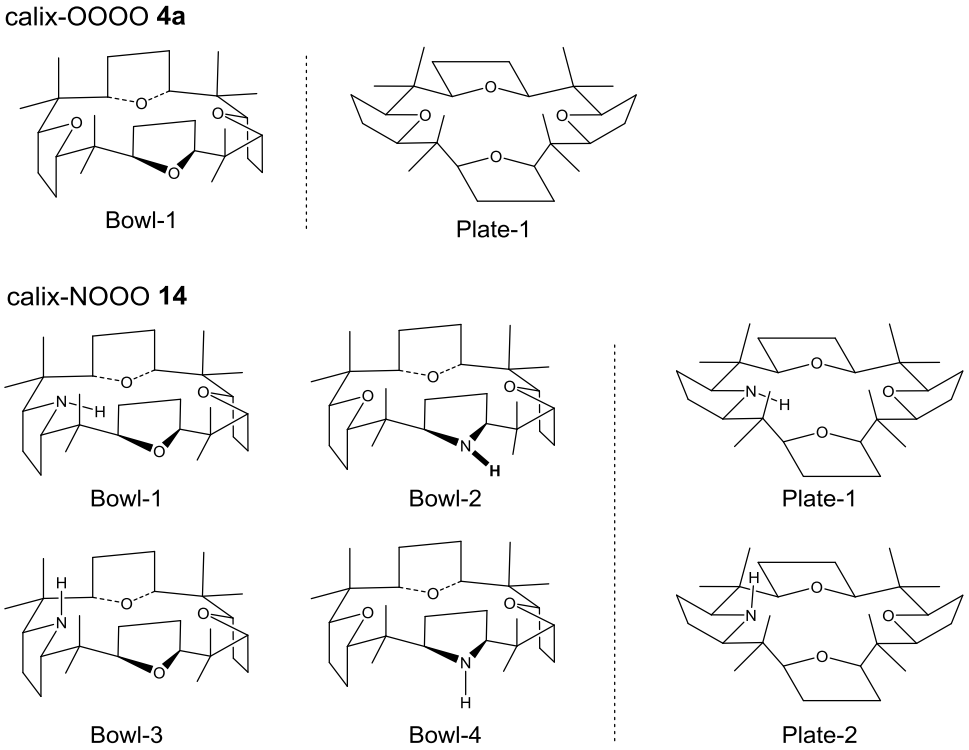

calix-NNOO **12**

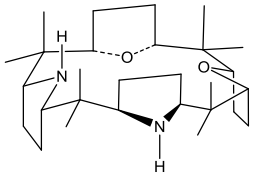

Bowl-1

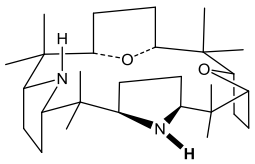

Bowl-2

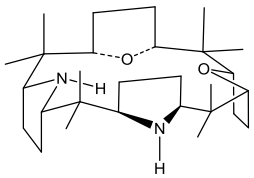

Bowl-3

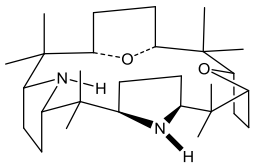

Bowl-4

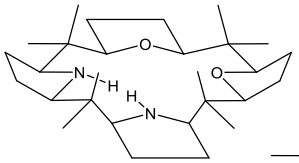

Plate-1

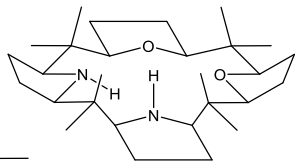

Plate-2

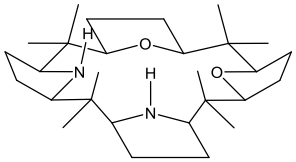

Plate-3

calix-NONO **13**

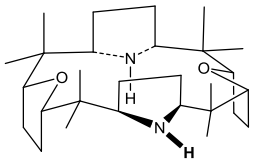

Bowl-1

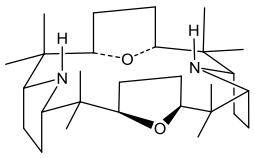

Bowl-2

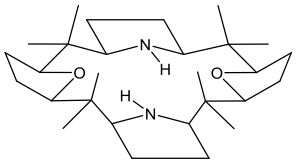

Plate-1

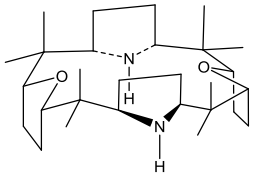

Bowl-3

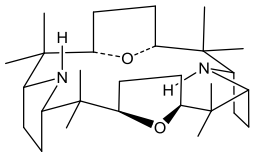

Bowl-4

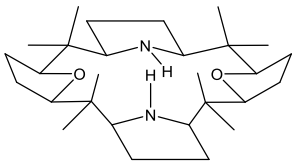

Plate-2

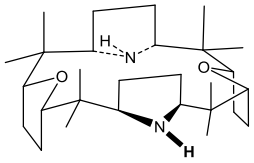

Bowl-5

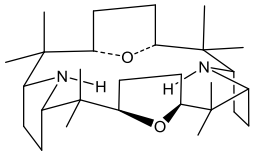

Bowl-6

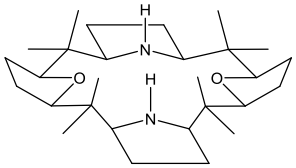

Plate-3

calix-NNNO **11**

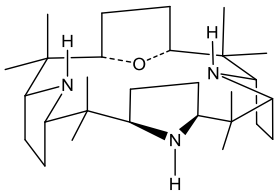

Bowl-1

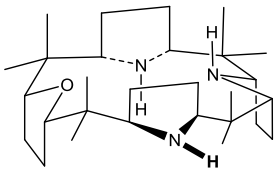

Bowl-2

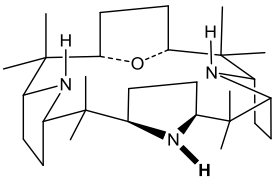

Bowl-3

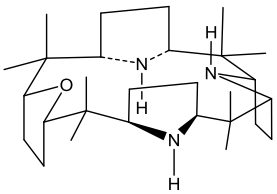

Bowl-4

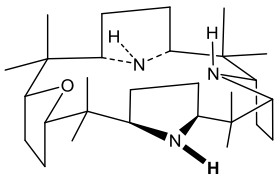

Bowl-5

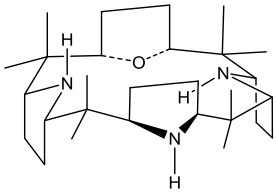

Bowl-6

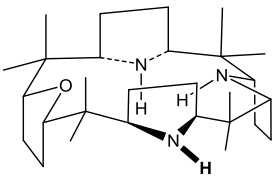

Bowl-7

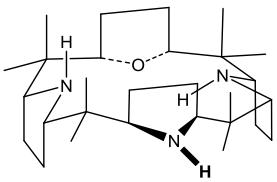

Bowl-8

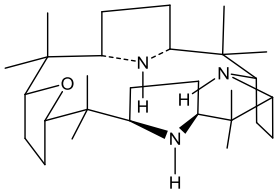

Bowl-9

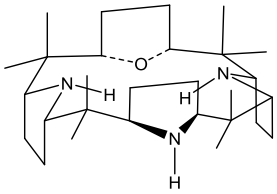

Bowl-10

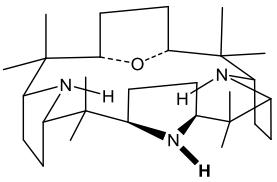

Bowl-11

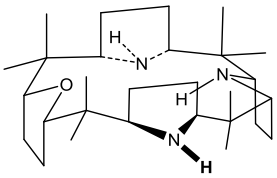

Bowl-12

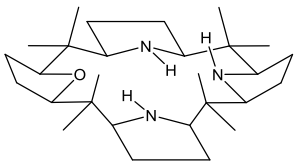

Plate-1

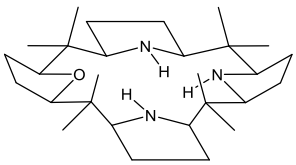

Plate-2

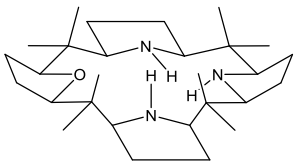

Plate-3

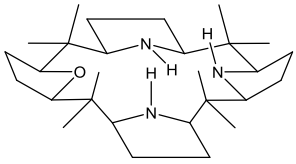

Plate-4

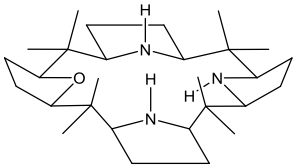

Plate-5

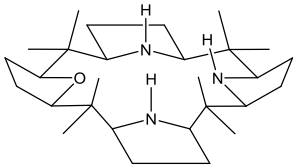

Plate-6

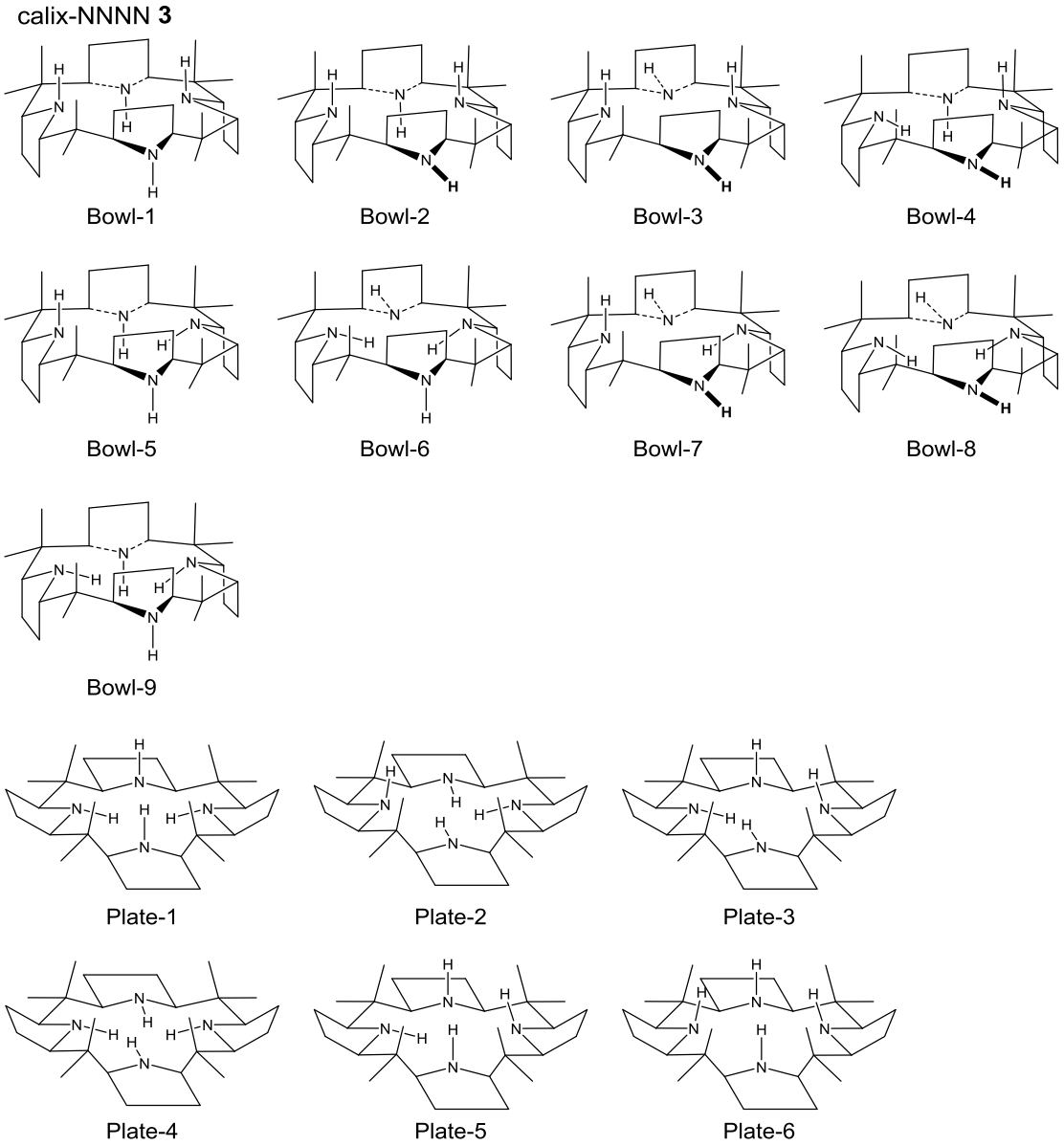

Figure 41. The 57 possible geometries (bowl and plate) of calix-compounds **3**, **4a** and **11** – **14**

The most stable calculated bowl and plate conformations are visualized in Figure 42 together with their relative free energies.

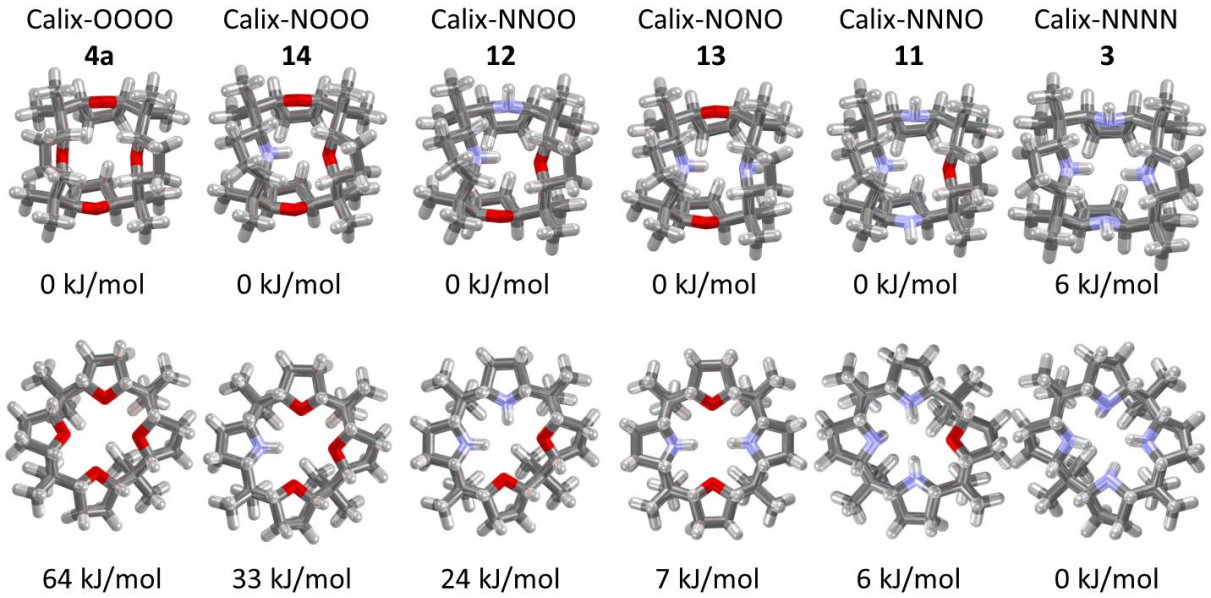

Figure 42. Geometries and relative free energies (298 K) for the most stable bowl (above) and plate (below) conformations of the six calix-derivatives

4.2. Why does the oxygen/nitrogen content affect the stability of the plate conformation?

In order to understand what the effect of oxygen/nitrogen content in the calix-compounds have on the stability of the plate conformers, we performed some PIXEL interaction energies on dimers containing pyrrole and thetrahydrofuran (THF). The dimers were generated using orientation and distances found in the plate conformers of the various calix-compounds. PIXEL interaction energies of these dimers are presented in Table 7. As it can be seen from Table 7, dimers of pyrrolidine…pyrrolidine and pyrrolidine…THF are stable (negative values). The coulombic, polarization and dispersion interactions are all stabilizing with the repulsion being also relatively important. For THF…THF dimers, however, the geometry becomes unstable by 15 kJ/mol. An analysis of the various terms of PIXEL energies reveal that this is due to disfavored coulombic interactions. Having two oxygen atoms in close proximity is just disfavored. This would explain why as we increase the content of oxygen in the heterocalix[4]arene molecules, the plate conformations became considerably less stable.

	E_{total}	E_{coul}	E_{pol}	E_{disp}	E_{rep}
Pyr…Pyr	-4	-30	-13	-14	53
Pyr…THF	-6	-29	-11	-12	46
THF…THF	15	15	-3	-5	8

Table 7. PIXEL energies for the pyrrolidine…pyrrolidine, pyrrolidine…THF and THF…THF dimers as presented in Figure 40.[8] Energies are given in kJ/mol

4.3. Summary of conformer's stabilities

In summary, compounds calix-OOOO **4a**, calix-NOOO **14** and calix-NNOO **12** do clearly prefer the bowl conformations to the plate conformations. For calix-NONO **13**, calix-NNNO **11** and calix-NNNN **3**, the stabilities of the plates and bowls are all within 7 kJ/mol difference (relative free energies, Table 6). For calix-NNNN **3**, the plate is favored over the bowl conformations.

We noted that adjacent rings are located closer to each other than opposite rings in the calix-compounds. This can explain why the calix-NNOO **12** and calix-NONO **13** compounds have very different conformational energies for the plate forms.

5. Crystallographic aspects of the calix-compounds

5.1. Previously known forms

The crystal structure of calix-OOOO (DIVVOT):

- Z' = 1, P-1
- Bowl conformation (as predicted)
- Main interaction is dimer type
- Predicted morphology is chunky crystals

The crystal structure of calix-NNNN (MUYWOT)

- Z' = 1, $P2_1/c$
- Plate conformation (as predicted)
- Main interaction is a 1-dimension chain (continuous)
- Predicted morphology is needles

[8] Energies cited in Table 7: Ecoul = coulombic interaction; Epol = polarization interaction; Edisp = dispersion interaction; Erep = repulsion interaction

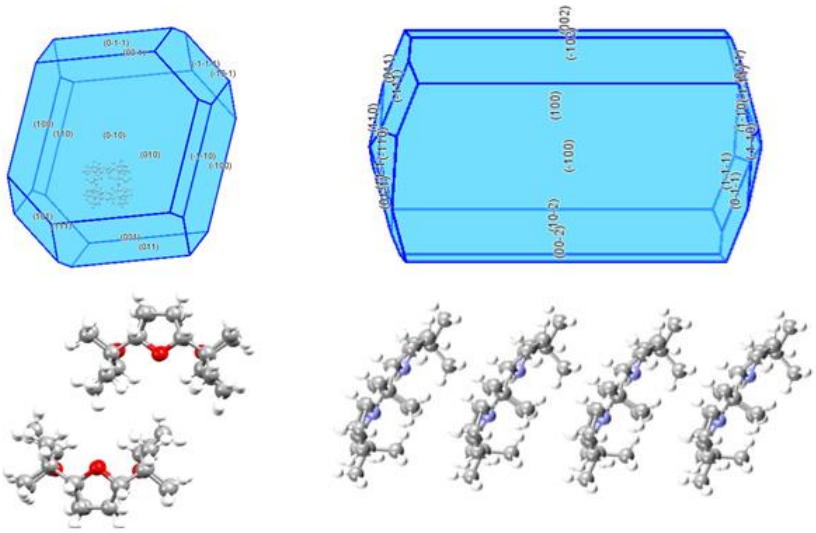

Figure 43. Predicted crystal morphologies (BFDH, upper) and dominant intermolecular interaction (lower) observed in the crystal structures of calix-OOOO **4a** and calix-NNNN **3** (DIVVOT and MUYWOT, left and right respectively).

5.2. Crystal structures of the calix[n]tetrahydrofuran[4-n]pyrrolidines 11 – 14

A set of crystallization experiments was performed for all compounds until crystals large enough for X-ray diffraction were obtained. Single crystals of calix-NNOO **12**, calix-NONO **13** and calix-NOOO **14** were grown using ethyl acetate as solvent. Difficulties to grow a crystal sufficient for an X-ray diffraction analysis were observed with calix-NNNO **11** using ethyl acetate. Crystals were obtained as very thin and fragile needles and the structure could not be determined. A single crystal of calix-NNNO **11** was successfully grown by slow evaporation of dichloromethane. In the same time, crystallizations were tested in presence of acid to crystallize a salt and secure the position of the hydrogen atoms in the α-position of the heteroatoms. A salt of calix-NNNO **11** with TFA as acid was obtained and is presented in the annex (page 163).

As previously described, the calix-NNNN **3** and calix-OOOO **4a** isosters were either present in the solid state in the bowl-like or the plate-like conformers (Figure 43). In Figure 44, the conformations observed in the crystals are summarized indication at the same time the observed space group of the lattice: calix-NNNO **11** and calix-NONO **13** crystallized in the monoclinic $P2_1/c$ as calix-NNNN **3** and present the same plate-like conformation. The other two derivatives, the calix-NNOO **12** and calix-NOOO **14** belong to the triclinic P-1 and showed the bowl-like conformation previously observed with calix-OOOO **4a**. The molecules are totally disordered therefore the differentiation between the oxygen and nitrogen atoms in the crystal was not possible. The structures has been refined by Mme Stoeckli and the occupancy of each atom was fixed for each site depending of the macrocycle (Calix-NNNO **11**: N 0.75, O 0.25; Calix-NNOO **12**: N 0. 50, O 0.50; Calix-NONO **13**: N 0. 50, O 0.50; Calix-NOOO **14**: N 0. 25, O 0.75).

Intramolecular hydrogen bonds were detected in calix-NNNO **11** and calix-NONO **13** but it was not the case for calix-NNOO **12** and calix-NOOO **14**. The bowl-like conformation is not "suitable" for hydrogen bonding because the distances are too big.

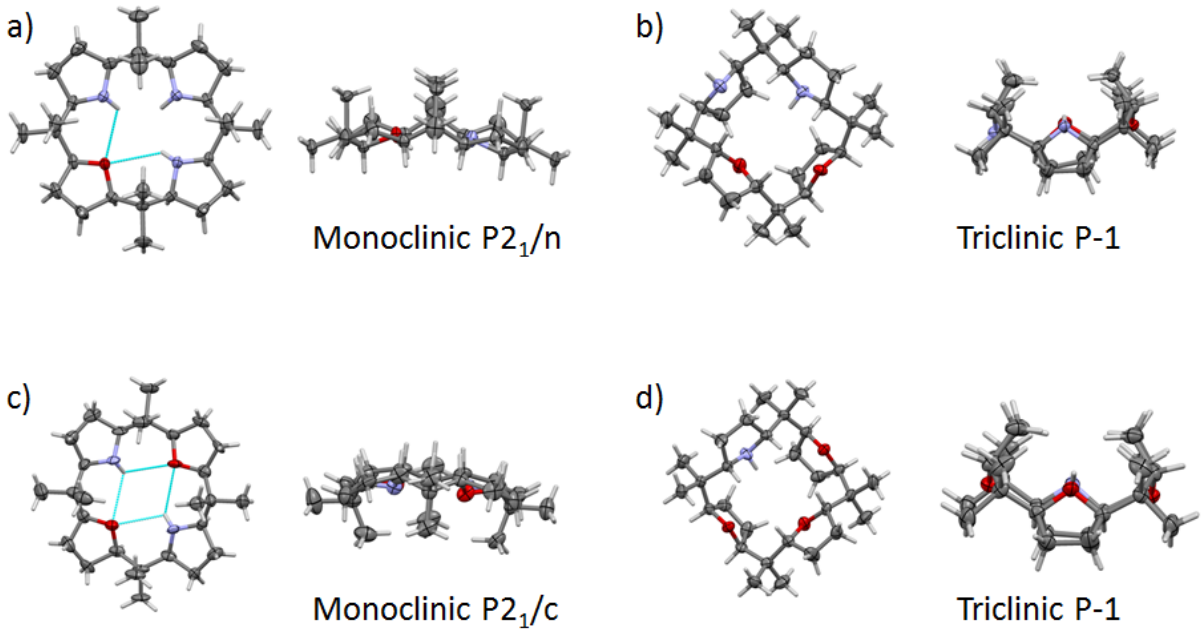

Figure 44. Molecular structures and space groups of the calix-compounds. a) calix-NNNO **11**; b) calix-NNOO **12**; c) calix-NONO **13**; d) calix-NOOO **14**. N-H···O hydrogen bonds are shown as blue dotted lines. Top views (left); side views (right)

Together with the two already known X-ray structures, we have the collection of six different crystalline structures. The structures can be classified in three main types: 1) Triclinic-(bowl), 2) Monoclinic-I-(plate) and 3) Monoclinic-II-(plate). This classification is possible because some of the calix-derivatives are isostructural. Calix-OOOO **4a**, calix-NNOO **12** and calix-NOOO **14** are isostructural and crystallized in the triclinic P-1 space group with similar cell dimensions. Calix-NNNN **3**, calix-NNNO **11** and calix-NONO **13** are isostructural and crystallized in the monoclinic P2$_1$/c space groups where calix-NNNN **3** crystallized in different cell dimensions compared to calix-NNNO **11** and calix-NONO **13**. A summary of the crystal structures adopted by these calix-compounds and their crystallographic information is given in Figure 45 and Table 8.

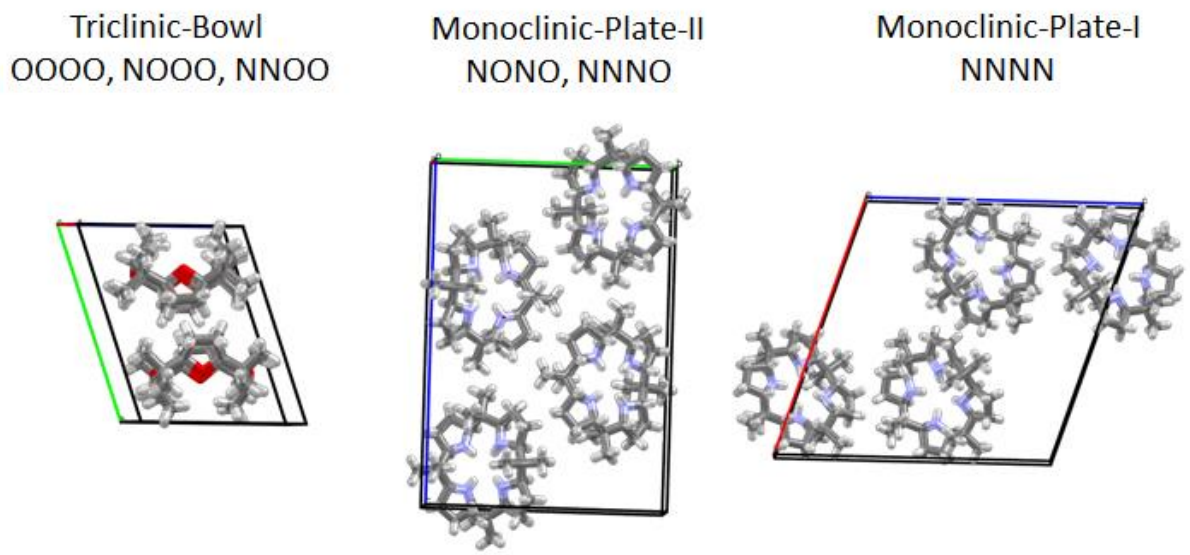

Figure 45. The three types of crystal structures found for the various calix-compounds

Structure type	**Triclinic-bowl**			**Monoclinic-II-(plate)**		**Monoclinic-I-(plate)**
X-Ray Structure Code	DIVVOT	-	-	-	-	MUYWOT
Molecular	OOOO	NOOO	NNOO	NONO	NNNO	NNNN
Structure	**4a**	**14**	**12**	**13**	**11**	**3**
Conformation	Bowl	Bowl	Bowl	Plate	Plate	Plate
Space Group	P-1	P-1	P-1	$P2_1/c$	$P2_1/c$	$P2_1/c$
a (Å)	10.379	10.511	10.509	6.262	6.261	20.825
b (Å)	11.028	11.047	11.084	17.128	17.128	6.331
c (Å)	12.882	12.894	12.699	25.187	25.187	21.050
α (°)	80.0	80.0	80.3	90	90	90
β (°)	70.2	69.7	69.8	104.3	104.3	108.3
γ (°)	71.8	71.8	71.3	90	90	90
T (K)	300	300	173	173	200	173
R-factor (%)	7.2	4.7	7.1	10.9	4.2	9.9

Table 8. Summary of crystallographic information for the previously known forms (DIVVOT, MUYWOT) and the new crystal forms discovered in this thesis

5.3. Microscopic morphologies of the calix-compounds

Images of the crystallites grown for each of the calix-compounds are given in Figure 46 except for the calix-OOOO **4a**, which was not resynthesized in this thesis.

Compounds having the plate conformations in the crystals display needles of slightly different aspect ratios (Figure 46). By contrast, crystals of compounds having the bowl conformers

appear as chunky prims. The stacking of plates formed by the calix-derivatives in their plate conformation gives rise to favorable continuous interaction (Figure 43). Due to this stacking interaction, crystal growth is clearly favored in the direction of the stacks, resulting in needle morphologies. The packing of the calix-derivatives present in their bowl conformations shows dimers as shown in Figure 43. Dimer formation is presumably a fast event. As the dimers are satisfying, packing of those dimers into the crystal has not a particular directional benefit in any specific direction. As a consequence, crystal growth has a good chance to be similar in all directions resulting in chunky crystals.

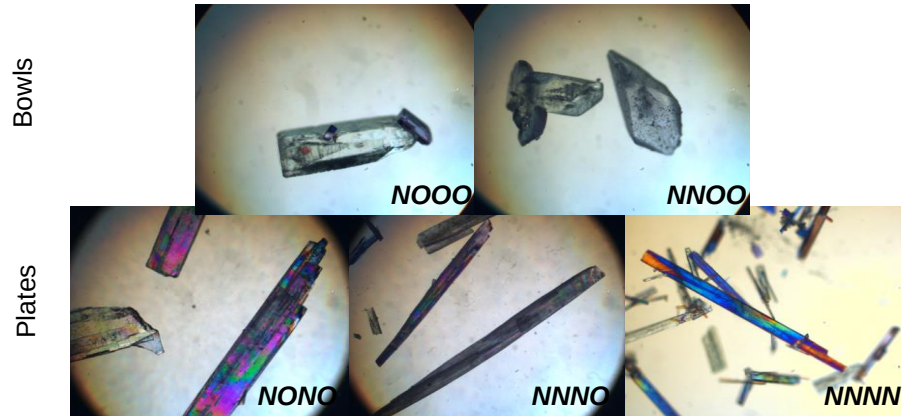

Figure 46. Images of the growth crystals under the polarized microscope

5.4. Behavior of the compounds upon heating and melting

Melting points of these initial set of crystals were recorded and are summarized in Table 9. Together with the melting experiments (capillary and micro hot-stage melting points), DSC measurements were also recorded.

These crystals showed a strange behavior upon melting. This unexpected special behavior made the actual measurement of the melting points complicated with both methods. The heat fluxed measured by DSC did not show any endothermic event for all compounds. The DSC showed no event at all at the transition temperature measured by eye. Melting was completely undetectable via this technique: no heat flux during the heating (experiment repeated twice). We then used a hot-stage microscope and a Buchi 510 instrument to observe the changes during heating of our compounds. The melting points recorded by both methods differed (Table 9).

For the melting point determination using the hot-stage under the microscope we used unpolarized light as well as cross-polarized light. Both visual detections gave the same results and no special behavior could be detected using polarized light. We observed transitions between the crystals as it is at room temperature and complete melting. This observation is illustrated in Figure 47 with calix-NNNO **11**. A pre-melting or sintering phenomena, consisting of the only melting of the shape of the crystals, was observed before the real melting point of the middle of the primitive cell (on a more or less wide range of temperature

depending of the compound). This pre-melting may vary depending of the chosen crystal to observe under microscope and could make the distinction of the melting point difficult. Once the melting point was observed, the heat was stopped and the resulting liquids were cooled to r.t. Recrystallization from the melting were sometimes observed with one or both techniques (Table 9). Pictures taken from the melting at different temperatures using the microscope were shown in the annex (page 168).

Moreover, the discrepancy of melting temperatures between the hot-stage microscope and the Buchi instrument as well as the big ranges of melting (e.g. calix-NNNN **3** 245 – 269 °C) suggests that perhaps various events may be taking place. The samples turned brown in various cases. Hence, there is the possibility of melting and decomposition occurring simultaneously. Further investigation is needed to understand the behavior of these materials upon heating.

Compound	**Conformation**	**Morphology**	**Melting Point (°C) Microscope**	**Melting Point (°C) Buchi**	**Recrystallization (°C) Buchi/(microscope)**
OOOO **4a**	Bowl	-	-	-	-
NOOO **14**	Bowl	Prisms	246	227-229	223/(183)
NNOO **12**[a]	Bowl	Prisms	238-239	-	-/(167)
NONO **13**	Plate	Needles	242	227-228	120/-
NNNO **11**[b]	Plate	Needles	249-255	238-240	No recryst.
NNNN **3**[b]	Plate	Needles	245-269	278	255/-

Table 9. Summary of melting points for the crystals obtained in this study. [a] This compound is only pure to 80%, which could affect the real melting point. Only the microscope melting point was measured but we expect this number not to be very accurate due to the impurities. [b] calix-NNNO **11** and calix-NNNN **3** compounds became brown upon heating so it is possible that they start decomposing already before the melting point

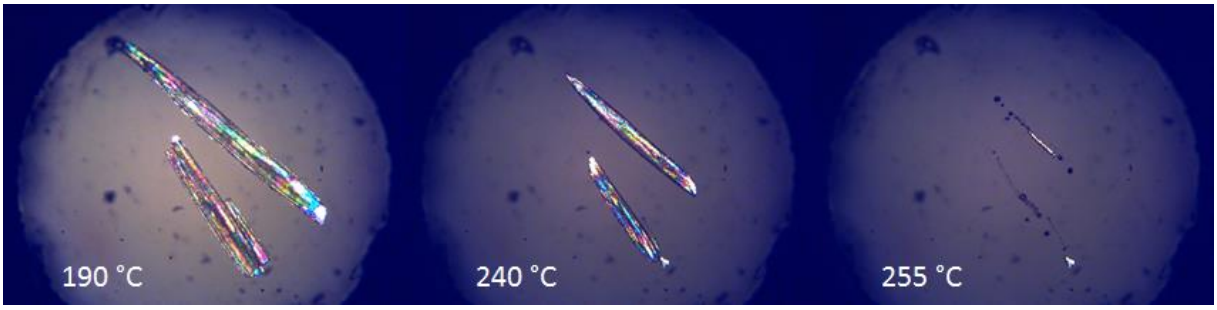

Figure 47. Photos of two crystals of calix-NNNO **11** taken under the microscope at three temperatures: 190 °C (no changes with r.t.), 240 °C (pre-melting was observed) and 255 °C (melting point)

5.5. Is polymorphism and conformational polymorphism possible for these compounds?

All the studied calix-compounds **3**, **4a** and **11** – **14** are similar. The only difference is the isosteric replacement of the heteroatoms which can be either N/O. It is reasonable to assume that this family of compounds may adopt similar crystal structures due to similar packing of the isosteric molecular units. The three compounds presenting the bowl conformation crystallized in three isostructural triclinic forms. The three remaining compounds crystallized in the plate conformations. The observed space groups of the crystals are two monoclinic forms (Figure 45).

In order to do a first theoretical evaluation as to whether polymorphism (and conformational polymorphism in particular) is possible for this class of compounds, all six of the calix-compounds were optimized into the three known lattice types experimentally observed. The relative energies of each compound "squeezed" into the three lattice types were calculated. The results are expressed for each compound relative to the energy value calculated for the bowl conformation inserted into the triclinic lattice (= reference value). A summary of the conformational free energies and relative lattice energies for all the compounds is given in Table 10. Green values indicate the experimental observations whilst yellow values indicate the possible occurrence of polymorphs.

According to the predictions, calix-NOOO **14** and calix-NNNN **3** should be capable to crystallize in different lattice structures as the lattice energy might compensate the difference in energy between the two conformations (see calix-NOOO **14** in Table 10). Calix-NOOO **14** showed identical relative lattice energy for the monoclinic-II-(plate) conformation compared to the reference value calculated for the insertion of the bowl conformation in to the triclinic lattice (0 kj/mol, Table 10). Based on the calculation this compound should be able to show polymorphism. These calculations also revealed that lattice observed for calix-NNNN **3** was not the most stable form. According to our calculations the monoclinic lattice by the presence of the plate conformation is the most stable crystalline form attainable. Surprisingly, the calculation indicates also that the crystalline form obtained (monoclinic-I-(plate)) is slightly less stable than the monoclinic-II-(plate) form by 5 kj/mol.

	Conformations			Crystal			
Compound	**Observed**	**Relative Free Energy (kJ/mol)**		**Observed**	**Relative Lattice Energy (kJ/mol)**		
		Bowl	**Plate**		**Triclinic-(bowl)**	**Monoclinic-II-(plate)**	**Monoclinic-I-(plate)**
OOOO	**Bowl**	**0**	64	**Triclinic-bowl**	**0**	53	61
NOOO	**Bowl**	**0**	33	**Triclinic-bowl**	**0**	0	11
NNOO	**Bowl**	**0**	24	**Triclinic-bowl**	**0**	8	22
NONO	**Plate**	0	**7**	**Monoclinic-II-(plate)**	0	**-21**	5
NNNO	**Plate**	0	**6**	**Monoclinic-II-(plate)**	0	**-17**	0
NNNN	**Plate**	6	**0**	**Monoclinic-I-(plate)**	0	-7	**-2**

Table 10. Summary of relative conformational free energies for bowls and plates of the calix-compounds (**3**, **4a** and **11** – **14**) and relative lattice energies for the three types of lattices expected for these compounds. Green shadows indicate structures observed experimentally; yellow shadows indicate lattice structures which should be accessible according to the calculated energetics

6. Conformational studies by ^{1}H NMR analysis in solution

NMR spectroscopy is an invaluable tool to study structure and dynamics involving molecules either in solution or solid state. Processes such as proton exchange or conformational interconversion may be monitored by variable-temperature NMR spectra, provided the interconversion rate is on the time scale of the NMR experiment. It was demonstrated by Kämmerer[155] and then Gutsche[156] that temperature-dependent ^{1}H NMR is a valuable technique for observing the interconversion between conformers of calix[4]arenes.

Figure 48 shows simulated spectra for a two-site exchange as the rate constant k of the process is progressively increased, from bottom to top. The parameters assumed in these simulations are given in the caption. It can be seen that, when no exchange takes place, i.e., when k = 0, two well resolved peaks may be readily identified, corresponding to the two different chemical environments at shifts ν_A = 240 Hz and ν_B = 160 Hz (0.6 and 0.4 ppm for ^{1}H spins at B_0 = 9.4 T). As the rate constant of the exchange/interconversion increases, or alternatively, as the temperature is increased, a progressive broadening of the peaks is

observed, until coalescence of the two peaks into a single broader one (k = 550 s^{-1}). As the temperature is further increased, a narrowing of this single average peak at $(\nu_A + \nu_B)/2$ = 200 Hz (0.5 ppm for ^{1}H at 9.4 T) takes place. Figure 49 shows simulations analogous to those of Figure 48 in the case where the two sites in exchange are in a 3:1 ratio. It is worth noting that, in the fast-exchange regime, in this case, the average environment is not at $(\nu_A + \nu_B)/2$.

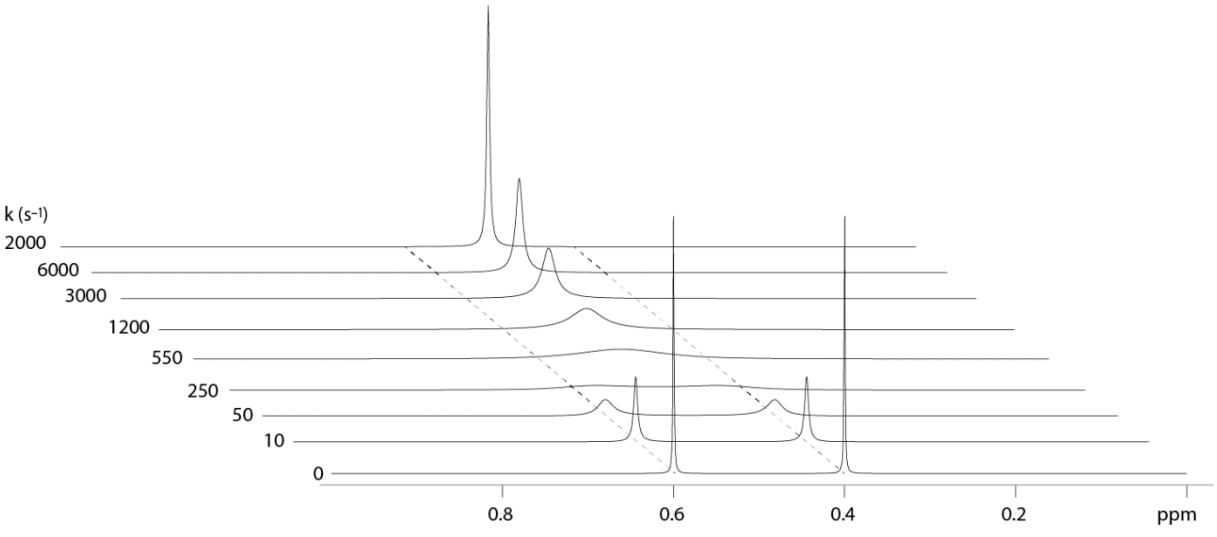

Figure 48. Simulated NMR spectra corresponding to two sites at ν_A = 240 and ν_A = 160 Hz (0.6 and 0.4 ppm for protons in a 9.4 T magnet) in 1:1 ratio as the exchange rate constant k is progressively increased. A line broadening of 0.5 Hz was assumed for both peaks. The two chemical shifts when $k \sim 0$ are indicated by dashed lines

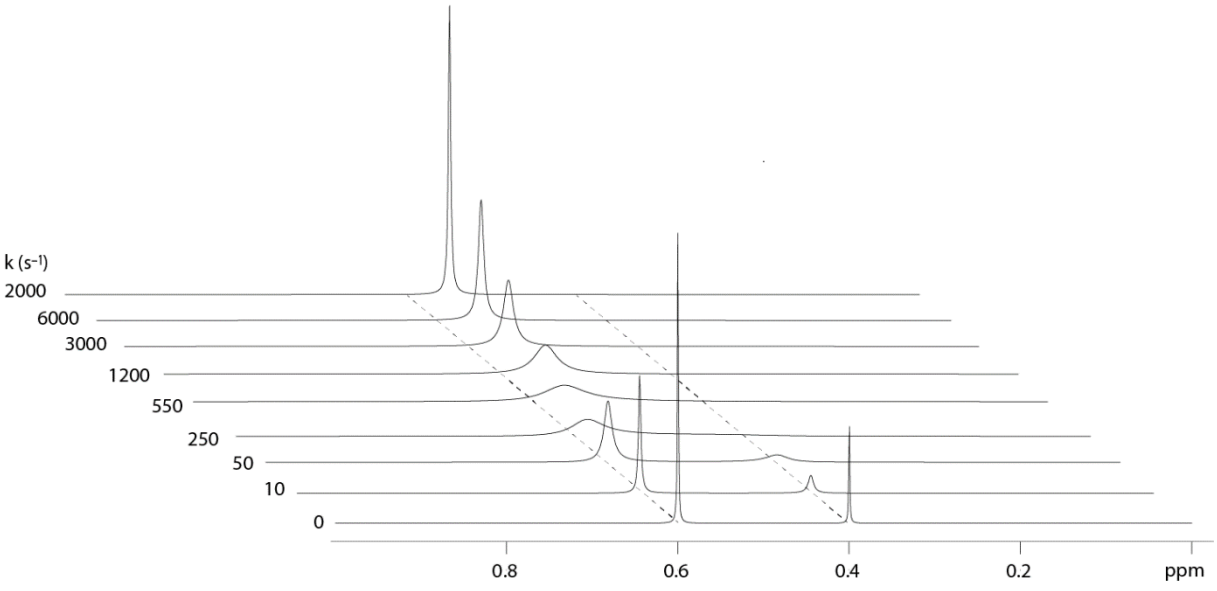

Figure 49. Simulations analogous to those of Figure 48 for two sites in 3:1 ratio

When the coalescence temperature is reached, the first-order rate constant k_c may be readily determined by $k_c = \pi \Delta\nu/\sqrt{2}$, where $\Delta\nu$ is the chemical shift difference when k ~ 0 Hz. At any other given temperature, the rate constant may be determined by numerical fit of the

experimental line shapes. The Gibbs activation energy $\Delta G^{\#}$ (in kcal/mol) can be then easily determined by the Eyring equation $\Delta G^{\#} = 4.574 \times 10^{-3} T \left(log \frac{T}{k} + 10.318 \right)$, where T is the temperature in K.

Interesting information might be obtained studying the ^{1}H NMR of calix-NOOO **14** and calix-NNNN **3** and their possible temperature-dependence. According to the calculations the two compounds were predicted to crystallize in different lattice structures. Correlating the observed crystal structures, the calculated predictions and the temperature-dependence of the ^{1}H NMR spectra might allow obtaining a complete picture of the conformational behavior as well in solution as in the crystal. The first NMR characterization of our calix-compounds was done with the goal to fully and unequivocally characterize the molecular structures after their synthesis. The ^{1}H NMR spectra of calix-NOOO **14** and calix-NONO **13** had to be measure at low temperature to obtain the ^{1}H and ^{13}C NMR spectra suitable for the full attribution of all the observed peaks. In contrast the calix-NNOO **12**, calix-NNNO **11** and calix-NNNN **3** could be easily analyzed at room temperature. As low temperature ^{1}H NMR spectra were needed for the complete attribution of the peaks of calix-NONO **13** this compound was added to the NMR study. Therefore the ^{1}H NMR spectra of the three compounds calix-NOOO **14**, calix-NONO **13** and calix-NNNN **3** were measured at variable temperatures from -55 °C to +55 °C.

The ^{1}H NMR spectra of calix-NNNN **3** measured from -55 °C to +55 °C did not reveal any dynamic conformational process (Figure 50). The signal which underwent the most pronounced changes was the amine signal of the pyrrolidine rings at around 2.1 ppm. At low temperatures (up to -15 °C) the –NH did not exchange with the traces of water in $CDCl_3$. The –NH coupled with the two equivalent neighboring protons (positions 2 and 5) therefore the signal was a triplet. At higher temperatures the exchange between the –NH and water became faster and the coupling was lost. The resulting –NH peak becomes broader. Concomitantly all the protons become broader, which indicates that the process observed at the –NH signal and due to the –NH signal is not exclusively suppressing the coupling due to an exchange mechanism. Our tentative interpretation attributes these effects to protonation-deprotonation of the pyrrolidine nitrogen atoms due to the presence (formation) of HCl by the solvent. This interpretation is compatible with the broadening of all the observed signals.

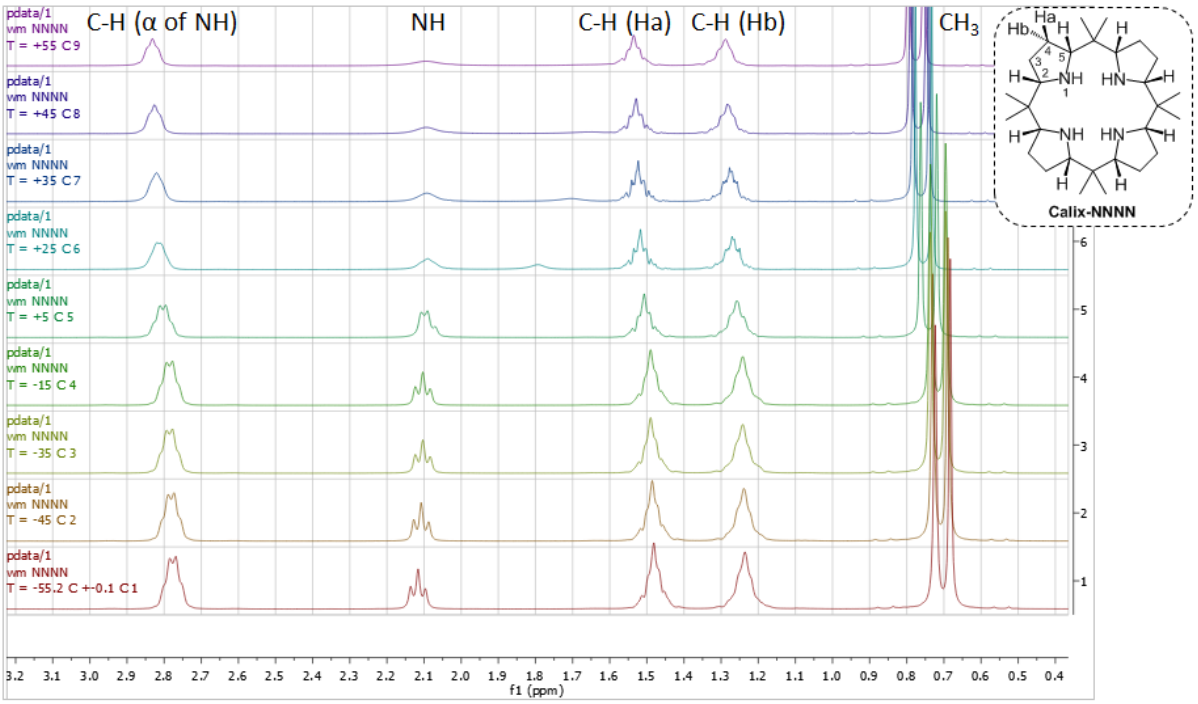

Figure 50. 400-MHz ^{1}H NMR spectra of calix-NNNN **3** IN $CDCl_3$ at variable temperatures (from -55 °C to +55 °C)

The studies of the low temperature ^{1}H NMR spectra of calix-NONO **13** showed a similar behavior (Figure 51). Moreover, we observed a considerable temperature dependent diamagnetic shift of the –NH signal by 0.203 ppm (Table 11) and concomitantly a broadening of the signal by increasing the temperature from -55 °C to +25 °C. A temperature dependent diamagnetic shift was also observed for all the other peaks. It may be notified that a bigger shift was observed for the protons located in the α-position of the nitrogen atom (+0.070 ppm) compared to the protons in the α-position of the oxygen atom (+0.015 ppm) (Table 11). A pronounced chemical shift of the protons Hb of the pyrrolidine rings was observed (+0.185 ppm) accompanied by coalescence with the peak 2' (Figure 51, 25 °C). At the lowest temperature of -55 °C, a new series of points started to appear (Figure 52). The occurrence of this new series of peaks at -55 °C is a clear indication of the occurrence of another minor conformer. Unfortunately further characterization of this isomer is hampered by the temperature limit imposed by the solvent. Signs of dynamic processes were observed with calix-NONO **13**.

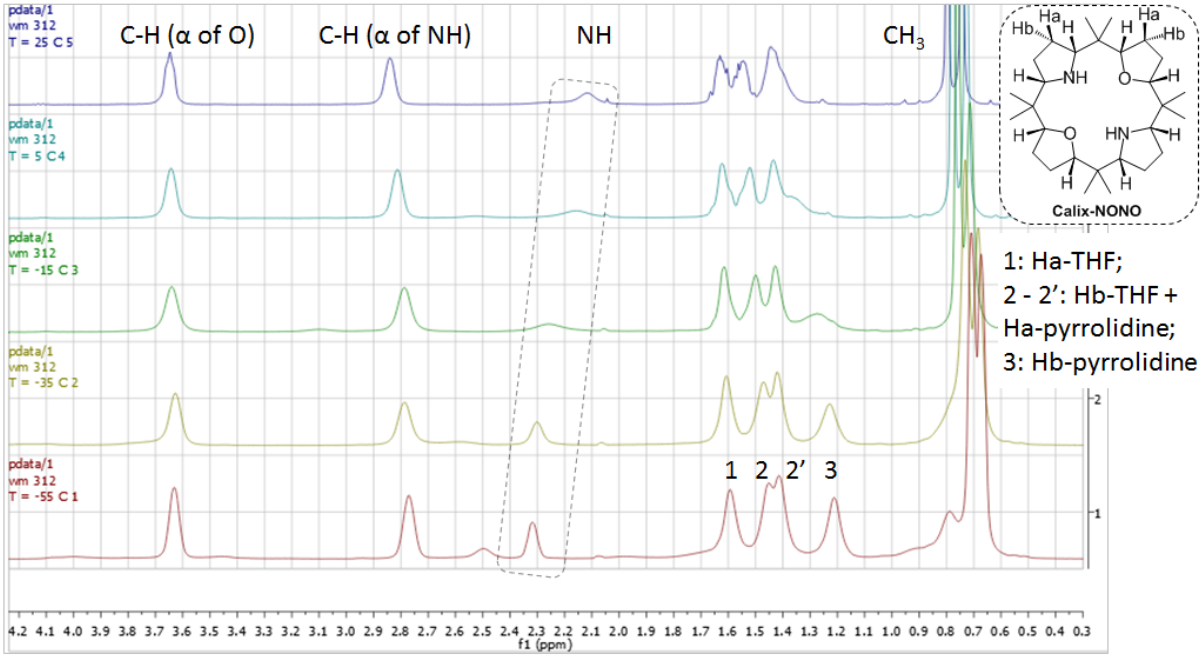

Figure 51. 400-MHz ^{1}H NMR spectra of calix-NONO **13** in $CDCl_3$ at variable temperatures (-55 °C to +25 °C)

T (°C)	Chemical shifts δ (ppm)								
	C-H (α of O)	C-H (α of NH)	–NH	1	2	2'	3	$–CH_3$	$–CH_3$
+25	3.646 (+0.015)	2.841 (+0.070)	2.115 (-0.203)	1.631 (+0.038)	1.539 (+0.088)	1.443 (+0.029)	~1.397 (+0.185)	0.797 (+0.088)	0.743 (+0.07)
+5	3.643	2.813	2.156	1.623	1.521	1.434	1.361	0.779	0.728
-15	3.640	2.788	2.254	1.614	1.499	1.428	1.274	0.760	0.714
-35	3.627	2.787	2.301	1.607	1.471	1.421	1.228	0.732	0.684
-55	3.631	2.771	2.318	1.593	1.451	1.414	1.212	0.709	0.673

Table 11. Chemical shifts observed in the ^{1}H NMR analysis of calix-NONO **13** in $CDCl_3$ depending of the temperature of analysis. Differences between the chemical shifts observed at -55 and +25 °C were shown in parentheses

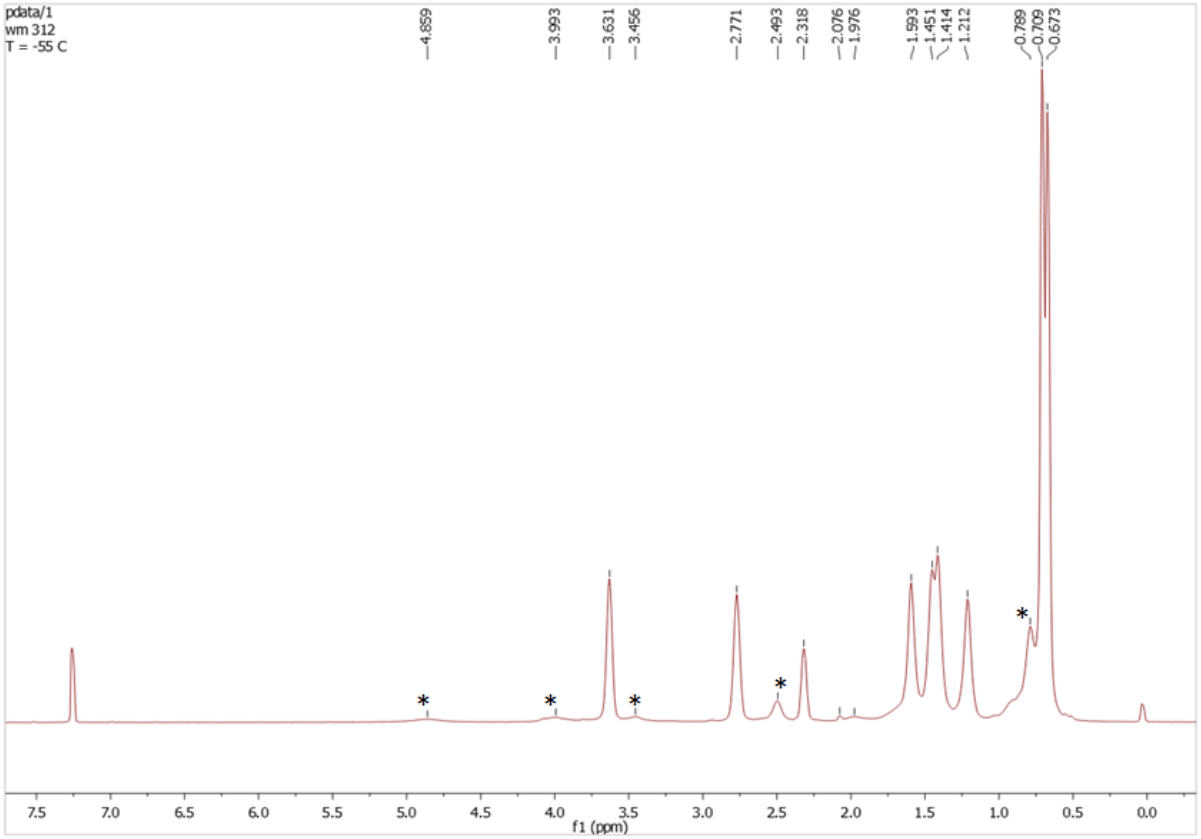

Figure 52. 400-MHz ^{1}H NMR spectra of calix-NONO **13** in $CDCl_3$ at -55 °C. *: New series of points observed only at this temperature

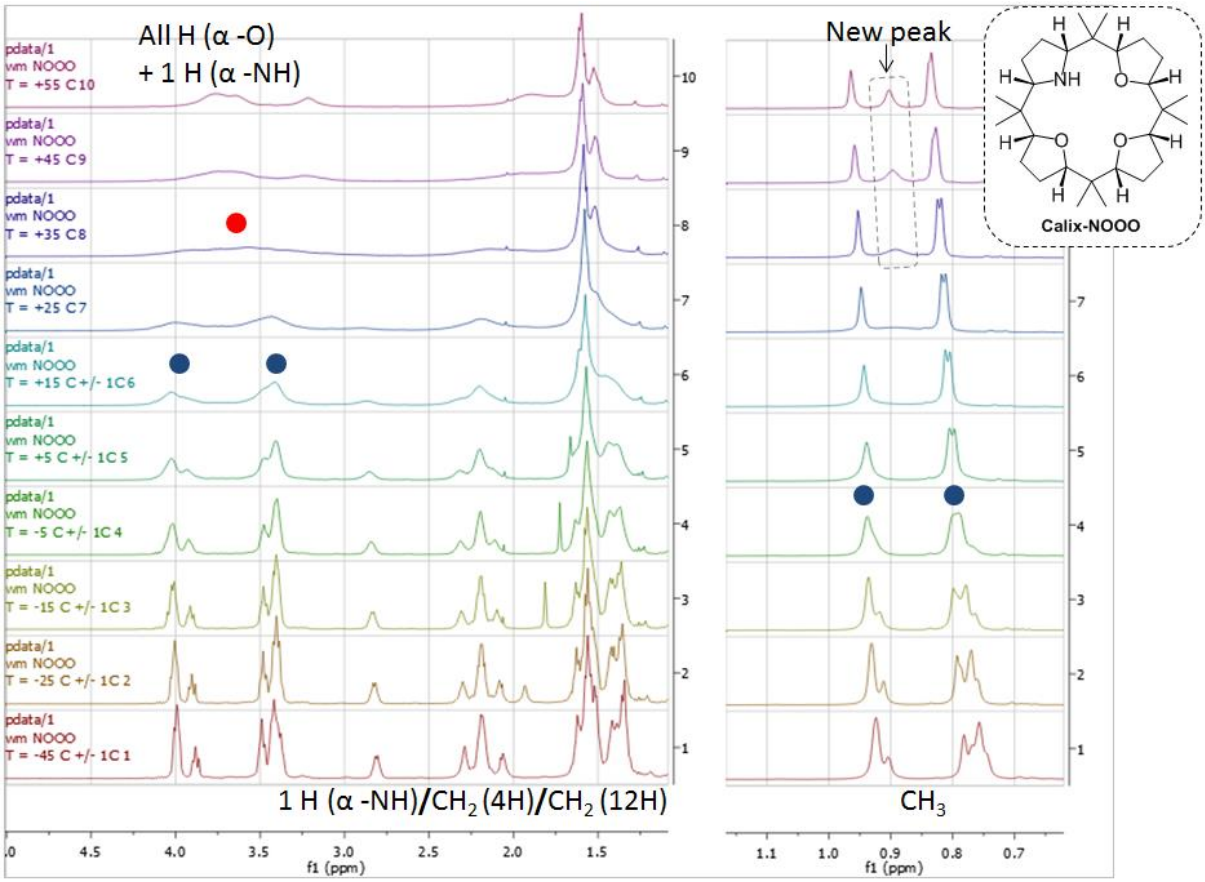

Figure 53. 400-MHz ^{1}H NMR spectra of calix-NOOO **14** in $CDCl_3$ at variable temperatures (-45 °C to +55 °C). Blue points: first coalescence; red points: supposed second coalescence

The calix-NOOO **14** showed complex behavior of the ^{1}H NMR spectra at variable temperatures (Figure 53). As the temperature increases, the signals for the α-(C-H) in the saturated heterocycles coalesce into large averaged signals. The same effect can be identified for the signal group attributed to the CH_3 groups. These coalescences are represented as blue point in Figure 53.

The protons in the α-position of the heteroatoms (around 4.0 ppm and 3.5 ppm) seemed to undergo a second coalescence (red point, Figure 53) at around +35 °C into an even larger signal from 3.0 to 4.5 ppm. At higher temperature, this signal seems to be split into new signals. The temperature limit of the solvent did not allow studying this process further.

For the methyl signals resonating at 0.94 and 0.8 ppm (Temperature -5 °C, Figure 53) a new peak started to appear around 0.90 ppm (measured at +55 °C) between the two broad signals representing the methyl groups at temperatures higher than +35 °C. This new peak is indicating the occurrence of a second dynamic process. In the temperature range from -45 to +55 °C the ^{1}H NMR spectra of the compound calix-NOOO **14** are compatible with the at least two independent dynamic processes with two different activation energies.

Methyl peaks at 0.924 ppm and 0.904 ppm (^{1}H NMR spectra at -45 °C) ppm were chosen for simulation of dynamic NMR using the WINDNMR software as additional tool to prove the existence of dynamic NMR processes occurring in compound calix-NOOO **14** (Figure 54).

We based the simulation according to the experimental results obtained at the lowest temperature performed (-45 °C) on the 400 MHz Brucker machine: a proportion of 77/33 (peak (a)/peak (b)) and a difference of 8 Hz between these two peaks.

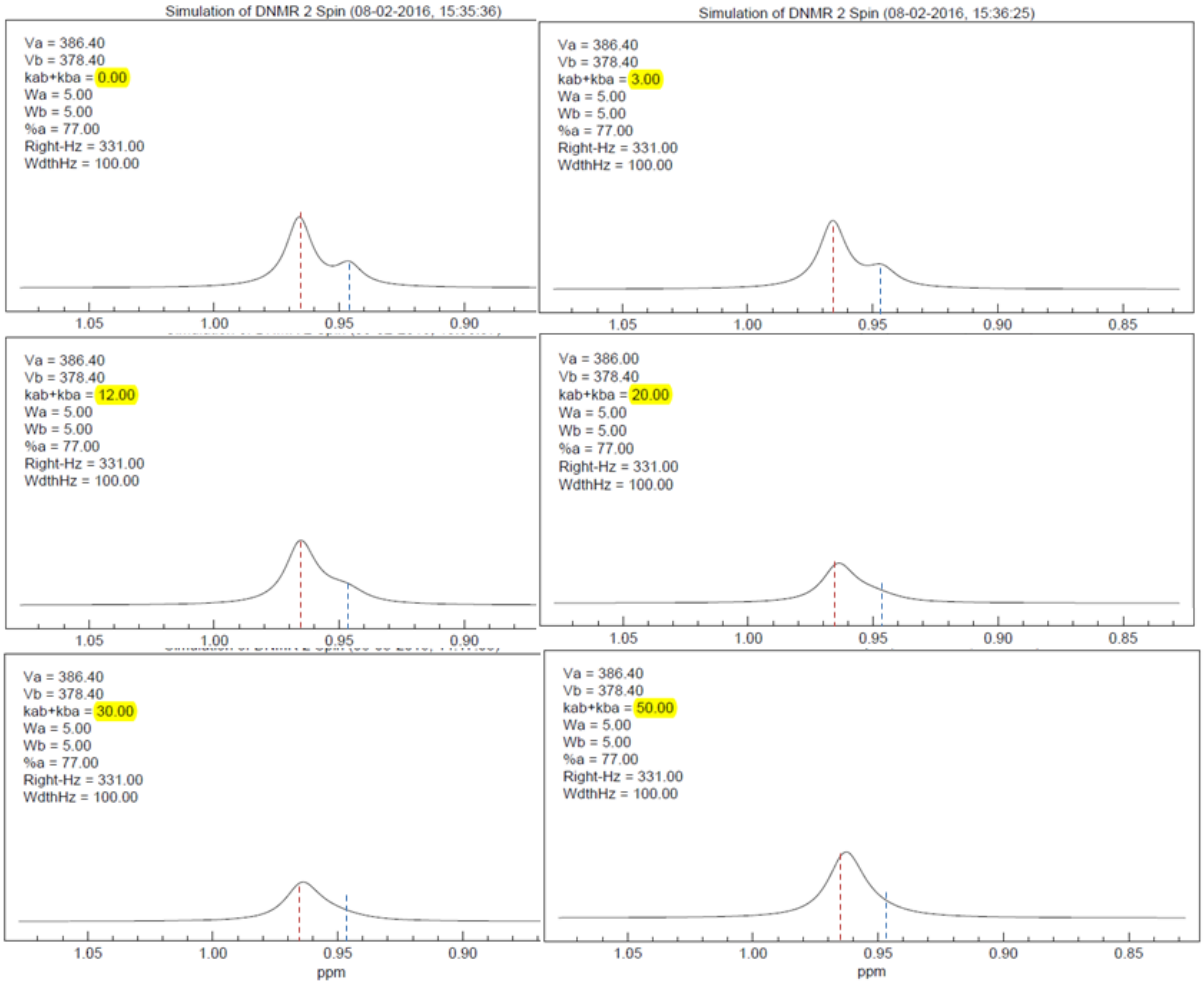

Figure 54. Simulation of dynamic NMR (DNMR) of selected methyl groups of calix-NOOO **14** at variable rate constant using WINDNMR software. Chemical shifts of the signals at -45 °C were showed as dotted line: red (peak (a)); blue (peak (b)). Simulated rate constant (k, in s^{-1}) was highlighted in yellow

As the rate constant *k* was increased, peak (b) disappeared and coalesced with peak (a). The simulation was very close to the observations made by the experimental NMR by increasing the temperature. Therefore we can justify the existence of dynamic NMR between these two peaks. Considering *k* values of = 0; 3; 12 and 20 s^{-1}, the peak (b) disappeared. No significant differences were observed between *k* = 20 and *k* = 30 s^{-1} so the coalescence should be around 20 s^{-1}. With a fast exchange of 50 s^{-1} the average peak became thinner.

Calculation of the first rate constant k_c with the formula $k_c = \pi \Delta\nu/\sqrt{2}$ afforded $k_c = 17.8$ s^{-1} (chemical shift of peak (a) and (b) taken at -45 °C). The Gibbs activation energy ($\Delta G^{\#}$) at the coalescence was therefore $\Delta G^{\#} = 4.574 \times 10^{-3}\, T\left(log\frac{T}{k} + 10.318\right) = 14.10$ kcal/mol.

7. Search for polymorphs for calix-NOOO 14

Calix-NOOO **14** was crystallized in the triclinic-(bowl) conformation. According to our calculation this compound could also crystallize in the monoclinic-II-(plate) conformation (Table 10). Different crystallizations experiments were realized trying to crystallize calix-NOOO **14** in this monoclinic-plate II conformation and show polymorphism.

7.1. Crystallizations experiments

7.1.1. Crystallizations in different solvents

Recrystallizations of the calix-compounds were usually carried out in EtOAc. A new set of crystallization with calix-NOOO **14** were performed using several solvents in which the compounds was successfully soluble at r.t. or by heating (Table 12).

Entry	Solvents	Solubility at r.t.	Hot	Crystals?
1	Heptane	Yes	-	Crystals on the walls
2	Toluene	Yes	-	Crystals (small squares) on the walls →**P-1**
3	Dioxane	No	Yes	Crystals →**Pbca**
4	Ethylene glycol dimethyl ether	No	Yes	Big needles on the walls →**Pbca**
5	Isopropyl ether	No	Yes	Kind of crystals as a tree on the walls, no single crystals
6	Benzyl alcohol	No	Yes	No evaporation →solution was heated, no crystals
7	MeOH	No	No	CH_2Cl_2/MeOH (1/1) Crystals (prism) but no single crystals

Table 12. New set of crystallizations of calix-NOOO **14**

Calix-NOOO **14** was put into small tubes (between 1.0 – 2.0 mg) and few drops of solvent were added. Heptane and toluene as solvent allowed the solubilization of **14** at r.t. (Table 12, Entries 1 and 2). A minimum amount of these solvents (typically 0.2 mL) was added to solubilize calix-NOOO **14** and then the tubes were placed into vials. The other solvents reported in Table 12 did not solubilize calix-NOOO **14** at r.t. Homogeneous solutions were obtained by warming the solutions with the heat gun (Table 12, Entries 3 to 6). Calix-NOOO **14** was insoluble in methanol so CH_2Cl_2 was added to solubilize the starting material in a 1/1 methanol/dichloromethane mixture (Table 12, Entries 7). The small tubes were placed into vials to avoid the solvent evaporation. After one week at r.t. no precipitation was observed. Holes were drilled into the plugs with needles to proceed at a slow evaporation of the solvents. The slow evaporation of the solvents allowed the precipitation of calix-NOOO **14** in few days. With the use of heptane and isopropyl ether as solvents, calix-NOOO **14** crystallized over the walls. These crystals were given to analyze in X-ray diffraction but

unsuitable crystals were obtained (Table 12, Entries 1 and 5). A white powder was obtained with the use of dioxane as solvent (Table 12, Entry 3). The 1/1 mixture of methanol/dichloromethane gave small prisms after the evaporation of a part of the solvent (Table 12, Entry 7). No single crystals among these prisms were found by Mme Stoeckli-Evans. Since benzyl alcohol has a high boiling point (205 °C), no evaporation of the solvent was observed at r.t. The tube was put into the fridge but no crystallization was observed after weeks (Table 12, Entry 6).

The tube with ethylene glycol dimethyl ether as solvent gave big needles on the walls after slow evaporation of the solvent (Table 12, Entry 4). This was the first experiment forming needles from crystallization experiments of of calix-NOOO **14**. The crystals were suitable for X-ray determination. Despite the macroscopic aspect of the calix-NOOO **14** crystals the X-ray structure determination showed that the molecules had bowl-conformation. The molecules were crystallizing in a new space group, the orthorhombic Pbca space group. Despite the promising macroscopic aspect of the crystal the crystallization had not placed the molecule in the predicted plate-conformation. This structure determination proofs that compound calix-NOOO **14** can crystallize in different polymorphic forms. Analyses of crystals grown in dioxane and toluene afforded the same bowl-conformation previously observed in Pbca and P-1 space groups, respectively.

7.1.2. Seeding experiment

In order to influence the crystallization of calix-NOOO **14**, seeding experiments were also tried. This method consist of adding a crystal (= the seed) into a solution of the wanted compound in order to start the crystallization. This method is mainly used to crystallize molecules in a specific polymorphic form[157-158] and to crystallize single crystal of protein.[159-160]

In our case, the idea was to add a crystal of calix-NONO **13** (the monoclinic-II-(plate) conformation) into a supersaturated solution of calix-NOOO to influence the conformational organization during the crystallization. Excess calix-NOOO **14** was solubilized in a small amount of hot EtOAc leaving some solid undissolved ligand as solid. This process guarantees the creation of a saturated solution. The excess of solid (undissolved ligand) was filtered with hot glassware and a needle of calix-NONO **13** was quickly dropped into the vial. Since we worked with a saturated solution, the precipitation occurred quickly therefore “the seed” had to be added quickly to the solution to avoid spontaneous crystallization. Several experiments were performed in order to correctly master the technique. After the addition of calix-NONO **13** at r.t., a quick precipitation of calix-NOOO **14** into very small cubes was observed within seconds. The X-ray determination of the cubes revealed that calix-NOOO **14** had crystallized a second time in the Pbca space group.

7.1.3. Crystallizations at high temperature

Our NMR studies suggest that dynamic processes occurred with calix-NOOO **14** at 55 °C. We tested crystallization of calix-NOOO **14** at higher temperatures using two solvents: $CHCl_3$ and EtOAc. Calix-NOOO **14** was dissolved in $CHCl_3$, respectively EtOAc, in NMR tubes. These NMR tubes were plunged in an oil bath and heated overnight at 65 °C. Since the NMR tubes are long thin tubes, the solvents did not evaporate immediately because the vapor condensed along the walls. In these conditions, the solvents slowly evaporated overnight. The calix-NOOO **14** was recovered as white solid in the tube containing $CHCl_3$ as solvent. Unfortunately the quality of the crystals obtained with EtOAc was not suitable for X-ray structure determination.

7.2. Polymorphic form found

Our trials to crystallize calix-NOOO **14** in new polymorphic forms has been partially successful: the crystallization experiments gave a new type of crystals with a different unit cell, but showing the same conformation of the molecule as the one obtained in our first structure determination. The calix-NOOO **14** has crystallized in two polymorphic forms: the triclinic P-1 and the orthorhombic Pbca forms. In both forms the conformation of the macrocycle is bowl-shaped. The crystallographic information and the molecular structure of the Pbca form are summerized in Table 13 and Figure 55b.

Structure type	Orthorhombic-bowl
Molecular Structure	NOOO **14**
Conformation	Bowl
Space Group	Pbca
a (Å)	12.099
b (Å)	24.722
c (Å)	17.524
α (°)	90.0
β (°)	90.0
γ (°)	90.0
T (K)	203
R-factor (%)	5.1

Table 13. Crystallographic data of the Pbca form of calix-NOOO **14**

The two triclinic P-1 and orthorhombic Pbca forms of calix-NNNO **14** are very similar (Figure 55). On the side views of the structures (Figure 55, right), aligning the two furan rings positioned opposite one another in the macrocycle revealed a slight change in the positioning of the rest of the structure. With this view, the two groups of methyl in the *meso*-position are almost aligned in the P-1 form which is not observed in the Pbca form.

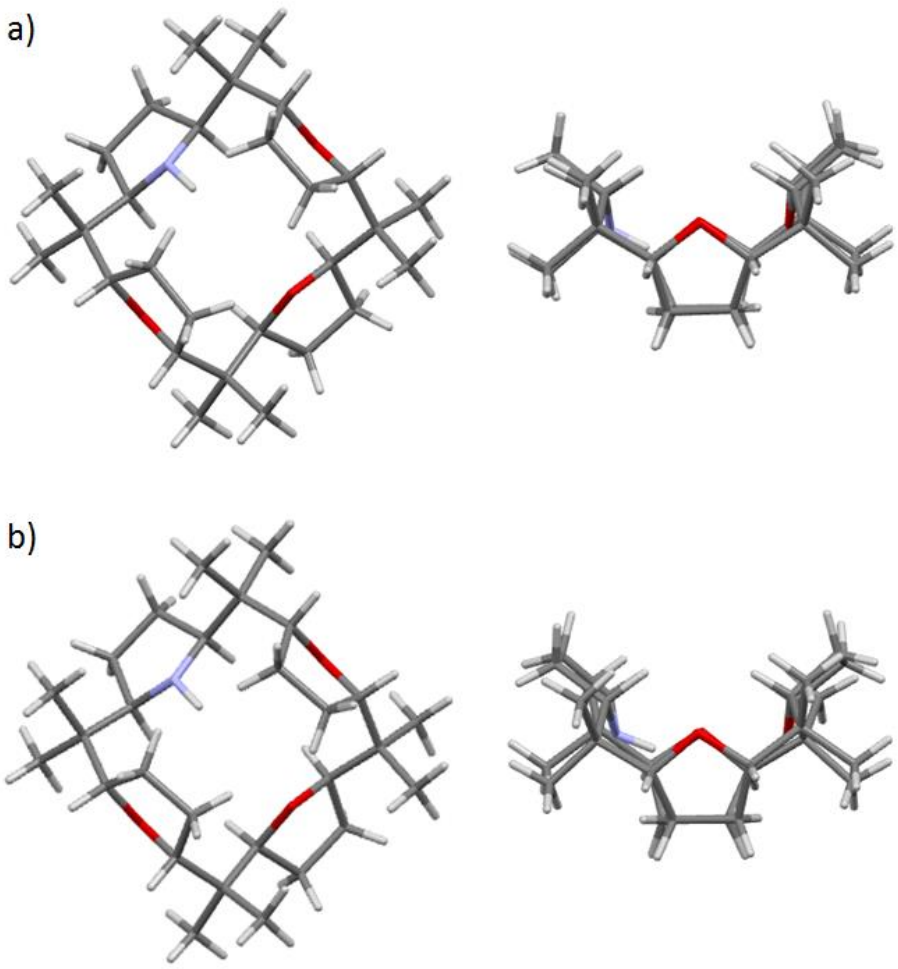

Figure 55. Comparison of the molecular structures of the P-1 and Pbca forms of calix-NOOO **14**. a) P-1 form; b) Pbca form. Top views (left); side views (right)

8. Conclusion

The conformational study of the six calix-compounds **3**, **4a** and **11** – **14** in the solid phase provided for the first time justifications on the presence of the two different conformations observed experimentally, namely the bowl-like and plate-like conformations. The presence of oxygen atoms close to each other in the macrocycle led to the bowl-conformation mainly cause by coulombic interactions. Thereby, calix-OOOO **4a**, calix-NNOO **12** and calix-NOOO **14** with adjacent THF rings present the bowl-conformation. Although the presence of supplementary hydrogen atom of the pyrrolidine ring in the macrocycle strongly increase the repulsion interaction (by 38 kj/mol), the other interactions all stabilize the plate-conformation. Calculations of the relative lattice energies of the six calix-compounds for the three lattices observed experimentally (one bowl- and two plate-conformations) allowed identifying calix-NOOO **14** as good candidate for polymorphism with the same lattice energy for the triclinic P-1 (bowl-like) and monoclinic $P2_1/c$ (plate-like) space groups. These directions allowed us to crystallize calix-NOOO **14** in the new orthorhombic Pbca (bowl-like) lattice.

The conformational study in solution by ^{1}H NMR at several temperatures (-55 °C to +55 °C in $CDCl_3$) of the three calix-NNNN **3**, calix-NONO **13** and calix-NOOO **14** revealed the presence of dynamic processes. Once again, calix-NOOO **14** was the compound showing the most changes with a complex behavior when the temperature was increased with the coalescence of several signals. For this compound, we were limited by the boiling point of the solvent (61.3 °C) and we believe we only observed a window of the full properties accessible with the NMR technique. The use of deuterated toluene, solvent in which calix-NOOO **14** is soluble at r.t., could afford additional information with a wider range of temperature (boiling point = 110.6 °C). Further analyses in conformal study of the calix-compounds together with NMR and computational methods

Chapter 5. Preliminary work on the synthesis of transition metal complexes using calix[n]tetrahydrofuran[4-n]pyrrolidines as ligands

1. Introduction

1.1. Tetraazamacrocycles as ligand

Polyazamacrocycles of adequate size and form can be tuned for efficient metal complexation. They are in general more powerful ligands than their linear polyamines counterparts. Cyclam and its derivatives are one of the most used saturated macrocyclic polyamines in coordination chemistry (see page 12 Chapter 1). Nowadays, metal complexes of cyclam derivatives containing one or several pendant arms connected to nitrogen atom(s) are increasingly studied in the development of novel therapeutic agents, especially for the complexation of copper-64 and zinc cations.[161-164] The copper-64 complexes presented in Figure 56a with a (methyl)benzoic acid or a bis(phosphinate) side arms found application in radiolabeling.[161, 164] Bicyclam derivatives (Figure 56b) are also studied and this class of compound shows strong anti-HIV activities.[161]

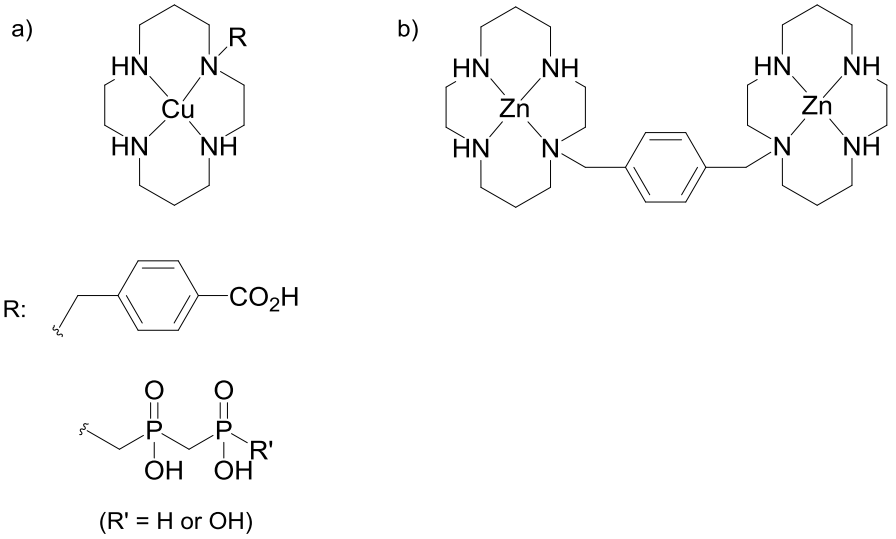

Figure 56. Recent pharmaceutical cyclam-derivatives

1.2. Reported complexes of heterocalix[4]arenes

Complex of calix[4]tetrahydrofuran 4a

In his paper concerning the synthesis and crystal structure determination of calix[4]tetrahydrofuran **4a** and **4b**, van Beylen[93] also reported the crystal structure of a complex of isomer **4a** with lithium picrate. The structure crystallized in the orthorhombic Pbca space group (refcode DIVVUZ). In this lithium complex, the four oxygen atoms binding

the cation are located in the same plan and formed the base of a very flat square pyramid. The lithium cation is forming the tip of the square pyramid (Figure 56). Although the isolation and characterization of compound **4a** has been reported over thirty years ago, this lithium picrate complex is the only structure of a metal complex of this type of macrocycles reported so far.

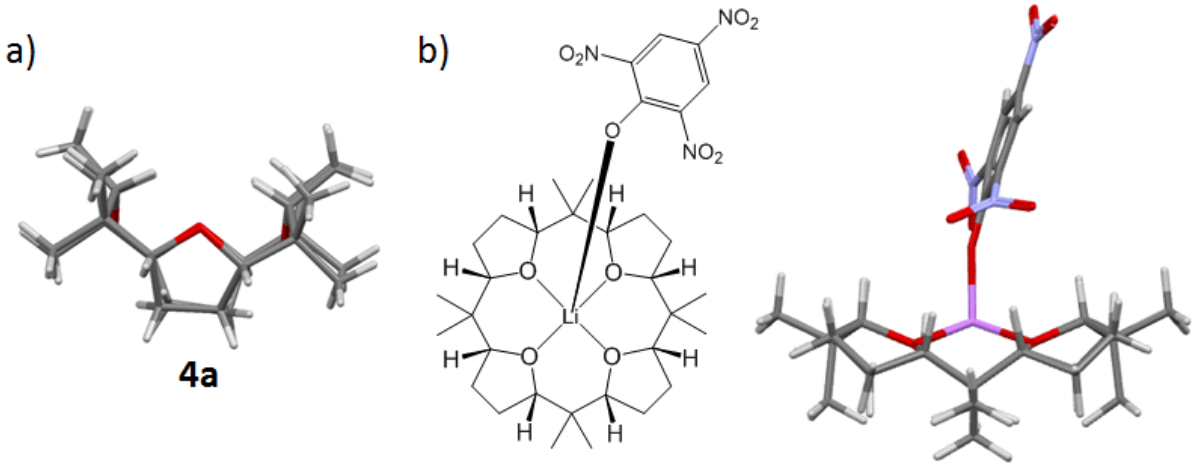

Figure 56. X-ray structures of calix-OOOO **4a** and its lithium picrate complex reported by van Beylen.[93] a) free ligand calix-OOOO **4a**; b) structure and molecular formula of the lithium picrate complex (refcode DIVVUZ)

Complexes of calix[4]pyrrolidine 3

With the successful synthesis and characterization of calix-NNNN **3** previously reported in the group, complexation studies were also undertaken using transition metals.[90] A series of transition metal complexes could be easily synthesized by the group. An equimolar amount of calix-NNNN **3** and a metal salt was heated to reflux in EtOH. The three Cu^{II}, Ni^{II} and Pd^{II} chloride complexes with calix-NNNN **3** as ligand were synthesized and structurally characterized. In a subsequent study the Mn^{II} acetate and chloride complexes were synthesized.[96] The structures of the five metal complexes are very similar and are illustrated here by the Ni^{II} complex (Figure 57). The four nitrogen atoms and the cation are arranged in a same plan (quadratic planar arrangement). The four –NH bonds point in a perpendicular direction to this plane. The two chlorides or the corresponding anions are situated above or below of this plane directly above or below the metal cation.

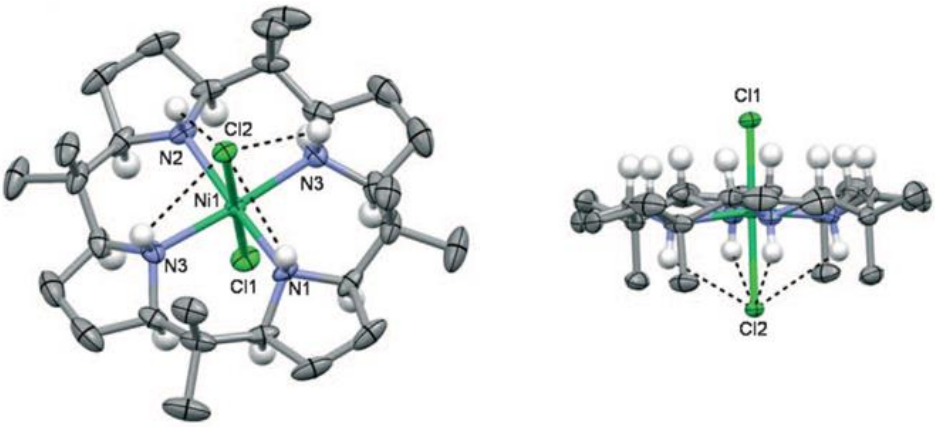

Figure 57. Molecular structure of the $Ni^{II}Cl_2$ complex of calix-NNNN **3** with thermal ellipsoids drawn at the 50% probability level. Dotted lines indicate NH···Cl interactions (solvent molecules and most hydrogen atoms have been removed for clarity)[90]

In a proof of concept study on the suitability of the metal complexes using our ligand our group studied the catalytic epoxidation of alkenes with the Mn^{II} acetate complex using hydrogen peroxide. Reasonable to good yields of product could be obtained using the Mn^{II} acetate complex as catalyst.[96] The biggest disadvantage hampering the use of the metal complexes of calix-NNNN **3** are: 1) the low yield of the ligand **3** (8% yield starting from calix[4]pyrrole **1** obtained in our standard conditions (0.3 equiv. of Pd/C); 2) the need of a large excess of Pd/C (9.5 equiv.) to accomplish the full conversion of the starting material and higher yield (75%). The hydrogenation under our standard conditions of the calix-compounds **7**, **9** and **10** mixing nitrogen and oxygen atoms in the macrocycle gave much better yields (35 – 78%). The saturated compounds **11**, **13** and **14** are good candidates for the synthesis of novel heterocalix[4]arene complexes.

2. Synthesis of transition metal complexes

Having developed the optimized synthesis of calix[n]tetrahydrofuran[4-n]pyrrolidines **11** – **14** sufficient quantities of the mixed macrocycles became available. With the goal to characterize the reactivity of these mixed ligands and to compare their reactivity with the parent compounds **1** and **2**, we started a preliminary study on the synthesis of transition metal complexes of these ligands. The two calix-NONO **13** and calix-NOOO **14** showed the best overall yields (36% and 33% respectively) and are more accessible in large quantities. For this reason these two compounds were chosen for the first set of complexation studies. Moreover the two free ligands showed different conformations in the solid state: a plate conformation similar to calix-NNNN **3** for calix-NONO **13** and a bowl conformation for calix-NOOO **14** similar to the conformation of the heterocalix[4]arenes and calix-OOOO **4a**.

2.1. Calix-NONO 13 as ligand

The first two tests of complexation were carried out with cobalt and nickel (cobalt chloride and nickel chloride). The colors changed in a characteristic manner during complexation (see Table 14). The general procedure for the complexation was the following: Calix-NONO **13** and the metal salt were added in equimolar amount to 1.0 mL anhydrous EtOH in 5-mL vials. The vials were sealed and the mixtures were magnetically stirred at 100 °C (Scheme 26). Reactions were stopped after 4 h of stirring. The reaction mixtures were cooled to r.t. and the solvent was removed. The crude materials were purified by filtration over neutral alumina (Al_2O_3) in a Pasteur pipette using CH_2Cl_2/MeOH (99/1) as mobile phase.

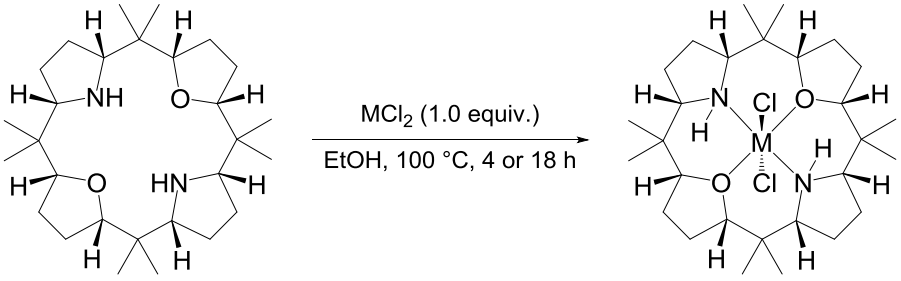

Scheme 26. Synthesis of complexes **29** – **30**. **29**: $CoCl_2$, EtOH, 100 °C, 4 h; **30**: $NiCl_2$, EtOH, 100 °C, 4 h; **31**: $CuCl_2$, EtOH, 100 °C, 18 h

The isolation of the products was facilitated by their color. The crude **29** and crude **30** were obtained as purple and yellow solids, respectively. Remaining starting material was also isolated during the purifications indicating that the reaction were not completed after 4 h. Crude **29** and **30** were solubilized in a CH_2Cl_2/cyclohexane (1/1) solutions and slow evaporation of these solutions gave big purple and yellow needles of complexes **29** (48%) and **30** (47%), respectively (Table 14 and Scheme 26).

Metal salts	Observed colors			
	Metal salt	Metal salt in solution	Reaction mixture	Pure product
$CoCl_2$*	Purple	Blue	Clear purple solution	Purple solid
$NiCl_2$*	Yellow	Clear yellow with precipitates	Clear yellow solution	Yellow solid
$CuCl_2$	Brown	Yellow	Colorless solution	Blue solid

Table 14. Colors observed in the different steps of the complexation reactions using calix-NONO **13** as starting material. *: The same colors were observed with the use of calix-NOOO **14** as starting material

An identical experiment was carried out with copper chloride except that the reaction was stirred for 18 h in EtOH at 100 °C (Scheme 26). Filtration on alumina in a Pasteur pipette (CH_2Cl_2/MeOH, 99/1) and crystallization of the resulting solid in a CH_2Cl_2/cyclohexane (1/1) solution afforded complex **31** (93%) as blue needles after the slow evaporation of the solution. A longer reaction time allowed the full conversion of the starting material **13** with a significant increase of the isolated yield compared to the two reactions stopped after 4 h with cobalt chloride and nickel chloride.

Analysis of these three set of needles by HRMS and X-ray diffraction confirmed the structures of the complexes **29** – **31** (Figure 58). The mass of the complexes losing one chloride was detected in the HRMS analyses $(M\text{-}Cl)^+$. The X-ray structures were very similar to the structures obtained with calix-NNNN **3** as ligand.[95] Whereas the X-ray analyses of the free calix-compounds **11** – **14** showed disorder, no disorder was observed in complexes **29** – **31**. The oxygen and nitrogen atoms could be differentiated.

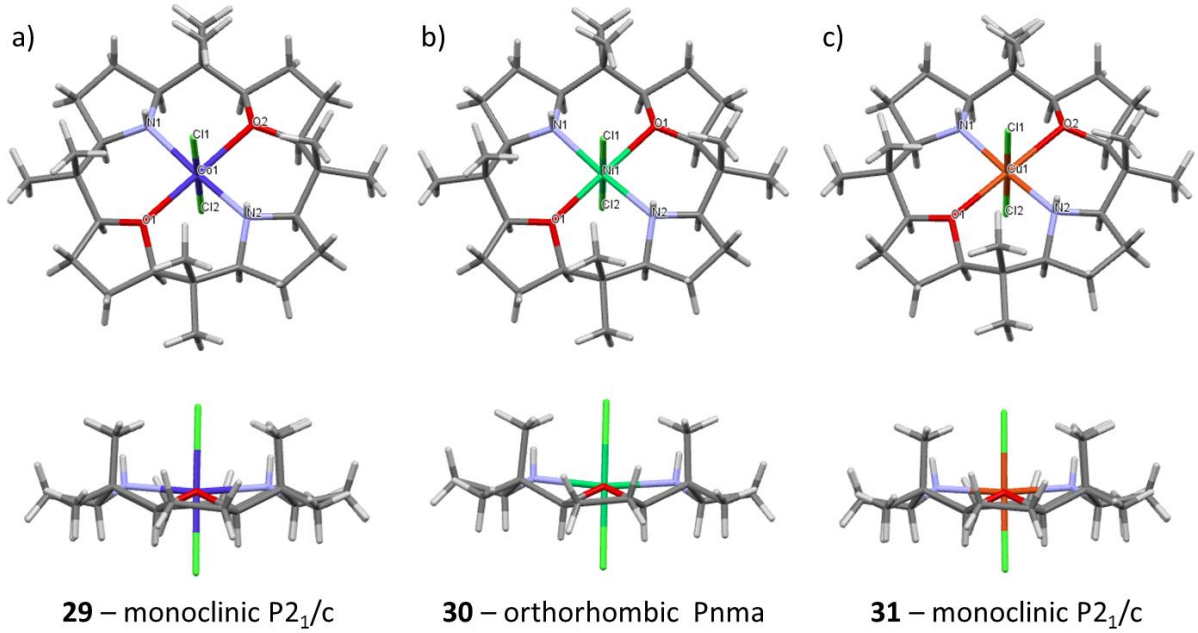

Figure 58. Molecular structures and space groups of complexes **29** – **31**. Top views (above); side views (below). a) Co-complex **29**; b) Ni-complex **30**; c) Cu-complex **31**

Distances between the metal and the heteroatoms in the solid state are reported in Table 15. The distances between the central metal and the nitrogen or oxygen and heteroatoms are relatively close in the three complexes although the three metals, especially the nickel, have different ionic radius (Ionic radius (in pm): Co^{II} = 88.5; Ni^{II} = 83 and Cu^{II} = 87). The largest difference observed are the distances between the metal and the oxygen atoms between the nickel and the copper complexes: Δ(M-O1) and Δ(M-O2) are respectively 0.1134 and 0.1199 Å (Table15). The two chloride atoms are not localized at the same distances of the metal. In the three complexes, the chloride atom pointing in the same direction of the eight hydrogen atoms positioned on the asymmetric carbon atoms (hydrogen α-NH and α-O) is closer to the metal (distance $M\text{-}Cl_2$ in Table 15) compared to the other chloride atom (Cl_1). Variations of distances and geometry of the macrocyclic structure keeping the four heteroatoms in a same plane should be limited in the complexes. If the metal possesses the appropriate ionic radius

for complexation, the distances in the resulting complex are mostly imposed by the structure of the ligand.

Complexes	Metal-Nitrogen	Distances (Å)	Metal-Oxygen	Distances (Å)	Metal-Chloride	Distances (Å)
29	Co-N_1	2.1184 (16)	Co-O_1	2.2414 (13)	Co-Cl_1	2.4824 (5)
	Co-N_2	2.1220 (17)	Co-O_2	2.2433 (13)	Co-Cl_2	2.3673 (6)
30	Ni-N_1	2.0881 (17)	Ni-O_1	2.2278 (10)	Ni-Cl_1	2.4636 (6)
	Ni-N_2	2.0932 (18)	Ni-O_2	2.2279 (10)	Ni-Cl_2	2.3568 (6)
31	Cu-N_1	2.0429 (12)	Cu-O_1	2.3412 (10)	Cu-Cl_1	2.3975 (4)
	Cu-N_2	2.0451 (13)	Cu-O_2	2.3478 (10)	Cu-Cl_2	2.3224 (4)

Table 15. Distances between the metal and the heteroatoms in complexes **29** – **31**. Standard deviation are shown under parentheses

2.2. Calix-NOOO 14 as ligand

Two complexation reactions were carried out with calix-NOOO **14** as ligand using cobalt chloride or nickel chloride as metal salts (Scheme 27).

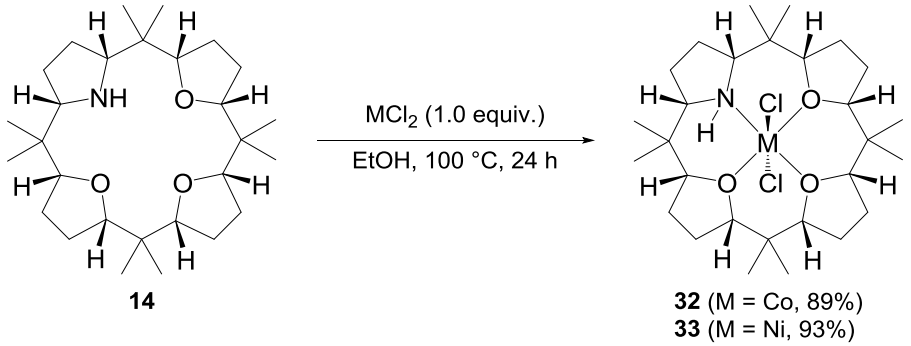

Scheme 27. Synthesis of complexes **32** and **33**

The reactions were carried using the same procedure as the complexation with calix-NONO **13** however the reaction time was prolonged to 24 h. The color changes were identical to those observed when calix-NONO **13** was used as ligand (Table 14). After 24 h the transformation was complete and the solvents were removed under reduced pressure. The crude solids were dissolved in a CH_2Cl_2/cyclohexane (1/1) solution and after evaporation of the solutions, crystals of **32** (89%) and **33** (93%) were obtained as purple and yellow needles, respectively. Analysis of these needles by HRMS and X-ray diffraction confirmed the structures (Figure 59). The loss of one chloride was also observed in the HRMS analyses of compounds **32** and **33**. The X-ray structures with calix-NOOO **14** are very similar to the previously obtained structures with calix-NONO **13** and calix-NNNN **3**. As the complexes **29** – **31**, no disorder was observed in these two complexes. The distances between the metal and the nitrogen and oxygen atoms were shown in Table 16. The distances are similar between the two complexes. The most notable difference is observed between the metal and the nitrogen atom with a difference of 0.0326 Å. In both complexes **32** and **33**, as in the three complexes

29 – **31**, the chloride atom in the same direction that the eight hydrogen atoms (α-NH and α-O) is closer to the metal than the other chloride atom (Table 16).

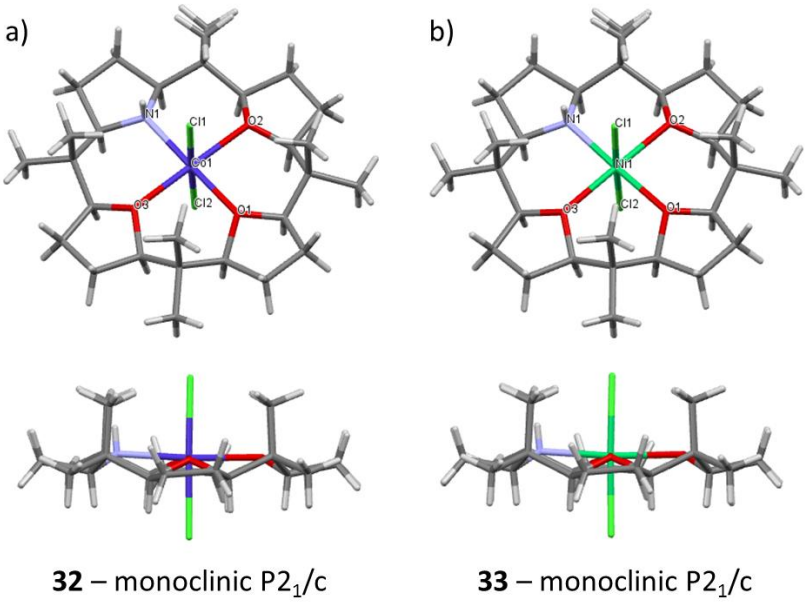

Figure 59. Molecular structures of complexes **32** and **33**. Top views (above); side views (below). a) Co-complex **32**; b) Ni-complex **33**

Complexes	Metal-Nitrogen	Distances (Å)	Metal-Oxygen	Distances (Å)	Metal-Chloride	Distances (Å)
32	$Co-N_1$	2.1397 (12)	$Co-O_1$	2.1768 (10)	$Co-Cl_1$	2.3990 (4)
			$Co-O_2$	2.2112 (10)	$Co-Cl_2$	2.3646 (4)
			$Co-O_3$	2.2088 (10)		
33	$Ni-N_1$	2.1071 (13)	$Ni-O_1$	2.1776 (11)	$Ni-Cl_1$	2.3756 (5)
			$Ni-O_2$	2.1959 (11)	$Ni-Cl_2$	2.3345 (5)
			$Ni-O_3$	2.1947 (11)		

Table 16. Distances between the metal and the heteroatoms in complexes **32** and **33**. Standard deviation are shown under parentheses

3. Conclusion

Five novel transition metal complexes were successfully synthesized and characterized by X-ray diffraction. Both ligands **13** and **14** led to the synthesis of very similar structures compared to complexes already synthesized in the group with calix-NNNN **3** as ligand. The complexation could be easily envisaged on a wider range of metals and could afford new structures for catalytic applications.

Chapter 6. Ring opened intermediates with 1,4-diketone function: a platform for synthetic modifications

1. General introduction

The key reaction for our synthesis of calix[n]furan[4-n]pyrroles is the oxidative ring opening of the furan ring(s) in calix[4]furan **2**. This transformation yields unsaturated or after hydrogenation saturated 1,4-diketone functions as part of the macrocyclic skeleton. The retrosynthetic approach to calix[3]furan[1]pyrrole **10** is illustrated in Scheme 28.

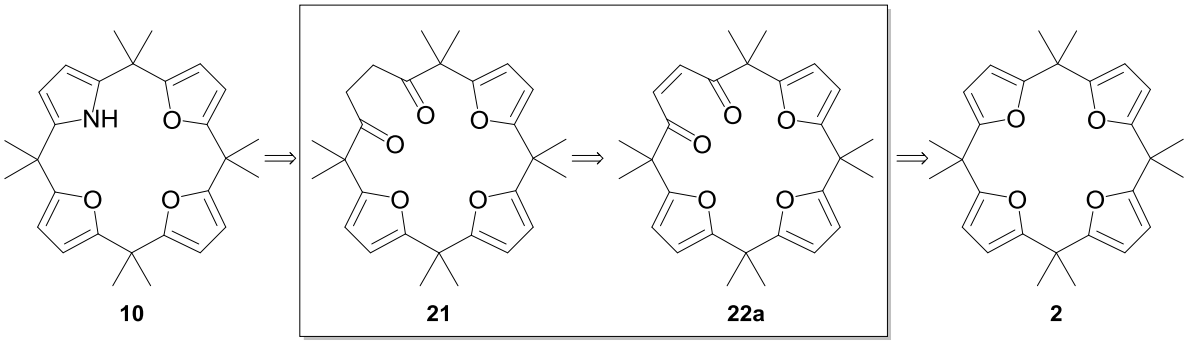

Scheme 28. The retrosynthesis of calix[3]furan[1]pyrrole **10** highlighting the mono-ring opened unsaturated **22a** and saturated intermediates **21**

These 1,4-diketones imbedded in the macrocycle allow many chemical transformations leading efficiently to a great variety of novel derivatives: formation of imine derivatives (Schiff bases), oximes, reduction to alcohols either by adding hydrides (addition of H^-) or organometallic reagents), 1,4-addition to the α,β-unsaturation of intermediate **22a** (Michael addition) to mention only a few possible transformations. The two ketone functions are part of the macrocycle. Including the 1,4-diketo function into a macrocyclic structure may influence the reactivity and/or the selectivity of the transformation. We focused our preliminary work on the modification of the most simple intermediates **21** and **22a** of this class, where the calix[4]furan **2** has undergone only one ring-opening reaction. The Figure 60 illustrates some of the envisaged interesting modifications starting from these two intermediates.

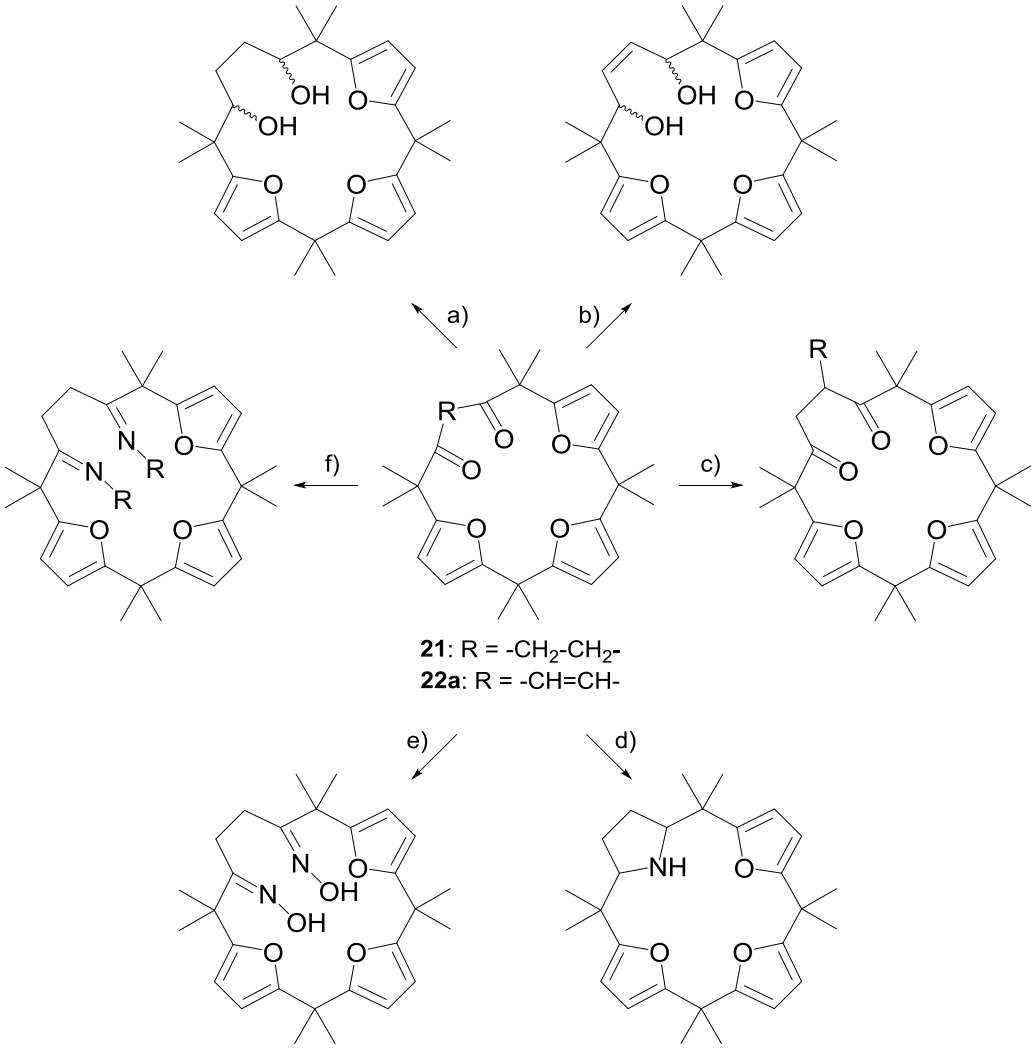

Figure 60. Modifications envisaged for the transformations of intermediate **21** or **22a**. a) and b) Reduction of keto function starting from **21** (and respectively **22a**). c) Michael addition from **22a**. d) Reductive amination from **21**. e) and f) oximes and respectively imines formation from **21**

A single crystal of ring-opened, hydrogenated compound **21** was successively grown. Its structure is presented in Figure 61 compared to calix[4]furan **2**. The molecule crystallized in the triclinic P-1 space group with the typical 1,3-alternating conformation of the three furan rings, very similar to the conformation observed for the calix[4]furan **2**. The angle between the two planes defined by the two carbonyl groups is 34.57 ° and the carbonyl double bonds are pointing into opposite directions.

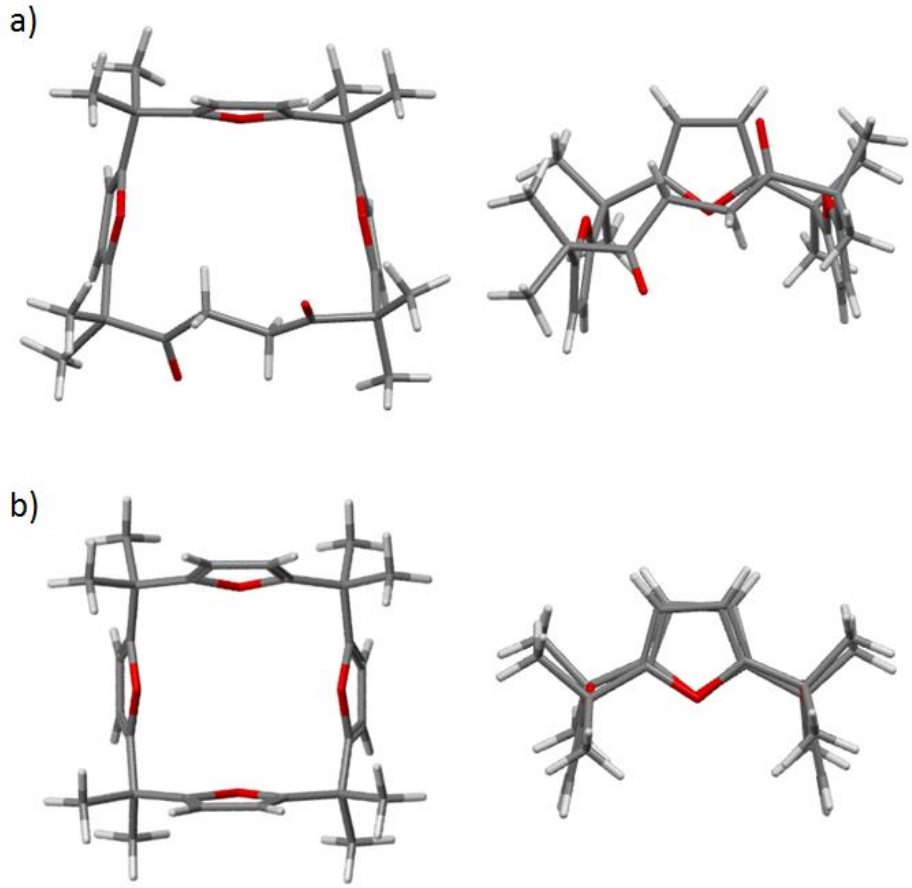

Figure 61. Structure of compound **21** as determined by X-ray diffraction compared to calix[4]furan **2**. Top view (left); side view (right). The points are the positions of the atoms resulting on the inversion of the two carbonyl groups (red points: oxygen; grey points: carbon; white points: hydrogen). a) compound **21**; b) calix[4]furan **2**

The conformation of the intermediate **21** is rather similar to the conformation of the calix[4]furan **2**, if one considered the arrangements of the three furan rings. The introduction of the 1,4-butadione unit just creates a linker between the two quaternary carbons connected to the α-positions of the furan rings. The linker imposes a longer distance and thereby enlarges the internal cavity delimited by the macrocyclic structure. This novel architecture allows selective modifications of the two keto functions. These structural variations might form a set of interesting ligands with tailored properties. A selected number of the possible transformations was tested with the goal to obtain and to characterize the novel structures. Optimization of the process was not the primary goal at this stage of our investigations. Another important objective of our studies was the exploration of the reactivity of these special diketones characterizing the influence of the macrocyclic structure on the chemical reactivity.

2. Synthesis of calix-1,4-diol

2.1. Inspiration

Toward the end of the 20th century, chemists are not solicited to just synthesize molecules but to furnish enantiomerically enriched compounds of high purity. This need has focused the activity of the synthetic community on asymmetric synthesis or stereoselective synthesis. The IUPAC definition of this term is: "stereoselective synthesis is a chemical reaction (or reaction sequence) in which one or more new elements of chirality are formed in a substrate molecule and which produces the stereoisomeric (enantiomeric or diastereoisomeric) products in unequal amounts".[165] According to IUPAC definition the term asymmetric synthesis is used for stereoselective synthesis of chiral compounds. The most efficient approach to the synthesis of enantiopure compounds is the so called enantioselective catalysis (earlier term used: asymmetric catalysis). Initially this approach was almost exclusively based on the use of metal catalyzed reactions, introducing the enantioselective element by tuning the ligand. Powerful enantiopure catalysts based on preferred ligand structures are used to promote these asymmetric reactions in stoichiometric but preferentially in catalytic amounts. Two well-known catalysts possess a 1,4-diol function: BINOL[9] and TADDOL[10] (Figure 62). The application of these two chiral ligands has been widely reported in the literature. The advantages of these two well-known ligands are: an easy preparation, a good affinity with several metals in different oxidation states, a high versatility and their successful application in various types of enantioselective reactions.[166-167]

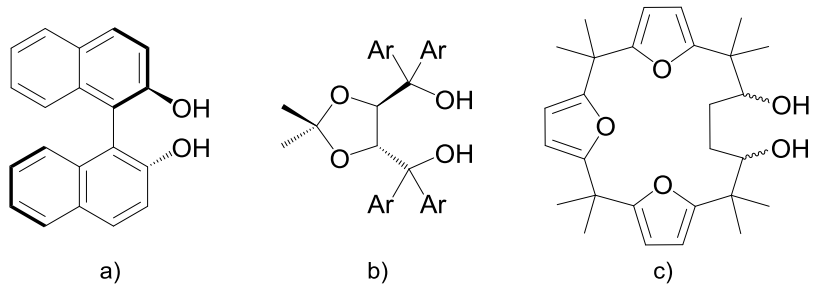

Figure 62. Two widely used 1,4-diol ligands in metal catalyzed enantioselective catalysis (a and b) compared to the target structure calix-1,4-diol. a) (*R*)-BINOL; b) structure of generic TADDOL; c) targeted calix-1,4-diol

Reducing both keto functions present in the structure of intermediate **21** should afford an interesting molecule containing a 1,4-diol function bearing two quaternary carbons in the α-position of the two diols (Figure 62c). The reduction of both carbonyl groups of **21** into a 1,4-diol function was studied to form the targeted calix-1,4-diol structure.

[9] IUPAC name: 1,1'-Bi-2-naphthol

[10] IUPAC name: α,α,α',α'-tetraaryl-2,2-disubstituted 1,3-dioxolane-4,5-dimethanol

2.2. First synthesis of calix-1,4-diols 34a and 34b

Three reducing agents were tested, namely sodium cyanoborohydride ($NaBH_3CN$), sodium borohydride ($NaBH_4$) and lithium aluminium hydride ($LiAlH_4$). $NaBH_3CN$, a weak reducing agent, is usually used for the transformation of imines to amines typically in a so called reductive amination reactions. The reduction of ketones to alcohols is usually not achieved by this reagent.[168] We tested the reaction with $NaBH_3CN$ as a reference. We wanted to make sure, that no reaction occurs between sodium cyanoborohydride and compound **21**. The goal was to use this reagent in a reductive amination reaction using the macrocycle **21** or derivatives of this macrocycle as added ligand (see page 115).

When compound **21** was treated with $NaBH_3CN$ in EtOH at reflux for 2 h no reaction was observed. The unreacted starting material **21** was quantitatively recovered in the crude material (Table 17, Entry 1, page 114). $NaBH_3CN$ was a suitable reducing agent in our tests of the reductive amination.

Under the same conditions, the use of $NaBH_4$ as reductive agent led to the formation of two products with greatly different R_f values in TLC (Cy/EtOAc 7/3, R_f(**34a**) = 0.5; R_f(**34b**) = 0.25). The two fractions were easily isolated by silica gel chromatography: the first fraction (**34a**) was isolated using Cyclohexane/EtOAc (8/2) as mobile phase. Increasing the polarity changing the solvent to a Cyclohexane/EtOAc (6/4) mixture allowed the isolation of the second fraction **34b**. Analysis of the two fractions by MS and NMR spectroscopy revealed that the two fractions are isomers obtained as result of the reduction of both carbonyl groups to the alcohol function (Scheme 29). The two isomers **34a** and **34b** were isolated as white powders in 40% and 38% yield, respectively.

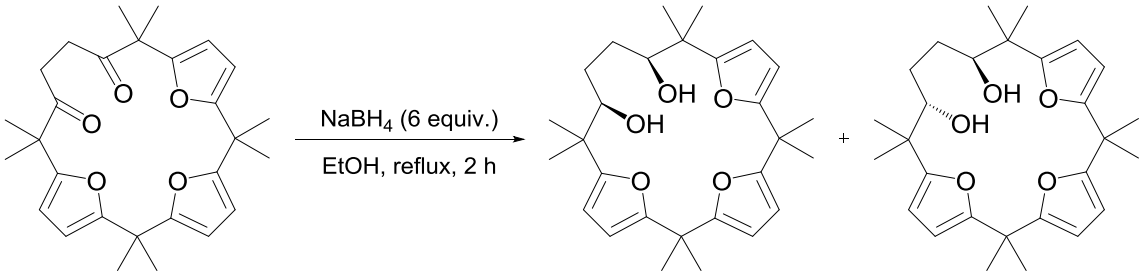

Scheme 29. Synthesis of the two isomeric calix-1,4-diols **34a** and **34b** using sodium borohydride as reducing agent

With two stereocenters, four isomers of compound **34** could be drawn connected between them in pairs of enantiomers: the *rac*-compound and the *meso*-compound (Figure 63). The separation of the *rac*-compound from the *meso*-compound is easy and the separation of the two enantiomers present in the *rac*-compound is difficult.

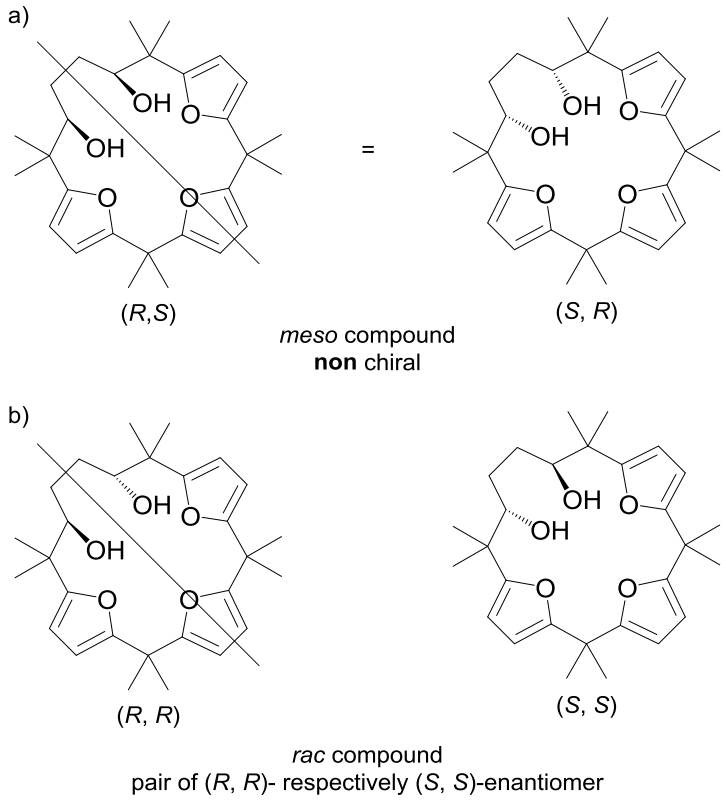

Figure 63. Repartition of the four different diastereoisomers in two fractions in terms of symmetry. a) *meso*-compound; b) *rac*-compound

Our GC method did not separate the two compounds **34a** and **34b** as they showed the same retention time under our conditions (Figure 64). For separating the novel calix-1,4-diol compounds **34a** and **34b**, polar compounds with two alcohol functions, we developed a reverse phase method using the UPLC technology. A fast and efficient method was created (see experimental part) allowing to separate the two different diastereoisomers (separation within 6 min with the UPLC technology compared to 30 min with the GC method, Figure 64).

To attribute the structures of the two fractions we tried to grow single crystals for an X-ray analysis of both fractions. We successfully obtained a mono-crystal from fraction 2 which corresponds to the diastereoisomer **34b**. The compound crystallized in the triclinic P-1 space group and revealed to be the *rac*-compound (mixture of the the (*S*, *S*)- and the (*R*,*R*)-enantiomers. The presence of two independent molecules in the asymmetric unit cell was observed (Figure 65a). The structural differences of these two independent molecules are minor. The Figure 65b shows the overlay of the two independent molecules, one in black and the other in red. Both of the "central" furan rings (in front of the 1,4-diol function) of the black molecule, respectively the red molecule, point in the same opposite direction of their neighboring furan rings but with a different angle.

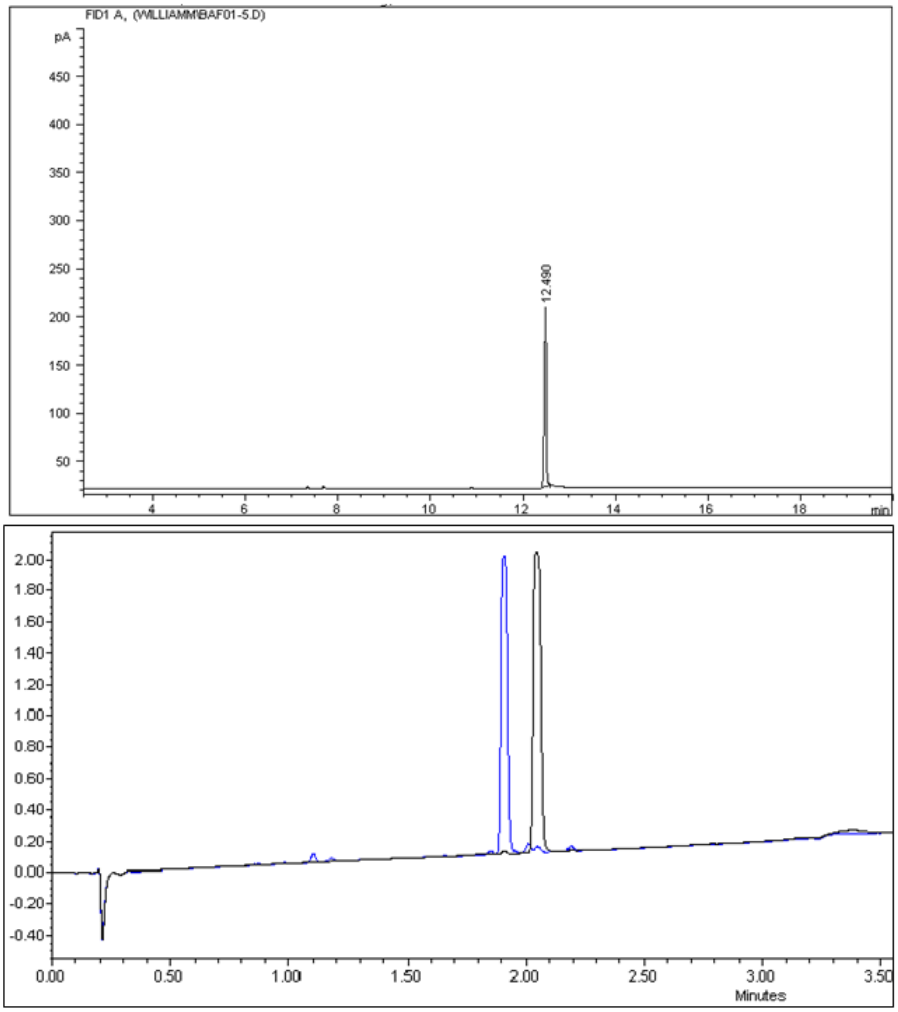

Figure 64. GC analysis of **34a** and **34b** (above) and UPLC analysis (below). In UPLC: **34b** (blue, 1.91 min); **34a** (black, 2.05 min)

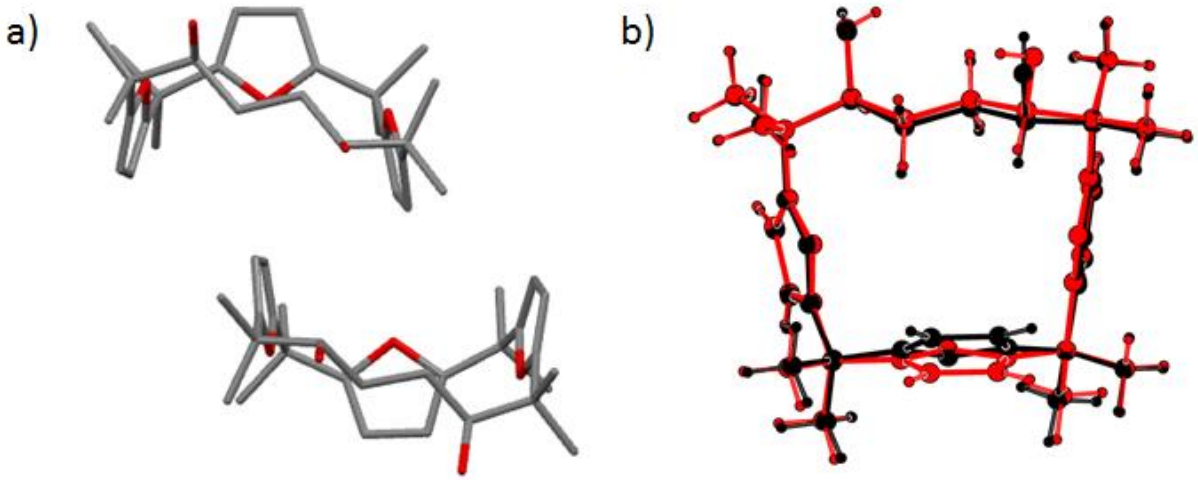

Figure 65. Molecular structure of **34b**. a) Molecular structure of the two independent molecules of **34b** determined by X-ray diffraction (the hydrogens were omitted for clarity); b) Overlay of these two independent molecules found in the asymmetric unit cell

The two fractions showed almost identical ^{13}C NMR and small differences in their ^{1}H NMR spectra. The major differences in the ^{1}H NMR spectra are observed for the peaks attributed to the $–CH_2$ protons and for the peak of one of the methyl signals (Figure 66). The $–CH_2$ groups should give two different signals: one signal for each of the diastereotopic protons of the A,A',B,B'-system. The multiplet appearing at 1.29 – 1.23 ppm is present at the same position for both diastereoisomers. The multiplet for the second diastereotopic proton occurs at 1.11 – 1.02 ppm for **34b** and 0.79 – 0.71 ppm for **34a**. The peaks for the four magnetically different methyl groups appear in two clusters: Two signals occur at 1.56 and 1.58 ppm, whereas the other two signals are observed between 1.21 and 1.15 ppm. The signals for the methyl groups at 1.56 – 1.58 ppm are almost undistinguishable between the two diastereoisomer **34a** and **34b**. These signals are attributed to the methyl groups situated between two furan rings. The signals occurring between 1.21 and 1.15 ppm are attributed to the methyl groups between a furan ring on one side and the aliphatic chain on the other side. The two signals for the methyl group of **34a** are close to each other (respectively 1.21 and 1.18 ppm) while the signal for one of the methyl groups of **34b** occurs at lower chemical shift (respectively 1.21 and 1.15 ppm).

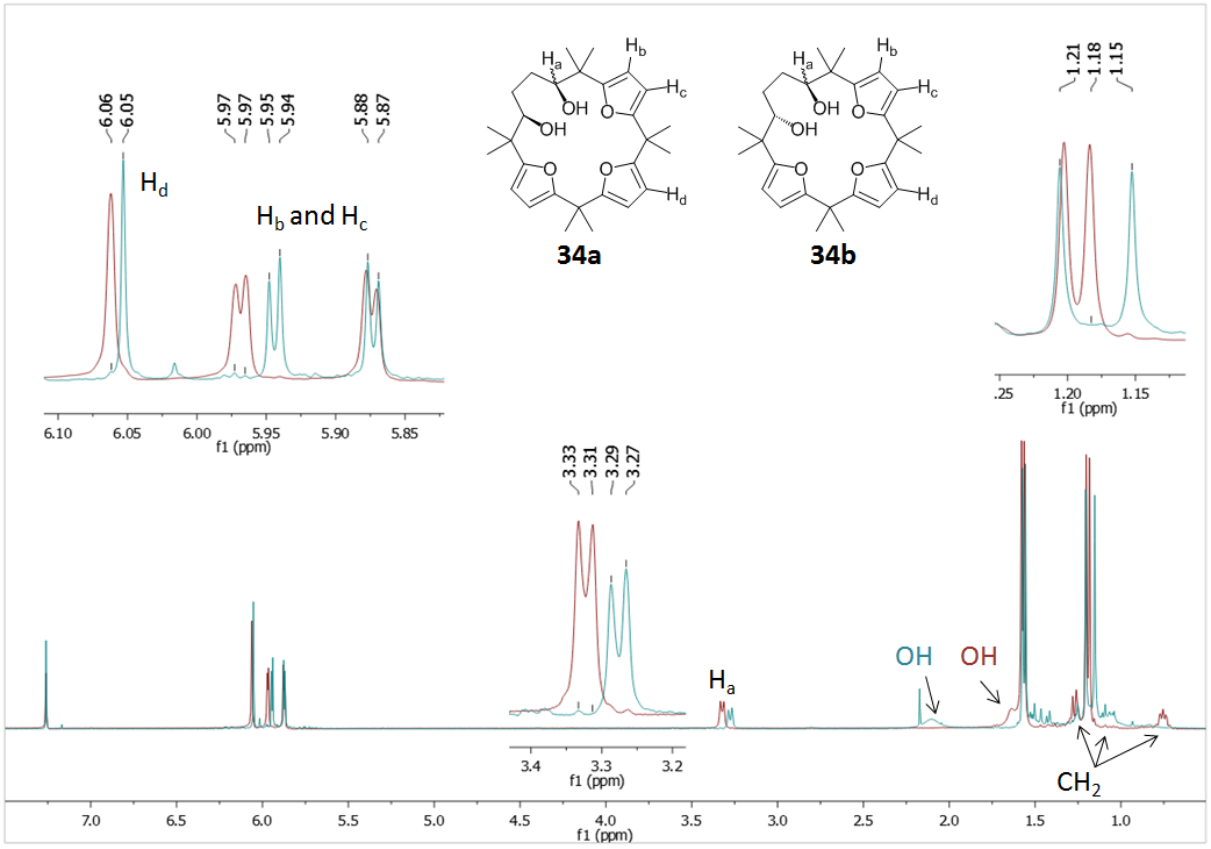

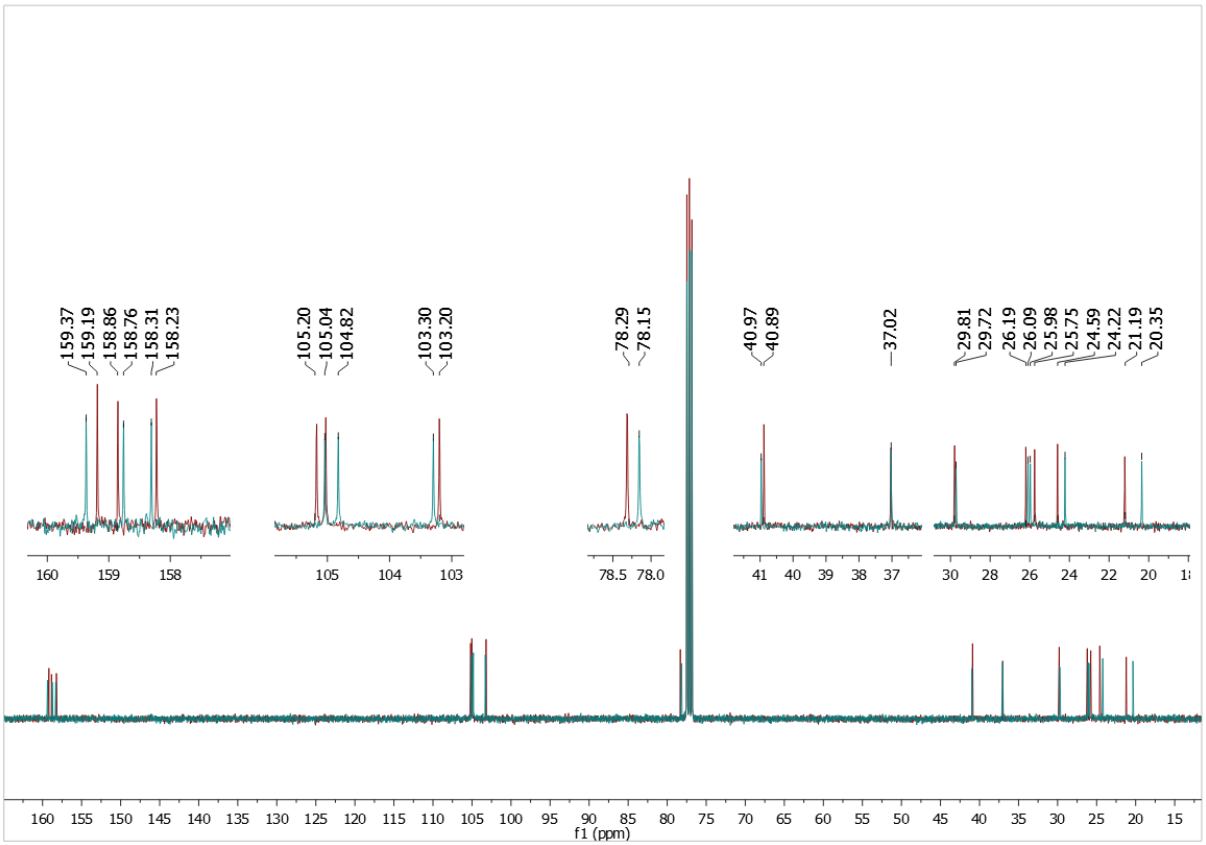

Figure 66. Comparison of 400-MHz ^{1}H (above) and ^{13}C NMR (below) spectra of **34a** and **34b**. Brown spectra: **34a**; blue spectra: **34b**

In summary the differences observed in the NMR spectra are subtle but characteristic despite the massive difference in polarity between the two diastereoisomers as observed in TLC or UPLC. As expected the melting points of the two fractions were also significantly different. A melting point of 165 °C was observed for the *meso*-compound **34a** while the melting point determined for the racemate **34b** was significantly higher (204 – 206 °C). Visually the two solids were easy to distinguish: **34b** was an expanded and light solid and **34a** was a powder. Thereby, **34b** occupied a more important space in the vial it was kept compared to an identical mass of **34a**.

2.3. Screening conditions

With our UPLC method we could screen different conditions in order to study the diastereoselectivity of the reduction (see Table 17). Treatment of compound **21** with $NaBH_4$ in EtOH at reflux for 2 h afforded the two diastereoisomers in the same 50/50 ratio (Table 17, Entry 2). Changing the reducing agent to $LiAlH_4$ in THF led after 2 h at reflux to a 70/30 diastereoselectivity in favor of **34a** (Table 17, Entry 3). When the reaction was carried out at lower temperature (r.t. and 0 °C), a slower conversion was observed and 4 h reaction were needed to convert all the starting material **21** (Table 17, Entry 4 and 5). Better diastereoselectivities were obtained at lower temperatures to reach an 89/11 ratio at 0 °C as shown in the UPLC in Figure 67 and Table 17, Entry 5.

Entry	Reducing agent	Reaction conditions	Ratio **34a**/**34b**(%)
1	$NaBH_3CN$	EtOH, reflux, 2 h	No reaction
2	$NaBH_4$	EtOH, reflux, 2 h	50/50
3	$LiAlH_4$	THF, reflux, 2.5 h	70/30
4	$LiAlH_4$	THF, r.t., 4 h	85/15
5	$LiAlH_4$	THF, 0 °C, 4 h	89/11

Table 17. Screening of the ketone's reduction of compound **21** (6 equiv. of reducing agent was used in each experiment)

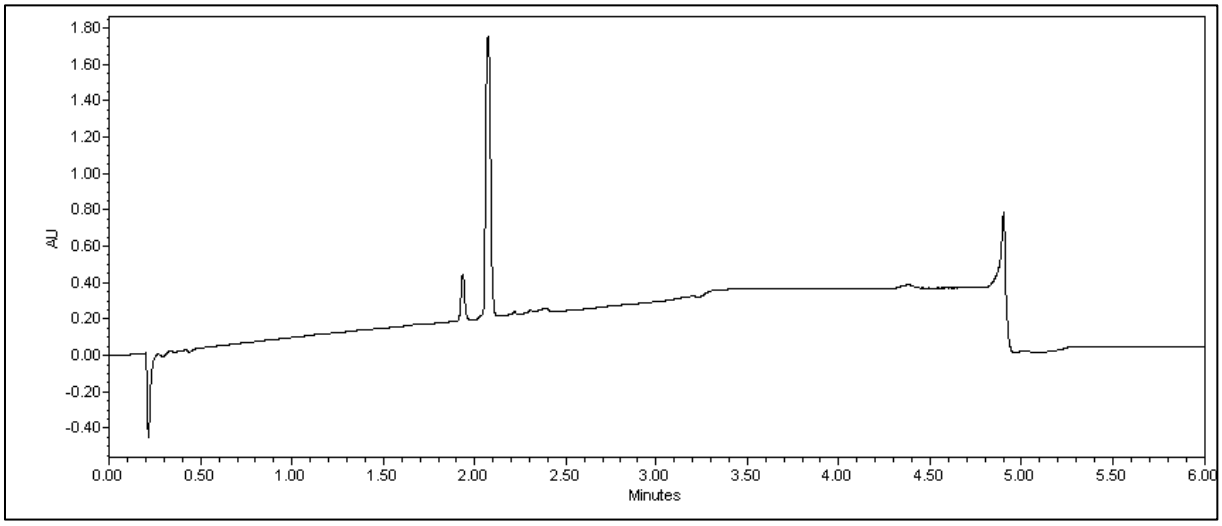

Figure 67. UPLC analysis of the crude material after reduction of ketones of compound **21** ($LiAlH_4$, THF, 0 °C, 4 h; see Entry 5 Table 17). Ratio: **34a**/**34b** = 89/11. Peaks at 0.2 and 4.9 min are respectively the injection and the change of mobile phase to equilibrate the column before a new injection

2.4. Conclusion

The transformation of the ketone functions of compound **21** led to the formation of the two diastereoisomers **34a** and **34b**. The X-ray structure determination of fraction 2 (**34b**) allowed to attribute unambiguously the chemical structures (= relative configurations) to the two isolated fractions. The reduction was studied using $NaBH_4$ and $LiAlH_4$ as reducing agent leading to diastereoselectivity in favor of *meso*-compound using $LiAlH_4$ at lower temperatures.

3. Synthesis of pyrrolidine function via reductive amination of compound 21

3.1. Context of the reaction in the project

Following the unsatisfactory yields obtained on the synthesis of calix[4]pyrrolidine **3** *via* the hydrogenation of calix[4]pyrrole **1**, an alternative sequence was tested in our group by Dr. Vsevolod Khlebnikov. This sequence was based on the reductive amination of the four saturated 1,4-diketone functions of compound **35** to form calix[4]pyrrolidine **3** (Scheme 30). Using the procedure successively applied for the synthesis of calix[n]furan[4-n]pyrroles **7** – **10** developed in chapter 2, the tetra-ring-opening of calix[4]furan **2** with *m*-CPBA followed by the reduction of the alkene functions led to the formation of compound **35**. Compound **35** should then be reductively aminated to give the calix[4]pyrrolidine **3**. Unfortunately, this alternative approach did not lead to the formation of calix[4]pyrrolidine **3**.

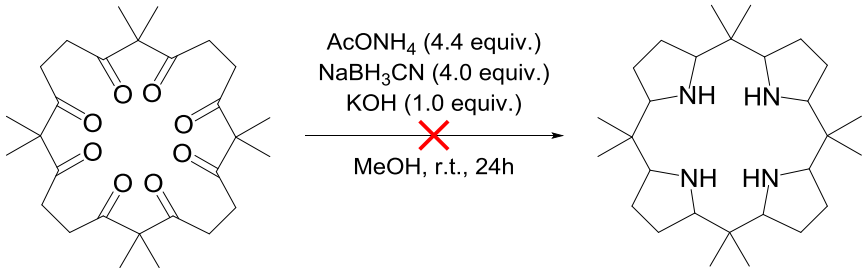

Scheme 30. Proposed alternative synthesis of calix[4]pyrrolidine **3**

3.2. Synthesis of compound 36

The reductive amination with $AcONH_4$ as amine source was carried out on compound **21** (Scheme 31). The reaction conditions were based on a procedure reported by Jones *et al*. on the formation of 2,5-dialkylpyrridines *via* the reductive amination of 1,4-diketones.[169] Methanol was the reported solvent for the synthesis. Since compound **21** was not soluble in methanol, a (1/1) dichloromethane/methanol mixture was used. Treatment of compound **21** with $AcONH_4$, $NABH_3CN$ and potassium hydroxide (KOH) led after 24 h at r.t. to full conversion of **21** and to the formation of compound **36** in 75% in the crude material (GC analysis). Recrystallization of the crude material in EtOAc (one night in the fridge) afforded macrocycle **36** in 25% yield as white solid.

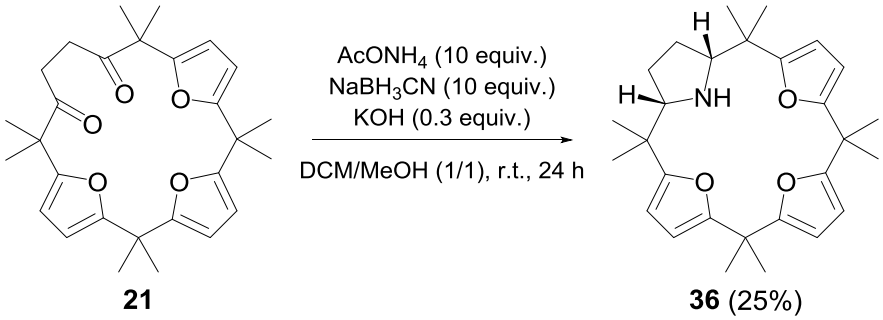

Scheme 31. Synthesis of calix[3]furan[1]pyrrolidine **36**

The molecular structure of compound **36** was determined by X-ray diffraction analysis of suitable crystals obtained by crystallization from EtOAc (Figure 68). Compound **36** crystallized in the monoclinic $P2_1/n$ space group with the 1,3-alternate bowl conformation. The X-ray structure secured the position of the protons located in the α–position of the –NH (*cis*-pyrrolidine). The proton on the nitrogen has been localized pointing towards the center of the macrocycle; the proton was located in a different Fourier map and was freely refined.

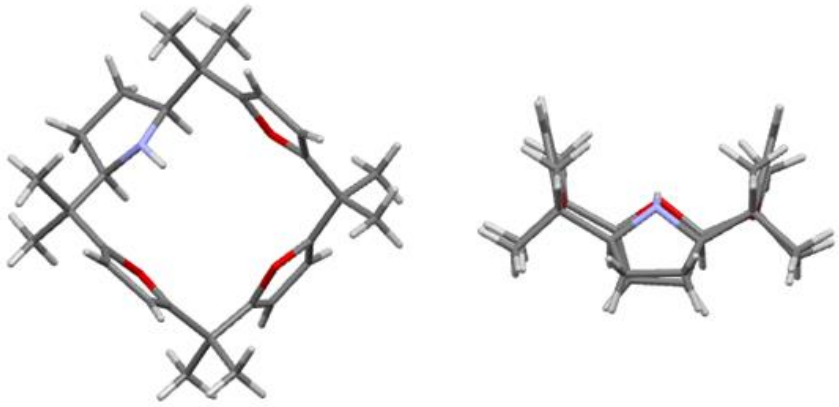

Figure 68. Molecular structure of **36**. Top view (left); side view (right)

4. Synthesis of unsymmetrical calix[n]furan[4-n]pyrroles

4.1. Isolation and characterization of side product 37

During the optimization of the synthesis of calix[3]furan[1]pyrrole **10** (see chapter 2), one of the first large-scale experiment of the ring-opening of calix[4]furan **2** (7.17 grams) into compound **22a** led to the isolation of an interesting side product during the purification process (Scheme 32). As was found out later, the speed of the separation process is crucial for obtaining good yields of compound **22a** (see page 33 Chapter 2). In our initial experiments the isolation revealed to be time consuming. In this specific experiment the chromatography had to be interrupted overnight, as most of the product had already been recovered.

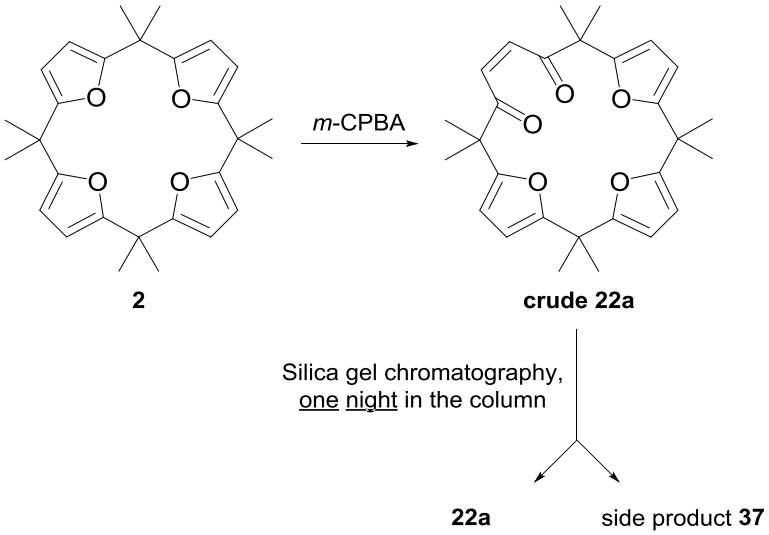

Scheme 32. Process leading to the isolation of side product **37**

The day after, a new product appeared under compound **22a** on the TLC (Cy/EtOAc 8/2, R_f(**22a**) = 0.68; R_f(**37**) = 0.63). This side product was isolated pure (400 mg, 5% yield) and we were able to fully characterize it.

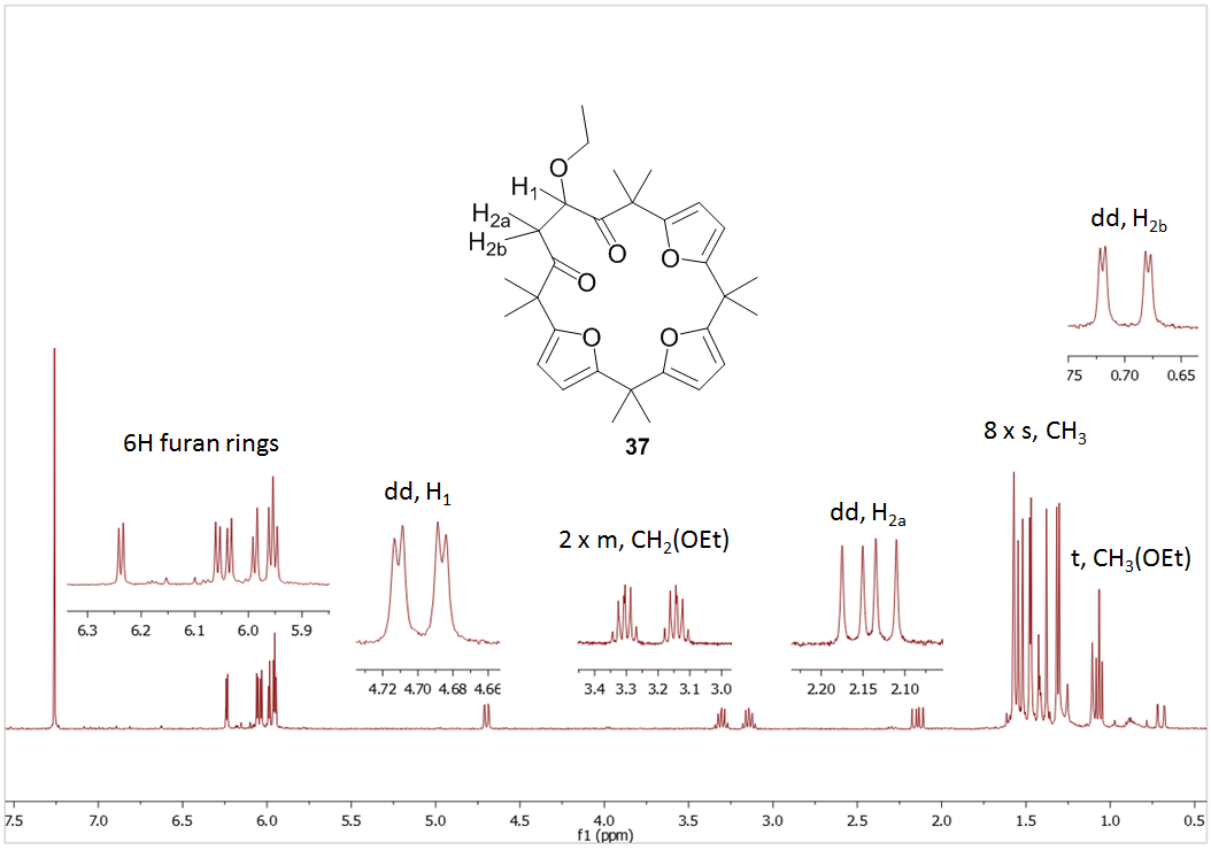

Figure 69. 400-MHz ^{1}H NMR spectra of compound **37**

However the symmetry of the macrocycle had been lost and an ethyl group had been added. Eight singulets were observed in the region between 1.25 and 1.50 ppm, indicating that each methyl group had its own chemical environment and therefore its characteristic chemical

shift. The analyses of the ^{1}H, ^{13}C NMR and MS spectra were compatible with the structure proposed in Figure 69. This product would be the result of the addition of ethanol on the double bond in the starting material **22a**. The protons of the CH_2-group α to the keto function are diastereotopic and H_{2a} and H_{2b} appear therefore as two distinct doublets of doublet (dd) in the ^{1}H NMR spectra with significantly different chemical shifts (2.14 ppm (H_{2a}) compared to 0.7 ppm (H_{2b})). Proton H_{2a} (respectively H_{2b}) coupled with its geminal partner H_{2b} (respectively H_{2a}) with a germinal coupling constant of 16 Hz and additionally the vicinal coupling to proton H_1 is observed (coupling 10 Hz respectively 2 Hz). The two protons from the O–CH_2 group from the ethyl chain are also diastereotopic as the two peaks at 3.31 ppm and 3.14 respectively are two multiplets, which can be interpreted as quintet like multiplet derived from a signal which should be theoretically a doublet of quadruplet having similar coupling constants.

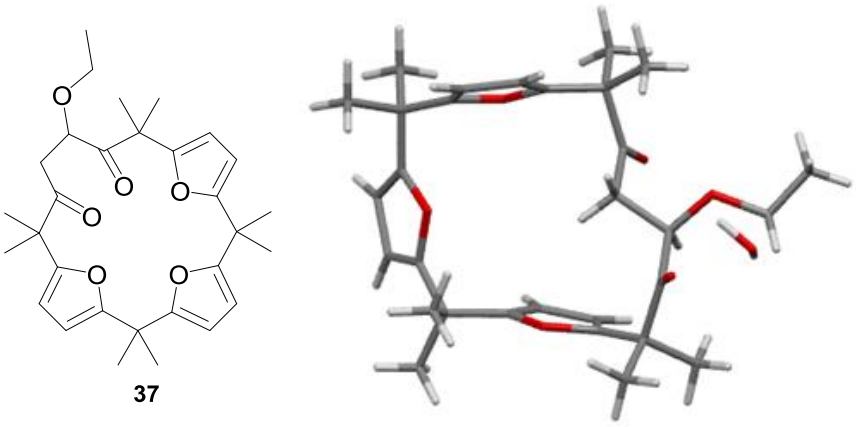

Figure 70. Structure (left) and molecular structure (right) of compound **37**

A crystal of sufficient size for an X-ray diffraction analysis was grown. The X-ray structure is in full agreement with our previous structure proposals (Figure 70). The molecule crystallized in the monoclinic $P2_1/n$ space group and incorporated a molecule of water. The two diastereotopic hydrogens H_{2a} and H_{2b} point in significantly different directions which should explain the difference in their chemical shifts. One of the protons is directing toward the shielding region of the opposite aromatic furan ring while the other is pointing outside of the macrocycle. The proton in direction to the furan ring should be in higher field (H_{2b}, 0.7 ppm, Figure 69) than the other (H_{2a}, 2.14 ppm).

As this compound was formed during the overnight stay of the compound on the silica gel column without the formal presence of ethanol a reasonable proposal for the mechanism of formation has to be proposed (Scheme 33). We therefore propose that under the influence of the acidity of the silica the EtOAc of the solvent might have been partially hydrolyzed thereby forming ethanol. Ethanol, as a nucleophile attacks the activated double bond of compound **22a**.

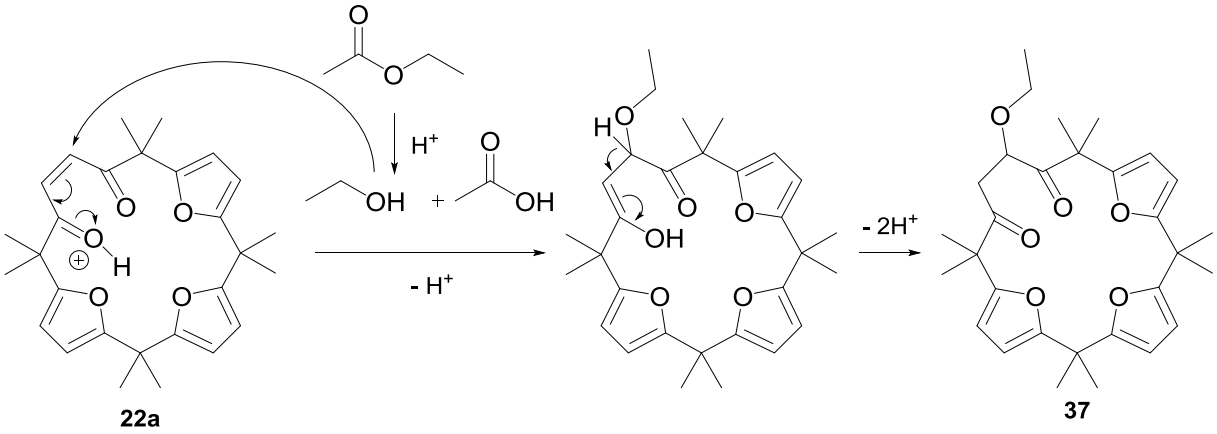

Scheme 33. Proposed mechanism for the formation of compound **37**

4.2. Ring closing reaction on compound 37

A sufficient amount of compound **37** (400 mg) was isolated to test the ring-closing reaction on this type of 2-substituted-1,4-diketone intermediate. Compound **37** was solubilized in EtOH and treated with an excess of $AcONH_4$ (10 equiv.) at 85 °C (Scheme 34). The product did not precipitate out of the solution as we had observed in the synthesis of calix[3]furan[1]pyrrole **10** and calix[2]furan[2]pyrrole **8**. After 4 h, TLC and GC analysis showed complete disappearance of the starting material and to our surprise the formation of two products. No change in the product distribution was observed if the reaction was run for longer reaction times (6 h). Dichloromethane was added and the mixture was washed with water to remove the excess of $AcONH_4$. Evaporation of the solvent led to the crude material containing the two products in a 52/48 ratio (GC). The difference of polarity of the two compounds was big enough to allow a separation of the two compounds by chromatography (Cy/EtOAc 7/3, R_f = 0,69 and 0,27). The first fraction was isolated with Cy/EtOAc (95/5) as mobile phase and then the polarity of the eluent was considerably increased (7/3 mixture) allowing to elute the pure second fraction.

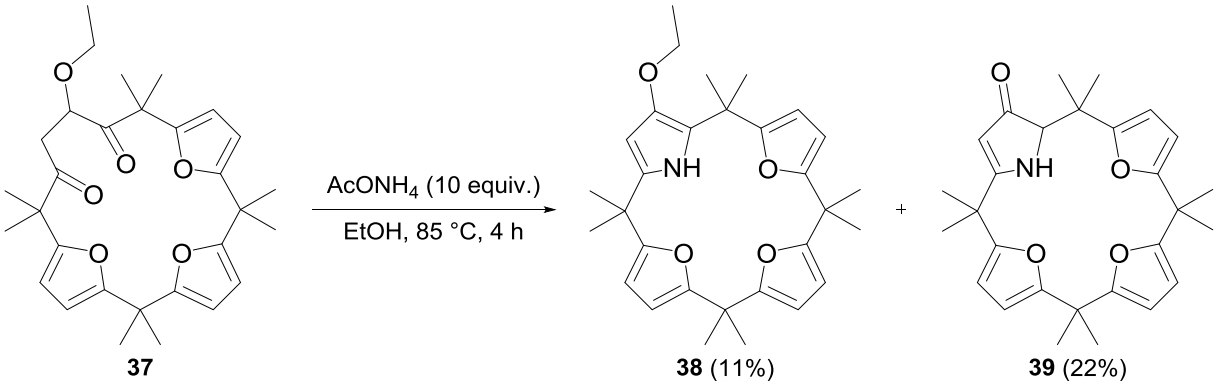

Scheme 34. Paal-Knorr synthesis starting from compound **37**

The ^1H NMR spectra of the first fraction were compatible with the proposed structure **38** derived from the planned Paal-Knorr reaction (Scheme 34). The analysis of the 1D/2D NMR and MS spectra of the second fraction is compatible with the structure **39**, a compound which

is the hydrolysis product of **38**. The formation of compound **39** is the consequence of a hydrolysis step leading to compound **38** present as a mixture of two tautomeric forms (Scheme 35). The formation of the pyrrole ring using $AcONH_4$ involves the liberation of two molecules of water by pyrrole ring in the reaction mixture. The presence of water in the slightly acidic reaction medium (one molecule of acetic acid is formed per pyrrole) favors the hydrolysis of the ether chain to form compound **39** as a mixture of its keto-enol tautomers **39** and **39'**. The two compounds **38** and **39** were isolated in respectively 11% and 22% yield. These compounds were isolated as clean as possible for full characterization. This explains the relatively low isolated yield compared to the conversion observed in GC.

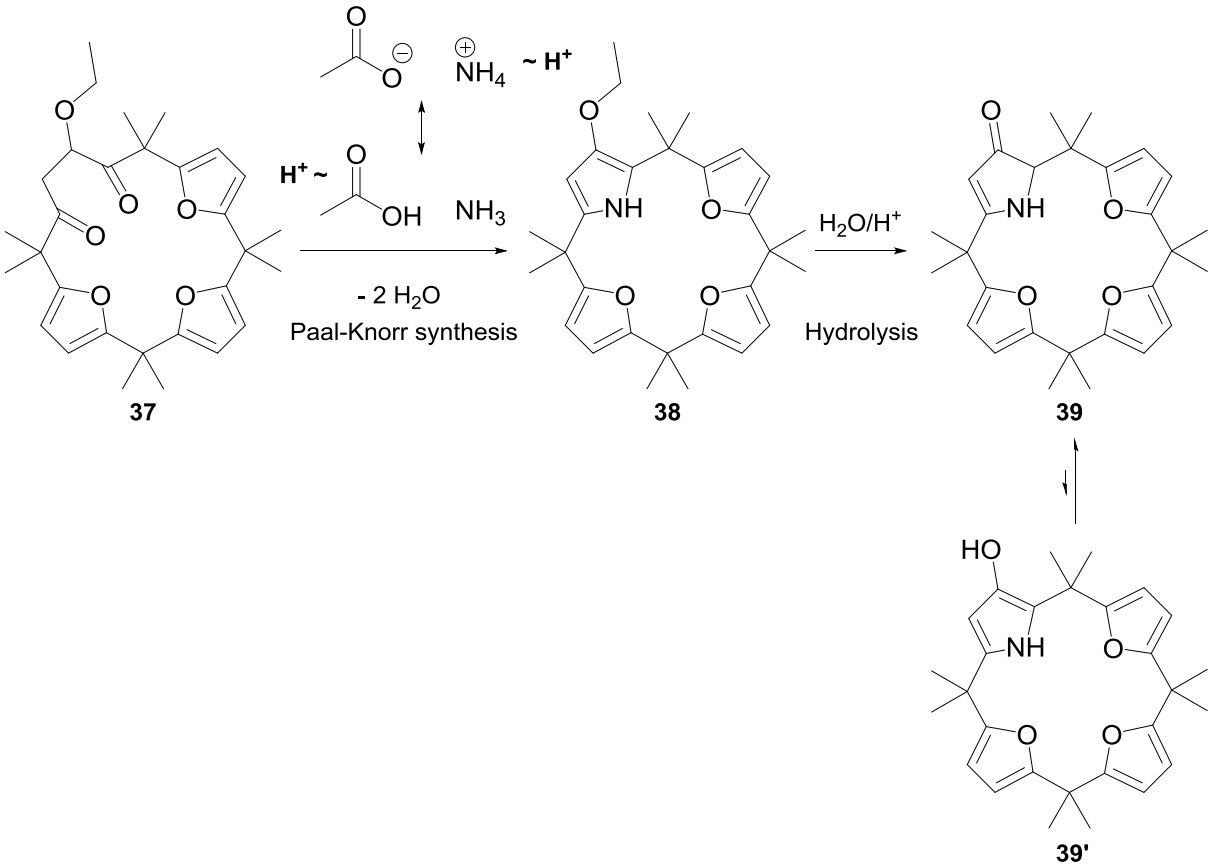

Scheme 35. Proposed formation of **39** from compound **38**

4.3. Synthesis of substituted calix[3]furan[1]pyrrole 41

The isolation and characterization of side product **37** revealed the ease, by which nucleophile can add to the activated double bond. This result induced us to study this strategy as an approach to the synthesis of unsymmetrically substituted calix[n]furan[4-n]pyrroles containing a 3-substituted pyrrole ring in the macrocycle.

Diethyl malonate, a classical Michael donor (nucleophile) for 1,4-addition of α,β-unsaturated was chosen to test this reaction. Treatment of compound **22a** in THF with diethyl malonate and sodium hydride (NaH) as base led after one night at r.t. to the formation of a compound present in 62% in the crude material (GC analysis). The solvent was removed using the

rotavap and the resulting oil was purified by silica gel chromatography to afford compound **40** in 55% yield, 95% purity by GC analysis (Scheme 36).

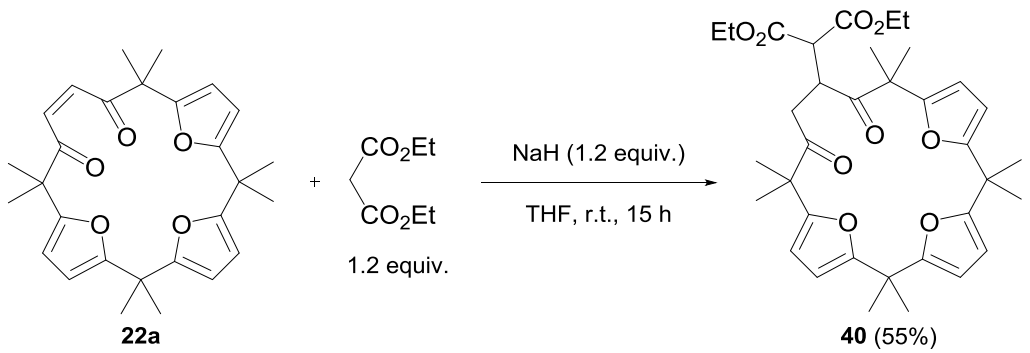

Scheme 36. Synthesis of compound **40**

Compound **40** was submitted to the ring-closing reaction using 4.5 equiv. of $AcONH_4$ in EtOH at 85 °C in a Schlenck tube. No precipitation of the product was observed during the reaction. After 4 h, the GC analysis indicated the formation of a unique product in 95% purity. Dichloromethane was added to the reaction and then the reaction mixture was washed with water. After collecting the organic layers and removing the solvent under reduced pressure using the rotavap, the residue was purified by silica gel chromatography (Cy/EtOAc 95/5). The HRMS analysis of the fraction indicated a molecular weight (MW) of 518.2905g.mol^{-1}. This molecular weight clearly indicates the loss of one of the carboethoxy groups (molecular weight of the expected compound **42**: MW = 589.7290) (Scheme 37). Moreover, while two different quadruplets were observed for the $-CH_2$ of the –OEtyl chain in the ^{1}H NMR analysis of compound **40**, only one quadruplet is present in the ^{1}H NMR spectrum of the isolated fraction **41**. These spectral data are compatible with the occurrence of one decarboxylation during the reaction forming compound **41** as unique isolated product and no traces of compound **42** were detected. Compound **41** was isolated in 67% yield as a white solid in excellent purity (GC analysis). The introduction of this unique "side arm" with an ester function is an excellent starting point of further transformations, introducing *via* easy and high-yielding reactions all sorts of novel side chains or fixing the macrocycle on surfaces.

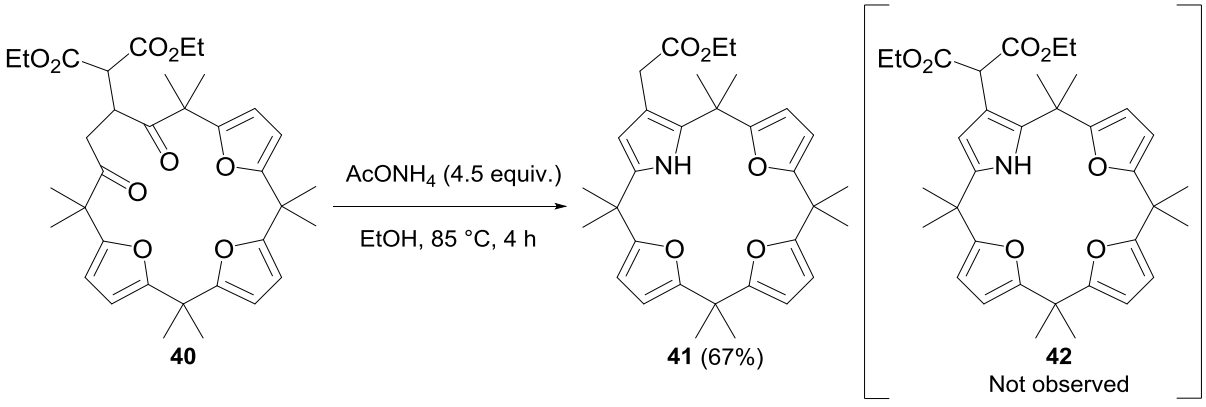

Scheme 37. Synthesis of compound **41**

5. Conclusion

Intermediates **22a** and **21** revealed to be valuable compounds for the synthesis of novel molecules with varied functions. Only a few transformations of the catalogue of possible modifications were tested so far. Calix-1,4-diols **34a** and **34b** are interesting structures but resolution of the *meso*- and *rac*-compounds by introducing substituents to obtain enantiomerically pure compounds would be needed before thinking to study these compounds as potential catalysts. The most attractive of the studied transformation was the synthesis of non-symmetrical calix[3]furan[1]pyrroles introducing a selective substitution on the pyrrole ring. This 3-substituted pyrrole ring came from nucleophilic addition on the unsaturation of intermediate **22a** followed by a ring closing Paal-Knorr reaction. The use of diethyl malonate as nucleophiles have been tested reliably leading in good yields to the new non-symmetrical calix[3]furan[1]pyrrole **41**.

Chapter 7. Conclusion and perspectives

Conclusion

The objectives, developing an efficient synthesis of the four calix[n]furan[4-n]pyrroles **7** – **10** and studying their hydrogenation to fully saturated macrocycles **7** – **14**, were achieved. Although three of the four aromatic macrocycles containing both furan and pyrrole rings were synthesized for the first time more than fifty years ago, especially the low yield to these compounds prohibited in-depth studies of their properties and potential applications. Optimizing their synthesis based on the selective ring-opening of calix[4]furan **2** brought an easy and scalable access to the four isomers. Having developed an easy access may inspire renewed interests from the scientific community. The (geometric) resemblance with the structures of the "pigments of life" predicts interesting and important properties of this class of ligands. Having made available a systematic and complete series of isoelectronic ligands should facilitate the interpretation of the results.

During the optimization the different steps were varied as to detect the best conditions for larger scale experiments. Over the years gram quantities of the four isomers **7** – **10** were isolated. With these heterocalix[4]arenes in hand, the hydrogenation study, made in preliminary studies by Guillaume Journot in the group, could be examined and efficient conditions for the hydrogenation were developed. The hydrogenation reaction was remarkably selective: With three of the four calix[n]furan[4-n]pyrroles the formation of a unique diastereoisomer in good to excellent yield was observed. A respectable amount (hundreds of mg) of these saturated macrocycles was also isolated. Being a synthetic group we decided to share our materials with scientific colleagues specialized in studies using specific physicochemical methods or interested in the application of these compounds e.g. in catalysis. Time restraints obviously limited the breadth of studies, which could be undertaken.

Both the fully saturated macrocyclic structures, as their aromatic parent compounds, are easy to crystallize. The structures in the crystals of the entire family of calix-compounds could be determined by X-ray diffraction. The calix[n]furan[4-n]pyrroles, containing four aromatic rings, all crystallized in the 1,3-alternate conformation (bowl-like conformation) reported for the calix[4]arenes. The saturated calix[n]tetrahydrofuran[4-n]pyrrolidines showed two different conformations: the 1,3-alternate conformation (bowl-like) and an almost planar conformation (plate-like). With the help of Prof. Aurora Cruz-Cabeza (University of Manchester, UK) the conformational manifold of this class of compounds was studied using computational methods. Computational calculations predicted the presence of two conformers and explain the trend from bowl- to plate- conformation. The calculations thereby induced us to study preferentially the crystallization of calix-NOOO **14**, which is predicted to be present in both conformations. These studies lead to the detection of an isomorph: the orthorhombic Pbca form. This isomorph however showed the same conformation of the compound. The switch to the alternative conformer has not (yet) been observed. As next step calculations of the relative lattice energies of the six fully saturated heterocycles in this Pbca form will be done with the goal to identify other isomers which might be crystallized in this symmetry of the unit cell.

As preliminary studies five novel transition metal complexes were synthesized using the mixed ligands, namely calix-NONO **13** and calix-NOOO **14**. No in-depth studies on the properties of these metal complexes have been carried out yet.

As it is often the case in chemistry research, our "calix" project was full of unpredicted obstacles. These obstacles allowed taking new directions either to reach the initial goal or to define new ambitions relative to the first goal. Originally, the project on the hydrogenation of calix[n]furan[4-n]pyrroles was born from the difficulties observed on the synthesis of calix[4]pyrrolidine **3** from the well-known calix[4]pyrrole. The four years spent on the project allowed reaching our objectives with the contribution of an efficient and scalable synthesis of the four saturated heterocalix[4]arenes **11** – **14**. This work led to several other not yet finished or unexplored projects.

Perspectives

During our work on the optimization of the synthesis of calix[n]furan[4-n]pyrroles **7** – **10** a collaboration started with the group of Professor Christophe Thomas (ParisTech, France). They developed a synthesis of biodegradable polyesters by a tandem catalysis using tetradentate salen ligands (Figure 38).[170] A collaborative project between our two groups was started studying the formation of metal complexes using the calix[n]furan[4-n]pyrroles as ligands. No new useful catalyst based on our ligands has been fully characterized yet. To our delight the activity of some complexes synthesized *in situ* could successfully be tested.

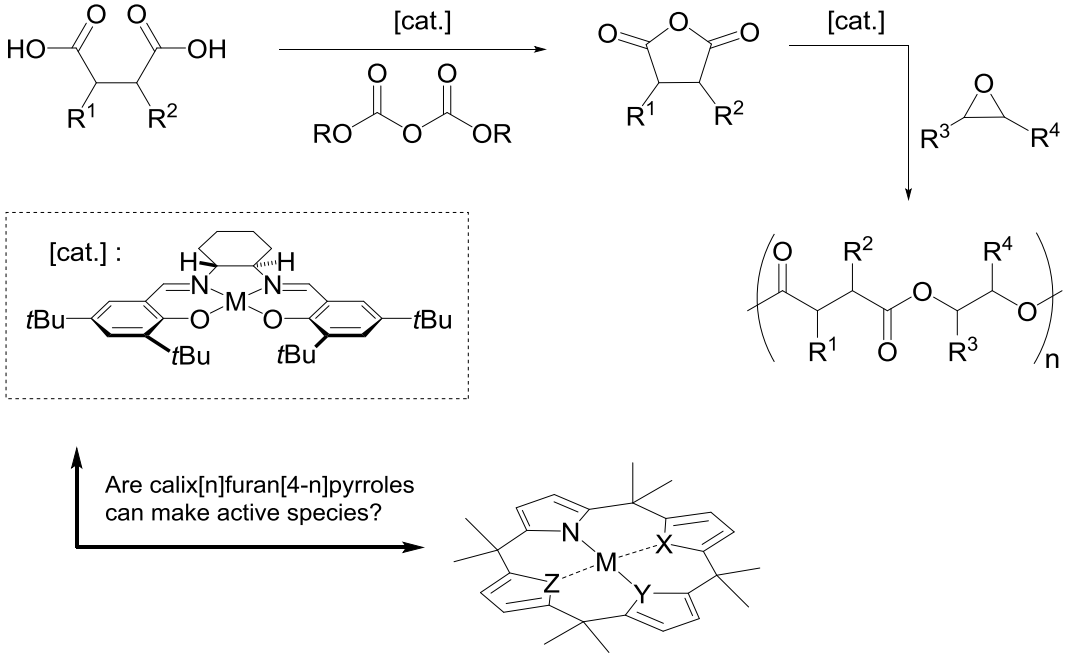

Scheme 38. Synthesis of aliphatic polyesters by tandem catalysis reported by the group of Christophe Thomas.[170] M = Cr-Cl; Al-Cl; Co; Mn-Cl. X = Y = Z = NH or O.

Secondly, an ambitious idea is based on the recent collaboration with Prof. Karl Kadish's group working on electrochemistry. So far the oxidation of the aromatic calix-compounds was studied. The electrochemical reduction of calix[4]pyrrole **1** in presence of acid, might be a way to circumvent the disappointingly difficult hydrogenation to our target compound calix[4]pyrrolidine **3** (Scheme 39). A success in the formation of calix[4]pyrrolidine **3** with this alternative synthetic access would be an extraordinary way to come full circle.

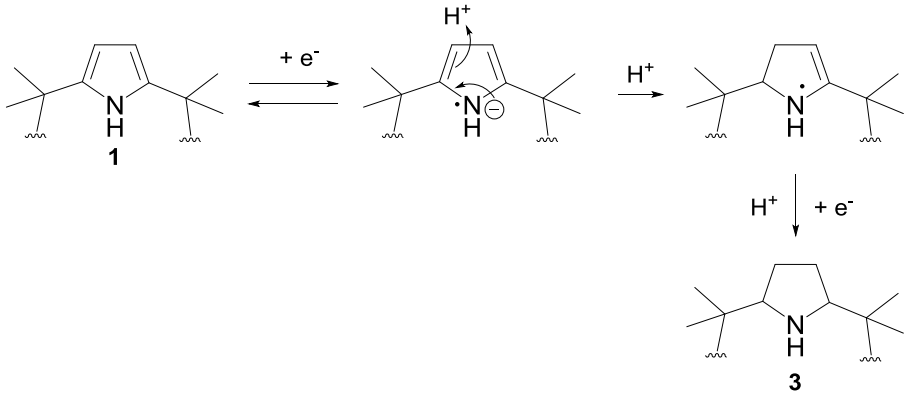

Scheme 39. Proposed hypothetical synthesis of **3** *via* electrochemical hydrogenation

Thirdly, the synthesis of calix-1,4-diols stopped with the synthesis and characterization of the *meso*- and *rac*-compounds. The next step of this project would be the resolution of the C_{2v} rac-compound: formation of a diastereoisomeric mixture with the addition of a chiral auxiliary. The separation of these diastereoisomers followed by the removal of the auxiliary would give the two enantiopure (*S, S*) and (*R, R*) compounds. One of the most common methods for the resolution of diol-compounds is be the mono acylation using chiral catalyst such as (*S*)-proline and boric acid[171], a chiral phosphoric acid[172] or enzymatic resolution using lipases[173], just to cite a few.

As a final proposal, applying the synthesis of an unsymmetrical substituted calix[3]furan[1]pyrrole *via* Michael addition on the unsaturated 1,4-diketone intermediate opens many interesting new opportunities. Several other analogues could be synthesized with various substituents and the full hydrogenation of these products might lead to interesting ligands with a side arm (Scheme 40) with similar applications than cyclam derivatives.

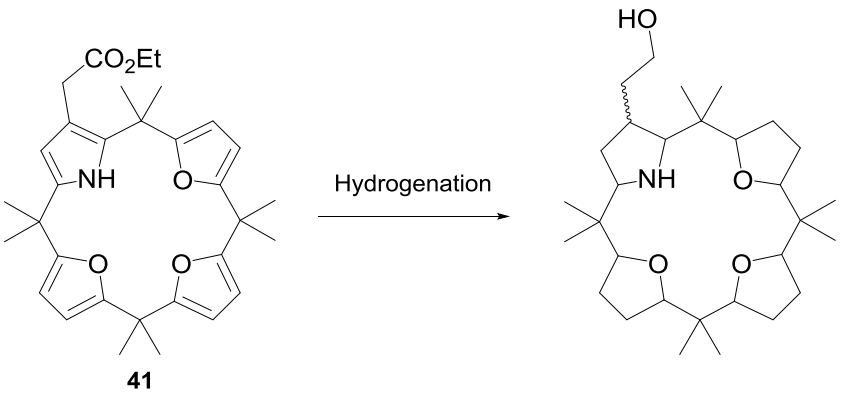

Scheme 40. Supposed hydrogenation substituted calix[3]furan[1]pyrrole **41**

Chapter 8. Experimental part

1. General information

Standard solvents

For the purpose of chromatography and extractions, technical grade solvents were distilled under reduced pressure using the rotavapor.

Solvent	Abbreviation used
Chloroform	$CHCl_3$
Cyclohexane	Cyclohexane
Dichloromethane	CH_2Cl_2
Ethyl acetate	EtOAc
Methanol	MeOH
Trimethylamine	Et_3N

Solvents for reaction

solvent	Abbreviation used	Quality
Acetic acid (glacial)	AcOH	VWR Chemicals, analaR Normapur
Chloroform	$CHCl_3$	Honeywell Burdick & Jackson, p.a.*, ACS reagent
Dichloromethane	CH_2Cl_2	Honeywell Burdick & Jackson, p.a., ACS reagent
Dioxane	Dioxane	ROMIL-SpS
Ethanol	EtOH	Honeywell Burdick & Jackson, p.a. or Aldrich p.a. ≥99.8%
Ethyl acetate	EtOAc	Honeywell Burdick & Jackson, p.a., ACS reagent
Methanol	MeOH	VWR Chemicals, analaR Normapur
Tetrahydrofuran	THF	Aldrich, anhydrous ≥99.9%

*p.a.: pro analysis

Reagents. Unless otherwise noted, all reagents were obtained commercially and used without further purification.

Reagent	Abbreviation used	Quality
3-chloropenbenzoic acid	*m*-CPBA	Acros Organics, technical grade (70-75%)*
Acetone	Acetone	Aldrich, CHROMASOLV® PLUS, for HPLC, ≥99.9%
Ammonium acetate	$AcONH_4$	Aldrich, ≥98%**
Bromine	Br_2	Acros organics, p.a.
Butyl lithium	*n*-BuLi	Aldrich, 2.5M in hexane
$Cobalt^{II}$ chloride	$CoCl_2$	Aldrich, purum p.a., ≥98%
$Copper^{II}$ chloride	$CuCl_2$	Aldrich, 99%
Diethyl malonate	Diethyl malonate	Aldrich, ReagentPlus®, 99%

Furan	Furan	Aldrich, ACS reagent, ≥99%
Hydrochloric acid	HCl	VWR Chemicals, analaR Normapur, 37%
Hydrogen	H_2	Carbagaz 45
Lindlar catalyst 5%	Lindlar catalyst	Aldrich, 5% Pd on calcium carbonate, poisoned with lead
Lithium aluminum hydride	$LiAlH_4$	Aldrich, reagent grade, 95%
Nickel^{II} chloride	$NiCl_2$	Aldrich, 98%
Palladium on carbon 10%	Pd/C	Aldrich, 10% Pd basis
Potassium hydroxide	KOH	Acros organics, extra pure, pellets
Potassium permanganate	$KMnO_4$	Aldrich, ACS reagent, ≥99%
Pyrrole	Pyrrole	Aldrich, reagent grade, 98%
Sodium cyanoborohydride	$NaBH_3CN$	Aldrich, reagent grade, 95%
Sodium borohydride	$NaBH_4$	Aldrich, purum p.a., ≥96%
Sodium hydride	NaH	Aldrich, 95%
Sulfuric acid	H_2SO_4	Carlo Erba, for analysis
Trifluoroacetic acid	TFA	Aldrich, ReagentPlus®, 99%
Zinc dust	Zn	Aldrich, ≥98%

*_m_-CPBA) was technical grade (70-75%, the amount used were calculated assuming 72.5%); **Ammonium acetate was kept in the fridge and dry under reduced pressure for 1 h before to be used (hygroscopic)

Heating/cooling. For reactions at low temperature, ice bath with salt (0 °C to -5 °C) and acetone/liquid nitrogen bath (-78 °C) were used. For heating reactions, oil baths (40-200 °C) were used.

Melting points. Melting points were measured on a Buchi 510 melting instrument.

Thin layer chromatography (TLC). Analytical thin layer chromatography was performed on Merck precoated glass-backed TLC plates (silica gel 60 F254) and visualized by UV lamp (254 nm) and potassium permanganate ($KMnO_4$) stain.

Columns chromatography. Columns chromatography were carried out on silica gel 60 Å, 32-63 (Brunschwig) and aluminium oxide Fluka for chromatography, Brockmann activity I. Technical grade solvents were employed, which were distilled using the rotavapor prior to use. Concentration of the collected fractions under reduced pressure was performed by rotary evaporation at 40 °C at the appropriate pressure. Purified compounds were further dried under high vacuum (0.3 Torr). Yields refer to purified and spectroscopically pure compounds, unless stated otherwise.

Gas chromatography (GC). GC analyses were recorded on an Agilent 6850A, column Agilent Technologies (Part Number 19091Z-413E, Length (m): 30; Diam. (mm): 0.320; film (µm): 0.25).

GC method used for macrocyclic structures: Injection volume (µL): 1.0; Inlet Temp. (°C): 280; Inlet Pres. (PSI): 10.32; Flow (mL/min.): 45.6; Detector Temp (°C): 280; Flow (mL/min.): H_2: 40.0, Air: 450, N_2: 45. Gradient: 220°C for 2min, 220°C to 300°C by heating 5°C/min then 300°C for 10min. Total time: 28min.

GC method used for the small models: Injection volume (µL): 1; Inlet Temp. (°C): 280; Inlet Pres. (PSI): 5.74; Flow (mL/min.): 45.6; Detector Temp (°C): 280; Flow (mL/min.): H_2:40.0, Air 450, N_2:45. Gradient: 50°C for 3min, 50°C to 300°C by heating 15°C/min then 300°C for 8min. Total time: 28min.

Gradient: Macrocyclic structures (left) and small models (right)

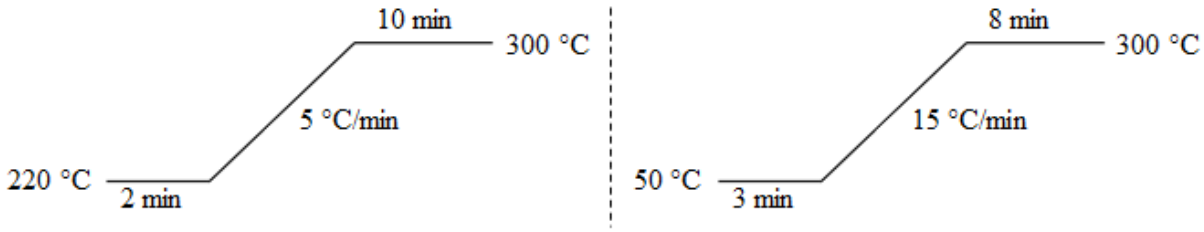

Ultra performance liquid chromatography (UPLC). UPLC analyses were recorded on a Acquity UPLC Waters (Software: Empower), column 1.7 µm Acquity BEH C18, Length (mm): 50; Diam. (mm): 2.1.

Method:

Low pressure: 0 psi; High pressure: 15000 psi; weak wash: 600 µl: strong wash: 200 µl; seal wash: 5 min; equilibration time: 0.1 min; T (°C) sample: off; ; T (°C) column: off; λ UV detector: 220 nm; injection volume (µL):1.0;

Gradient : solution A: water/acetonitrile/formic acid (90/10/0.1); solution B: acetonitrile; proportion of solution B (%): 40 % for 3 min then 100 % for 1.5 min then 40 % for 1.5 min; Flow (ml/min): 0.6 for 3.0 min then 1.0 for 1.5 min then 0.6 for 1.5 min. Total time: 6 min

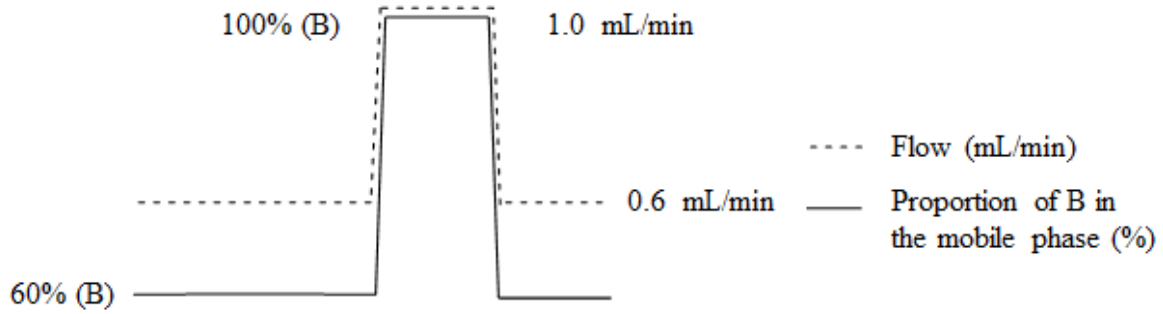

Infrared Spectroscopy (IR). Perkin Elmer Spectrum One version B FT-IR (Software: Spectrum version 5.0.1) or an ATR Thermo Scientific Nicolet iS5 FT-IR (Software: OMNIC) were used for obtaining IR spectra. KBr pellets (KBr – Fluka puris p. a) were prepared for the analysis of solid substances and thick oil like substance with the Perkin Elmer apparatus. The absorption bands between 4000 and 400 cm-1 were measured. The intensity of the spectrum was divided into four parts with the abbreviations *s* (intense), *m* (medium intensity), *w* (weak) and *br* (broad).

Nuclear Magnetic Spectroscopy (NMR). NMR spectra were recorded using a Bruker Avance 400 spectrometer operating at 400.13 MHz (^{1}H) and 100.63 MHz (^{13}C). The NMR

solvents were purchased from Cambridge Isotope Laboratories. ^{1}H NMR spectroscopy chemical shifts are quoted in ppm relative to internal tetramethylsilane TMS (δ= 0.00 ppm) or $CDCl_3$ (δ= 7.26 ppm). ^{13}C NMR spectroscopy chemical shifts are quoted in ppm relative to internal tetramethylsilane TMS (δ= 0.00 ppm) or $CHCl_3$ (δ= 77.16 ppm). The chemical shift is given in ppm in the descending order and the coupling constant *J* in Hz. The multiplicity of signals were given abbreviations *s* (singlet), *d* (doublet), *t* (triplet), *q* (quartet), *quint* (quintet), *dd* (doublet of doublet), *dt* (doublet of triplet), *br* (broad) and *m* (multiplet).

Mass Spectroscopy (MS). The mass spectra measurements for ESI (electro-spray ionization) were recorded with a Finnigan LCQ mass spectrometer. The high resolution mass spectroscopy measurements (HRMS) were recorded on a Waters UPLC-QTOFMS coupled with a SYNAPT G2. The ionization used was ESI (electro-spray ionization).

X-ray crystallography. The intensity data were collected at 173K (-100°C) on a Stoe Mark II-Image Plate Diffraction System [1] equiped with a two-circle goniometer and using MoKα graphite monochromated radiation (λ = 0.71073 Å). The structures were solved by Direct methods using the program SHELXS-97 [2]. The refinement and all further calculations were carried out using SHELXL-97 [2] or SHELXL-2014 [3]. The non-H atoms were refined anisotropically, using weighted full-matrix least-squares on F^2. A semi-empirical (multi-scan) absorption correction was generally applied using the MULABS routine in PLATON [4].

If the NH H-atoms could be located in a difference Fourier map they were refined with distance restraints: N-H = 0.88(2) Å with $U_{iso}(H) = 1.2U_{eq}(N)$. If the NH H-atoms could not be located in a difference Fourier map they were included in calculated positions and treated as riding atoms: N-H = 0.88 Å with $U_{iso}(H) = 1.2U_{eq}(N)$.

The remainder of the H-atoms were included in calculated positions and treated as riding atoms: C-H = 0.99 and 0.98 Å for CH_2 and CH_3, respectively, with $U_{iso}(H) = 1.5U_{eq}$(C-methyl) and $1.2U_{eq}$(C) for other H atoms.

References:

[1] Stoe & Cie. (2009). *X-Area V1.52 & X-RED32 V1.48 Software*. Stoe & Cie GmbH, Darmstadt, Germany.

[2] Sheldrick, G. M. (2008) Acta Cryst. A64, 112-122.

[3] Sheldrick, G. M. (2015) Acta Cryst. C71, 3-8.

[4] Spek, A. L. (2009). Acta Cryst. D65, 148-155.

2. Synthetic procedures and characterizations

2.1. Synthesis of calix[n]furan[4-n]pyrroles 7 – 10

2.1.1. Large scale synthesis of calix[4]furan 2

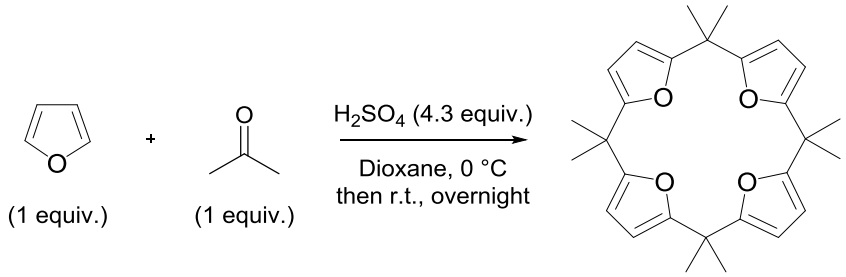

2

A precooled (0 °C) 90.5% sulfuric acid (175.5 mL, 2.956 mol, 4.3 equiv.) was added dropwise to a stirred precooled (0 °C) mixture of acetone (50.48 mL, 0.688 mol), furan (50.0 mL, 0.688 mol), and dioxane (800 mL). Upon addition of sulfuric acid, the reaction mixture turned dark purple and some precipitation of product was observed. The reaction mixture was stirred overnight at r.t., then separated in two equivalent portions in 2-L Erlenmeyer flasks equipped with stirring bars. Water (400 mL in each Erlenmeyer flask) was added and the acid was neutralized (pH = 14) by addition of NaOH pellets under stirring (around 240 g in total). Crude product was filtered off, washed with water (2 x 40 mL), methanol (until no more discoloration of the product was observed) and then dried vacuum (mass crude material = 56 g). Recrystallization of the tan solid from dioxane (10 g per batch of crystallization, around 70 mL of dioxane) gave 26.09 g (35% yield) of' colorless small needles.

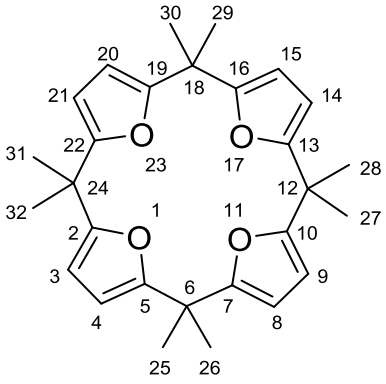

^{1}H NMR ($CDCl_3$, 298K) δ 5.89 (s, 8 H, C-H(3, 4, 8, 9, 14, 15, 20, 21)), 1.48 (s, 24 H, CH_3(25, 26, 27, 28, 29, 30, 31, 32));

13C NMR (CDCl3) δ 158.51 (C(2, 5, 7, 10, 13, 16, 19, 22)), 103.07 (C(3, 4, 8, 9, 14, 15, 20, 21)), 36.55 (C(6, 12, 18, 24)), 25.49 (C(25, 26, 27, 28, 29, 30, 31, 32)).

MS calcd for $C_{28}H_{32}O_4$ 432.23, found 433.4 (M+H)+.

See additional analyses in "R. Pajewski, R. Ostaszewski, J. Jurczak, *Org. Prep. Proced. Int.* **2000**, *32*, 394".

2.1.2. Synthesis of calix[1]furan[3]pyrrole 7

Synthesis of compound **17**

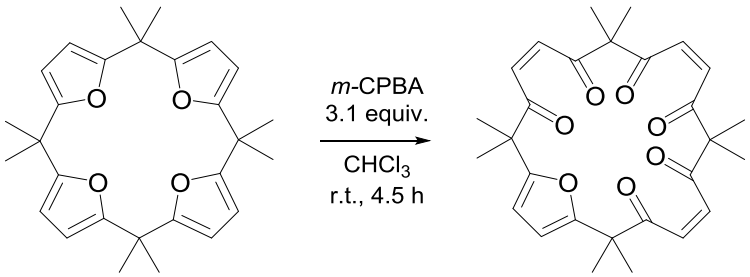

2 **17**

To a magnetically stirred 500-mL round-bottomed flask containing Calix[4]furan **2** (4.46g, 10.3 mmol) solubilized at r.t. in chloroform (250 mL) was added *m*-CPBA (7.61 g, 32.0 mmol, 3.1 equiv.) in one portion. After being stirred for 4.5 h at r.t., the crude reaction mixture was washed with three portions of saturated aqueous $NaHCO_3$ and once with saturated aqueous NaCl. The organic layer was dried over anhydrous Na_2SO_4. The solvent is removed in vacuum, leaving a yellow solid. The residue was purified by column chromatography (SiO_2, CH_2Cl_2/EtOAc, 97/3) to yield 3.13 g (63%) of compound **17** as a yellow solid.

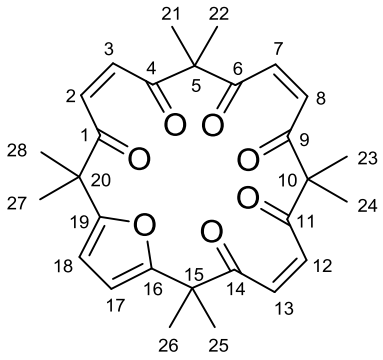

^{1}H NMR ($CDCl_3$, 298K) δ 6.65 (s, 2 H, C-H(7, 8)), 6.50 (d, ^{3}J(2, 3) and ^{3}J(13, 12) = 12.0 Hz, 2 H, C-H(2, 13 or 3, 12)), 6.23 (s, 2 H, C-H(17, 18)), 6.16 (d, ^{3}J(2, 3) and ^{3}J(13, 12) = 12.0 Hz, 2 H, C-H(2, 13 or 3, 12)), 1.46 (s, 12 H, CH_3(21, 22, 23, 24 or 25, 26, 27, 28)), 1.41 (s, 12 H, CH_3(21, 22, 23, 24 or 25, 26, 27, 28));

^{13}C NMR ($CDCl_3$) δ 203.56 (C=O), 202.71 (C=O), 199.78 (C=O), 157.41 (C(16, 19)), 140.20 (C(2, 3 or 12, 13)), 135.13 (C(7, 8)), 128.95 (C(2, 3 or 12, 13)), 107.11 (C(17, 18)), 61.10 (C(5, 10 or 15, 20)), 48.17 (C(5, 10 or 15, 20)), 22.61 (CH_3), 22.33 (CH_3).

MS calcd. for $C_{28}H_{32}O_7$ 580.2, found 503.3 (M+Na)+.

See additional analyses in "P. D. Williams and E. LeGoff, *J. Org. Chem.*, 1981, **46**, 4143".

X-ray: Suitable crystals of 1**7** were obtained as colorless rods by slow evaporation of a solution in dichloromethane. The structure crystallized in the monoclinic $P2_1/c$ space group. The compound crystallized with two conformationally similar molecules per asymmetric unit.

Synthesis of compound **20**

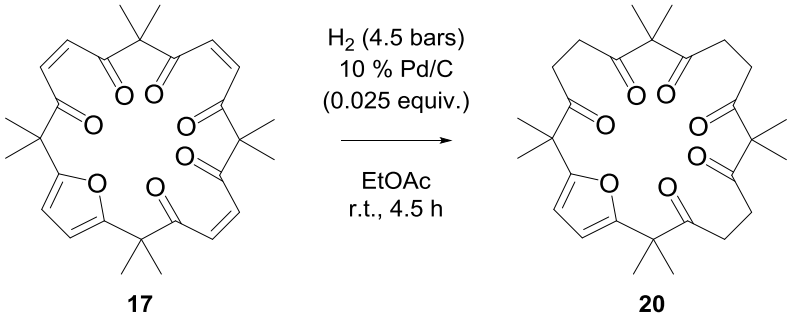

17 **20**

A suspension of 10% Pd/C (83 mg, 0.078 mmol, 0.025 equiv.) in a solution of **17** (1.50 g, 3.12 mmol) in EtOAc (200 mL) was shaken under 4.0 bars of H_2 for 3 h at 20 °C in a Parr apparatus. The catalyst was filtered off under celite and washed with $CHCl_3$. The filtrate was dried under vacuum and the resulting residue was purified by recrystallization in EtOH to yield 1.06 g (70 %) of compound **20** as colorless prisms.

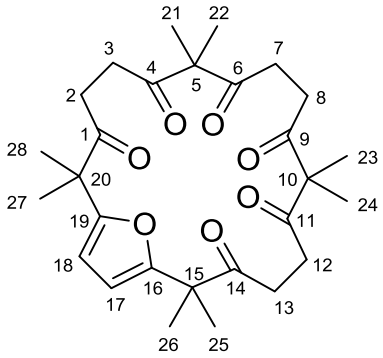

^{1}H NMR ($CDCl_3$, 298K) δ 6.15 (s, 2 H, C-H(17, 18)), 2.66 (s, 4 H, C-H(7, 8)), 2.59 (m, 8 H, C-H(2, 3, 12, 13)), 1.47 (s, 6 H, CH_3(21, 22, 23, 24 or 25, 26, 27, 28)), 1.37 (s, 12 H, CH_3(21, 22, 23, 24 or 25, 26, 27, 28));

^{13}C NMR ($CDCl_3$) δ 210.09 (C=O), 209.46 (C=O), 208.27 (C=O), 157.25 (C(16, 19)), 106.72 (C(17, 18)), 62.01 (C(15, 20)), 48.78 (C(5, 10)), 32.69 (C(7, 8)), 32.05 (C(2, 3, 12, 13), 23.44 (CH_3), 20.98 (CH_3).

MS calcd. for $C_{28}H_{38}O_7$ 486.2, found 509.5 (M+Na)+.

See additional analyses in "P. D. Williams and E. LeGoff, *J. Org. Chem.*, 1981, **46**, 4143".

Synthesis of calix[1]furan[3]pyrrole **7**

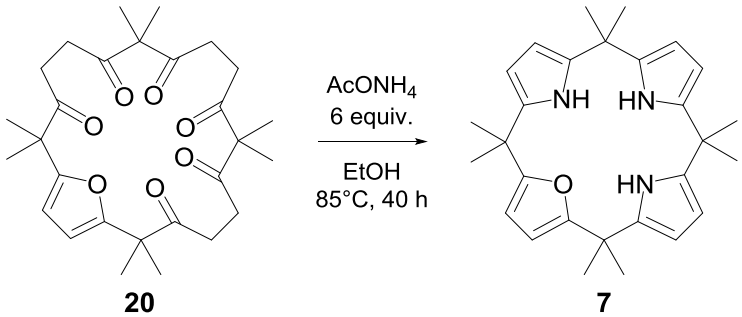

20 **7**

In a Schlenk tube were introduced **20** (983 mg, 2.02 mmol) and EtOH (60 mL). Then, $AcONH_4$ (934 mg, 12.1 mmol, 6 equiv.) was added to the slurry, and the mixture was warmed

at 85 °C for 40 h. The solvent was partially removed under vacuum leading to the precipitation of **7**. The reaction mixture was filtered off, washed with ethanol and dried under vacuum. The residue was purified by recrystallization in EtOH to yield 523 mg (60%) of compound **7** as colorless crystals.

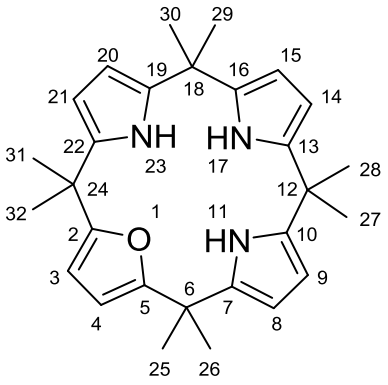

IR (ATR) 3441.6*s*, 2971.6*s*, 2931.5*m*, 2870*m*, 1579.1*w*, 1414.2*m*, 1359.9*m*, 1232.2*m*, 1043.4*m*, 953.5*w*, 758.0*s*, 725.3*m*, 704.3*s*;

^{1}H NMR ($CDCl_3$) δ 7.20 (bs, 1 H, N-H(17)), 6.81 (bs, 2 H, N-H(11, 23)), 6.05 (s, 2 H, C-H(3, 4)), 5.93 (d, *J* = 2.8 Hz, 2 H, C-H(14, 15)), 5.87 (dd, ^{3}J(8, 9) and ^{3}J(20, 21) = 3.2 Hz, ^{4}J(8, 11) and ^{4}J(21, 23) = 3.6 Hz, 2 H, C-H(8, 21)), 5.83 (dd, ^{3}J(8, 9) and ^{3}J(20, 21) = 2.8 Hz, ^{4}J(9, 11) and ^{4}J(20, 23) = 3.2 Hz, 2 H, C-H(9, 20)), 1.51 (s, 24H, CH_3);

^{13}C NMR ($CDCl_3$) δ 159.83 (C(2, 5)), 138.72 (C(13, 16)), 137.91 (C(7, 22 or 10, 19)), 137.61 (C(7, 22 or 10, 19)), 104.48 (C(3, 4)), 103.21 (C(14, 15)), 102.98 (C(8, 21 or 9, 20)), 102.25 (C(8, 21 or 9, 20)), 36.28 (C(6, 24 or 12, 18)), 35.36 (C(6, 24 or 12, 18)), 29.41 (CH_3), 27.70 (CH_3).

Melting point: 263°C.

MS calc. for $C_{28}H_{35}N_3O$ 429.3, found 430.7 (M+H)+, 452.7 (M+Na)+.

HRMS calcd. for $C_{28}H_{36}N_3O^+$ 430.2853, found 430.2858 (M+H)+.

X-ray: Suitable crystals of **7** were obtained as colorless plates by slow evaporation of a solution in dichloromethane. The structure crystallized in the tetragonal $P4_1$ space group.

2.1.3. Synthesis of calix[2]furan[2]pyrrole 8

Synthesis of compound **16**

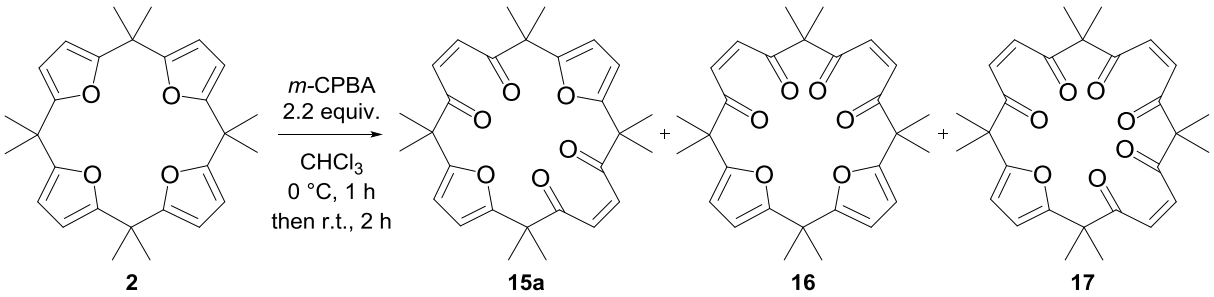

To a magnetically stirred 500-mL round-bottomed flask containing Calix[4]furan **2** (3.0 g, 6.94 mmol) dissolved in $CHCl_3$ (200 mL) at 0 °C was added *m*-CPBA (3.63 g, 15.3 mmol, 2.2 equiv.) in one portion. The reaction mixture was stirred at 0 °C for 1 h and at 20 °C for an

additional 2 h. The crude reaction mixture was washed with three portions of saturated aqueous $NaHCO_3$ and once with saturated aqueous NaCl. The organic layer was dried over anhydrous Na_2SO_4. The solvent was removed in vacuum. The residue was purified by column chromatography (SiO_2, Cyclohexane/EtOAc, 9/1) to yield 1.26g (39%) of compound **16** as a yellow solid, then the solvent was changed to (CH_2Cl_2/EtOAc, 97/3) to yield 1.07g (33%) of compound **15a** and 316 mg (9%) of compound **17** as yellow solids.

- Compound **16**

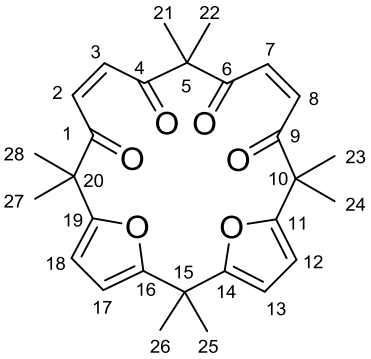

^{1}H NMR ($CDCl_3$, 298K) δ 6.38 (d, ^{3}J(2, 3) and ^{3}J(8, 7) = 11.9 Hz, 2 H, C-H(3, 7)), 6.08 (d, ^{3}J(12, 13) and ^{3}J(18, 17) = 3.2 Hz, 2 H, C-H(12, 18)), 5.96 (d, ^{3}J(13, 12) and ^{3}J(17, 18) = 3.2 Hz, 2 H, C-H(13, 17)), 5.79 (d, ^{3}J(2, 3) and ^{3}J(8, 7) = 11.9 Hz, 2 H, C-H(2, 8)), 1.61 (s, 6 H, CH_3(21, 22, or 25, 26)), 1.55 (s, 12 H, CH_3(23, 24, 27, 28)), 1.22 (s, 6 H, CH_3(21, 22, or 25, 26));

^{13}C NMR ($CDCl_3$) δ 206.22 (C(1 or 9)), 197.93 (C(1 or 9)), 159.49 (C(11,19 or 14, 16)), 155.42 (C(11,19 or 14, 16)), 141.37 (C(2, 8 or 3, 7)), 155.42 (C(2, 8 or 3, 7)), 106.70 (C(12, 18 or 13, 17)), 104.53 (C(12, 18 or 13, 17)), 60.68 (C(5 or 15)), 48.88 (C(10, 20)), 37.04 (C(5 or 15)), 29.73 (CH_3), 25.19 (CH_3), 24.07 (CH_3), 20.16 (CH_3).

MS calcd. for $C_{28}H_{32}O_6$ 464.2, found 487.3 (M+Na)+.

See additional analyses in "P. D. Williams and E. LeGoff, *J. Org. Chem.*, 1981, **46**, 4143".

- Compound **15a**

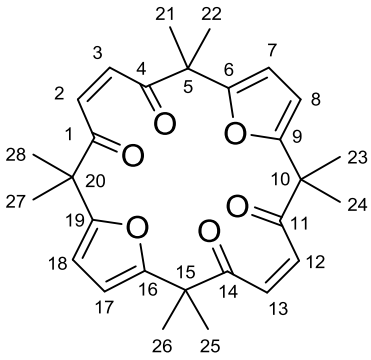

^{1}H NMR ($CDCl_3$, 298K) δ 6.11 (s, 4 H, C-H(7, 8, 17, 18)), 6.08 (s, 4 H, C-H(2, 3, 12, 13)), 1.47 (s, 24 H, CH_3);

^{13}C NMR ($CDCl_3$) δ 202.57 (C(1, 4, 11, 14)), 157.02 (C(6, 9, 16, 19)), 134.29 (C(2, 3, 12, 13)), 107.15 (C(7, 8, 17, 18)), 48.35 (C(5, 10, 15, 20)), 23.25 (CH_3).

MS calcd. for $C_{28}H_{32}O_6$ 464.2, found 487.2 (M+Na)+

See additional analyses in "P. D. Williams and E. LeGoff, *J. Org. Chem.*, 1981, **46**, 4143".

Synthesis of compound **19**

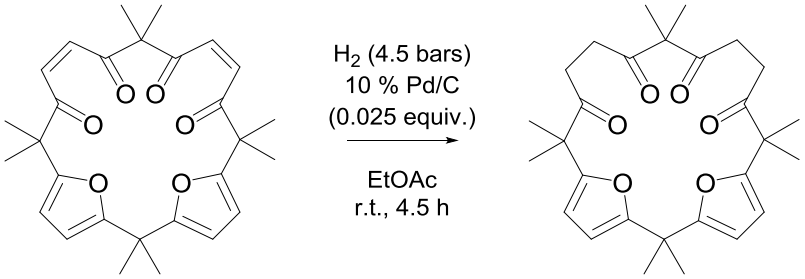

16 **19**

A suspension of 10% Pd/C (57 mg, 0.054 mmol, 0.025 equiv.) in a solution of **16** (1.0 g, 2.15 mmol) in EtOAc (170 mL) was shaken under 4.0 bars of H_2 for 3 h at 20 °C in a Parr apparatus. The catalyst was filtered off under celite and washed with $CHCl_3$. The filtrate was dried under vacuum and the resulting residue was purified by recrystallization in EtOH to yield 782 mg (78%) of compound **19** as colorless prisms.

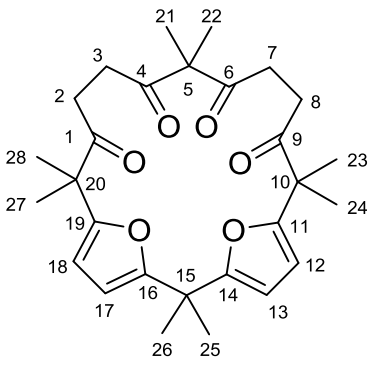

^{1}H NMR ($CDCl_3$, 298K) δ 6.02 (s, 4 H, C-H(12, 13, 17, 18)), 2.58 (m, 4 H, C-H(2, 8 or 3, 7)), 2.43 (m, 4 H, C-H(2, 8 or 3, 7)), 1.54 (s, 6 H, CH_3), 1.42 (s, 12 H, CH_3), 1.29 (s, 6 H, CH_3);

^{13}C NMR ($CDCl_3$) δ 210.04 (C(1, 9, or 4, 6)), 208.15 (C(1, 9, or 4, 6)), 159.18 (C(11, 19 or 14, 16)), 156.10 (C(11, 19 or 14, 16)), 105.99 (C(12, 18 or 13, 17)), 104.40 (C(12, 18 or 13, 17)), 63.4 (C(5)), 48.57 (C(10, 20)), 36.88 (C(15)), 32.14 (C(2, 8 or 3, 7)), 32.11 (C(2, 8 or 3, 7)), 25.76 (CH_3), 23.41 (CH_3), 20.64 (CH_3).

MS calcd. for $C_{28}H_{36}O_6$ 468.25, found 491.5 (M+Na)+.

See additional analyses in "P. D. Williams and E. LeGoff, *J. Org. Chem.*, 1981, **46**, 4143".

Synthesis of calix[2]furan[2]pyrrole **8**

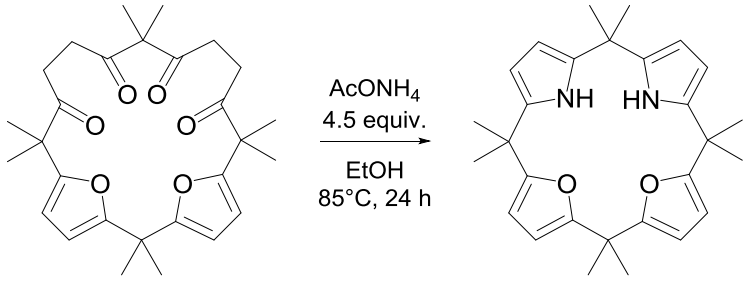

19 **8**

In a Schlenk tube were introduced **19** (916 mg, 1.95 mmol) and ethanol (25 mL). Then, $AcONH_4$ (678 mg, 8.80 mmol, 4.5 equiv.) was added to the slurry, and the mixture was

heated at 85 °C for 24 h. The solvent was partially removed under vacuum, the reaction mixture was filtered off and washed with ethanol to yield 674 mg (80%) of compound **8** as a white powder.

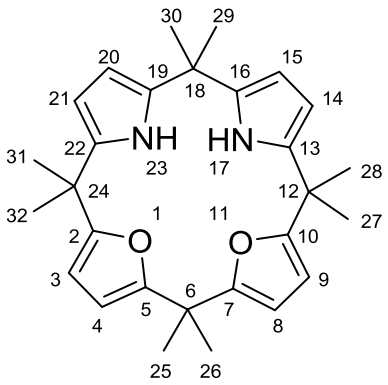

IR (KBr): 3443.1*m*, 2973.2*m*, 2935.1*w*, 1556.4*m*, 1415.2*w*, 1364.1*m*, 1240.4*m*, 1028.4*m*, 954.2*m*, 765.0*m*, 729.8*m*, 706.4*m*;

^{1}H NMR ($CDCl_3$, 298K) δ 6.93 (bs, 2 H, N-H(17, 23)), 5.98 (d, ^{3}J(3, 4) and ^{3}J(9, 8) = 3.1 Hz, 2 H, C-H(3, 9)), 5.95 (d, ^{3}J(4, 3) and ^{3}J(8, 9) = 3.1 Hz, 2 H, C-H(4, 8)), 5.89 (dd, ^{3}J(14, 15) and ^{3}J(21, 20) = 3.0 Hz, ^{4}J(14, 17) and ^{4}J(21, 23) = 2.8 Hz, 2 H, C-H(14, 21)), 5.86 (dd, ^{3}J(15, 14) and ^{3}J(20, 21) = 3.0 Hz, ^{4}J(15, 17) and ^{4}J(20, 23) = 2.8 Hz, 2 H, C-H(15, 20)), 1.50 (s, 24 H, CH_3);

^{13}C NMR ($CDCl_3$) δ 159.09 and 158.94 (C(quat.furan)), 137.97 and 137.83 (C(quat.pyrrole)), 104.37 and 103.58 (C(furan)), 103.09 and 102.00 (C(pyrrole)), 36.74 (C(6 or 18)), 36.08 (C(12, 24)), 35.35 (C(6 or 18)), 29.75 (CH_3), 27.77 (CH_3), 27.61 (CH_3), 25.65 (CH_3).

Melting point: 238.9°C.

MS calcd. for $C_{28}H_{34}N_2O_2$ 430.2, found 453.4 (M+Na)+.

HRMS calcd. for $C_{28}H_{34}N_2O_2Na^+$ 453.2512 found 453.2516.

X-ray: Suitable crystals of **8** were obtained as colorless plates by slow evaporation of a solution in dichloromethane. The structure crystallized in the tetragonal $P4_1$ space group.

2.1.4. Synthesis of calix[2]furan[2]pyrrole 9

Synthesis of compound **18**

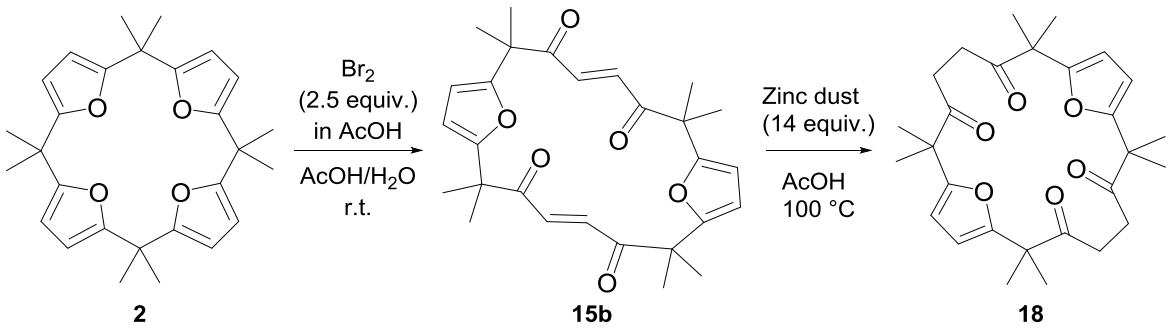

A magnetically stirred, 1-L, single-necked round-bottomed flask was charged with finely powdered calix[4]furan **2** (6.00 g, 13.9 mmol) in glacial acetic acid **(**780 mL) and distilled water (24 mL). To this vigorously stirred suspension was dropwise added, over a period of about 3 h, a solution of Br_2 (1.8 mL, 34.7 mmol, 2.5 equiv.) in glacial acetic acid (120 mL), during which time the suspension takes on a bright yellow color. After the addition, stirring is

continued for an additional hour and then the crude product is suction filtered and washed with methanol. The crude product **15b** was dried under vacuum to give a yellow solid (4.18-4.50 g, 65-70% yield) and the next step was realized without other purification.

In a 2-L Erlenmeyer flask was placed glacial acetic acid (1 L), in which **15b** (4.5 g) was dissolved with heating on a hot plate. When **15b** was completely soluble, the flask was removed from the heat, and while the mixture was still hot, zinc dust (8.9 g, 135.6 mmol, 14 equiv.) was added in portions with efficient swirling so as to prevent bumping. Reaction was cold to r.t., the excess of zinc and precipitated zinc salts were filtered and washed with $CHCl_3$. The colorless filtrate was poured into two volumes of water, the organic phase removed, and the upper aqueous phase extracted once with more $CHCl_3$. The combined organic layers were washed with saturated aqueous $NaHCO_3$ (until pH = 9), brine and then dried over anhydrous Na_2SO_4. The solvent was removed in vacuum. EtOH was added and the insoluble solid was filtered, washed with EtOH and dried under vacuum to yield 4.11 g (95%; 63% over two steps) of compound **18** as a colorless powder.

Compound **18** could also be obtained starting from the *cis*-isomer **15a** using the same procedure with identical 95% yield. Compound **15a** was obtained during the ring-opening of calix[4]furan with 2.2 equiv. of *m*-CPBA (page 36).

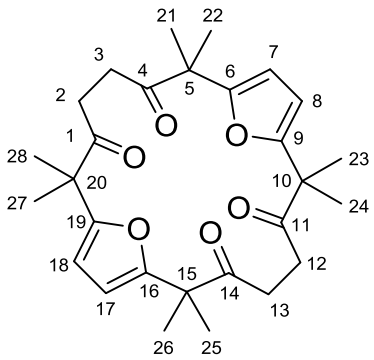

^{1}H NMR ($CDCl_3$, 298K) δ 6.16 (s, 4 H, C-H(7, 8, 17, 18)), 2.45 (s, 8 H, C-H(2, 3, 12, 13)), 1.42 (s, 24 H, CH_3);

^{13}C NMR ($CDCl_3$) δ 209.39 (C(1, 4, 11, 14)), 157.47 (C(6, 9, 16, 19)), 106.44 (C(7, 8, 17, 18)), 48.78 (C(5, 10, 15, 20)), 30.95 (C(2, 3, 12, 13)), 23.05 (CH_3).

MS calcd. for $C_{28}H_{36}O_6$ 468.25, found 491.5 (M+Na)+.

See additional analyses in "P. D. Williams and E. LeGoff, *J. Org. Chem.*, 1981, **46**, 4143".

Synthesis of calix[2]furan[2]pyrrole **9**

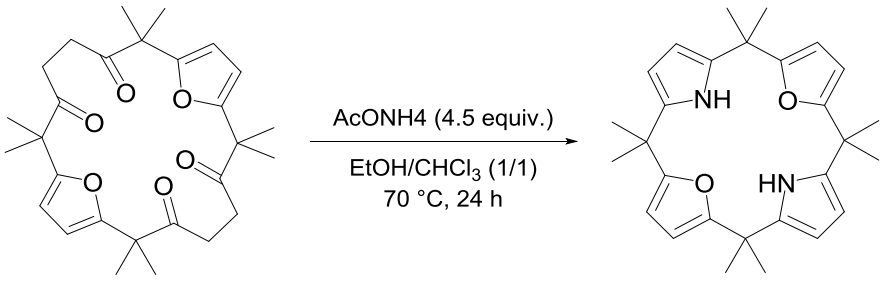

18 **9**

In a Schlenk tube were introduced **18** (2.62 g, 5.59 mmol), chloroform (60 mL) and ethanol (60 mL). Then, $AcONH_4$ (1.94 g, 25.2 mmol, 4.5 equiv.) was added to the slurry, and the mixture was heated at 70°C for 24 h. The solvent was partially removed under vacuum

leading to the formation of a precipitate. The precipitate was filtered off, washed with ethanol and dried under vacuum. The residue was purified by a quick silica gel chromatography (Cyclohexane/CH_2Cl_2, 1/1) to yield 2.03 g (84%) of compound **9** as colorless crystals.

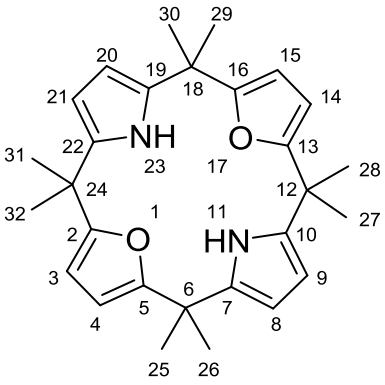

IR (KBr): 3448.3*s*, 2972.7*s*, 2935.4*m*, 1552.9*m*, 1416.8*w*, 1236.3*m*, 1113.4*m*, 1028.0*m*, 954.6*m*, 785.9*m*, 757.6*s*, 725.8*m*, 705.8*s*, 487.1*w*;

^{1}H NMR ($CDCl_3$, 298K) δ 7.19 (bs, 2 H, N-H(11, 23)), 6.04 (s, 4 H, C-H(3, 4, 14, 15)), 5.85 (d, ^{4}J(8, 11) = ^{4}J(9, 11) and ^{4}J(20, 23) = ^{4}J(21, 23) = 2.8 Hz, 4 H, C-H(8, 9, 20, 21)), 1.54 (s, 24 H, CH_3);

^{13}C NMR ($CDCl_3$) δ 159.98 (C(2, 5, 13, 16)), 137.07 (C(7, 10, 19, 22)), 104.25 (C(3, 4, 14, 15)), 102.44 (C(8, 9, 20, 21)), 36.25 (C(6, 12, 18, 24)), 27.90 (CH_3).

Melting point: 231.2°C.

HRMS calcd. for $C_{28}H_{34}N_2O_2Na^+$ 453.2512 found 453.2517 (M+Na)+.

X-ray: Suitable crystals of **9** were obtained as colorless needles by slow evaporation of a solution in dichloromethane. The structure crystallized in the tetragonal $P4_3$ space group.

2.1.5. Synthesis of calix[3]furan[1]pyrrole 10

Synthesis of compound **22a**

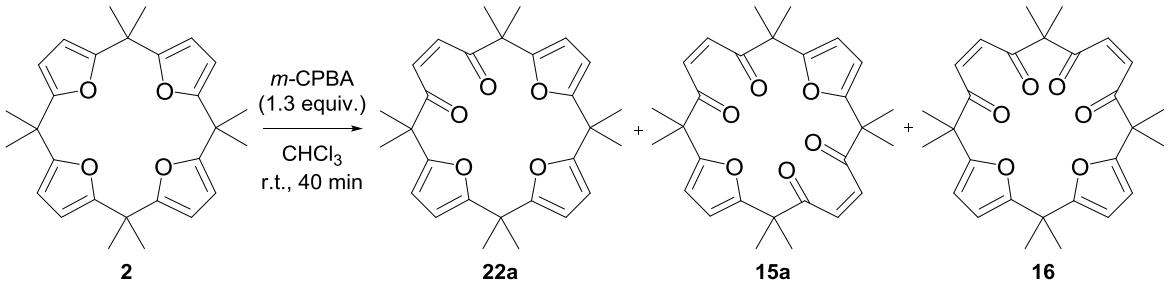

To a magnetically stirred 1-L round-bottomed flask containing Calix[4]furan **2** (10 g, 23.1 mmol) dissolved in $CHCl_3$ (400 mL) at r.t. was added *m*-CPBA (7.15 g, 30.0 mmol, 1.3 equiv.) in one portion. The reaction mixture was stirred at r.t. for 40 min. The crude reaction mixture was washed with three portions of saturated aqueous $NaHCO_3$ and once with saturated aqueous NaCl. The organic layer was dried over anhydrous Na_2SO_4. The solvent was removed in vacuum, leaving a yellow solid. The residue was purified by silica gel chromatography (cyclohexane/EtOAc, 97/3) to yield 880 mg of recovered starting material **2** (9%) as a white powder, 5.77 g (56%) of compound **22a** as a yellow solid then the solvent

was changed to (cyclohexane/EtOAc, 8/2) to yield 1.32 g (12%) of compound **16** and 321 mg (3%) of compound **15a** as yellow solids.

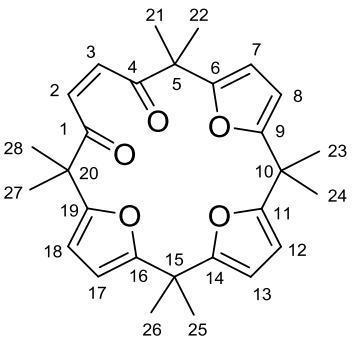

IR (ATR): 2977*m*, 2937*m*, 2873*m*, 1793*m*, 1692*s*, 1549*m*, 1466*m*, 1385*m*, 1368*m*, 1258*m*, 1157*m*, 1110*m*, 1058*s*, 1021*s*, 956*s*, 779*s*, 730*m*;

^{1}H NMR ($CDCl_3$, 298K) δ 6.00 (s, 2 H, C-H(12, 13)), 5.95 (d, ^{3}J(4, 5) = 3.2 Hz, 2 H, C-H(7, 18 or 8, 17)), 5.91 (d, ^{3}J(4, 5) = 3.2 Hz, 2 H, C-H(7, 18 or 8, 17)), 5.88 (s, 2 H, C-H(2, 3)), 1.59 (s, 12 H, CH_3(23, 24, 25, 26)), 1.42 (s, 12 H, CH_3(21, 22, 27, 28));

^{13}C NMR ($CDCl_3$) δ 203.83 (C=O), 159.27 (C(quat.furan 9, 16)), 158.57 (C(quat.furan 11, 14)), 154.90 (C(quat.furan 6, 19)), 133.54 (C(2, 3)), 106.76 (C(furan 7, 18 or 8, 17)), 104.33 (C(furan 7, 18 or 8, 17)), 103.46 (C(furan 12, 13)), 48.28 (C(meso 5, 20)), 37.01 (C(meso 10, 15)), 25.17 (C(23, 24, 25, 26)), 23.64 (C(21, 22, 27, 28)).

Melting point: 129°C.

HRMS calcd. for $C_{28}H_{33}O_5^+$ 449.2328, found 449.2327 (M+H)+.

Synthesis of compound **21**

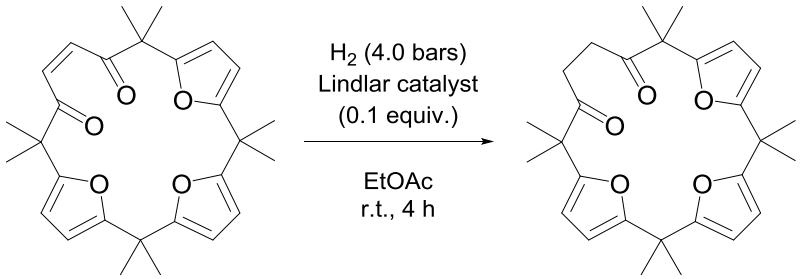

22a **21**

A suspension of Lindlar catalyst (5% $Pd/CaCO_3$, poisoned by $Pb(OAc)_4$, 2.28 g, 1.07 mmol, 0.1 equiv.) in a solution of **22a** (4.80 g, 10.7 mmol) in EtOAc (250 mL) was shaken under 4.0 bars of H_2 for 4 h at r.t. in a Parr apparatus. The catalyst was filtered off under celite and washed with $CHCl_3$. The colorless filtrate was dried under vacuum and the resulting slightly yellow residue was washed with EtOH to yield 4.59 g (95%) of compound **21** as a colorless/clear yellow powder.

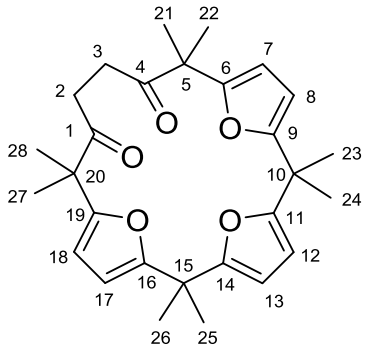

IR (KBr): 3420.6*bs*, 2978.3*m*, 2937.4*m*, 1711.4*s*, 1552.0*m*, 1469.8*m*, 1260.3*m*, 1022.37*m*, 954.6*m*, 778.7*m*, 709.64*w*;

^{1}H NMR ($CDCl_3$, 298K) δ 6.02 (s, 2 H, C-H(furan)), 6.01 (s, 4 H, C-H(furan)), 2.16 (s, 4 H, C-H(2, 3)), 1.55 (s, 12 H, CH_3(23, 24, 25, 26)), 1.37 (s, 12 H, CH_3(21, 22, 27, 28));

^{13}C NMR ($CDCl_3$) δ 210.50 (C=O), 159.71 (C(quat.furan)), 158.03 (C(quat.furan)), 155.60 (C(quat.furan)), 106.29 (C(furan)), 104.79 (C(furan)), 104.27 (C(furan)), 49.01 (C(meso)), 36.92 (C(meso)), 32.00 (C(2, 3)), 25.73 (C(23, 24, 25, 26)), 22.83 (C(21, 22, 27, 28)).

Melting point: 106.8°C.

MS calcd. for $C_{28}H_{34}O_5$ 450.24, found 473.4 (M+Na)+.

HRMS calcd. for $C_{28}H_{35}O_5^+$ 451.2484, found 451.2487(M+H)+.

X-ray: Suitable crystals of **21** were obtained by slow evaporation of a solution in dichloromethane. The structure crystallized in the triclinic P-1 space group.

Synthesis of calix[3]furan[1]pyrrole **10**

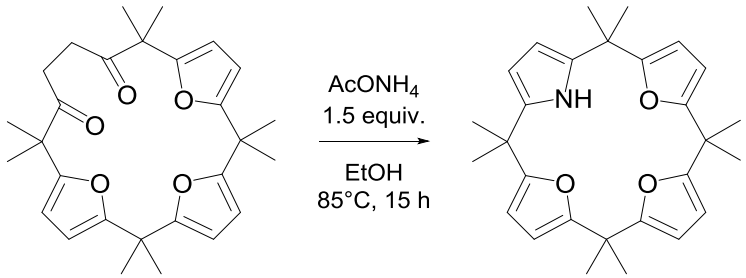

21 **10**

In a Schlenk tube were introduced **21** (2.32 g, 5.15 mmol) and ethanol (100 mL). Then, $AcONH_4$ (595 mg, 7.72 mmol, 1.5 equiv.) was added to the slurry, and the mixture was warmed overnight at 85 °C leading to the formation of a precipitate. The solvent was partially removed under vacuum and the solid was filtered off, washed with ethanol and dried under vacuum. The residue was recrystallized in dioxane to yield 1.93 g (87%) of compound **10** as colorless prisms.

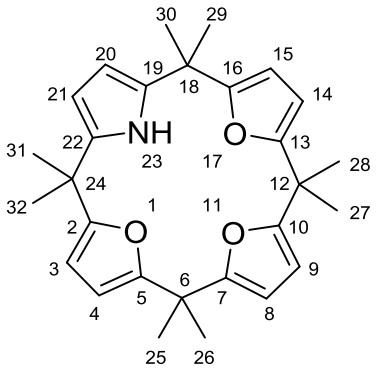

IR (KBr): 3445.5*m*, 2973.2*m*, 2936.4*w*, 1557.3*m*, 1449.8*w*, 1364.1*m*, 1262.8*m*, 1027.9*m*, 955.1*m*, 778.3*m*, 760.0*m*, 731.3*m*, 706.7*m*;

^{1}H NMR ($CDCl_3$, 298K) δ 7.44 (bs, 1 H, N-H(23)), 5.98 (s, 4 H, C-H(3, 4, 14, 15)), 5.96 (s, 2H, C-H(8, 9)), 5.82(d, ^{4}J(20, 23) = ^{4}J(21, 23) = 2.7 Hz, 2 H, C-H(20, 21)), 1.54 (s, 12 H, CH_3), 1.52 (s, 12 H, CH_3);

^{13}C NMR ($CDCl_3$) δ 159.35 (C(quat.furan)), 159.26 (C(quat.furan)), 158.48 (C(quat.furan)), 137.71 (C(19, 22)), 104.19 (C(furan)), 103.87 (C(furan)), 103.55 (C(furan)), 101.71 (C(20, 21)), 36.96 (C(meso)), 36.22 (C(meso)), 28.15 (CH_3), 26.23 (CH_3).

Melting point: 221.6°C.

MS calcd. for $C_{28}H_{33}NO_3$ 431.2, found 454.4 (M+Na)+.

HRMS calcd. for $C_{28}H_{33}NO_3Na^+$ 454.2353, found 454.2356 (M+Na)+.

X-ray: Suitable crystals of **10** were obtained by recrystallization from dioxane. The structure crystallized in the tetragonal $P4_1$ space group.

2.2. Hydrogenation of calix[n]furan[4-n]pyrroles 7 – 10

2.2.1. Synthesis of calix[1]tetrahydrofuran[3]pyrrolidine 11

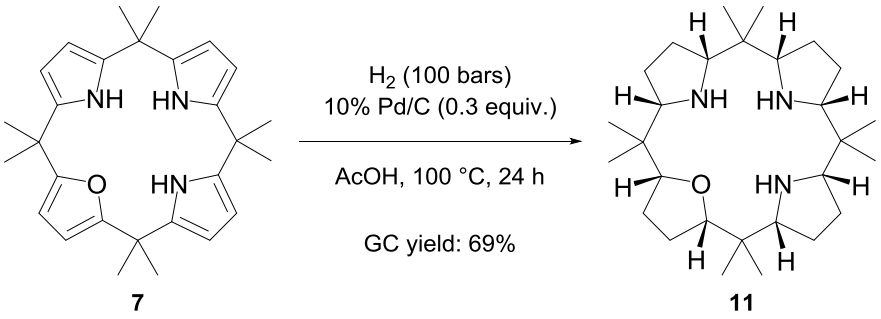

Calix[1]furan[3]pyrrole **7** (450 mg, 1.05 mmol) and Pd/C 10% (334 mg, 0.31 mmol) were placed in a test tube (125 x 15 mm) containing a small cross stirring bar. AcOH (10 mL) was added and the test tube was placed inside an autoclave vessel containing AcOH (25 mL). The autoclave was closed, put under magnetic stirring, filled with hydrogen (100 bars) and heated at 100 °C for 24 h. Stirring was stopped, the reaction was cold down to room temperature (around 1 h) and then hydrogen was removed from the autoclave. The reaction mixture was filtered through celite and the solid was successively washed with AcOH (2 x 5 mL) and CH_2Cl_2 (2 x 5 mL). The combined filtrate and washings were washed with 2M aqueous NaOH (until pH = 14). The organic layer was then separated and the aqueous phase was extracted with CH_2Cl_2 (2 x 10 mL). The collected organic layers were washed with brine,

dried over K_2CO_3, and concentrated under reduced pressure. The residue was purified by successive recrystallization in EtOAc to yield 164 mg (35%) of compound **11** as colorless needles.

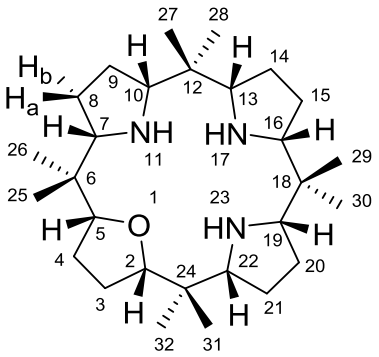

IR (ATR) 3349.5*m*, 2968*s*, 2869.2*m*, 2639.3*w*, 1465.3*m*, 1395.4*s*, 1357.3*m*, 1262.8*m*, 1107.2*m*, 1060.1*s*, 953.6*m*, 905.1*m*, 878.1*m*, 778.7*s*, 601.9*w*;

^{1}H NMR ($CDCl_3$, 298K) δ 3.57 (m, 2 H, C-H(αO(2, 5))), 2.91 (m, 2 H, C-H(αN(10, 19))), 2.84 (m, 2 H, C-H(αN(7, 22))), 2.73 (m, 2H, C-H(αN(13, 16))), 2.49 (bs, 1H, N-H(17)), 1.77 (bs, 2H, N-H(11, 23)), 1.67–1.55 (m, 4 H, CH_2(3, 4)), 1.57–1.22 (m, 12 H, CH_2(8, 9, 14, 15, 20, 21)), 0.79 (s, 6 H, CH_3(26, 32)), 0.78 (s, 6 H, CH_3(28, 30)), 0.74 (s, 6 H, CH_3(28, 30)), 0.71 (s, 6 H, CH_3(25, 31));

^{13}C NMR ($CDCl_3$) δ 90.07 (C(2, 5)), 71.59 (C(13.16)), 70.04 (C(7, 22)), 69.23 (C(10, 19)), 39.30 (C(6, 24)), 38.53 (C(12, 18)), 27.72 (C(14, 15)), 27.15 (C(3, 4)), 26.31 (C(27, 30 + 8, 21 or 9, 20)), 25.75 (C((8, 21 or 9, 20))), 24.95 (C(25, 32)), 12.09 (C(26, 31)), 11.61 (C(28, 29)).

Melting point: 251-252°C.

MS calcd. for $C_{28}H_{52}N_3O^+$ 446.4, found 446.7 (M+H)+.

HRMS calcd. for $C_{28}H_{52}N_3O^+$ 446.4105, found 446.4109 (M+H)+.

X-ray: Suitable crystals of **11** were as colorless thin needles obtained by slow evaporation of a solution in dichloromethane. The structure crystallized in the monoclinic $P2_1/n$ space group. The molecule is totally disordered with the N and O positions occupying alternative sites: O1/N1, O2/N2, O3/N3 and O4/N4. The structure has been refined and the occupancy of each atom was fixed for each site as: N: 0.75; O: 0.25.

2.2.2. Synthesis of calix[2]tetrahydrofuran[2]pyrrolidine 12

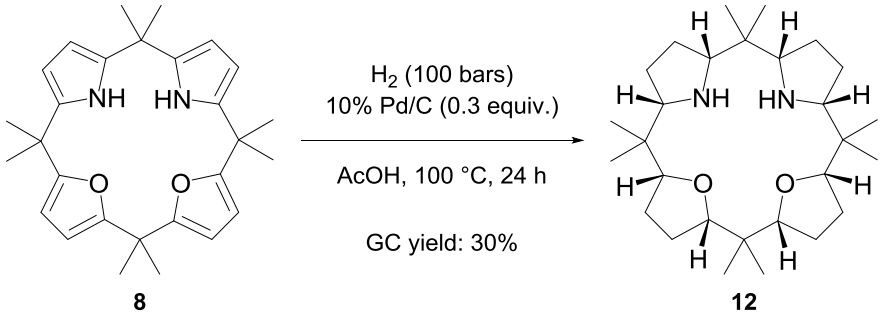

8 **12**

Calix[2]furan[2]pyrrole **8** (180 mg, 0.42 mmol) and Pd/C 10% (134 mg, 0.13 mmol) were placed in a test tube (125 x 15 mm) containing a small cross stirring bar. AcOH (5 mL) was added and the test tube was placed inside an autoclave vessel containing AcOH (25 mL). The

autoclave was closed, put under magnetic stirring, filled with hydrogen (100 bars) and heated at 100 °C for 24 h. Stirring was stopped, the reaction was cold down to room temperature (around 1 h) and then hydrogen was removed from the autoclave. The reaction mixture was filtered through celite and the solid was successively washed with AcOH (2 x 5 mL) and CH_2Cl_2 (2 x 5 mL). The combined filtrate and washings were washed with 2M aqueous NaOH (until pH = 14). The organic layer was then separated and the aqueous phase was extracted with CH_2Cl_2 (2 x 10 mL). The collected organic layers were washed with brine, dried over K_2CO_3, and concentrated under reduced pressure. The residue was purified by recrystallization in EtOAc to yield 21 mg (15%) of compound **12** in 80% purity.

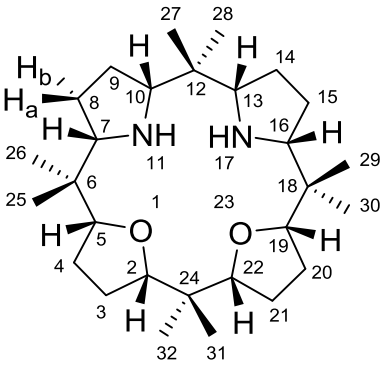

^{1}H NMR ($CDCl_3$, 298K) δ 8.86 (bs, 2 H, N-H(11 or 17)), 8.34 (bs, 2 H, N-H(11 or 17)), 4.15 (m, 4 H, C-H(2, 5, 19, 22)), 3.39 (m, 4 H, C-H(7, 10, 13, 16)), 2.05 (m, 4 H, CH_2(8a, 9a, 14a, 15a)), 1.95 (m, 4 H, CH_2(8b, 9b, 14b, 15b)), 1.76 (m, 4 H, CH_2(3a, 4a, 20a, 21a)), 1.58 (m, 4 H, CH_2(3b, 4b, 20b, 21b)), 1.36 (s, 12 H, CH_3(26, 28, 30, 32)), 0.86 (s, 12 H, CH_3(25, 27, 29, 31));

^{13}C NMR ($CDCl_3$) δ 85.61 (C(2, 5, 19, 22)), 74.01(C(7, 10, 13, 16)), 39.18 (C(6, 12, 18, 24)), 25.91 (C(3, 4, 20, 21)), 25.67 (C(25, 27, 29, 31)), 23.38 (C(8, 9, 14, 15)), 13.76 (C(26, 28, 30, 32)).

HRMS calcd. for $C_{28}H_{51}N_2O_2^+$447.3945, found 447.3947 (M+H)+.

X-ray: Suitable crystals of **12** were obtained as colorless plates by recrystallization from EtOAc. The structure crystallized in the triclinic P-1 space group. The molecule is totally disordered with the N and O positions occupying alternative sites: O1/N1, O2/N2, O3/N3 and O4/N4. The structure has been refined and the occupancy of each atom was fixed for each site as: N: 0. 5; O: 0.5.

2.2.3. Synthesis of calix[2]tetrahydrofuran[2]pyrrolidine 13

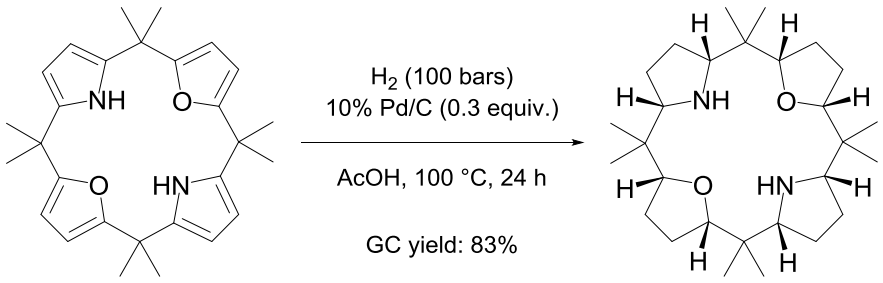

9 **13**

Calix[2]furan[2]pyrrole **9** (1.0 g, 2.32 mmol) and 10% Pd/C (740 mg, 0.70 mmol, 0.3 equiv.) were placed in a glass cylinder (280 x 35 mm) containing a cross stirring bar. AcOH (25 mL) was added and the cylinder was placed inside an autoclave vessel. The autoclave was closed,

put under magnetic stirring, filled with hydrogen (100 bars) and heated at 100 °C for 24 h. Stirring was stopped, the reaction was cold down to room temperature (around 1 h) and then hydrogen was removed from the autoclave. The reaction mixture was filtered through celite and the solid was successively washed with AcOH (2 x 5 mL) and CH_2Cl_2 (2 x 30 mL). The combined filtrate and washings were washed with 2M aqueous NaOH (until pH = 14). The organic layer was then separated and the aqueous phase was extracted with CH_2Cl_2 (2 x 30 mL). The collected organic layers were washed with brine, dried over K_2CO_3, and concentrated under reduced pressure. The residue was purified by recrystallizations in EtOAc to yield 668 mg (64%) of compound **13** as colorless needles in 99% purity.

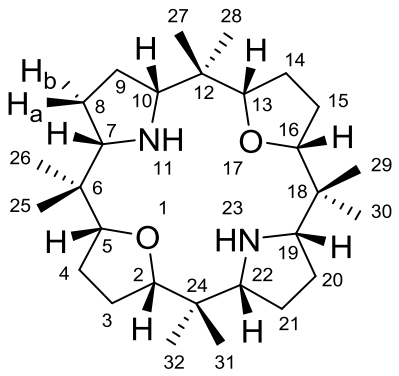

IR (KBr): 3368.3*m*, 2973.5*s*, 2870.4*s*, 2822.5*s*, 2639.8*m*, 1611.4*w*, 1575.0*w*, 1469.0*s*, 1398.6*s*, 1370.2*s*, 1334.5*m*, 1284.7*m*, 1212.1*m*, 1061.6*s*, 932.7*m*, 869.7*m*, 783.4*m*, 529.5*m*;

^{1}H NMR ($CDCl_3$, 218K) δ 3.64 (s, 4 H, C-H(2, 5, 13, 16)), 2.77 (s, 4 H, C-H(7, 10, 19, 22)), 2.32 (m, 2 H, N-H(11, 23)), 1.60 (m, 4 H, CH_2(3a, 4a, 14a, 15a)), 1.44 (m, 8 H, CH_2(3b, 4b, 14b, 15b, 8a, 9a, 20a, 21a)), 1.22 (m, 4 H, CH_2(8b, 9b, 20b, 21b)), 0.71 (s, 12 H, CH_3(26, 28, 30, 32)), 0.68 (s, 12 H, CH_3(25, 27, 29, 31));

^{13}C NMR ($CDCl_3$) δ 88.74 (C(2, 5, 13, 16)), 69.97 (C(7, 10, 19, 22)), 38.90 (C(6, 12, 18, 24)), 26.93 (C(3, 4, 14, 15)), 26.52 (C(8, 9, 20, 21)), 25.12 (C(25, 27, 29, 31)), 11.71 (C(26, 28, 30, 32)).

HRMS calcd. for $C_{28}H_{51}N_2O_2^+$ 447.3945, found 447.3941 (M+H)+.

X-ray: Suitable crystals of **13** were obtained as colorless needles by recrystallization from EtOAc. The structure crystallized in the monoclinic $P2_1/c$ space group. The molecule is totally disordered with the N and O positions occupying alternative sites: O1/N1, O2/N2, O3/N3 and O4/N4. The structure has been refined and the occupancy of each atom was fixed for each site as: N: 0.5; O: 0.25.

2.2.4. Synthesis of calix[3]tetrahydrofuran[1]pyrrolidine 14

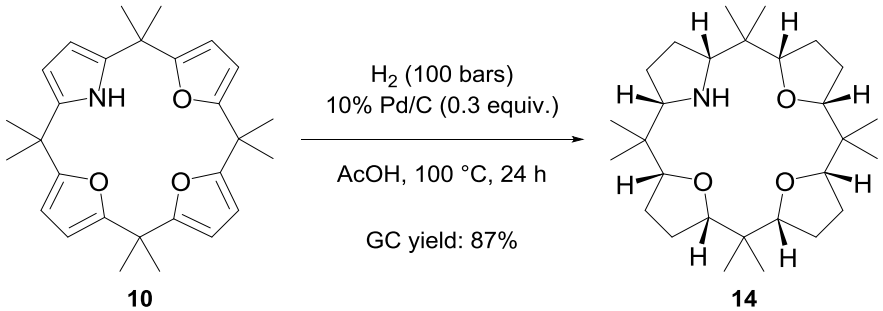

10 **14**

Calix[3]furan[1]pyrrole **10** (1.0 g, 2.32 mmol) and 10% Pd/C (740 mg, 0.70 mmol, 0.3 equiv.) were placed in a glass cylinder (280 x 35 mm) containing a cross stirring bar. AcOH (25 mL) was added and the cylinder was placed inside an autoclave vessel. The autoclave was closed, put under magnetic stirring, filled with hydrogen (100 bars) and heated at 100 °C for 24 h. Stirring was stopped, the reaction was cold down to room temperature (around 1 h) and then hydrogen was removed from the autoclave. The reaction mixture was filtered through celite and the solid was successively washed with AcOH (2 x 5 mL) and CH_2Cl_2 (2 x 30 mL). The combined filtrate and washings were washed with 2M aqueous NaOH (until pH = 14). The organic layer was then separated and the aqueous phase was extracted with CH_2Cl_2 (2 x 30 mL). The collected organic layers were washed with brine, dried over K_2CO_3, and concentrated under reduced pressure. The residue was purified by recrystallizations in EtOAc to yield 736 mg (71%) of compound **14** as colorless crystals.

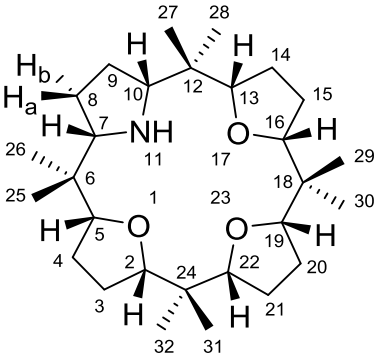

IR (KBr): 2967.5*s*, 2873.5*s*, 2820.2*m*, 2671.4*w*, 1469.9*m*, 1391.9*s*, 1374.6*m*, 1361.0*m*, 1085.2*s*, 1071.5*s*, 1042.2*s*, 999.5*m*, 981.0*m*;

^{1}H NMR ($CDCl_3$, 231K) δ 4.02 (m, 2 H, C-H(αO)), 3.91 (m, 1 H, C-H(αO)), 3.51 (m, 1 H, C-H(αO)), 3.43 (m, 2H, C-H(αO)), 3.43 (m, 1H, C-H(αN)), 2.85 (m, 1H, C-H(αN)), 2.33–2.11 (m, 4 H, CH_2), 1.66–1.30 (m, 12 H, CH_2), 0.96 (s, 6 H, CH_3), 0.94 (s, 3 H, CH_3(29, 30)), 0.82 (s, 3 H, CH_3), 0.81 (s, 3 H, CH_3), 0.80 (s, 6 H, CH_3), 0.79 (s, 3 H, CH_3);

^{13}C NMR ($CDCl_3$, 231K) δ 88.12 (C(αO)), 87.83 (C(αO)), 87.77 (C(αO)), 80.89 (C(αO)), 80.03 (C(αO)), 79.86 (C(αO)), 68.43 (C(αN)), 62.06 (C(αN)), 39.32 (C(meso)), 39.30 (C(meso)), 39.15 (C(meso)), 38.76 (C(meso)), 28.94, 27.32, 26.77, 26.74, 26.33, 26.26, 26.13, 26.03, 26.00, 25.85 (CH_2), 18.89, 17.89, 17.71, 17.46 (CH_3).

Melting point: 243°C.

HRMS calcd. for $C_{28}H_{50}NO_3^+$ 448.3785, found 448.3787 (M+H)+.

X-ray: Suitable crystals of **14** were obtained as colorless cubes by recrystallization from EtOAc. The structure crystallized in the triclinic P-1. The molecule is totally disordered with the N and O positions occupying alternative sites: O1/N1, O2/N2, O3/N3 and O4/N4. The structure has been refined and the occupancy of each atom was fixed for each site as: N: 0.25; O: 0.75.

2.3. Synthesis of half macrocycle models 24 and 25

Synthesis of compound **24**

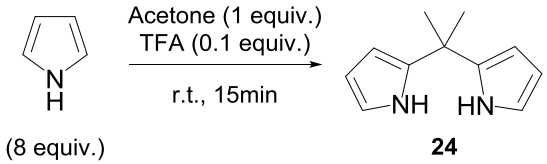

In a round-bottom flask were introduced pyrrole (21.00 mL, 0.304 mol, 8 equiv.) and acetone (2.82 mL, 38.0 mmol). The flask was equipped with a reflux condenser. The mixture was stirred for 5 minutes, then trifluoroacetic acid (0.293 mL, 3.80 mmol, 0.1 equiv.) was added and the mixture was stirred for an additional 15 minutes. After stirring, CH_2Cl_2 was added and the reaction mixture was basified with 5% sodium hydroxide and washed with saturated brine. The aqueous layer was extracted two times with CH_2Cl_2. The combined organic layers were dried with Na_2SO_4, and the solvent was removed under vacuum. The residue was purified by distillation using Kugelrohr to yield 3.97 g (60%) of compound **24** as pale yellow crystals.

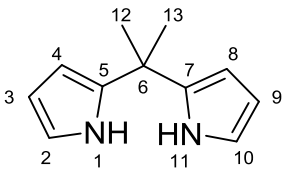

^{1}H NMR ($CDCl_3$, 298K) δ 7.72 (bs, 2 H, N-H(1, 11)), 6.62–6.60 (m, 2 H, pyrrolic-H(2, 10)), 6.15–6.13 (m, 2 H, pyrrolic-H(3, 9)), 6.11–6.09 (m, 2 H, pyrrolic-H(4, 8)), 1.59 (s, 6 H, CH_3(12, 13));

^{13}C NMR ($CDCl_3$) δ 139.24 (C(5, 7)), 117.19 (C(2, 10)), 107.91 (C(3, 9)), 103.87 (C(4, 8)), 35.52 (C(6)), 29.46 (C(12, 13)).

MS calcd for $C_{11}H_{14}N_2$: 174.11, found 174.01 (M).

See additional analyses in –B. J. Littler, M. A. Liller, C. –H. Hung, R. W. Wagner, D. F. O'Shea, P. D. Boyle, J. S. Lindsey, *J. Org. Chem.* **1999**, 64, 1391-1396.

Synthesis of compound **25**

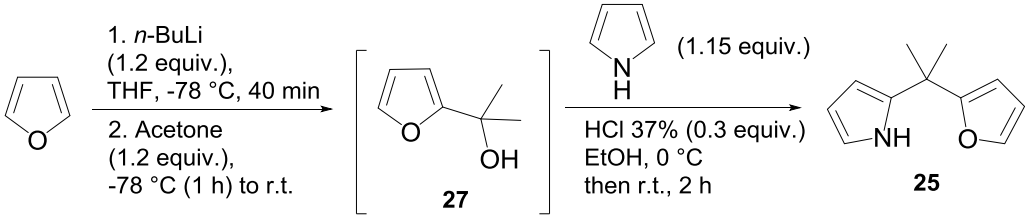

In a round-bottom flask were introduced furan (2.08 mL, 29.5 mmol) and anhydrous THF (20 mL). The reaction mixture was cold at -78 °C and then *n*-BuLi (1.6 M in cyclohexane, 22 mL, 35.3 mmol, 1.2 equiv.) was added dropwise. Once the addition was completed, the reaction mixture was stirred at -78 °C for 40 min. Acetone (2.62 mL, 35.3 mmol, 1.2 equiv.) was added at -78 °C and the reaction was stirred for an additional 1 h. The reaction was warmed to r.t. (around 1 h, colorless to clear yellow liquid). The reaction was quenched with saturated

aqueous NH_4Cl and the aqueous layer was extracted three times with EtOAc. The combined organic layers were washed with brine, dried over Na_2SO_4 and the solvent was removed under reduced pressure to yield 1.70 g (46%) of compound **27** as yellow liquid.

In a round-bottom flask were introduced pyrrole (1.08 mL, 15.5 mmol, 1.15 equiv.) and EtOH (1.5 mL). The reaction mixture was cold at 0 °C and compound **27** (1.70 g, 13.5 mmol) was added dropwise at 0 °C over a period of 15 min. The reaction was warmed to r.t. and then stirred for 2 h at r.t. After 2 h, distilled water was added to the orange solution, the organic layer was isolated and washed with saturated aqueous $NaHCO_3$ and brine. The solvent was removed under reduced pressure. The residue was purified by silica gel chromatography (Cyclohexane/CH_2Cl_2, 8/2) to yield 379 mg (16%) of compound **25** as colorless oil. The oil was kept in the fridge under argon and turned dark orange after few days. ^{1}H NMR and GC analysis did not change despite this change of color.

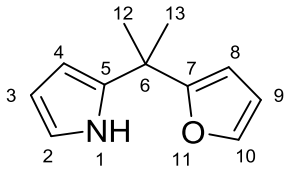

IR (ATR): 3415.3*br*, 2974.0*w*, 2934.6*w*, 2869.2*w*, 1557.5*w*, 1504.6*w*, 1463.6*w*, 1417.1*w*, 1383.3*w*, 1361.3*w*, 1260.3*w*, 1237.0*w*, 1158.8*m*, 1099.7*w*, 1080.9*w*, 1033.7*m*, 1017.0*m*, 1006.5*m*, 950.0*w*, 925.5*m*, 882.8*w*, 790.3*m*, 714.5*s*, 598.0*m*;

^{1}H NMR ($CDCl_3$, 298K) δ 8.12 (bs, 1 H, N-H(1)), 7.36 (d, ^{3}J(9, 10) = 0.8 Hz, 1 H, C-H(10)), 6.69 and 6.68 (system AB, J(A, B) = 4 Hz, 1 H, C-H(2)), 6.31 and 6.30 (system AB, J(A, B) = 3 Hz, 1 H, C-H(9)), 6.15 and 6.14 (system AB, J(A, B) = 5.6 Hz, 1 H, C-H(3)), 6.07 (d, ^{3}J(8, 9) = 3.2 Hz, 1 H C-H(8)), 6.06–6.04 (m, 1 H, C-H(4)), 1.68 (s, 6 H, C-H(12, 13));

^{13}C NMR ($CDCl_3$) δ 161.35 (C(7)), 141.53 (C(10)), 138.14 (C(5)), 116.87 (C(2)), 110.06 (C(9)), 107.92 (C(3)), 103.81 (C(4)), 103.36 (C(8)), 36.30 (C(6)), 27.91 (C(12, 13)).

HRMS calcd for $C_{11}H_{13}NO$: 176.1051, found 176.1059 (M)

2.4. Hydrogenation of models

Synthesis of compound **26**

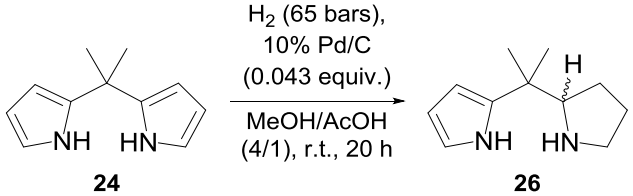

24 **26**

In an autoclave vessel were introduced compound **24** (2 g, 11.5 mmol), 10% Pd/C (524 mg, 0.49 mmol, 0.043 equiv. Pd), MeOH/AcOH 4/1 (50 mL). The suspension was stirred for 20 h at r.t. under 65 bar of H_2. Then the Pd/C was filtered through celite, the solid was washed with CH_2Cl_2 and the combined filtrate concentrated under reduced pressure to give a yellow slurry to which 2M NaOH (180 mL) and CH_2Cl_2 (100 mL) were added. The aqueous phase was extracted with CH_2Cl_2 (three times), the combined organic layers was dried over K_2CO_3 and

concentrated under reduced pressure. The resulting residue purified by silica gel chromatography (EtOAc/MeOH/Et_3N, 95/5/1) to yield 1.66 g (81%) of compound **26** as colorless crystals.

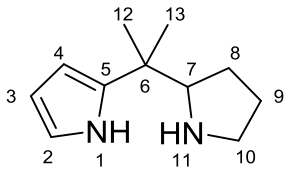

IR (KBr): 3150.4*m*, 3080.7*m*, 2965.8*m*, 2966.5*s*, 2871.8*s*, 1688.4*w*, 1566.6*m*, 1422.9*s*, 879.8*m*, 714.2*s*;

^{1}H NMR (CDCl3, 298K) δ 10.23 (bs, 1 H, N-H(1)), 6.67 (m, 1 H, pyrrolic-H(2)), 6.09 (m, 1 H, pyrrolic-H(3)), 5.92 (m, 1 H, pyrrolic-H(4)), 3.09 (t, 3J(2, 3) = 7.9 Hz, 1 H, C-H(7)), 2.90–2.87 (m, 2 H, CH_2(10)), 1.87 (bs, 1 H, N-H(11)), 1.78–1.70 (m, 1 H, CH_2(8)), 1.67–1.51 (m, 2 H, CH_2(9)), 1.31 (s, 3H, CH_3(12)), 1.23 (s, 3 H, CH_3(13)), 1.22–1.12 (m, 1 H, CH_2(8));

^{13}C NMR (CDCl3) δ 139.65 (C(5)), 116.15 (C(2)), 106.58 (C(3)), 103.97 (C(4)), 69.08 (C(7)), 46.87 (C(10)), 37.43 (C(5)), 29.62 (C(12)), 27.10 (C(8)), 26.03 (C(9)), 25.00 (C(13)).

Melting point: 79.2°C.

MS calcd for $C_{11}H_{18}N_2$: 178.15, found 179.3 (M+H)+.

Synthesis of compound **28**

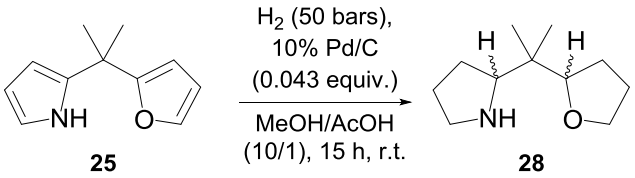

In an autoclave vessel were introduced compound **25** (106 mg, 0.61 mmol), 10% Pd/C (524 mg, 0.027 mmol, 0.045 equiv. Pd), MeOH/AcOH 10/1 (1.1 mL). The suspension was stirred for 15 h at r.t. under 50 bar of H_2. Then the Pd/C was filtered through celite, the solid was washed with CH_2Cl_2 and the combined filtrate concentrated under reduced pressure to give a yellow slurry to which 5% NaOH (180 mL) and CH_2Cl_2 (100 mL) were added. The aqueous phase was extracted with CH_2Cl_2 (three times), the combined organic layers was dried over Na_2SO_4 and concentrated under reduced pressure. The resulting residue purified by neutral alumina gel chromatography (Al_2O_3, EtOAc then EtOAc/MeOH, 9/1) to yield 31 mg (28%) of compound **28** as a clear yellow oil.

^{1}H NMR and ^{13}C NMR analysis of the isolated product revealed the presence of two diastereoisomers of compound **28** in the fraction in a ratio 70/30. These two diastereoisomers are presented as major (70%) and minor (30%) in the descriptions. The positions of the protons were attributed without taking account of the two diastereoisomers for the multiplets.

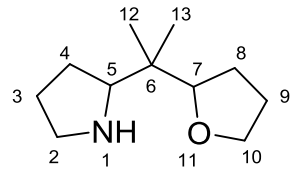

^{1}H NMR (CDCl3, 298K) δ 3.82–3.73 (m, C-H(10)), 3.73–3.64 (m, C-H(7)), 3.08–2.76 (m, C-H(6, 9)), 2.10 (bs, N-H(1)), 3.82–3.73 (m, C-H(10)), 1.86–1.60 (m, C-H(3, 4, 8, 9)), 1.50–1.39 (m, C-H(4)), 0.88 (s, CH_3(major)), 0.85 (s, CH_3(minor)), 0.80 (s, CH_3(minor)), 0.76 (s, CH_3(major));

^{13}C NMR (CDCl3) δ 86.07 (C(7)major), 84.62 (C(7)minor), 68.34 (C(10)major), 68.29 (C(10)minor), 66.59 (C(5)major), 65.71 (C(5)minor), 47.05 (C(2)major), 46.94 (C(2)minor), 39.11 (C(6)major), 38.84 (C(6)minor), 26.63 (C(8)major), 26.54 (C(8)minor), 26.41 (C(4)major + minor), 26.11 (C(3 or 9)minor), 26.04 (C(9 or 3)major), 25.95 (C(9 or 3)minor), 25.41 (C(3 or 9)major), 20.08 (C(13)major), 19.89 (C(13)minor), 19.54 (C(12)minor), 17.74 (C(12)major).

HRMS calcd for $C_{11}H_{22}NO^{+}$: 184.1713, found 184.1702 (M+H)+.

2.5. Synthesis of transition metal complexes

2.5.1. Complexes with calix-NONO 13 as ligand

Synthesis of cobalt^{II} complex **29**

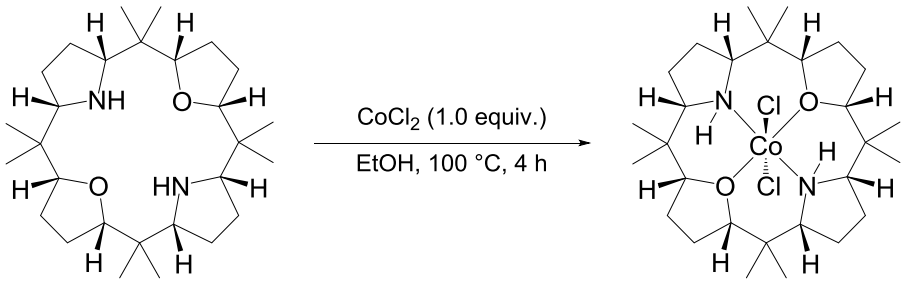

Cobalt^{II} chloride (2.9 mg, 0.022 mmol, purple solid) and compound **13** (10 mg, 0.022 mmol) were added in 5-mL vial containing anhydrous EtOH (1 mL). Cobalt^{II} chloride took a blue color in EtOH and then turned clear purple in few seconds. The vial was sealed and the reaction was stirred at 100 °C for 4 h. The clear purple reaction mixture was then cooled to r.t. and the solvent was removed under reduced pressure. The resulting purple solid was purified by chromatography (Al_2O_3, CH_2Cl_2/MeOH 99/1) in a Pasteur pipette to yield 6.2 mg (48%) of compound **29** as a purple powder. Slow evaporation at r.t. of a CH_2Cl_2/cyclohexane (1/1) solution containing **29** gave crystals of **29** as purple needles.

HRMS calcd for $C_{28}H_{50}ClCoN_2O_2$: 540.2893, found 540.2881 (M-Cl)+.

X-ray: Suitable crystals of **29** were obtained as purple needles by slow evaporation in a (1/1) solution of cyclohexane/dichloromethane. The structure crystallized in the monoclinic $P2_1/c$ space group.

Synthesis of nickel^{II} complex **30**

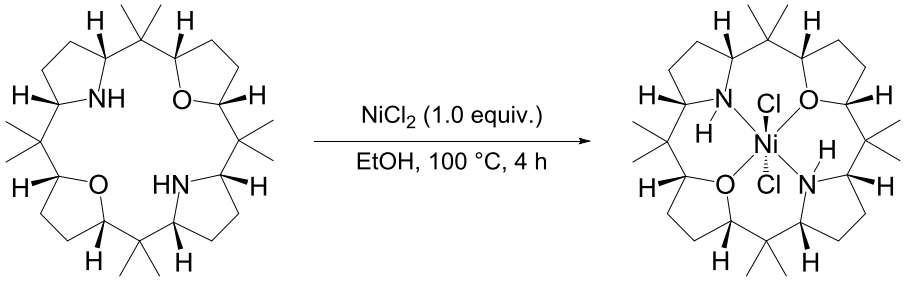

13 **30**

Nickel^{II} chloride (2.9 mg, 0.022 mmol, yellow solid) and compound **13** (10 mg, 0.022 mmol) were added in 5-mL vial containing anhydrous EtOH (1 mL). The vial was sealed and the reaction was stirred at 100 °C for 4 h. The clear yellow reaction mixture contained precipitates which solubilized in around 30 min. The clear yellow reaction mixture was then cooled to r.t. and the solvent was removed under reduced pressure. The resulting green/yellow solid was purified by chromatography (Al_2O_3, CH_2Cl_2/MeOH 99/1) in a Pasteur pipette to yield 6.1 mg (47%) of compound **30** as a yellow solid. Slow evaporation at r.t. of a CH_2Cl_2/cyclohexane (1/1) solution containing **30** gave crystals of **30** as yellow needles.

HRMS calcd for $C_{28}H_{50}ClN_2NiO_2$: 539.2914, found 539.2903 (M-Cl)+.

An undetermined peak with a mass of 549.32 (M-Cl + 10)+ was observed. Short investigation showed this peak could be without certainty the loose of the two Cl and addition of formate adduct.

X-ray: Suitable crystals of **30** were obtained as yellow needles by slow evaporation in a (1/1) solution of cyclohexane/dichloromethane. The structure crystallized in the orthorhombic Pnma space group.

Synthesis of copper^{II} complex **31**

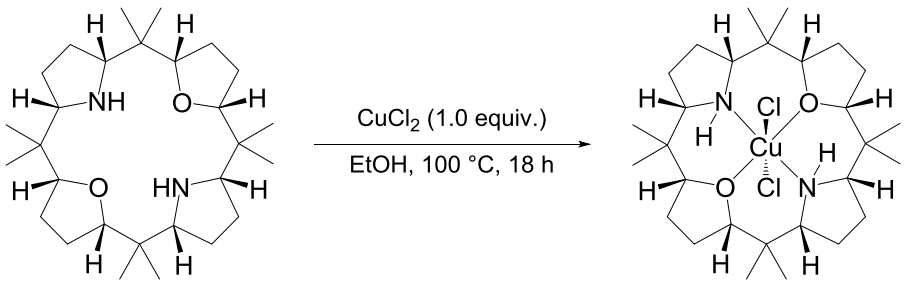

13 **31**

Copper^{II} chloride (3.0 mg, 0.022 mmol, brown solid) and compound **13** (10 mg, 0.022 mmol) were added in 5-mL vial containing anhydrous EtOH (1 mL). Copper^{II} chloride took a yellow color in EtOH. The vial was sealed and the reaction was stirred at 100 °C for 18 h. In few minutes at 100 °C the reaction mixture became colorless. The colorless reaction mixture was then cooled to r.t. and the solvent was removed under reduced pressure. The resulting blue

solid was purified by chromatography (Al_2O_3, CH_2Cl_2/MeOH 99/1) in a Pasteur pipette to yield 12.1 mg (93%) of compound **31** as a blue solid. Slow evaporation at r.t. of a CH_2Cl_2/cyclohexane (1/1) solution containing **31** gave crystals of **31** as blue needles.

HRMS calcd for $C_{28}H_{50}ClCuN_2O_2$: 544.2857, found 544.2861 (M-Cl)+.

X-ray: Suitable crystals of **31** were obtained as blue needles by slow evaporation in a (1/1) solution of cyclohexane/dichloromethane. The structure crystallized in the monoclinic $P2_1/c$ space group.

2.5.2. Complexes with calix-NOOO 14 as ligand

Synthesis of cobalt^{II} complex **32**

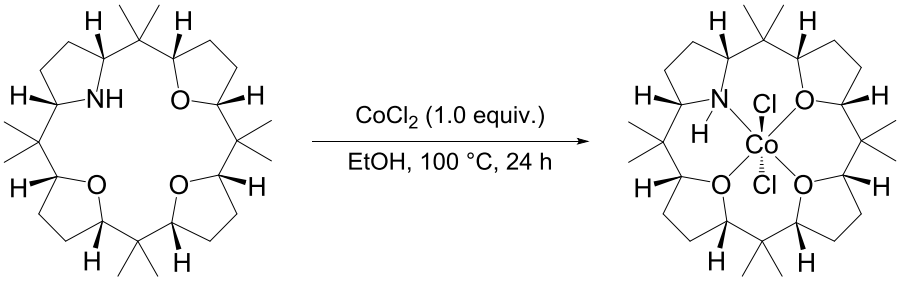

14 **32**

Cobalt^{II} chloride (2.9 mg, 0.022 mmol, purple solid) and compound **14** (10 mg, 0.022 mmol) were added in 5-mL vial containing anhydrous EtOH (1 mL). Cobalt^{II} chloride took a blue color in EtOH and then turned clear purple in few seconds. The vial was sealed and the reaction was stirred at 100 °C for 24 h. The clear purple reaction mixture was then cooled to r.t. and the solvent was removed under reduced pressure. No more starting material was observed by TLC analysis (Al_2O_3, CH_2Cl_2/MeOH 99/1). Slow evaporation at r.t. of a CH_2Cl_2/cyclohexane (1/1) solution containing **29** (12 mg) yielded 11.5 mg (89%) of compound **32** as purple needles.

HRMS calcd for $C_{28}H_{49}ClCoNO_3$: 541.2733, found 541.2718 (M-Cl).

X-ray: Suitable crystals of **32** were obtained as purple needles by slow evaporation in a (1/1) solution of cyclohexane/dichloromethane. The structure crystallized in the monoclinic $P2_1/c$ space group.

Synthesis of nickel^{II} complex **33**

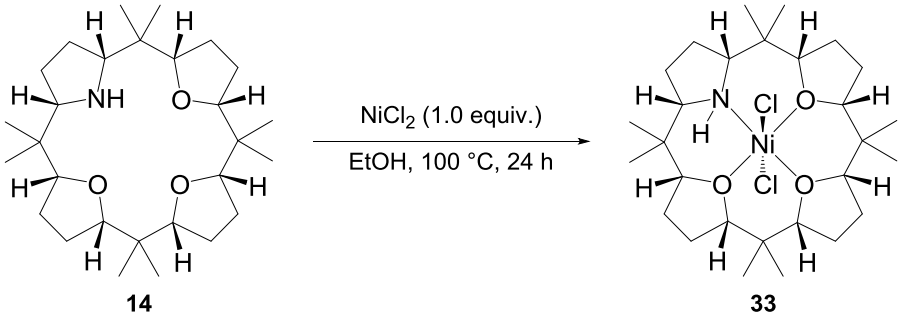

14 **33**

Nickel^{II} chloride (2.9 mg, 0.022 mmol, yellow solid) and compound **14** (10 mg, 0.022 mmol) were added in 5-mL vial containing anhydrous EtOH (1 mL). The vial was sealed and the reaction was stirred at 100 °C for 24 h. The clear yellow reaction mixture contained precipitates which solubilized in around 30 min. The clear yellow reaction mixture was then cooled to r.t. and the solvent was removed under reduced pressure. No more starting material was observed by TLC analysis (Al_2O_3, CH_2Cl_2/MeOH 99/1). Slow evaporation at r.t. of a CH_2Cl_2/cyclohexane (1/1) solution containing **29** (13 mg) yielded 12 mg (93%) of compound **33** as yellow needles.

HRMS calcd for $C_{28}H_{49}ClNNiO_3$: 540.2754, found 540.2755 (M-Cl)+.

An undetermined peak with a mass of 550.3 (M-Cl + 10)+ was observed. Short investigation showed this peak could be without certainty the loose of the two Cl and addition of formate adduct.

X-ray: Suitable crystals of **33** were obtained as yellow needles by slow evaporation in a (1/1) solution of cyclohexane/dichloromethane. The structure crystallized in the monoclinic $P2_1/c$ space group.

2.6. Synthesis of calix-1,4-diols 34a and 34b

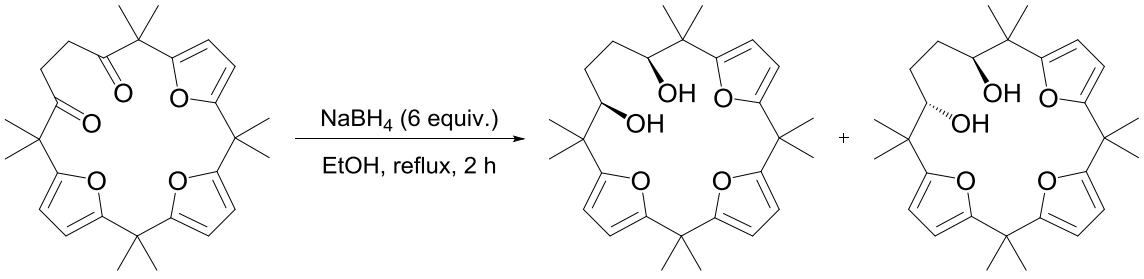

21 **34a** **34b**

$NaBH_4$ (504 mg, 13.3 mmol, 6 equiv.) was added to a solution of compound 21 (1.0 g, 2.22 mmol) in EtOH (90 mL). The reaction mixture was refluxed for 2 h. After being cold to r.t. the reaction mixture was slowly quenched with a saturated aqueous NH_4Cl solution. Water and EtOAc were added and the organic layer was isolated. The aqueous layer was extracted once with EtOAc and then the combined organic layer was washed with brine and and dried over Na_2SO_4. The solvent was removed under reduced pressure and the residue was purified

by silica gel chromatography (Cyclohexane/EtOAc, 8/2) to yield 400 mg (40% yield) of compound **34a** as white solid. The solvent was then changed to (Cyclohexane/EtOAc, 6/4) to yield 380 mg (38% yield) of compound **34b** as white solid.

- Compound **34a**

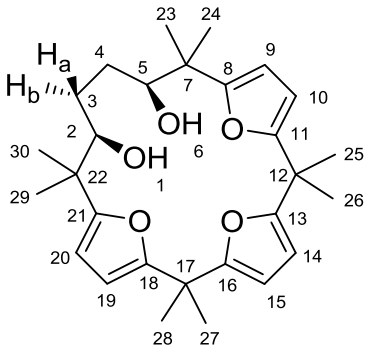

IR (ATR): 3552.7*w*, 3350.5*br*, 2973.8*m*, 2925.6*w*, 2.873.2*w*, 1547.5*w*, 1467.2*w*, 1441.5*w*, 1384.4*w*, 1368.1*w*, 1263.4*w*, 1110.1*m*, 1023.0*s*, 981,1*s*, 953.1*s*, 786.8*s*

^{1}H NMR (CDCl$_3$, 298K) δ 6.06 (s, 2 H, C-H(14, 15)), 5.97 (d, ^{3}J(9, 10 and 19, 20) = 3.2 Hz, 2 H, C-H(9, 20 or 10, 19)), 5.87 (d, ^{3}J(9, 10 and 19, 20) = 3.2 Hz, 2 H, C-H(9, 20 or 10, 19)), 3.32 (d, ^{3}J(2, 3 and 4, 5) = 8 Hz, 2 H, C-H(2, 5)), 1.64 (bs, 2 H, O-H(1, 6)), 1.58 (s, 6 H, C-H(25, 27)), 1.56 (s, 6 H, C-H(26, 28)), 1.29–1.23 (m, 2 H, C-Ha or C-Hb(3, 4)), 1.20 (s, 6 H, C-H(23, 29)), 1.18 (s, 6 H, C-H(24, 30)), 0.79–0.71 (m, 2 H, C-Ha or C-Hb(3, 4));

^{13}C NMR (CDCl$_3$) δ 159.20 (C(8, 21)), 158.84 (C(11, 18)), 158.22 (C(13, 16)), 105.17 (C(9, 20 or 10, 19)), 105.03 (C(14, 15)), 103.20 (C(9, 20 or 10, 19)), 78.29 (C(2, 5)), 40.88 (C(7, 22)), 37.02 (C(12, 17)), 29.79 (C(3, 4)), 26.18 (C(25, 27)), 25.76 (C(26, 28)), 24.59 (C(23, 29)), 21.18 (C(24, 30)).

Melting point: 162 °C.

HRMS calcd. for $C_{28}H_{39}O_5^+$ 455.2797, found 455.2801 (M+H)+.

- Compound **34b**

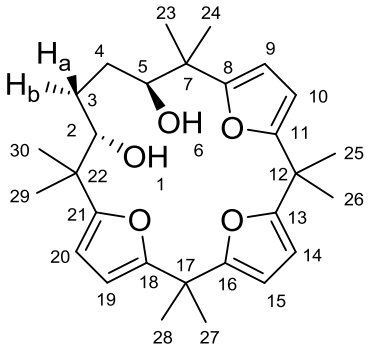

IR (ATR): 3264.8*br*, 2969.7*w*, 2933.2*w*, 2850.3*w*, 1549.7*w*, 1464.7*w*, 1366.3*m*, 1267.2*w*, 1193.2*m*, 1151.2*m*, 1096.2*s*, 1068.23*s*, 1020.2*s*, 974.0*s*, 790.1*s*, 713.6*m*;

^{1}H NMR (CDCl$_3$, 298K) δ 6.05 (s, 2 H, C-H(14, 15)), 5.94 (d, ^{3}J(9, 10 and 19, 20) = 3.2 Hz, 2 H, C-H(9, 20 or 10, 19)), 5.87 (d, ^{3}J(9, 10 and 19, 20) = 3.2 Hz, 2 H, C-H(9, 20 or 10, 19)), 3.28 (d, J = 8.8 Hz, 2 H, C-H(2, 5)), 2.10 (bs, 2 H, O-H(1, 6)), 1.57 (s, 6 H, C-H(25, 27)), 1.56 (s, 6 H, C-H(26, 28)), 1.27–1.24 (m, 2 H, C-Ha or C-Hb(3, 4)), 1.21 (s, 6 H, C-H(23, 29)), 1.15 (s, 6 H, C-H(24, 30)), 0.10–1.04 (m, 2 H, C-Ha or C-Hb(3, 4));

^{13}C NMR (CDCl$_3$) δ 159.37 (C(8, 21)), 158.76 (C(11, 18)), 158.31 (C(13, 16)), 105.04 (C(9, 20 or 10, 19)), 104.82 (C(14, 15)), 103.30 (C(9, 20 or 10, 19)), 78.15 (C(2, 5)), 40.97 (C(7,

22)), 37.02 (C(12, 17)), 29.72 (C(3, 4)), 26.09 (C(25, 27)), 25.98 (C(26, 28)), 24.22 (C(23, 29)), 20.35 (C(24, 30)).

Melting point: 205 °C.

HRMS calcd. for $C_{28}H_{39}O_5^+$ 455.2797, found 455.2796 (M+H)+.

X-ray: Suitable crystals of **34b** were obtained as colorless plates by slow evaporation of a solution in deuterated chloroform. The structure crystallized in the triclinic P-1space group. Two independent molecules crystallized in the asymmetric unit.

2.7. Synthesis of compound 36

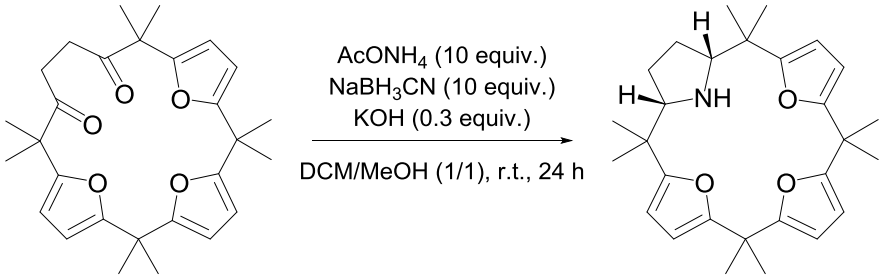

$AcONH_4$ (513 mg, 6.66 mmol, 10 equiv.), KOH (11 mg, 0.20 mmol, 0.3 equiv.) and $NaBH_3CN$ (418 mg, 6.66 mmol, 10 equiv.) were successively added to a solution of compound **21** (300 mg, 0.67 mmol) in a 1/1 mixture of CH_2Cl_2/MeOH (11 mL). The reaction mixture was stirred at r.t. for 24 h. The reaction mixture was quenched with a saturated aqueous NH_4Cl solution (pH = 6-7). The aqueous layer was extracted three times with CH_2Cl_2 and the combined organic layer was dried over Na_2SO_4. The solvent was removed under reduced pressure. The residue was recrystallized in EtOAc and the mixture was let crystallized one night at 4 °C in the fridge. Filtration yielded 73 mg of compound **36** (25% yield) as a white solid.

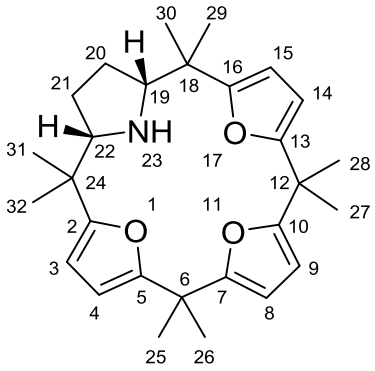

IR (ATR): 2968.9*m*, 2937.5*w*, 2871.3*w*, 1557.7*m*, 1462.1*w*, 1406.9*w*, 1389.3*w*, 1361.6*w*, 1261.1*m*, 1203.0*m*, 1151.9*m*, 1108.1*m*, 1023.7*m*, 953.3*m*, 777.2*s*, 725.6*w*, 714.3*w*, 576.3*w*;

^{1}H NMR ($CDCl_3$, 298K) δ 6.01 (s, 2 H, C-H(8, 9)), 5.90 (d, ^{3}J(3, 4) and = ^{3}J(14, 15) = 3.2 Hz, 2 H, C-H(3, 15 or 4, 14)), 5.76 (d, ^{3}J(3, 4) and = ^{3}J(14, 15) = 2.8 Hz, 2 H, C-H(3, 15 or 4, 14)), 3.00 (m, 2 H, C-H(19, 22)), 1.66 (bs, 1 H, N-H(23)), 1.54 (s, 6 H, C-H(25, 27)), 1.52 (s, 6 H, C-H(26, 28)), 1.32–1.25 (m, 4 H, C-H(20, 21)), 1.13 (s, 6 H, C-H(29, 31)), 1.09 (s, 6 H, C-H(30, 32));

^{13}C NMR ($CDCl_3$) δ 160.77 (C(2, 16)), 158.92 (C(7, 10)), 158.20 (C(5, 13)), 104.41 (C(3, 15 or 4, 14)), 103.45 (C(3, 15 or 4, 14)), 103.42 (C(8, 9)), 65.55 (C(19, 22)), 38.30 (C(18, 24)),

36.91 (C(6, 12)), 26.58 (C(29, 31)), 25.69 (C(25, 27)), 25.03 (C(26, 28)), 24.85 (C(20, 21)), 19.77 (C(30, 32)).

Melting point: 210 °C.

HRMS calcd. for $C_{28}H_{38}NO_3^+$ 436.2852, found 436.2862 (M+H)+.

X-ray: Suitable crystals of **36** were obtained as colorless cubes by slow evaporation of a solution in dichloromethane. The structure crystallized in the monoclinic $P2_1/n$ space group.

2.8. Synthesis of compounds 38 and 39

2.8.1. Characterization of side product 37

Compound **37** was isolated during the purification of compound **22a** by silica gel chromatography when a part of the crude product was let overnight in the column (See page 116 Chapter 6).

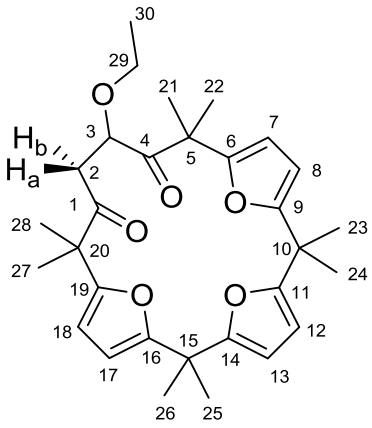

IR (ATR): 3128*w*, 2979*m*, 2934*m*, 2871*w*, 1712*s*, 1552*m*, 1464*m*, 1384*m*, 1366*m*, 1262*m*, 1205*m*, 1151*m*, 1122*s*, 1080*m*, 1023*s*, 798*s*, 784*s*, 708*m*;

^{1}H NMR (CDCl$_3$, 298K) δ 6.23 (d, ^{3}J(C-H(furan)) = 3.2 Hz, 1 H, C-H(furan)), 6.06 (d, ^{3}J(C-H(furan)) = 3.2 Hz, 1 H, C-H(furan)), 6.02 (d, ^{3}J(C-H(furan)) = 3.2 Hz, 1 H, C-H(furan)), 5.98 (d, ^{3}J(C-H(furan)) = 3.2 Hz, 1 H, C-H(furan)), 5.95 (t, ^{3}J(C-H(furan)) = 3.2 Hz, 2 H, C-H(furan)), 4.70 (dd, ^{3}J(2a, 3) = 9.6 Hz and ^{3}J(2b, 3) = 1.6 Hz, 1 H, C-H(3)), 3.31 (m, 1 H, C-H(29)), 3.14 (m, 1 H, C-H(29)), 2.14 (dd, ^{2}J(2a, 2b) = 16.0 Hz and ^{3}J(2a, 3) = 10.0 Hz, 1 H, C-H(2a)), 1.57 (s, 6 H, CH_3), 1.52 (s, 3 H, CH_3), 1.48 (s, 3 H, CH_3), 1.47 (s, 3 H, CH_3), 1.38 (s, 3 H, CH_3), 1.32 (s, 3 H, CH_3), 1.30 (s, 3 H, CH_3), 1.07 (t, ^{3}J(29, 30) = 7.2 Hz, 3 H, C-H(30)), 0.70 (dd, ^{2}J(2a, 2b) = 16.0 Hz and ^{3}J(2b, 3) = 2.0 Hz, 1 H, C-H(2b));

^{13}C NMR (CDCl$_3$) δ 210.43 (C=O), 208.81 (C=O), 159.93 (C(quat.furan), 159.88 (C(quat.furan), 158.58 (C(quat.furan), 157.86 (C(quat.furan), 155.91 (C(quat.furan), 153.73 (C(quat.furan), 108.17 (C(furan), 106.37 (C(furan), 106.21 (C(furan), 104.93 (C(furan), 103.72 (C(furan), 103.67 (C(furan), 76.65 (C(3)), 65.72 (C(29)), 49.23 (C(meso)), 47.76 (C(meso)), 39.15 (C(2)), 37.02 (C(meso)), 36.71 (C(meso)), 26.68 (CH_3), 25.95 (CH_3), 25.59 (CH_3), 25.47 (CH_3), 24.23 (CH_3), 22.99 (CH_3), 22.25 (CH_3), 21.69 (CH_3), 15.28 (C(30)).

Melting point: 109°C.

HRMS calcd. for $C_{30}H_{39}O_6^+$ 495.2747, found 495.2742 (M+H)+.

X-ray: Suitable crystals of **37** were obtained as colorless cubes by slow evaporation of a solution in dichloromethane. The structure crystallized in the monoclinic $P2_1/n$ space group.

2.8.2. Synthesis of compounds 38 and 39

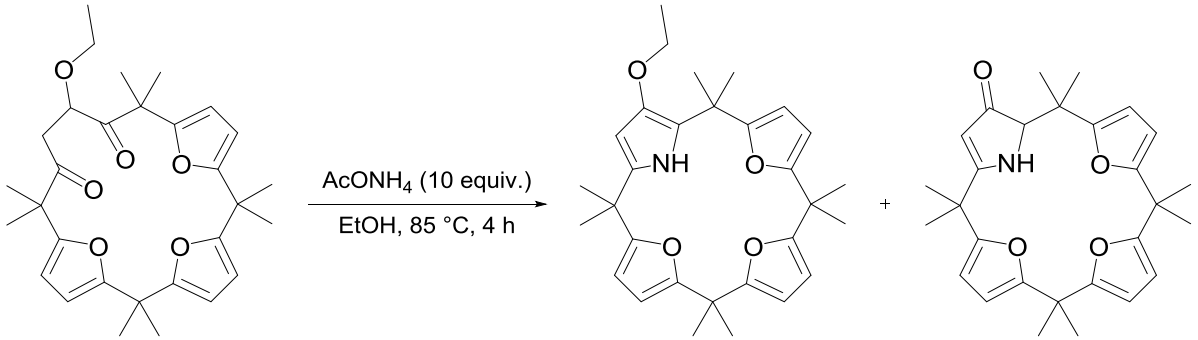

In a Schlenk tube were introduced compound **37** (50 mg, 0.10 mmol) and EtOH (3 mL). Then, $AcONH_4$ (78 mg, 1.01 mmol, 10 equiv.) was added to the slurry, and the mixture was warmed at 85 °C for 4 h. CH_2Cl_2 was added and the reaction mixture was washed with water and then brine. The organic layer was dried over Na_2SO_4 and the solvent was removed under reduced pressure. The residue was purified by silica gel chromatography (Cyclohexane/EtOAc 95/5) to yield 5.4 mg (11%) of compound **38** as colorless powder. The solvent was then changed to (Cyclohexane/EtOAc 7/3) to yield 10 mg (22%) of compound **39** as clear yellow powder.

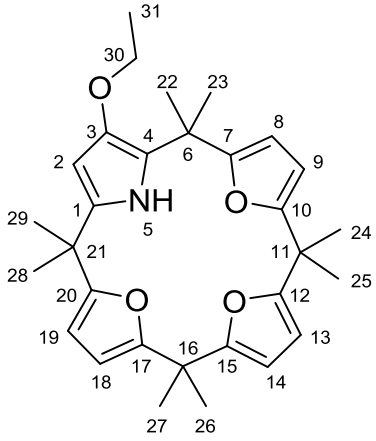

- Compound **38**

IR (ATR): 2985.3*w*, 2923.6*w*, 2854.1*w*, 1729.1*m*, 1707.3*m*, 1553.4*w*, 1456.3*w*, 1365.3*w*, 1297.3*w*, 1258.7*m*, 1237.1*m*, 1194.6*m*, 1152.5*m*, 1098.9*m*, 1043.9*m*, 1033.2*s*, 954.1*m*, 784.7*s*, 729.2*w*, 715.9*w*;

^{1}H NMR ($CDCl_3$, 298K) δ 6.35 (bs, 1 H, N-H(5)), 6.01 (q, ^{3}J(C-H(furan)) = 6.8 Hz, 2.8 Hz, 2 H, C-H(furan)), 5.98 (d, ^{3}J(C-H(furan)) = 3.2 Hz, 1 H, C-H(furan)), 5.96 (d, ^{3}J(C-H(furan)) = 3.2 Hz, 2 H, C-H(furan)), 5.94 (d, ^{3}J(C-H(furan)) = 3.2 Hz, 1 H, C-H(furan)), 5.66 (d, ^{4}J(2, 5) = 3.2 Hz, 1 H, C-H(2)), 3.90 (q, ^{3}J(30, 31) = 6.8 Hz, 2 H, C-H(30)), 1.57 (s, 6 H, CH_3), 1.54 (s, 6 H, CH_3), 1.53 (s, 6 H, CH_3), 1.45 (s, 6 H, CH_3), 1.32 (t, ^{3}J(30, 31) = 7.2 Hz, 3 H, C-H(31)) ;

^{13}C NMR ($CDCl_3$) δ 159.54 (C(quat.furan), 159.47 (C(quat.furan), 159.17 (C(quat.furan), 158.51 (C(quat.furan), 158.45 (2 x C(quat.furan), 141.02 (C(quat.pyrrole), 132.77 (C(quat.pyrrole), 119.02 (C(3)), 104.99 (C(furan), 104.84 (C(furan), 103.76 (C(furan), 103.74 (C(furan), 103.67 (C(furan), 103.64 (C(furan), 93.48 (C(2)), 67.06 (C(30)), 36.99 (C(meso)), 36.90 (C(meso)), 36.81 (C(meso)), 36.60 (C(meso)), 28.56 (CH_3), 26.69 (CH_3), 25.99 (CH_3), 25.91 (CH_3), 15.66 (C(31)).

Melting point: 132 – 134 °C.

HRMS calcd. for $C_{30}H_{37}NO_4^+$ 476.2801, found 476.2807 (M+H)+.

- Compound **39**

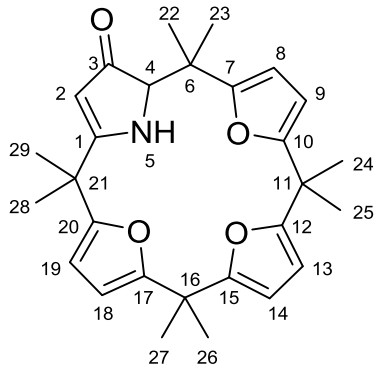

IR (ATR): 3216*br*, 2968*m*, 2924*m*, 2872*w*, 2850*w*, 1697*s*, 1557*w*, 1464*w*, 1364*w*, 1260*w*, 1207*w*, 1155*w*, 1110*w*, 1028*w*, 956*w*, 778*m*, 726*w*;

^{1}H NMR (CDCl$_3$, 298K) δ 6.24 (bs, 1 H, N-H(5)), 6.05 (d, ^{3}J(C-H(furan)) = 2.8 Hz, 1 H, C-H(furan)), 6.02 (d, ^{3}J(C-H(furan)) = 3.2 Hz, 1 H, C-H(furan)), 5.99 (d, ^{3}J(C-H(furan)) = 3.2 Hz, 1 H, C-H(furan)), 5.97 (d, ^{3}J(C-H(furan)) = 3.2 Hz, 1 H, C-H(furan)), 5.89 (d, ^{3}J(C-H(furan)) = 3.2 Hz, 1 H, C-H(furan)), 5.78 (d, ^{3}J(C-H(furan)) = 3.2 Hz, 1 H, C-H(furan)), 5.02 (t, ^{4}J(2, 4) = 2.0 Hz, 1 H, C-H(2)), 4.09 (t, ^{4}J(2, 4) = 1.6 Hz, 1 H, C-H(4)), 1.57 (s, 3 H, CH_3), 1.55 (s, 6 H, CH_3), 1.54 (s, 3 H, CH_3), 1.54–bis (s, 3 H, CH_3), 1.52 (s, 3 H, C-H(28)), 1.28 (s, 3 H, C-H(22)), 0.85 (s, 3 H, C-H(23));

^{13}C NMR (CDCl$_3$) δ 173.36 (C(3)), 159.59 (C(20)), 158.99 (C(quat.furan), 158.93 (C(quat.furan), 158.85 (C(quat.furan), 158.70 (C(quat.furan), 158.60 (C(quat.furan), 145.37 (C(1)), 142.32 (C(2)), 104.23 (C(furan), 104.17 (C(furan), 104.14 (C(furan), 104.07 (C(furan), 103.77 (C(furan), 103.75 (C(furan), 63.48 (C(4)), 38.46 (C(6)), 37.48 (C(meso)), 37.05 (C(meso)), 37.00 (C(meso)), 27.71 (CH_3), 25.97 (CH_3), 25.72 (CH_3), 25.67 (CH_3), 25.62 (CH_3), 24.07 (CH_3), 24.06 (CH_3), 18.19 (CH_3).

Melting point: 233 – 235 °C.

HRMS calcd. for $C_{28}H_{34}NO_4$ 448.2488, found 448.2488 (M+H)+.

2.9. Synthesis of substituted calix[3]furan[1]pyrrole 41

2.9.1. Synthesis of compound 40

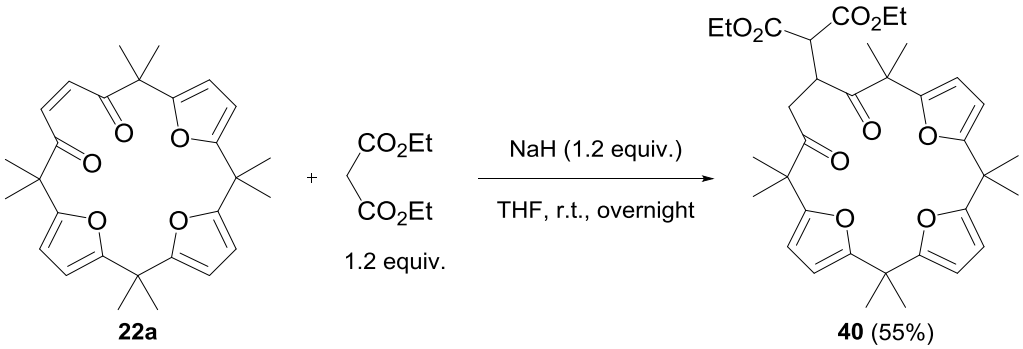

22a **40** (55%)

Diethyl malonate (213 µl, 1.40 mmol, 1.2 equiv.) and NaH (34 mg, 1.40 mmol, 1.2 equiv.) were successively added to a solution of **22a** (523 mg, 1.17 mmol) in anhydrous THF (5 ml) in a Schlenk tube. NaH solubilized in the mixture within second accompanied with a release of gas and a change of color of the reaction mixture from colorless to a light orange color. After stirring the reaction mixture overnight at r.t. the solvent was removed under reduced

pressure using the rotavap. The yellow oil was purified by silica gel chromatography (Cy/EtOAc 96/4) to yield 411 mg (95% purity, 55% yield) of compound **40** as white solid.

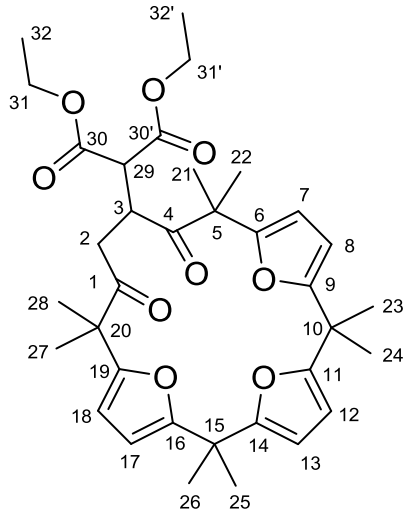

IR (ATR): 2977.9*w*, 2937.7*w*, 1732.4*s*, 1708.7*m*, 1550.2*w*, 1467.2*w*, 1454.3*w*, 1382.7*w*, 1366.0*w*, 1292.4*w*, 1240.1*m*, 1196.7*w*, 1154.5*m*, 1107.1*m*, 1040.4*m*, 1022.4*m*, 953.1*m*, 783.8*s*, 727.5*w*;

^{1}H NMR ($CDCl_3$, 298K) δ 6.07 (d, ^{3}J(C-H(furan)) = 3.2 Hz, 1 H, C-H(furan)), 6.01 (d, ^{3}J(C-H(furan)) = 3.2 Hz, 1 H, C-H(furan)), 5.97 (d, ^{3}J(C-H(furan)) = 3.2 Hz, 2 H, C-H(furan)), 5.95 (d, ^{3}J(C-H(furan)) = 3.2 Hz, 1 H, C-H(furan)), 5.93 (d, ^{3}J(C-H(furan)) = 3.2 Hz, 1 H, C-H(furan)), 4.11 (q, ^{3}J(31, 32) = 7.2 Hz, 1 H, C-H(31)), 4.11–bis (q, ^{3}J(31, 32) = 7.2 Hz, 1 H, C-H(31)), 4.04 (q, ^{3}J(31', 32') = 7.2 Hz, 2 H, C-H(31')), 3.85–3.80 (m, 1 H, C-H(3)), 3.55 (d, ^{3}J(3, 29) = 10.0 Hz, 1 H, C-H(29)), 1.65 (s, 3 H, CH_3), 1.60 (s, 3 H, CH_3), 1.58 (s, 3 H, CH_3), 1.56 (s, 3 H, CH_3), 1.52 (s, 3 H, CH_3), 1.42 (s, 3 H, CH_3), 1.40 (s, 3 H, CH_3), 1.28 (s, 3 H, CH_3), 1.28–bis (s, 2 H, C-H(2)), 1.21 (t, ^{3}J (31, 32) = 7.2 Hz, 3 H, C-H(32)) 1.20 (t, ^{3}J (31', 32') = 7.2 Hz, 3 H, C-H(32'));

^{13}C NMR ($CDCl_3$) δ 210.17 (C=O), 209.38 (C=O), 168.56 (C(30, 30')), 159.74 (C(quat.furan), 159.69 (C(quat.furan), 158.27 (C(quat.furan), 158.25 (C(quat.furan), 155.45 (C(quat.furan), 155.40 (C(quat.furan), 106.77 (C(furan), 106.45 (C(furan), 104.76 (C(furan), 104.16 (C(furan), 103.59 (C(furan), 103.58 (C(furan), 61.48 (C(31)), 61.42 (C(31')), 53.27 (C(29)), 48.49 (C(5 or 20)), 48.36 (C(5 or 20)), 42.36 (C(3)), 37.04 (C(10 or 15)), 36.94 (C(10 or 15)), 27.06 (CH_3), 26.22(CH_3), 26.01 (CH_3), 25.70 (CH_3), 25.12 (CH_3), 24.47 (CH_3), 23.65 (2 or CH_3), 23.61 (2 or CH_3), 23.57 (2 or CH_3), 14.12 (C(32, 32')).

Melting point: 87 – 88 °C.

HRMS calcd. for $C_{35}H_{44}O_9Na^+$ 631.2883, found 631.2867 (M+Na)+.

2.9.2. Synthesis of compound 41

In a Schlenk tube were introduced **40** (411 mg, 95% pure, 0.64 mmol) and ethanol (22 mL). Then, $AcONH_4$ (222 mg, 2.89 mmol, 4.5 equiv.) was added to the slurry, and the mixture was warmed at 85 °C for 4 h. Dichloromethane (40 ml) was added to the reaction and then the reaction mixture was washed with water (3 x 20 ml). The organic layers were combined and dried over Na_2SO_4. The solvent was removed under reduced pressure using the rotavap. The residue was purified by silica gel chromatography (Cy/EtOAc 95/5) to yield 224 mg (67%) of compound **41** as white solid.

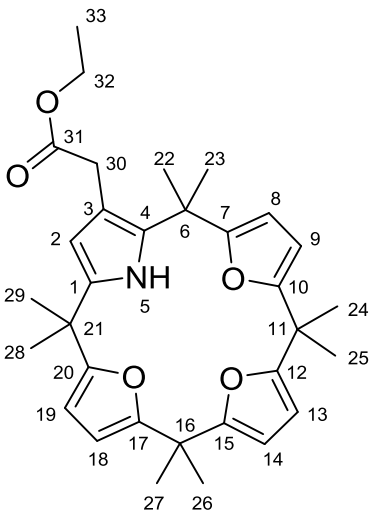

IR (ATR): 3436.3*w*, 2972.1*w*, 2930.6*w*, 2867.3*w*, 1736.3*m*, 1557.4*w*, 1445.3*w*, 1379.7*w*, 1362.2*w*, 1257.7*w*, 1235.1*w*, 1202.5*w*, 1152.5*w*, 1118.1*w*, 1060.8*w*, 1022.3*m*, 952.6*m*, 778.3*s*, 731.7*w*, 709.28*w*;

^{1}H NMR ($CDCl_3$, 298K) δ 6.81 (bs, 1 H, N-H(5)), 6.03 and 6.02 (system AB, J(A, B) = 4 Hz, 2 H, C-H(13, 14)), 5.97 and 5.95 (system AB, J(A, B) = 8 Hz, 2 H, C-H(8, 9 or 18, 19)), 5.95 and 5.92 (system AB, J(A, B) = 12 Hz, 2 H, C-H(8, 9 or 18, 19)), 5.79 (d, ^{4}J(2, 5) = 3.2 Hz, 1 H, C-H(2)), 4.16 (q, ^{3}J(32, 33) = 7.2 Hz, 2 H, C-H(32)), 3.55 (s, 2 H, C-H(30)), 1.57 (s, 6 H, CH_3), 1.53 (s, 12 H, CH_3), 1.46 (s, 6 H, CH_3), 1.27 (t, ^{3}J(32, 33) = 7.2 Hz, 3 H, C-H(33));

^{13}C NMR ($CDCl_3$) δ 127.97 (C=O), 159.39 (C(12, 15)), 159.35 (C(quat.furan), 158.80 (C(quat.furan), 158.47 (C(quat.furan), 158.24 (C(quat.furan), 135.52 (C(1)), 131.92 (C(4)), 109.03 (C(3)), 105.83 (C(2)), 105.01 (C(furan), 104.67 (C(furan), 103.79 (C(furan), 103.75 (C(furan), 103.65 (C(furan), 103.60 (C(furan), 60.58 (C(32)), 37.66 (C(6)), 36.95 and 36.86 (C(11, 16)), 36.16 (C(21)), 33.91 (C(30)), 28.43 (C(28, 29)), 27.50 (C(22, 23)), 25.91 and 25.88 (C(24, 25, 26, 27)), 14.39 (C(33)).

Melting point: 113 – 114°C.

HRMS calcd. for $C_{32}H_{40}NO_5^+$ 518.2906, found 518.2905 (M+H)+

Chapter 9. Annex

1. Cyclic voltammograms

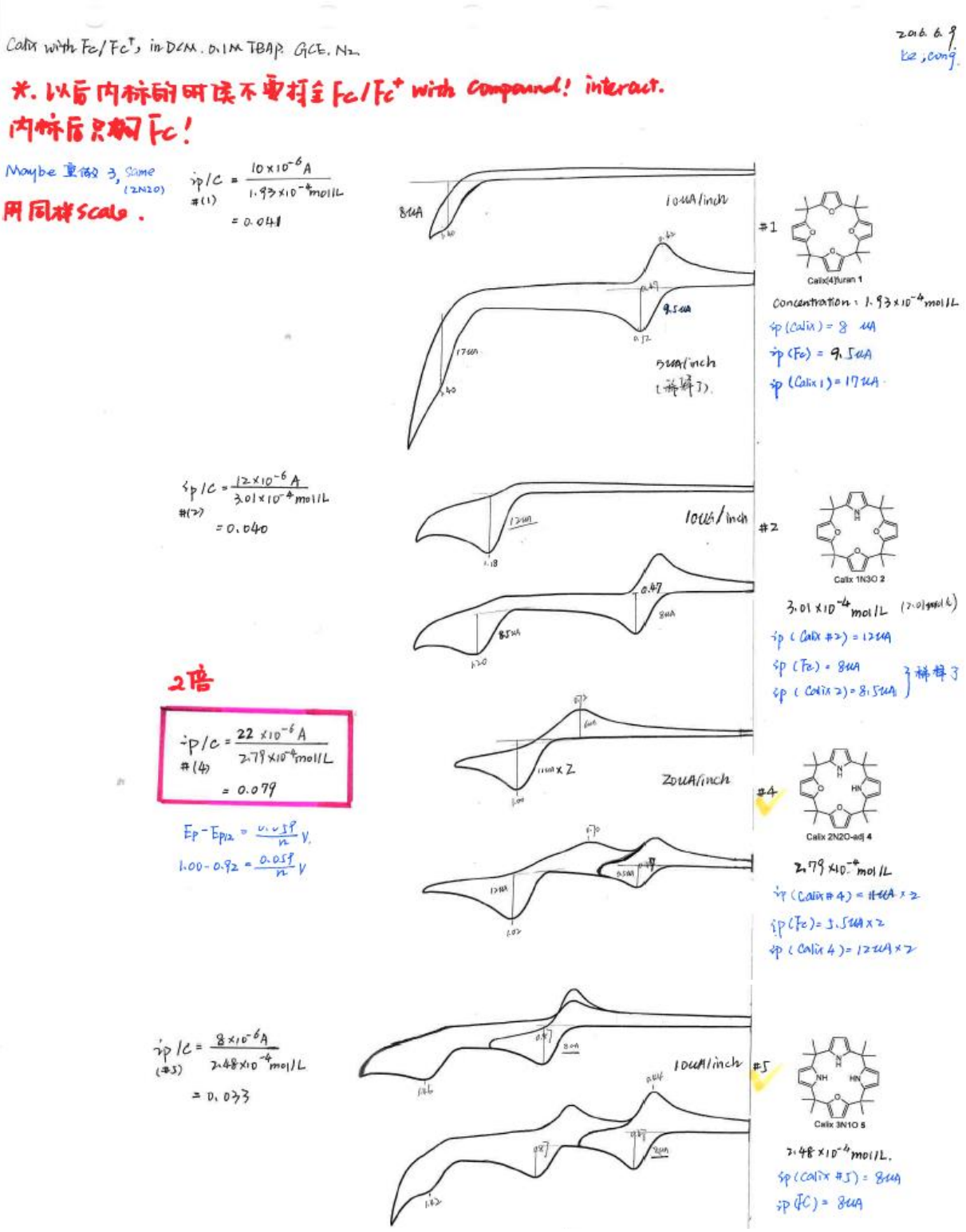

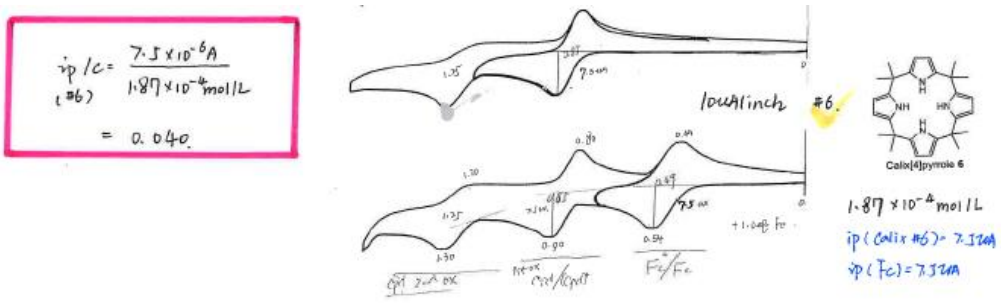

Figure 71. Cyclic voltammetry of compounds **1**, **2**, **7**, **8** and **10**, with and without Fc^+/Fc, 0.1M TBAP. Scan rate = 0.1V/s

2. Characterization of a salt of calix-NNNO 11 with TFA

Difficulties occurred to obtain a single crystal of the free ligand calix-NNNO **11**. To validate the position of the hydrogen atoms located on the α-position of the heteroatoms, a series of crystallization in presence of different acids were tested. The use of TFA led to structure characterization. Calix-NNNO **11** (3 mg, $6.73.E^{-6}$ mol) was solubilized in a minimum of CH_2Cl_2 in a small tube and TFA (2 µL, $2.61E^{-5}$ mol) was added (Scheme 41). After slow evaporation of the solution, the resulting product was not sufficient for an X-ray analysis. The crude material was solubilized in MeOH and the tube was placed in a vial in which isopropyl ether was added for diffusion. The vial was closed and the after few days (diffusion but no crystallization), the caps drilled and a slow evaporation of the solvent occurred. This evaporation led to the formation of crystals of compound **43** which could be successfully analyzed by X-ray determination (Figure 41).

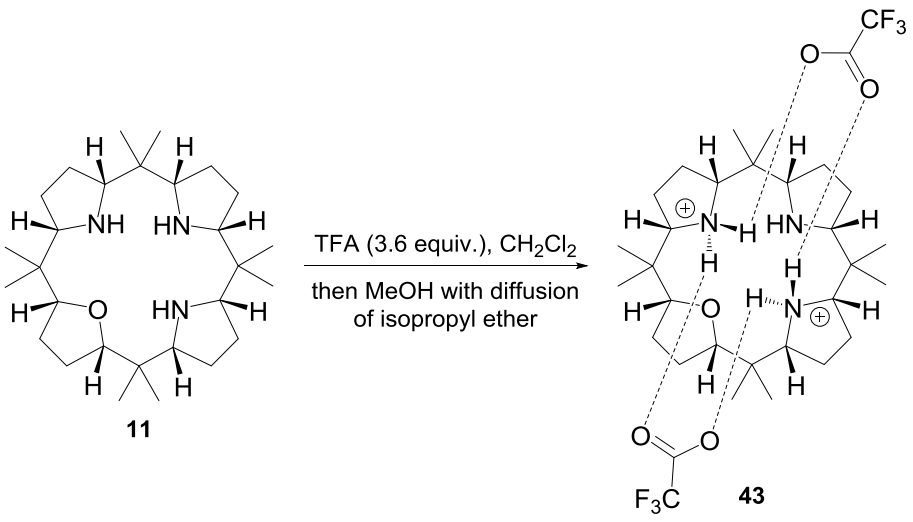

Scheme 41. Synthesis of calix-NNNO salt **43** with TFA as counteranion

The structure crystallized in the monoclinic C2/c space group and showed the protonation of the two pyrrolidines located in front of each other in the macrocycle and two molecules of TFA as counteranion (Scheme 41).

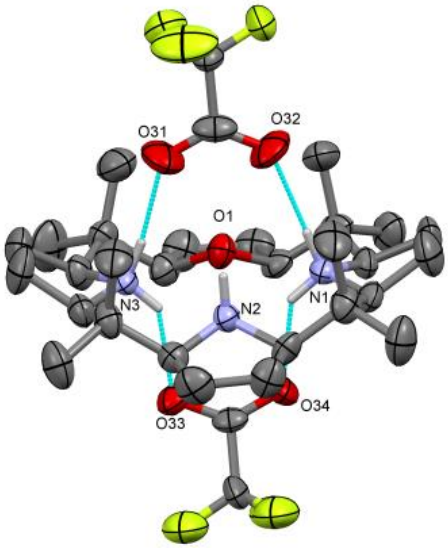

Figure 72. Molecular structure of the calix-NOOO salt **43** with TFA as counteranion. Hydrogen atoms were omitted for clarity. The displacement ellipsoids are drawn at the 30% probability level and the intramolecular hydrogen bonds as dashed blue lines

3. X-ray determination of side products

When optimizing the synthetic route of calix[n]furan[4-n]pyrroles **7** – **10** and their hydrogenations to calix[n]tetrahydrofuran[4-n]pyrrolidines **11** – **14**, the purifications by recrystallization were sometimes performed several times on the filtrate to isolate as much product as possible. When crystallizations were pushed to their limits, we sometimes were able to crystallize by product instead of the wanted product of the reaction. Here are three molecules for which suitable crystals for an X-ray analysis were grown and the structures deserved to be presented. These structures were not fully characterized.

Molecule 1:

During an hydrogenation of calix[2]furan[2]pyrrole **9** (100 bars of H_2, 0.3 equiv. of 10% PD/C, AcOH, 100 °C, 24 h, see page 50 Scheme 21) a side product was observed together with calix-NONO **13** after crystallization of the crude material in EtOAc. A GC-MS analysis of the fraction revealed that the unknown compound has a mass of 438 $g.mol^{-1}$ (M - 8 compared to compound **13**). The intermediate **44** (Figure 77) with the reduction of the furan rings only was our first prediction but this compound was previously reported by Guillaume Journot and a different retention time was observed in GC (**44**: 15.15 min; side product: 11.3 min).

Further crystallizations allowed isolating calix-NONO **13** as solid and a crystal was grown from the resulting filtrate. X-ray analysis of this crystal revealed the structure of compound **45** (Figure 78) with unexpectedly the reduction of the pyrrole rings and the furan rings stayed

unchanged. The structure crystallized in the triclinic P-1 space group and present the 1,3-alternate conformation.

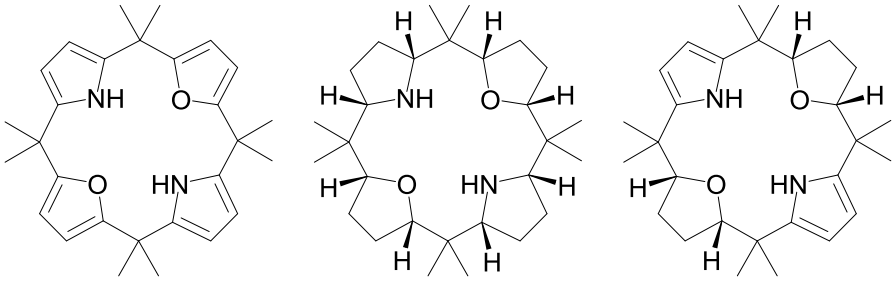

Figure 77. Characterized products involved in the hydrogenation of compound **9**

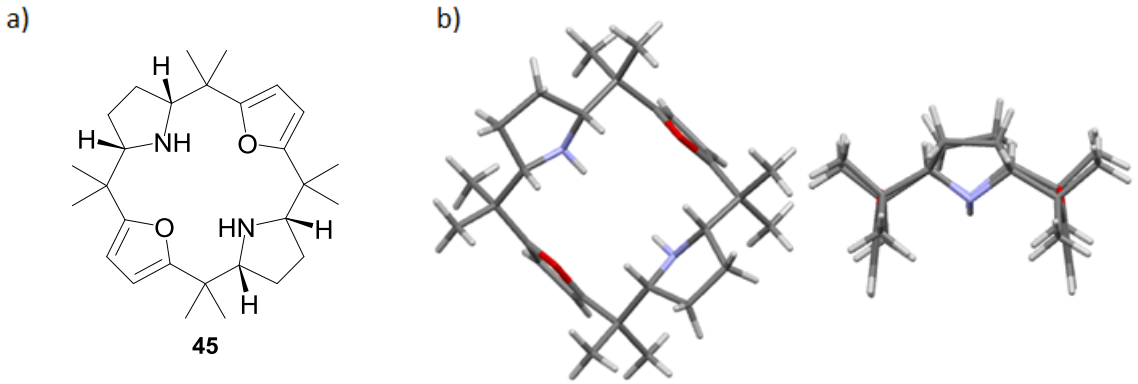

Figure 78. Structure (a) and molecular structure (b) of compound **45**. Top view (left); side view (right)

<u>Molecule 2:</u>

After reduction of tetraketone **16** by hydrogenation (4.0 bars of H_2, 10% Pd/C (0.025 equiv.), EtOAc, r.t., 4.5 h) a 72% yield was obtained by recrystallization in EtOH (Scheme 42a). Usually the hydrogenation of compound **16** gave 78% yield (see page 37 Chapter 2). The filtrate was concentrated and another recrystallization was performed leading to the formation of a unique crystal. An X-ray determination was performed on the crystal and the structure of compound **46** was obtained (Scheme 42b and Figure 79). The structure of compound **46** crystallized in the monoclinic $P2_1/c$ space group and showed a contraction of the macrocycle (15-membered ring compared to the 18-membered ring compound **19**), the formation of a cyclopentanone and an alcohol function. The proposed mechanism for the formation of compound **46** is illustrated in Scheme 42b. An intramolecular rearrangement from compound **19** led in one step to the formation of the side product **46**.

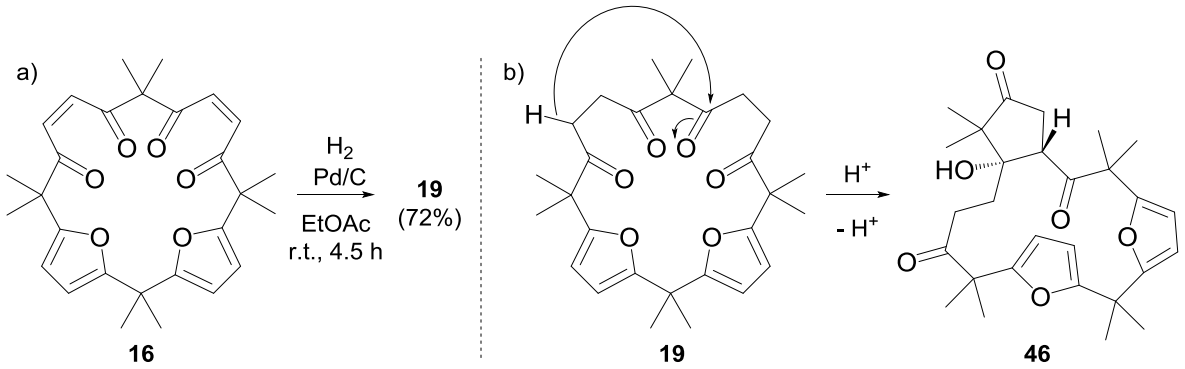

Scheme 42. Synthesis of compound **19** and its rearrangement into compound **46**. a) Hydrogenation of **16** in compound **19**; b) formation of compound **46** from compound **19**

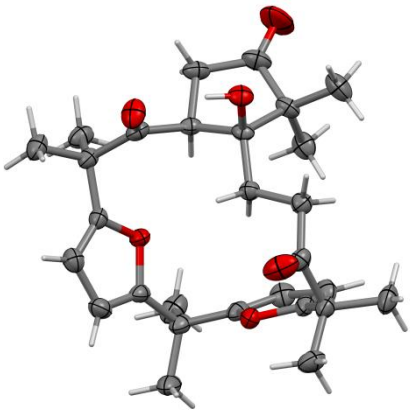

Figure 79. Molecular structure of compound **46**. The displacement ellipsoids are drawn at the 50% probability level

Molecule 3:

After a hydrogenation reaction on tetraketone **15a** to reduce the unsaturated 1,4-diketone functions (95%, Scheme 43), another single crystal was obtained from a filtrate after several recrystallizations. The analysis of the crystal surprisingly afforded the structure of compound **47** crystallizing in the triclinic P-1 space group (Figure 80).

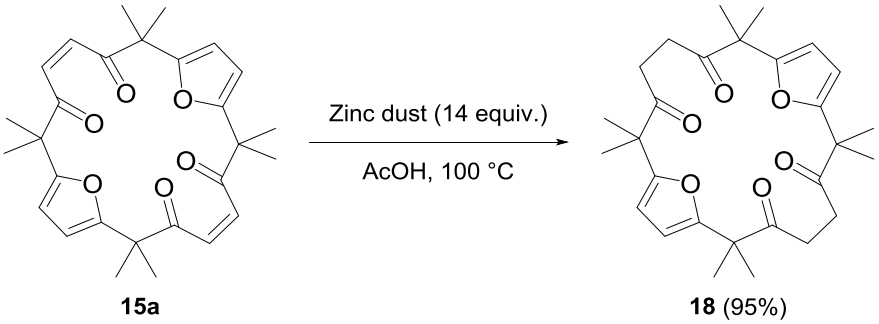

Scheme 43. Synthesis of compound **18**

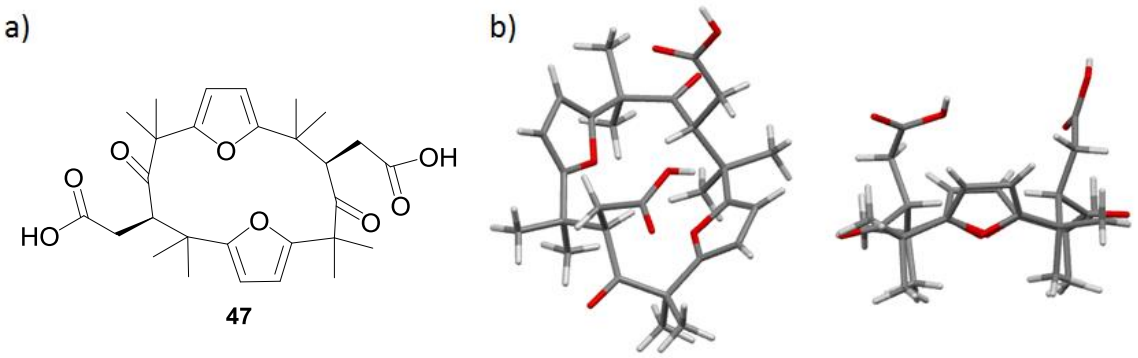

Figure 80. Structure (a) and molecular structure (b) of compound **47**. Top view (left); side view (right)

The structure of compound **47** is characterized by 1) a 14-membered macrocycle; 2) two furan rings at opposite position in the macrocycle; 3) a ketone and a $–CH_2COOH$ function at the two other positions. Both carboxylic acid chain point in the same direction and have a (*R*)-configuration.

With respect to the structure of compound **47**, this product came from a compound structurally closed to calix[4]furan **2** having undergone the same transformations during the synthesis of calix[n]furan[4-n]pyrrole compounds. The reactions leading to compound **47** in a retrospective way are: 1) an hydrogenation (4.0 bars of H_2, 10% Pd/C (0.025 equiv.), EtOAc, r.t., 4.5 h) and 2) a ring-opening reaction using *m*-CPBA as oxidative agent (*m*-CPBA (2.2 equiv.), $CHCl_3$, 1 h at 0 °C then 2 h at r.t.). A retrosynthesis was proposed to understand how this compound **47** could have been formed (Scheme 44). Under the hydrogenation reaction, compound **47** should come from the unsaturated analogue **48** with the two α,β-unsaturated carboxylic acid functions having a ketone in the γ-position (= 1,4-diketone function). This function should come from the oxidation of a furan ring in the presence of *m*-CPBA. This function is connected in the macrocycle by two successive atoms of carbon, meaning the furan was a 2,3-disubstituted ring in the origin macrocycle **50**. As illustrated by the oxidation of disubstituted furan ring in Figure 81, the oxidation of 2,3-disubtituted furan leads to the formation of an aldehyde function. The oxidation of compound **50** to **48** should go through the intermediate **49** with two α,β-unsaturated aldehyde functions. Compound **50** involves the formation of the *O*-confused bis(furan-2-yl)methane **51**. Although *N*-confused dipyrromethane[174] or *N*-confused calix[4]pyrroles[175] were reported in literature, compound 51 or "*O*-confused" calix[4]furan were not reported.

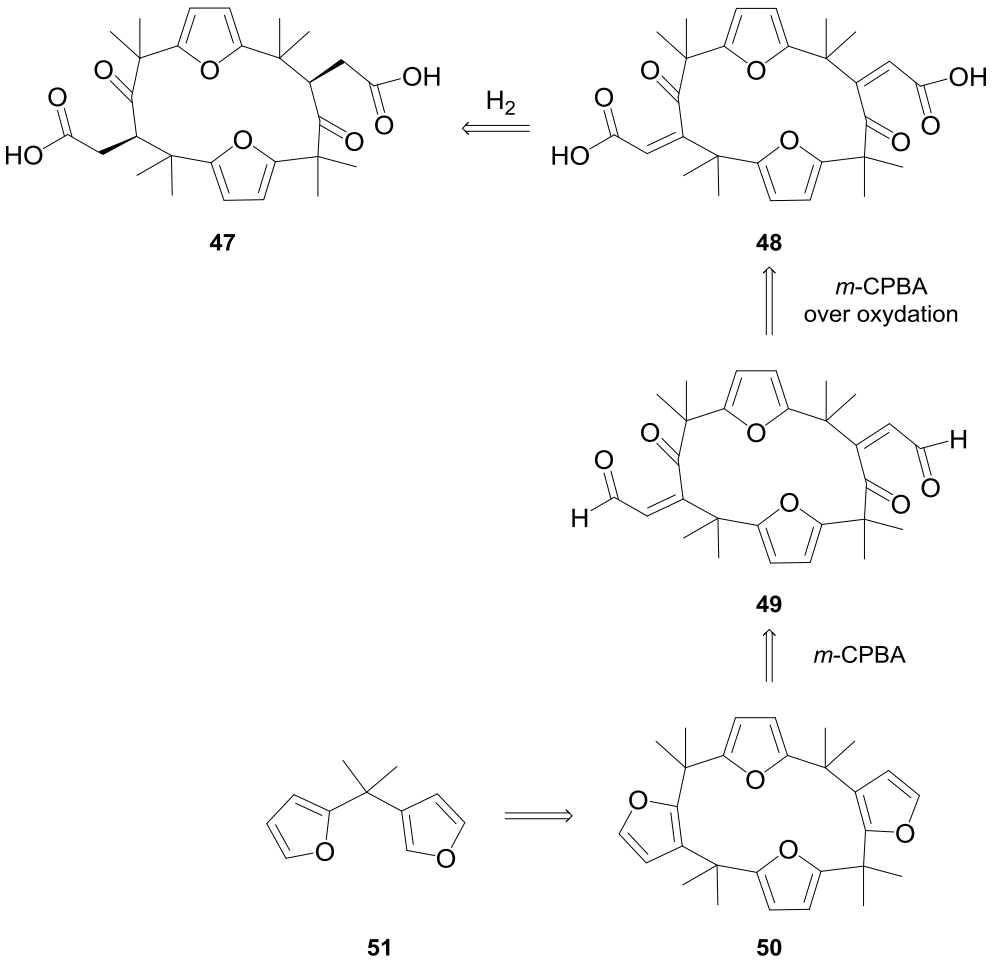

Scheme 44. Proposed retrosynthesis for the formation of compound **47**

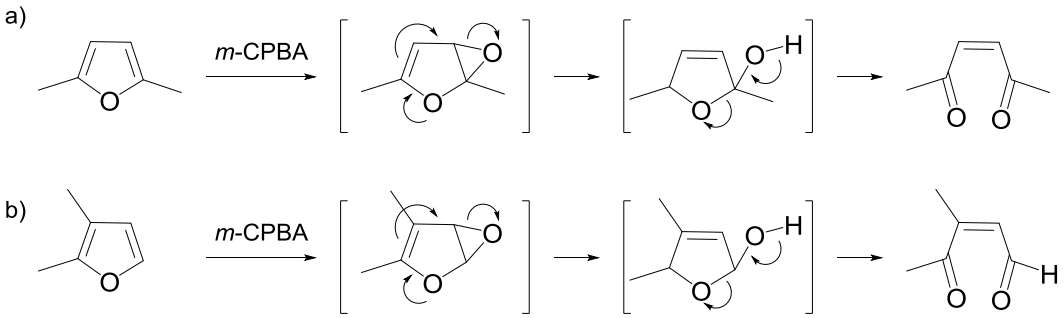

Figure 81. Oxidation of di-substituted furan ring with *m*-CPBA. a) Oxidation of 2,5-dimethyl furan; b) Oxidation of 2,3-dimethyl furan

4. Photos of crystals taken under the microscope during melting point experiments

-Calix-NNNN **3**

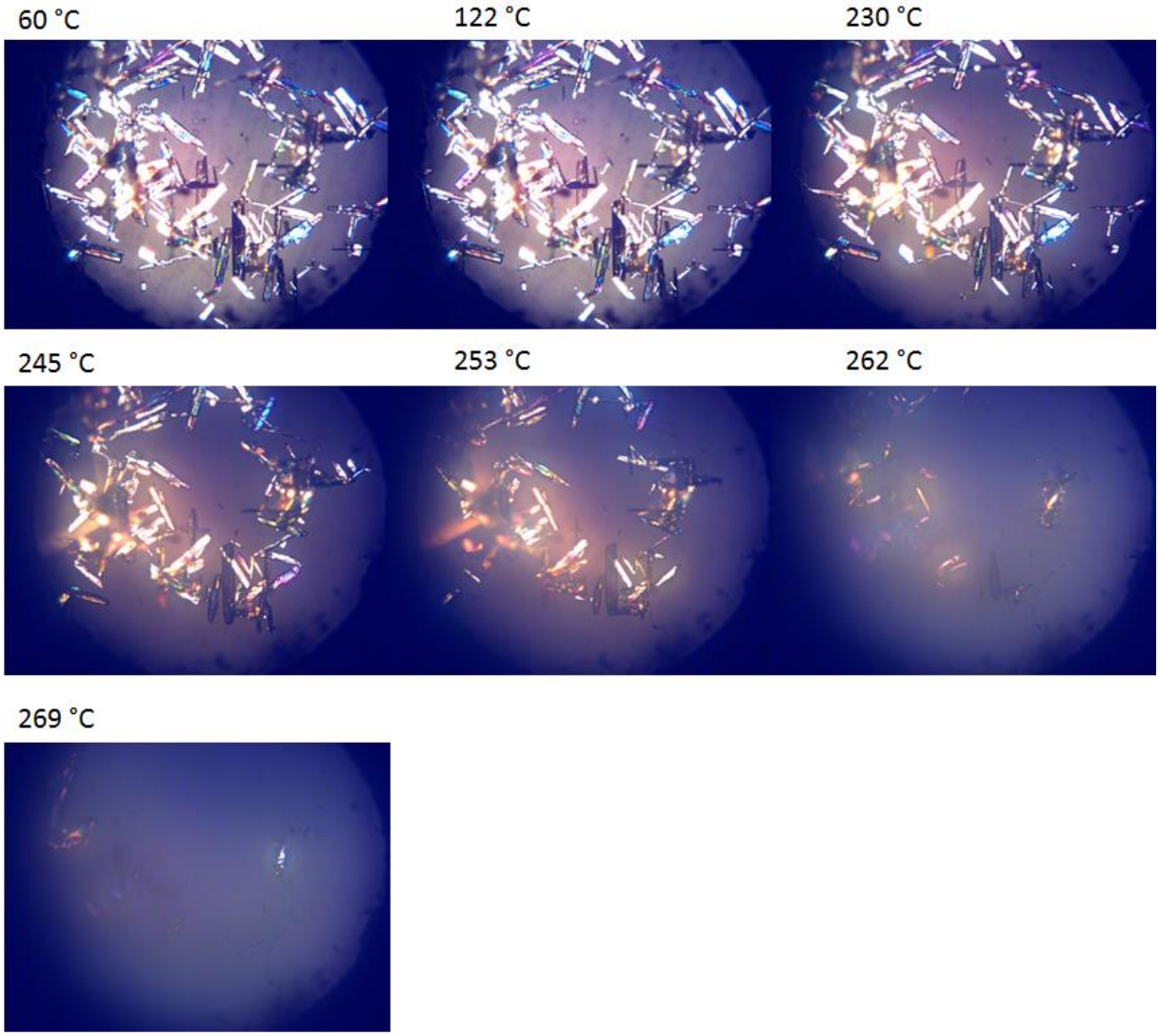

-Calix-NNNO **11**

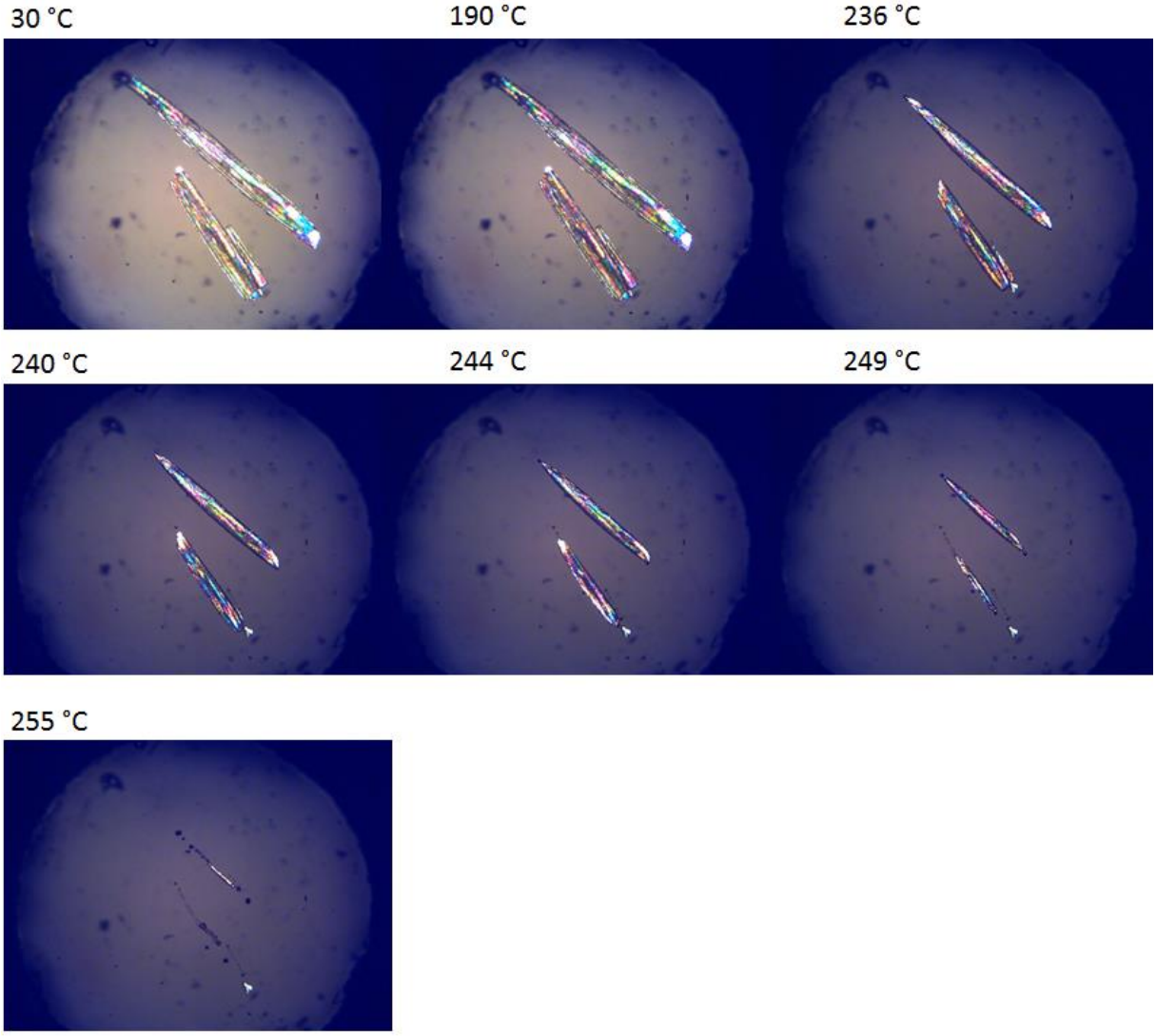

-Calix-NNOO **12**

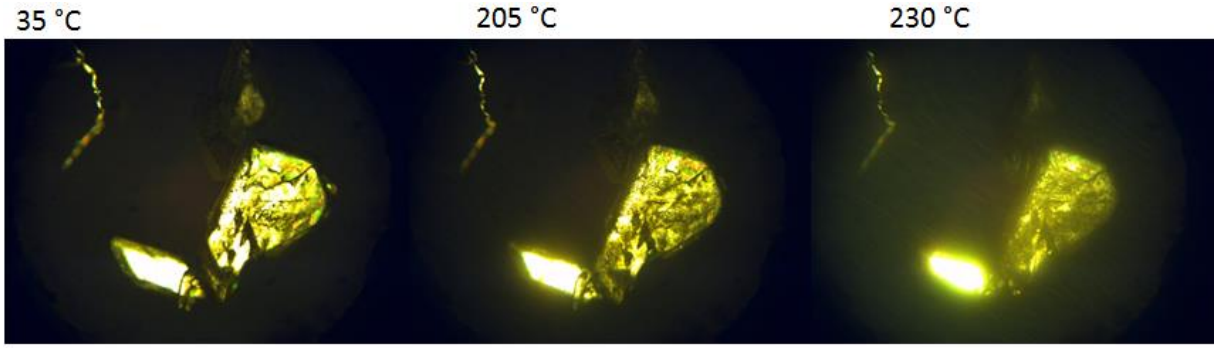

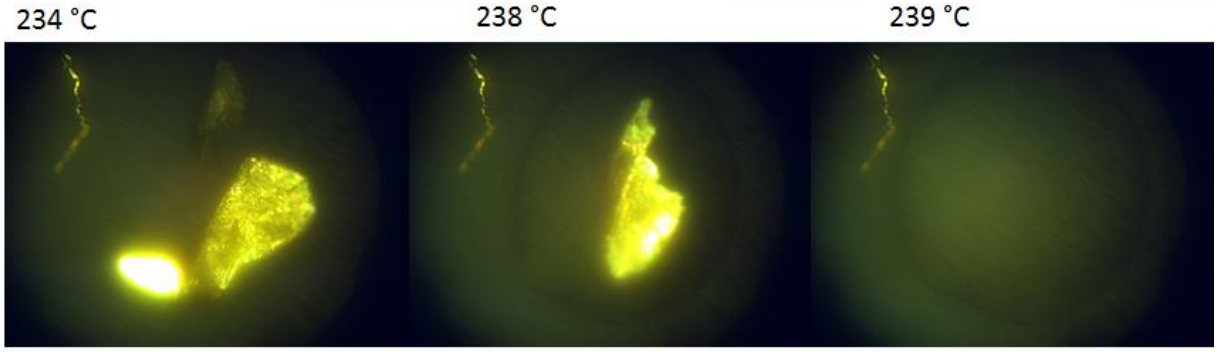

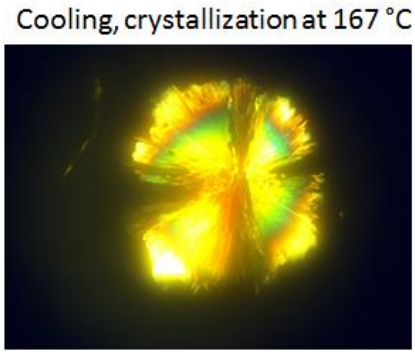

-Calix-NONO **13**

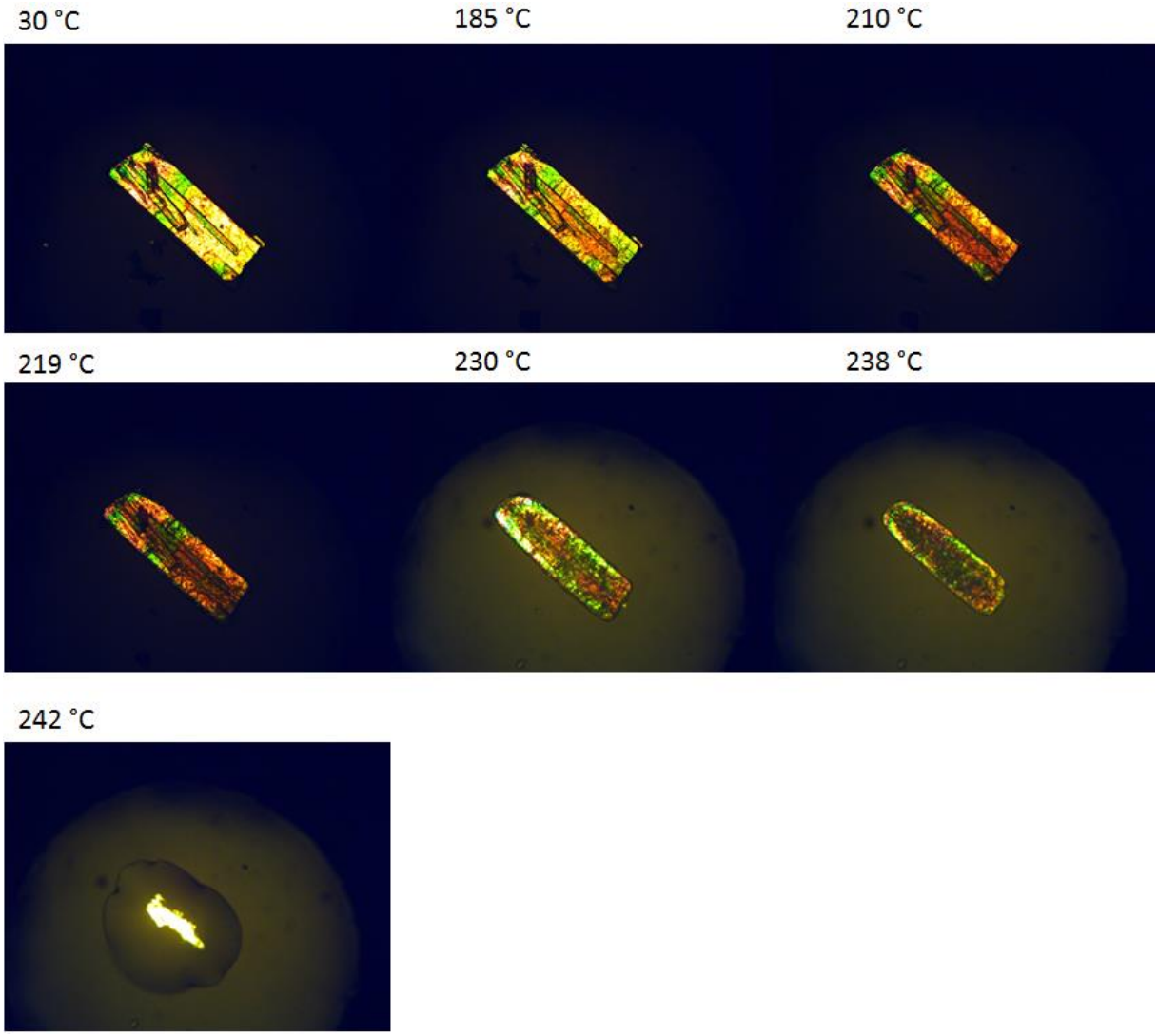

-Calix-NOOO **14**

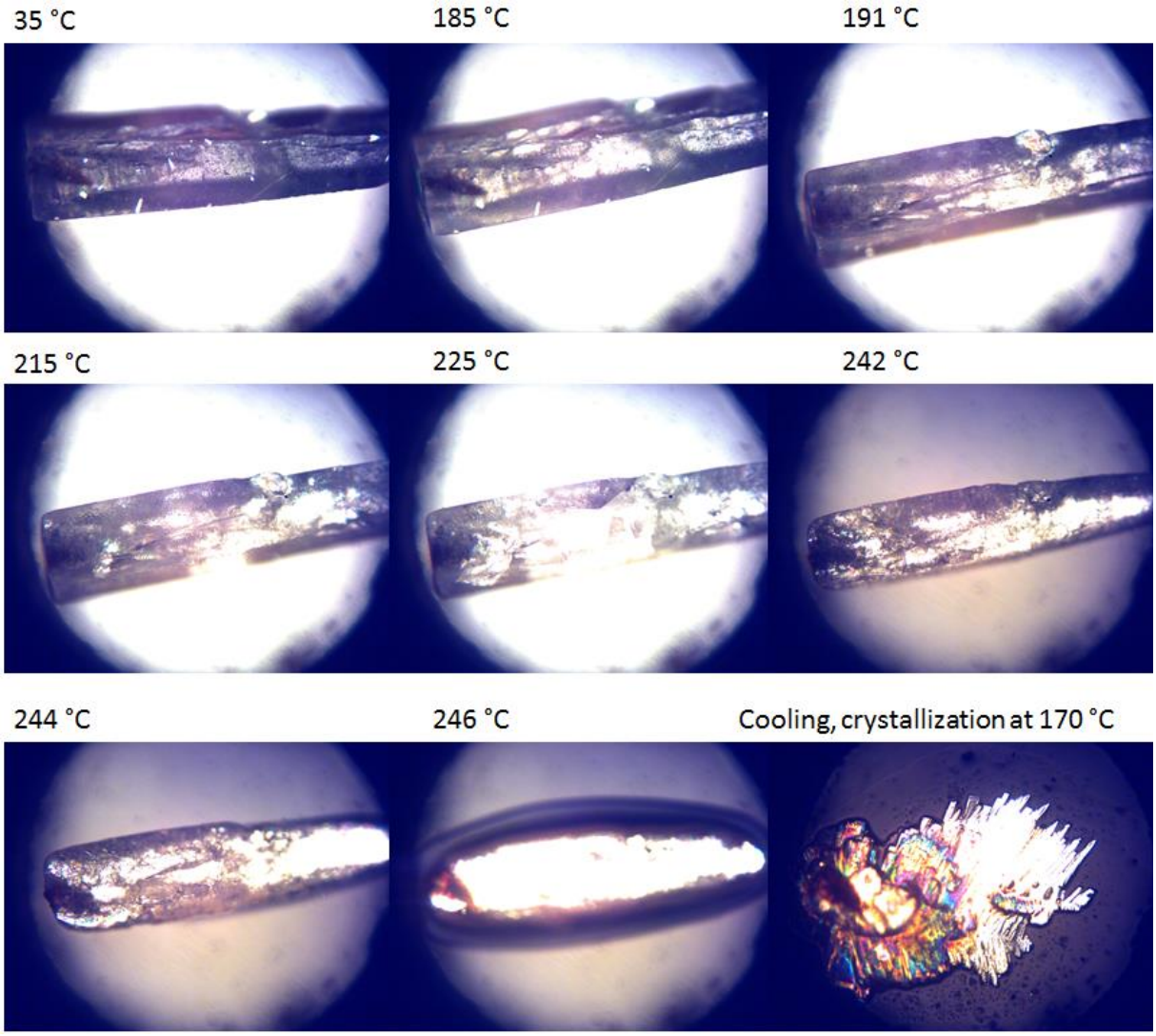

The crystal observed during cooling was heated to observed the second melting

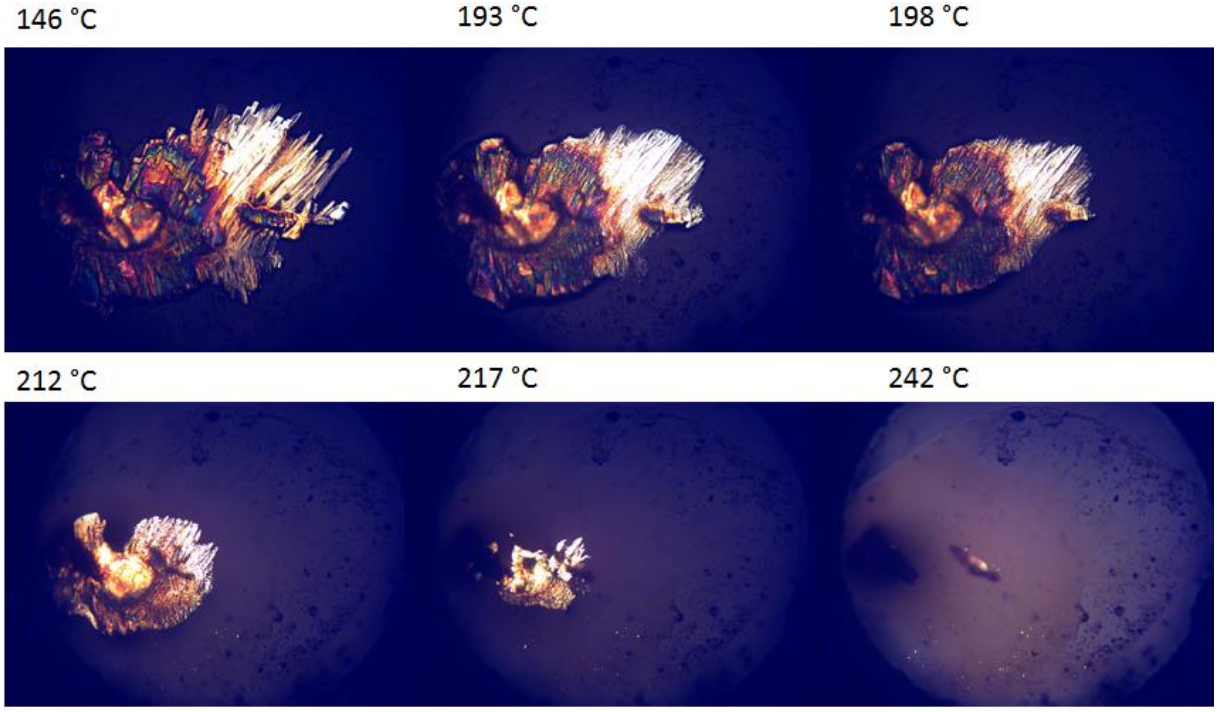

Chapter 10. References

[1] L. Ruzicka, *Helv. Chim. Acta,* **1926**, *9*, 715-729.
[2] L. Ruzicka, *Helv. Chim. Acta,* **1926**, *9*, 230-248.
[3] S. Fujimoto, K. Yoshikawa, M. Itoh, T. Kitahara, *Biosci. Biotech. Bioch.,* **2002**, *66*, 1389-1392.
[4] A. B. Smith, T. A. Rano, N. Chida, G. A. Sulikowski, J. L. Wood, *J. Am. Chem. Soc.,* **1992**, *114*, 8008-8022.
[5] A. K. Ghosh, C. Liu, *J. Am. Chem. Soc.,* **2003**, *125*, 2374-2375.
[6] P. K. Park, S. J. O'Malley, D. R. Schmidt, J. L. Leighton, *J. Am. Chem. Soc.,* **2006**, *128*, 2796-2797.
[7] B. M. Trost, G. Dong, J. A. Vance, *J. Am. Chem. Soc.,* **2007**, *129*, 4540-4541.
[8] G. Ehrlich, J. Hassfeld, U. Eggert, M. Kalesse, *Chem. Eur. J.,* **2008**, *14*, 2232-2247.
[9] B. M. Trost, G. Dong, *Nature,* **2008**, *456*, 485-488.
[10] S. Bonazzi, B. Cheng, J. S. Wzorek, D. A. Evans, *J. Am. Chem. Soc.,* **2013**, *135*, 9338-9341.
[11] J. N. deGruyter, W. A. Maio, *Org Lett,* **2014**, *16*, 5196-5199.
[12] I. Paterson, K. K. H. Ng, S. Williams, D. C. Millican, S. M. Dalby, *Ang. Chem. Int. Ed.,* **2014**, *53*, 2692-2695.
[13] E. M. Driggers, S. P. Hale, J. Lee, N. K. Terrett, *Nat. Rev. Drug. Discov.,* **2008**, *7*, 608-624.
[14] E. Marsault, M. L. Peterson, *J. Med. Chem.,* **2011**, *54*, 1961-2004.
[15] J. Mallinson, I. Collins, *Future. Med. Chem.,* **2012**, *4*, 1409-1438.
[16] X. F. Yu, D. Q. Sun, *Molecules,* **2013**, *18*, 6230-6268.
[17] J. M. Zuckerman, *Infect. Dis. Clin. N. Am.,* **2004**, *18*, 621-649.
[18] M. G. Sturgill, R. P. Rapp, *Ann. Pharmacother.,* **1992**, *26*, 1099-1108.
[19] D. J. Newman, G. M. Cragg, in *Macrocycles in Drug Discovery*, (Ed.: J. Levin),The Royal Society of Chemistry, **2015**, pp. 1-36.
[20] B. T. Kilbourn, J. D. Dunitz, L. A. R. Pioda, W. Simon, *J. Mol. Biol.,* **1967**, *30*, 559-563.
[21] L. Rose, A. T. A. Jenkins, *Bioelectrochemistry,* **2007**, *70*, 387-393.
[22] W. D. Woggon, *Chimia,* **1999**, *53*, 234-237.
[23] B. Kräutler, S. Ostermann, in *The Porphyrin Handbook* (Eds.: K. M. Smith, R. Guilard), Academic Press, Amsterdam, **2003**, pp. 229-276.
[24] B. Krautler, *Biochem. Soc. T.,* **2005**, *33*, 806-810.
[25] W. D. Woggon, *Accounts Chem. Res.,* **2005**, *38*, 127-136.
[26] H. Scheer, in *Chlorophylls and Bacteriochlorophylls: Biochemistry, Biophysics, Functions and Applications* (Eds.: B. Grimm, R. J. Porra, W. Rüdiger, H. Scheer), Springer Netherlands, Dordrecht, **2006**, pp. 1-26.
[27] A. R. Battersby, E. McDonald, *Accounts Chem. Res.,* **1979**, *12*, 14-22.
[28] A. R. Battersby, C. J. R. Fookes, G. W. J. Matcham, E. McDonald, *Nature,* **1980**, *285*, 17-21.
[29] A. R. Battersby, *Accounts Chem. Res.,* **1986**, *19*, 147-152.
[30] R. Bonnett, *Chem. Soc. Rev.,* **1995**, *24*, 19-33.
[31] T. D. Mody, *J. Porphyr. Phthalocya.,* **2000**, *4*, 362-367.
[32] L. B. Josefsen, R. W. Boyle, *Met. Based Drugs,* **2008**, *2008*.
[33] H. Huang, W. Song, J. Rieffel, J. F. Lovell, *Front. Phys.,* **2015**, *3*.
[34] A. Baeyer, *Ber. dtsch chem. Ges.,* **1872**, *5*, 280-282.
[35] A. Baeyer, *Ber. dtsch chem. Ges.,* **1872**, *5*, 1094-1100.
[36] L. H. Baekeland, *J. Ind. Eng. Chem.,* **1909**, *1*, 149-161.
[37] L. H. Baekeland, H. L. Bender, *Ind. Eng. Chem.,* **1925**, *17*, 225-237.
[38] A. Zinke, E. Ziegler, *Ber. dtsch chem. Ges.,* **1941**, *74*, 1729-1736.
[39] A. Zinke, E. Ziegler, *Ber. dtsch chem. Ges.,* **1944**, *77*, 264-272.
[40] Z. Wang, in *Comprehensive Organic Name Reactions and Reagents*, (Ed.: Z. Wang), John Wiley & Sons, Inc., **2010**, pp. 3183-3196.

[41] C. D. Gutsche, B. Dhawan, K. H. No, R. Muthukrishnan, *J. Am. Chem. Soc.,* **1981**, *103*, 3782-3792.
[42] C. D. Gutsche, in *Calixarenes: An Introduction: Edition 2*, (Ed.: J. F. Stoddard), The Royal Society of Chemistry, **2008**, pp. 1-276.
[43] B. V. Chelintzev, B. V. Tronov, S. G. Karmanov, *J. Russ. Chem. Soc.,* **1916**, *48*, 1210-1221.
[44] P. Rothemund, C. L. Gage, *J. Am. Chem. Soc.,* **1955**, *77*, 3340-3342.
[45] P. A. Gale, J. L. Sessler, V. Kral, V. Lynch, *J. Am. Chem. Soc.,* **1996**, *118*, 5140-5141.
[46] W. E. Allen, P. A. Gale, C. T. Brown, V. M. Lynch, J. L. Sessler, *J. Am. Chem. Soc.,* **1996**, *118*, 12471-12472.
[47] J. L. Sessler, A. Andrievsky, P. A. Gale, V. Lynch, *Angew. Chem. Int. Ed.,* **1996**, *35*, 2782-2785.
[48] D. Jacoby, C. Floriani, A. Chiesivilla, C. Rizzoli, *J. Chem. Soc., Chem. Comm.,* **1991**, 220-222.
[49] J. Jubb, D. Jacoby, C. Floriani, A. Chiesivilla, C. Rizzoli, *Inorg. Chem.,* **1992**, *31*, 1306-1308.
[50] C. Floriani, *Chem. Commun.,* **1996**, 1257-1263.
[51] L. Bonomo, E. Solari, R. Scopelliti, C. Floriani, *Chem. Eur. J.,* **2001**, *7*, 1322-1332.
[52] R. G. Ackman, W. H. Brown, G. F. Wright, *J. Org. Chem.,* **1955**, *20*, 1147-1158.
[53] M. Chastette, F. Chastrette, *J. Chem. Soc., Chem. Comm.,* **1973**, 534-535.
[54] M. Chastrette, F. Chastrette, J. Sabadie, *Org. Synth.,* **1988**, *50-9*, 856-859.
[55] M. D. Healy, A. J. Rest, *J. Chem. Soc., Perkin Trans. 1,* **1985**, 973-982.
[56] G.-A. Lee, W.-C. Wang, M. Shieh, T.-S. Kuo, *Chem. Commun.,* **2010**, *46*, 5009-5011.
[57] A. Nayak, J. Banerji, *J. Heterocyclic. Chem.,* **2014**, *51*, 1380-1384.
[58] K. Bowman-James, in *Encyclopedia of Inorganic and Bioinorganic Chemistry*, (Ed.: R. A. Scott), John Wiley & Sons, Ltd, **2011**, pp. 1-18.
[59] R. M. Izatt, J. S. Bradshaw, S. A. Nielsen, J. D. Lamb, J. J. Christensen, *Chem. Rev.,* **1985**, *85*, 271-339.
[60] K. E. Krakowiak, J. S. Bradshaw, D. J. Zameckakrakowiak, *Chem. Rev.,* **1989**, *89*, 929-972.
[61] K. E. Krakowiak, J. S. Bradshaw, R. M. Izatt, *J. Org. Chem.,* **1990**, *55*, 3364-3368.
[62] V. Alexander, *Chem. Rev.,* **1995**, *95*, 273-342.
[63] J. van Alphen, *Recl. Trav. Chim. Pay-B.,* **1936**, *55*, 835-840.
[64] J. van Alphen, *Recl. Trav. Chim. Pay-B.,* **1937**, *56*, 343-350.
[65] N. F. Curtis, *J. Chem. Soc.,* **1960**, 4409-4413.
[66] N. F. Curtis, D. A. House, *Chem. Ind. (London),* **1961**, 1708-1709.
[67] M. M. Blight, N. F. Curtis, *J. Chem. Soc.,* **1962**, 1204-1207.
[68] M. M. Blight, N. F. Curtis, *J. Chem. Soc.,* **1962**, 3016-3020.
[69] D. A. House, N. F. Curtis, *J. Am. Chem. Soc.,* **1962**, *84*, 3248-3250.
[70] N. F. Curtis, *Coordin. Chem. Rev.,* **1968**, *3*, 3-47.
[71] D. K. Cabbiness, D. W. Margerum, *J. Am. Chem. Soc.,* **1969**, *91*, 6540-6541.
[72] W. Nam, R. Ho, J. S. Valentine, *J. Am. Chem. Soc.,* **1991**, *113*, 7052-7054.
[73] R. Hage, J. E. Iburg, J. Kerschner, J. H. Koek, E. L. M. Lempers, R. J. Martens, U. S. Racherla, S. W. Russell, T. Swarthoff, M. R. P. van Vliet, J. B. Warnaar, L. v. d. Wolf, B. Krijnen, *Nature,* **1994**, *369*, 637-639.
[74] D. De Vos, T. Bein, *Chem. Commun.,* **1996**, 917-918.
[75] Z. J. Guo, P. J. Sadler, *Angew. Chem. Int. Ed.,* **1999**, *38*, 1513-1531.
[76] E. Kent Barefield, *Coordin. Chem. Rev.,* **2010**, *254*, 1607-1627.
[77] C. J. Pedersen, *J. Am. Chem. Soc.,* **1967**, *89*, 7017-7036.
[78] P. Muller, *Pure Appl. Chem.,* **1994**, *66*, 1077-1184.
[79] V. J. Thom, M. S. Shaikjee, R. D. Hancock, *Inorg. Chem.,* **1986**, *25*, 2992-3000.
[80] J. C. Dabrowiak, P. H. Merrell, D. H. Busch, *Inorg. Chem.,* **1972**, *11*, 1979-1988.
[81] J. S. Bradshaw, K. E. Krakowiak, R. M. Izatt, in *Chemistry of Heterocyclic Compounds*, (Eds.: J. S. Bradshaw, K. E. Krakowiak, R. M. Izatt), John Wiley & Sons, Inc., **2008**, pp. 1-29.
[82] G. W. Gokel, D. M. Dishong, C. J. Diamond, *J. Chem. Soc., Chem. Comm.,* **1980**, 1053-1054.
[83] R. A. Schultz, D. M. Dishong, G. W. Gokel, *J. Am. Chem. Soc.,* **1982**, *104*, 625-626.
[84] B. Dietrich, J. M. Lehn, J. P. Sauvage, *Tetrahedron Lett.,* **1969**, *10*, 2889-2892.

[85] G. W. Gokel, S. Korzeniowski, in *Macrocyclic Polyether Syntheses*, (Eds.: K. Hafner, J.-M. Lehn, C. W. Rees, P. von Ragué Schleyer, B. M. Trost, R. Zahnradník), Springer Berlin Heidelberg, **2012**, pp. 1-11.
[86] T. J. Hubin, *Coordin. Chem. Rev.,* **2003**, *241*, 27-46.
[87] J. C. Timmons, T. J. Hubin, *Coordin. Chem. Rev.,* **2010**, *254*, 1661-1685.
[88] "The Nobel Prize in Chemistry 1987". *Nobelprize.org.* Nobel Media AB 2014. Web. 29 Sep 2016. <http://www.nobelprize.org/nobel_prizes/chemistry/laureates/1987/>
[89] M. Ahmed, O. Meth-Cohn, *Tetrahedron Lett.,* **1969**, *10*, 1493-1496.
[90] V. Blangy, C. Heiss, V. Khlebnikov, C. Letondor, H. Stoeckli-Evans, R. Neier, *Ang. Chem. Int. Ed.,* **2009**, *48*, 1688-1691.
[91] Y. Kobuke, K. Hanji, K. Horiguchi, M. Asada, Y. Nakayama, J. Furukawa, *J. Am. Chem. Soc.,* **1976**, *98*, 7414-7419.
[92] K. E. Wiegers, S. G. Smith, *J. Org. Chem.,* **1978**, *43*, 1126-1131.
[93] M. Vanbeylen, B. Roland, G. S. D. King, J. Aerts, *J. Chem. Res., Synop.,* **1985**, 388-389.
[94] A. Corsini, J. M. Panoyan, *J. Inorg. Nucl. Chem.,* **1977**, *39*, 1449-1450.
[95] G. Journot, C. Letondor, R. Neier, H. Stoeckli-Evans, D. Savoia, A. Gualandi, *Chem. Eur. J.,* **2010**, *16*, 4224-4230.
[96] F. Bruyneel, C. Letondor, B. Basturk, A. Gualandi, A. Pordea, H. Stoeckli-Evans, R. Neier, *Adv. Synth. Catal.,* **2012**, *354*, 428-440.
[97] W. H. Brown, W. N. French, *Can. J. Chem.,* **1958**, *36*, 371-377.
[98] R. Crescenzi, E. Solari, C. Floriani, A. ChiesiVilla, C. Rizzoli, *Inorg. Chem.,* **1996**, *35*, 2413-2414.
[99] Y. S. Jang, H. J. Kim, P. H. Lee, C. H. Lee, *Tetrahedron Lett.,* **2000**, *41*, 2919-2923.
[100] A. Nagarajan, J. W. Ka, C. H. Lee, *Tetrahedron,* **2001**, *57*, 7323-7330.
[101] J. L. Sessler, D. Q. An, W. S. Cho, V. Lynch, D. W. Yoon, S. J. Hong, C. H. Lee, *J. Org. Chem.,* **2005**, *70*, 1511-1517.
[102] K. S. Park, S. O. Jung, I. Yoon, K. M. Park, J. Kim, S. S. Lee, J. S. Kim, *J. Incl. Phenom. Macro.,* **2001**, *39*, 295-301.
[103] S. M. Lim, H. J. Chung, K. J. Paeng, C. H. Lee, H. N. Choi, W. Y. Lee, *Anal. Chim. Acta,* **2002**, *453*, 81-88.
[104] C. A. T. dos Santos, A. L. Magalhaes, *J. Mol. Struc.-Theochem,* **2010**, *956*, 50-54.
[105] P. D. Williams, E. Legoff, *J. Org. Chem.,* **1981**, *46*, 4143-4147.
[106] G. Cafeo, F. H. Kohnke, G. L. La Torre, A. J. P. White, D. J. Williams, *Angew. Chem. Int. Ed.,* **2000**, *39*, 1496-1498.
[107] G. Cafeo, F. H. Kohnke, M. F. Parisi, R. P. Nascone, G. L. La Torre, D. J. Williams, *Org. Lett.,* **2002**, *4*, 2695-2697.
[108] G. Journot, Université de Neuchâtel, **2012**.
[109] R. Pajewski, R. Ostaszewski, J. Jurczak, *Org. Prep. Proced. Int.,* **2000**, *32*, 394-397.
[110] M. T. Barton, N. M. Rowley, P. R. Ashton, C. J. Jones, N. Spencer, M. S. Tolley, L. J. Yellowlees, *J. Chem. Soc. Dalton,* **2000**, 3170-3175.
[111] J. Bachmann, D. G. Nocera, *J. Am. Chem. Soc.,* **2004**, *126*, 2829-2837.
[112] J. Bachmann, D. G. Nocera, *J. Am. Chem. Soc.,* **2005**, *127*, 4730-4743.
[113] M. T. Barton, N. M. Rowley, P. R. Ashton, C. J. Jones, N. Spencer, M. S. Tolley, L. J. Yellowlees, *New J. Chem.,* **2000**, *24*, 555-560.
[114] A. J. Pistner, G. P. A. Yap, J. Rosenthal, *J. Phys. Chem. C,* **2012**, *116*, 16918-16924.
[115] A. J. Pistner, D. A. Lutterman, M. J. Ghidiu, Y.-Z. Ma, J. Rosenthal, *J. Am. Chem. Soc.,* **2013**, *135*, 6601-6607.
[116] Y. Cui, L. H. Zeng, Y. Y. Fang, J. L. Zhu, H. J. Xu, N. Desbois, C. P. Gros, K. M. Kadish, *ChemElectroChem,* **2016**, *3*, 110-121.
[117] D. Andrienko, *Cyclic Voltammetry,* **2008**.
[118] S. Sadki, P. Schottland, N. Brodie, G. Sabouraud, *Chem. Soc. Rev.,* **2000**, *29*, 283-293.
[119] G. Journot, R. Neier, H. Stoeckli-Evans, *Acta Crystallogr. E,* **2010**, *66*, O392-U2756.
[120] G. Journot, R. Neier, H. Stoeckli-Evans, *Acta Crystallogr. C,* **2012**, *68*, O119-O122.

[121] J. W. Cornforth, P. D. A. Hart, G. A. Nicholls, R. J. W. Rees, J. A. Stock, *Brit. J. Pharm. Chemoth.,* **1955**, *10*, 73-86.
[122] C. D. Gutsche, B. Dhawan, J. A. Levine, K. H. No, L. J. Bauer, *Tetrahedron,* **1983**, *39*, 409-426.
[123] G. D. Andreetti, R. Ungaro, A. Pochini, *J. Chem. Soc., Chem. Comm.,* **1979**, 1005-1007.
[124] K. Iwamoto, K. Araki, S. Shinkai, *J. Org. Chem.,* **1991**, *56*, 4955-4962.
[125] P. A. Gale, J. L. Sessler, V. Kral, *Chem. Commun.,* **1998**, 1-8.
[126] Y.-D. Wu, D.-F. Wang, J. L. Sessler, *J. Org. Chem.,* **2001**, *66*, 3739-3746.
[127] J. R. Blas, M. Márquez, J. L. Sessler, F. J. Luque, M. Orozco, *J. Am. Chem. Soc.,* **2002**, *124*, 12796-12805.
[128] A. Hazell, *Acta Crystallogr. C,* **1989**, *45*, 137-140.
[129] R. Pajewski, A. Pecak, R. Ostaszewski, J. Jurczak, *Acta Crystallogr. C,* **1999**, *55*, 1862-1864.
[130] P. Ballester, G. Gil-Ramírez, *Proc. Natl. Acad. Sci.,* **2009**, *106*, 10455-10459.
[131] S. K. Kim, J. L. Sessler, *Accounts Chem. Res.,* **2014**, *47*, 2525-2536.
[132] J.-B. Meng, D.-C. Fu, Y.-M. Wang, W.-L. Jia, X.-K. Yiao, H.-G. H Wang, *Jiegou Huaxue (Chin. J. Struct. Chem.),* **1992**, *11*, 376.
[133] S. Dey, K. Pal, S. Sarkar, *Tetrahedron Lett.,* **2007**, *48*, 5481-5485.
[134] P. G. Jones, P. Buenitschek, H. Hopf, *Z Kristallogr.,* **1994**, *209*, 777-778.
[135] R. J. Davey, *Cryst. Growth Des.,* **2002**, *2*, 675-676.
[136] H. G. Brittain, in *Polymorphism in Pharmaceutical Solids*, (Ed.: H. G. Brittain), Taylor & Francis, **1999**.
[137] J. Bernstein, *J. Phys. D: Appl. Phys.,* **1993**, *26*, B66.
[138] J. Bernstein, A. T. Hagler, *J. Am. Chem. Soc.,* **1978**, *100*, 673-681.
[139] A. J. Cruz-Cabeza, J. Bernstein, *Chem. Rev.,* **2014**, *114*, 2170-2191.
[140] J. Bauer, S. Spanton, R. Henry, J. Quick, W. Dziki, W. Porter, J. Morris, *Pharm. Res.,* **2001**, *18*, 859-866.
[141] F. Allen, *Acta Crystallogr. B,* **2002**, *58*, 380-388.
[142] C. R. Groom, I. J. Bruno, M. P. Lightfoot, S. C. Ward, *Acta Crystallogr. B,* **2016**, *72*, 171-179.
[143] M. D. Hanwell, D. E. Curtis, D. C. Lonie, T. Vandermeersch, E. Zurek, G. R. Hutchison, *J. Cheminform.,* **2012**, *4*, 1-17.
[144] M. J. frisch, *GAUSSIAN 09.(Gaussian inc, 2009)*.
[145] S. Grimme, *J. Comput. Chem.,* **2004**, *25*, 1463-1473.
[146] J. P. Perdew, K. Burke, M. Ernzerhof, *Phys. Rev. Lett.,* **1996**, *77*, 3865-3868.
[147] P. E. Blochl, *Phys. Rev. B,* **1994**, *50*, 17953-17979.
[148] G. Kresse, D. Joubert, *Phys. Rev. B,* **1999**, *59*, 1758-1775.
[149] S. Grimme, *J. Comput. Chem.,* **2006**, *27*, 1787-1799.
[150] G. Kresse, J. Hafner, *Phys. Rev. B,* **1993**, *47*, 558-561.
[151] G. Kresse, J. Hafner, *Phys. Rev. B,* **1994**, *49*, 14251-14269.
[152] G. Kresse, J. Furthmuller, *Comp. Mater. Sci.,* **1996**, *6*, 15-50.
[153] G. Kresse, J. Furthmuller, *Phys. Rev. B,* **1996**, *54*, 11169-11186.
[154] H. J. Monkhorst, J. D. Pack, *Phys. Rev. B,* **1976**, *13*, 5188-5192.
[155] H. Kämmerer, G. Happel, F. Caesar, *Die Makromolekulare Chemie,* **1972**, *162*, 179-197.
[156] C. D. Gutsche, L. J. Bauer, *J. Am. Chem. Soc.,* **1985**, *107*, 6052-6059.
[157] W. Beckmann, K. Nickisch, U. Budde, *Org. Process Res. Dev.,* **1998**, *2*, 298-304.
[158] S. A. Kulkarni, H. Meekes, J. H. ter Horst, *Cryst. Growth Des.,* **2014**, *14*, 1493-1499.
[159] E. A. Stura, I. A. Wilson, *J. Cryst. Growth,* **1991**, *110*, 270-282.
[160] C. Oswald, S. H. J. Smits, E. Bremer, L. Schmitt, *Int. J. Mol. Sci.,* **2008**, *9*, 1131-1141.
[161] X. Y. Liang, P. J. Sadler, *Chem. Soc. Rev.,* **2004**, *33*, 246-266.
[162] M. Shokeen, C. J. Anderson, *Accounts Chem. Res.,* **2009**, *42*, 832-841.
[163] L. M. P. Lima, D. Esteban-Gómez, R. Delgado, C. Platas-Iglesias, R. Tripier, *Inorg. Chem.,* **2012**, *51*, 6916-6927.
[164] T. David, V. Kubíček, O. Gutten, P. Lubal, J. Kotek, H.-J. Pietzsch, L. Rulíšek, P. Hermann, *Inorg. Chem.,* **2015**, *54*, 11751-11766.

[165] G. P. Moss, *Pure Appl. Chem.,* **1996**, *68*, 2193-2222.
[166] D. Seebach, A. K. Beck, A. Heckel, *Angew. Chem. Int. Ed.,* **2001**, *40*, 92-138.
[167] J. M. Brunel, *Chem. Rev.,* **2007**, *107*, Pr1-Pr45.
[168] C. F. Lane, *Synthesis-Stuttgart,* **1975**, 135-146.
[169] T. H. Jones, J. B. Franko, M. S. Blum, H. M. Fales, *Tetrahedron Lett.,* **1980**, *21*, 789-792.
[170] C. Robert, F. de Montigny, C. M. Thomas, *Nat. Commun.,* **2011**, *2*.
[171] M. Periasamy, V. D. Rao, M. Seenivasaperumal, *Tetrahedron-Asymmetr.,* **2001**, *12*, 1887-1890.
[172] C. M. Xie, D. H. Bai, S. H. Huang, X. S. Jia, R. Hong, *Asian. J. Org. Chem.,* **2014**, *3*, 277-280.
[173] A. Ghanem, H. Y. Aboul-Enein, *Chirality,* **2005**, *17*, 1-15.
[174] N. A. M. Pereira, T. M. V. D. Pinho e Melo, *Org. Prep. Proced. Int.,* **2014**, *46*, 183-213.
[175] S. Depraetere, M. Smet, W. Dehaen, *Angew. Chem. Int. Ed.,* **1999**, *38*, 3359-3361.